



Australian Government
Geoscience Australia

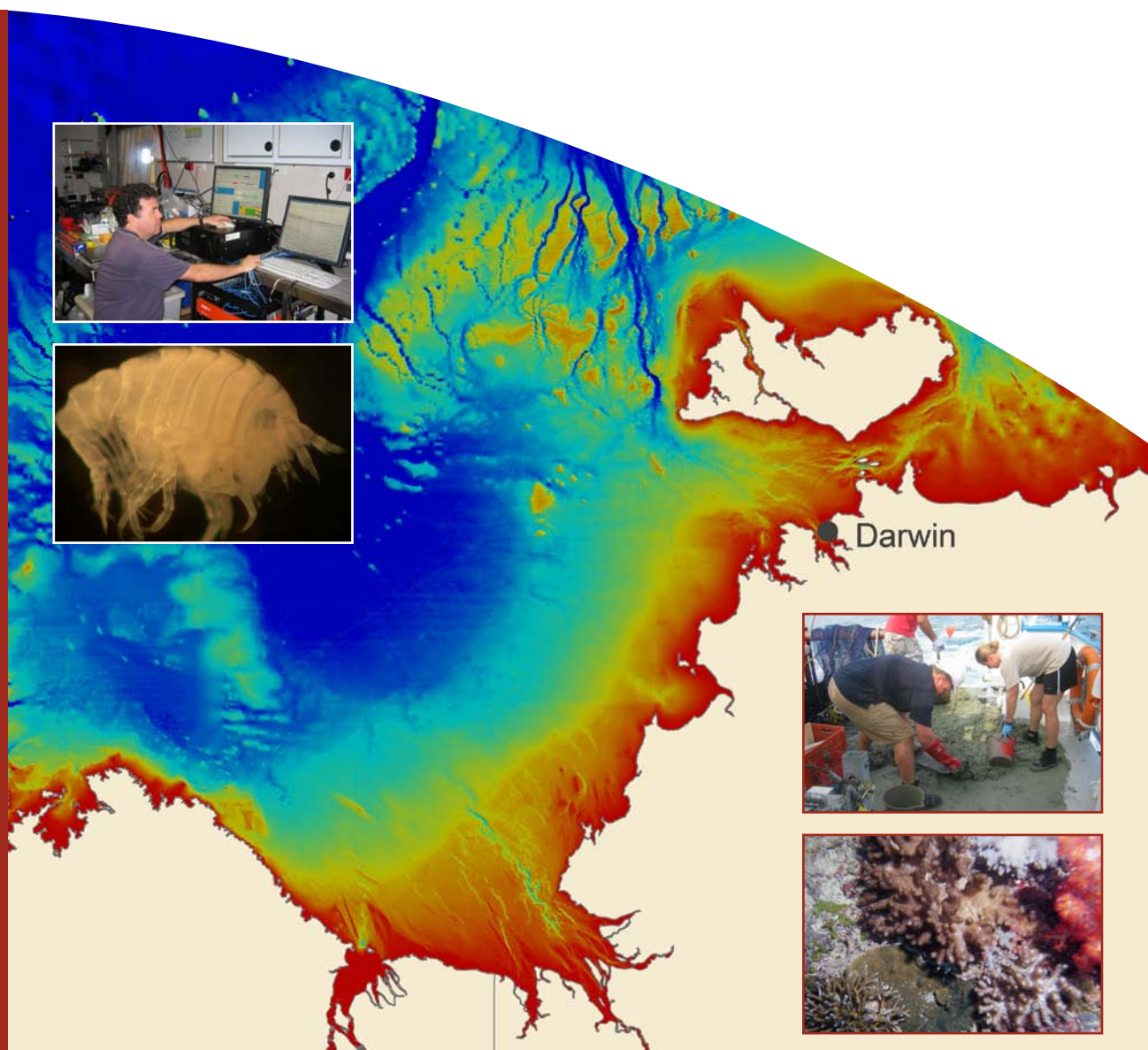
Seabed Habitats and Hazards of the Joseph Bonaparte Gulf and Timor Sea, Northern Australia

Rachel Przeslawski, James Daniell, Tara Anderson, J. Vaughn Barrie, Andrew Heap, Michael Hughes, Jin Li, Anna Potter, Lynda Radke, Justy Siwabessy, Maggie Tran, Tanya Whiteway and Scott Nichol

Record

2011/40

GeoCat #
72805



Seabed Habitats and Hazards of the Joseph Bonaparte Gulf and Timor Sea, Northern Australia

GEOSCIENCE AUSTRALIA
RECORD 2011/40

by

Rachel Przeslawski¹, James Daniell¹, Tara Anderson¹, J. Vaughn Barrie², Andrew Heap¹, Michael Hughes³, Jin Li¹, Anna Potter¹, Lynda Radke¹, Justy Siwabessy¹, Maggie Tran¹, Tanya Whiteway¹, Scott Nichol¹



Australian Government
Geoscience Australia

-
1. Geoscience Australia, GPO Box 378, Canberra, ACT 2601
 2. Geological Survey of Canada – Pacific, Natural Resources Canada, PO Box 6000, Sidney British Columbia, Canada
 3. Current Address: Office of the Chief Scientist, GPO Box 9839, Canberra, ACT 2601

Department of Resources, Energy and Tourism

Minister for Resources and Energy: The Hon. Martin Ferguson, AM MP

Secretary: Mr Drew Clarke

Geoscience Australia

Chief Executive Officer: Dr Chris Pigram



© Commonwealth of Australia (Geoscience Australia) 2011

With the exception of the Commonwealth Coat of Arms and where otherwise noted, all material in this publication is provided under a Creative Commons Attribution 3.0 Australia Licence (<http://creativecommons.org/licenses/by/3.0/au/>)

Geoscience Australia has tried to make the information in this product as accurate as possible. However, it does not guarantee that the information is totally accurate or complete. Therefore, you should not solely rely on this information when making a commercial decision.

ISSN 1448-2177

ISBN 978-1-921954-51-1

GeoCat # 72805

Bibliographic reference: Przeslawski, R., Daniell, J., Anderson, T., Barrie, J.V., Heap, A., Hughes, M., Li, J., Potter, A., Radke, R., Siwabessy, J., Tran, M., Whiteway, T., Nichol, S. 2011. Seabed Habitats and Hazards of the Joseph Bonaparte Gulf and Timor Sea, Northern Australia. Geoscience Australia, Record 2011/40, 69pp.

Contents

List of Figures	iv
List of Tables.....	v
Executive Summary.....	vi
Acronyms	vii
Acknowledgements	viii
1. Introduction.....	1
2. Habitats & Communities	6
2.1 Regional Summary of Habitats & Communities	6
2.2 Habitat Classifications	8
2.3 Regional-scale Geomorphology.....	11
2.4 Local-Scale Geomorphology	14
2.5 Biophysical Characterisation of Geomorphic Features.....	18
2.5.1 Banks.....	20
2.5.2 Terraces	21
2.5.3 Ridges.....	22
2.5.4 Plains	23
2.5.5 Valleys.....	24
2.6 Distinctive Habitats & Communities	25
2.6.1 <i>Sponge, Infaunal, and Coral Communities</i>	25
2.6.2 <i>Pockmark Communities</i>	26
2.7 Significant Habitats & Communities	26
2.8 Relationship between Biology and the Environment.....	30
3. Potential Hazards.....	37
3.1 Slope Instability	39
3.2 Fluid and Gas Expulsion.....	40
3.3 Elevated features / Hard ground.....	43
3.4 Erosion at the Seabed.....	44
3.5 Oceanographic Hazards at the Sea Surface.....	45
4. Biophysical Processes & Conceptual Models	49
5. Conclusions	59
6. References	61
Appendix A: Data Sources.....	70
Appendix B: Spatial interpolation of gravel and mud content in the JBG-TS	72
Appendix C: Ecology.....	74
Appendix D: Geomorphology & Sedimentology.....	104
Appendix E: Geochemistry.....	108
Appendix F: Geophysics.....	119
Appendix G: Physical Oceanography.....	129
Appendix H: GIS Data.....	153
Instructions for the CD-ROM	156

List of Figures

1. Introduction.....	1
Figure 1.1: Petroleum industry activity in the Joseph Bonaparte Gulf and Timor Sea region.	2
Figure 1.2: Bioregionalisations for the JBG based on IMCRA 4.0	3
 2. Habitats & Communities	 6
Figure 2.1: Key broadscale geomorphic features and ocean circulation patterns within the JBG-TS and adjacent region for wet (January) and dry (July) seasons.	7
Figure 2.2: Maps of biodiversity have been developed for Australia based on data from (a-b) demersal fish, (c) brittlestars, and (d) tropical and sub-tropical sponges.....	9
Figure 2.3: A habitat classification system based on regional-scale derivations of seascapes from combined interpolation of seven environmental factors in the JBG-TS	10
Figure 2.4: Palaeo-shoreline maps from the JBG-TS, with time series indicated on the line graph..	12
Figure 2.5: Map of JBG-TS geomorphology in the region of interest based on Harris et al (2005) and Heap and Harris (2008).	13
Figure 2.6: Geomorphic features from GA-0322 and GA-0325 survey areas.	15
Figure 2.7: Geomorphic features from GA-0322 and GA-0325 survey area A.....	16
Figure 2.8: Geomorphic features from GA-0322 and GA-0325 survey area B.....	16
Figure 2.9: Geomorphic features from GA-0322 and GA-0325 survey area C.....	17
Figure 2.10: Geomorphic features from GA-0322 and GA-0325 survey area D.....	17
Figure 2.11: The number of (a) epifaunal and (b) infaunal species collected from the survey areas, classified by geomorphic feature type.	19
Figure 2.12: Representative images of banks.	20
Figure 2.13: Representative images of terraces	21
Figure 2.14: Representative images of ridges.....	22
Figure 2.15: Representative images of plains.....	23
Figure 2.16: Representative images of valleys.	24
Figure 2.17: Sponge and octocoral gardens occurred along raised features of the JBG-TS.....	27
Figure 2.18: Scleractinian (reef-forming) corals recorded from several stations on the GA-322 and GA-325 survey.....	28
Figure 2.19: Map of GA-0322 and GA-0325 survey areas including bathymetric depth overlaid with species richness of (a) epifauna and (b) infauna.	32
Figure 2.20: Backscatter image of areas A, B, C, and D. Video habitat classifications (coloured dots) shown are overlaid on backscatter.	34
Figure 2.21: The locations of sponge and octocoral gardens and reef-forming hard corals found during surveys GA-322 and GA-325.....	36
Figure 3.1: Map of potential geohazards and other sub-surface features as identified from sub-bottom profiles (SBPs) collected from surveys GA-322 and GA-325.....	38
Figure 3.2: Slope map of the Joseph Bonaparte Gulf at: (a) a regional scale based on the 250 m Bathymetry grid of Australia (Whiteway 2009) and (b) a local scale based on multibeam bathymetry of the eastern JBG carbonate banks from surveys GA-0322 and GA-0325.	39
 3. Potential Hazards.....	 37
Figure 3.3: Sub-bottom profile from Geoscience Australia survey GA-0325 (Area A) showing possible slope failures on the flank of a terrace located on the outer shelf of JBG-TS.....	40
Figure 3.4: Sub-bottom profile from Geoscience Australia survey GA-0325 (Area B) showing possible faulting adjacent to the edge of a carbonate bank on the outer shelf of JBG-TS.....	41
Figure 3.5: Locations of pockmarks in the JBG-TS from multibeam sonar surveys.....	42
Figure 3.6: Sub-bottom profiles from Geoscience Australia survey GA-0325 (Area D)	43
Figure 3.7: Map of bedforms distributions from Lees (1992) and modified using additional data from Royal Australian Navy charts 316 and 318.....	44

Figure 3.8: Map of Bedload transport Shield's parameter	45
Figure 3.9: Statistics for annual significant wave height, H_s in metres at difference percentiles and mean.....	46
Figure 3.10: Statistics for annual significant wave height, H_s in metres, for different seasons.	47
Figure 3.11: Example 11-year time series showing wave conditions from a location in the outer gulf; 11 ° S, 129 ° E.....	48
4. Conceptual Models.....	49
Figure 4.1: A generalised habitat map showing the potential distribution of habitats and biological communities in the JBG-TS	
Figure 4.2: A conceptual model showing the biophysical processes operating in the eastern JBG-TS across the shelf.	53
Figure 4.3: A conceptual model showing the biophysical processes operating in the JBG-TS along the shelf.	54
Figure 4.4: A conceptual model showing the biophysical processes operating in Area D.	55
Figure 4.5: A conceptual model showing the biophysical processes operating in Area C	56
Figure 4.6: A conceptual model showing the biophysical processes operating in Area B	57
Figure 4.7: A conceptual model showing the biophysical processes operating in Area A	58

List of Tables

2. Habitats & Communities	6
Table 2.1: Key geomorphic features in the vicinity of the JBG-TS. Refer to Figure 2.1 for the location of these features.	13
Table 2.2: Summary of key biophysical variables used to characterise geomorphic features identified from the GA-0322 and GA-0325 seabed mapping surveys. Calculations are based on the values recorded at sampling stations. SR = species richness (number of species).....	18
Table 2.3: Species identifications of reef-forming corals collected from GA-325 which are included on the IUCN Red List. Depth at Station 52 = 28.5 m and Station 55 = 31.4 m.....	29
Table 2.4: List of abiotic factors that were significantly related to biological factors.....	31
3. Potential Hazards.....	37
Table 3.1: A listing of cyclones between 1997 and 2008 that produced significant wave heights larger than 5 m in gulf waters. LCP = lowest central pressure (hPa); LWS = largest wind speed (10-minute average; knots). Information was compiled from the Australian Bureau of Meteorology and the Joint Typhoon warning Centre.	48

Executive Summary

The Joseph Bonaparte Gulf and Timor Sea region (JBG-TS) is an area of significance for multiple resource needs, from marine planning to offshore industry development. As such, information on seabed environments in this region is of interest to both industry and marine management. Geoscience Australia is focussed on the collation and preparation of regional pre-competitive environmental datasets, the outputs of which can be used for pre and post-bid environmental assessments and for emergency response planning.

This report provides a spatial synthesis of seabed environments for the Joseph Bonaparte Gulf and Timor Sea region (JBG-TS) by identifying and describing significant habitats, communities, and potential geohazards. Data are sourced from existing literature, including publicly available industry data, as well as data collected from two seabed mapping surveys to the Van Diemen Rise in the eastern Timor Sea (GA-322 during August-September 2009 and GA-325 during July – August 2010).

The JBG-TS is dominated by offshore gradients in habitat complexity and species richness, with habitat heterogeneity and epifaunal species richness increasing offshore and infaunal species richness decreasing offshore. Most of the seabed of the JBG is flat and comprises soft sediments with associated taxa such as prawns and small infauna. Isolated rocky reefs occur near headlands, and sand banks occur in the inner JBG. The outer JBG-TS is scattered with banks and palaeoreefs which provide habitat for sessile invertebrates and fish. The Van Diemen Rise comprises carbonate banks, terraces, ridges and valleys on which rich sponge and octocoral gardens occur.

Reef-forming hard corals are rare in the JBG-TS, with the exception of isolated nearshore coral reefs and mixed coral and sponge gardens on carbonate banks of the Van Diemen Rise. Protected marine species have been recorded from the JBG, but most of these are pelagics or migrants (e.g., sea turtles, cetaceans, seahorses, sea snakes, sharks) and so their distribution within the region is unpredictable and dynamic. Exceptions include several species of reef-forming hard corals from the banks of the Van Diemen Rise that are listed as vulnerable or endangered. No species associated with gas or fluid seepage were recorded, although sample identifications from GA-325 are still pending.

The primary geological hazards are mass movements caused by erosion of the banks and the presence of subsurface gas and fluid. Both processes are likely to be ongoing and could be a more significant hazard in areas where these processes interact together. Fluid and/or gas escape is inferred throughout the JBG-TS, with pockmarks and gas chimneys relatively common in the soft sediments of valleys and plains. The strong tidal currents of the JBG increase risk of erosion and mobilisation of seabed sediments, and these hazards are greatest in the inner JBG where bedload transport is highest and bedforms such as dunes and banks are common. Oceanographic hazards at the surface associated with wave conditions show an offshore gradient, with increasing wave height with distance from shore. The most significant wave heights occur in January and July; however cyclone season occurs from December to March during which wave heights can reach up to 8 m in the outer JBG.

This report synthesises pre-competitive environmental data for the Australian offshore oil and gas industry, thereby allowing industry to put proposed developmental plans in a regional context. In particular, this study uses regional-scale data (10-100s km) to identify broad spatial patterns and to develop conceptual models for the JBG-TS region (e.g., geomorphology, seascapes, wave heights). Nevertheless, results from surveys GA-322 and GA-325 indicate that significant habitats, communities, and hazards also exist at a local scale (1-10s km), too small to be detected in regional-scale analysis, thus highlighting the continued importance of acquiring high-resolution geophysical data and robust biogeophysical sampling.

Acronyms

ALA	Atlas of Living Australia, an online database
EEZ	Australia's Exclusive Economic Zone
EPBC Act 1999	Environmental Protection and Biodiversity Conservation Act 1999
IUCN	International Union for the Conservation of Nature
JBG	Joseph Bonaparte Gulf
JBG-TS	The Joseph Bonaparte Gulf-Timor Sea region, as defined in this study to include the Petrel sub-basin, Malita Graben, and Darwin Shelf
JPDA	Joint Petroleum Development Area, an area shared by Australia and Timor-Leste and designated by the <i>Timor Sea Treaty</i>
OBIS	Ocean Biogeographic Information System, an online database
NRSMPA	National Representative System of Marine Protected Areas
SBP	Sub-bottom profile
SEWPaC	Australian Commonwealth Department of Sustainability, Environment, Water, Populations and Communities
TS	Timor Sea

Acknowledgements

Surveys GA-322 and GA-325 were conducted in collaboration with the Australian Institute of Marine Science, and we are particularly grateful to all scientific and ship crew involved. The following taxonomic experts provided species identifications for this report: Dr Belinda Glasby for sponges (Museum and Art Gallery of the Northern Territory (MAGNT)), Dr Chris Glasby and Charlotte Watson for worms ((MAGNT), Dr Richard Willan for molluscs (MAGNT), Dr Tim O'Hara for ophiuroids (Museum of Victoria (MV)), Kate Naughton for crinoids (MV), and Dr Carden Wallace and Dr Paul Muir for hard corals (Museum of Tropical Queensland). Dr Matthew McArthur (GA) assisted with identification of infauna, and Suzanne Horner sorted and curated specimens at the MAGNT. Thanks to Tony Watson, Greg O'Connell, Matthew Brown, Janice Trafford, Liz Webber, Bill Pappas and Billie Poignand for the provision and/or assistance with laboratory analyses (all at GA). The isotope analyses were undertaken at Environmental Isotopes Pty Ltd (Sydney). Shoaib Burq and Brad Cook (GA) prepared and provided some of the datasets for spatial interpolation. Dr Dianne Edwards (GA) provided advice on geological basins. Dr Peter Harris and Alfredo Chirinos provided valuable comments on this report prior to publication. This record is published with permission of the Chief Executive Officer of Geoscience Australia.

1. Introduction

1.1 BACKGROUND

The need to improve transparency and efficiency in the legislation guiding petroleum activities in Australian waters was highlighted in a review of the *Environmental Protection and Biodiversity Conservation Act* (EPBC) (Hawke 2009) and of the *Regulatory Burden on the Upstream Petroleum (Oil and Gas) Sector* (Productivity Commission 2009). The collation, management and distribution of environmental data was one area that was specifically identified as requiring modification in order to improve data submission processes and availability of data for both industry and government. In particular, it was recommended that pre-competitive environmental data should be collected by the Government and distributed by a central agency (Productivity Commission 2009) and that a landscape-scale approach to the collation of regional baseline datasets should be used (Hawke 2009). More recently, the Montara Commission of Inquiry produced its final report into the Montara oil spill of 2010, in which it identified that scientific and environmental data should be used to provide baseline information against which impact assessments could be made (Borthwick 2010).

Geoscience Australia is focussed on the collation and preparation of regional pre-competitive environmental datasets, the outputs of which can be used for pre and post-bid environmental assessments and for emergency response planning and assessments. The datasets and associated analyses presented in this report provide a spatial synthesis of seabed environments for the Joseph Bonaparte Gulf and Timor Sea region (JBG-TS).

The JBG-TS is an area of interest for multiple resource needs, from marine planning to offshore industry development. Petroleum industry interests are based on the high resource potential of the region, with hydrocarbon families and their purported source rocks occurring throughout the Bonaparte Basin (Bishop 1999; GA 2010; Logan et al. 2010; Zabanbark 2010). The first gas and oil-gas fields were discovered in 1970, and by 2010 approximately 100 wells had yielded more than 20 gas, oil and gas condensate fields (Zabanbark 2010). The JBG-TS is an area of active petroleum exploration and infrastructure development with existing gas and oil fields, pipelines, and ongoing acreage releases (GA 2010; [Figure 1.1](#)). In addition, the region is also the focus of interest for carbon capture and storage (CCS), with the first acreage release areas for CCS released in 2009 (www.ret.gov.au/resources/Documents/ccs/08-3465-11_Petrel_GHG_2009.pdf). As such, there is a need for regional pre-competitive datasets and syntheses such as the ones provided in this report.

In addition to industry, the JBG-TS is also of interest for the development of marine protected areas (MPAs) by the Department of Sustainability, Environment, Water, Population and Communities (SEWPaC). As part of the northern bioregion, the JBG-TS has been identified as a target of environmental research in order to identify gaps in our understanding of biodiversity across northern Australia (e.g., the National Environmental Research Program of SEWPaC). In addition, a large proportion of the JBG-TS has been included in the proposed Commonwealth marine reserve network as of October 2011 ([Figure 1.2](#)). These proposed reserves will form part of the National Representative System of Marine Protected Areas (NRSMPA) (DEWHA 2009; DEWHA 2010). Development and monitoring of the NRSMPA will require knowledge of existing biodiversity patterns, location of significant habitats and communities, and the potential to predict these habitats and communities when data are limited.

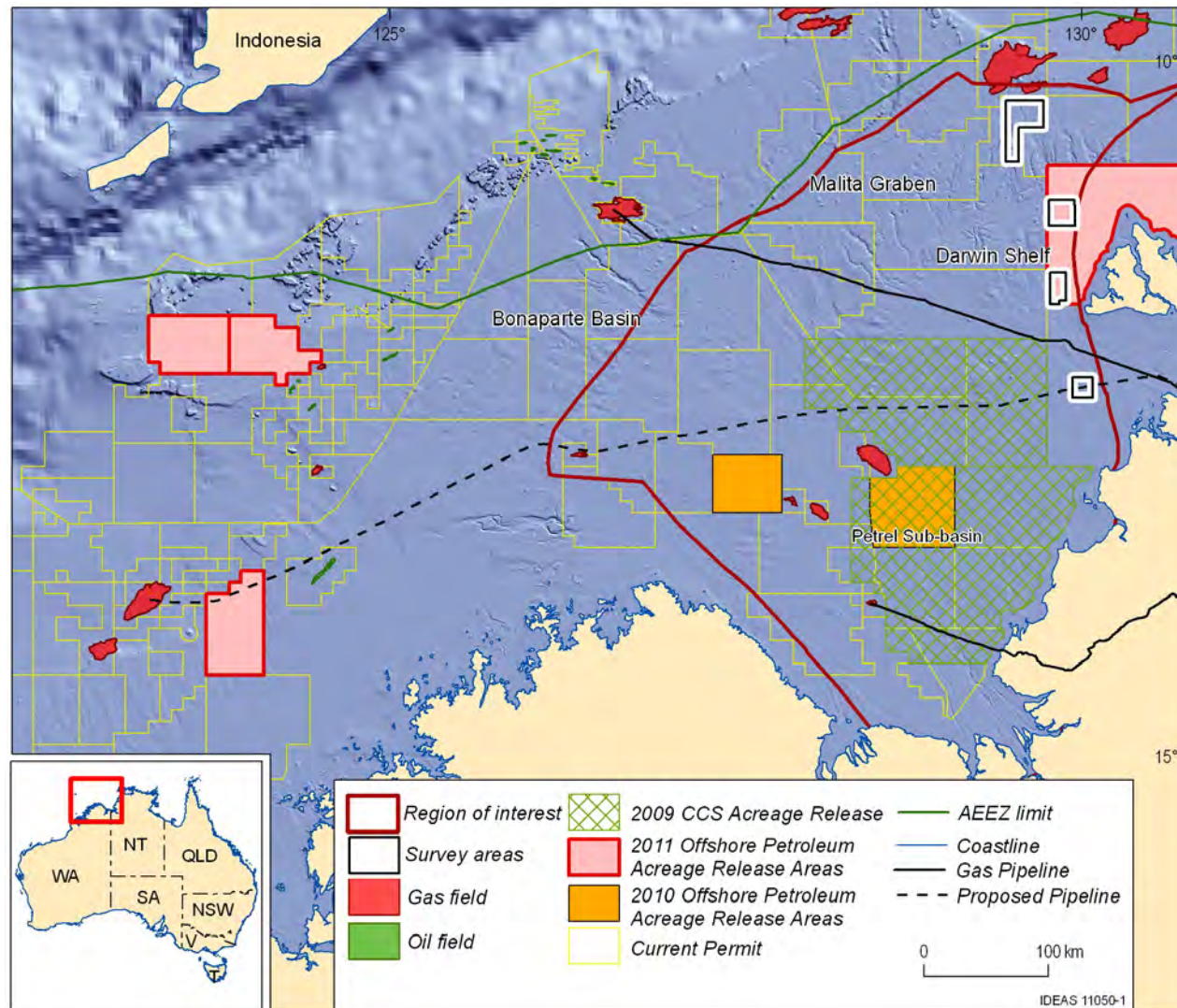


Figure 1.1: Petroleum industry activity in the Joseph Bonaparte Gulf and Timor Sea region.

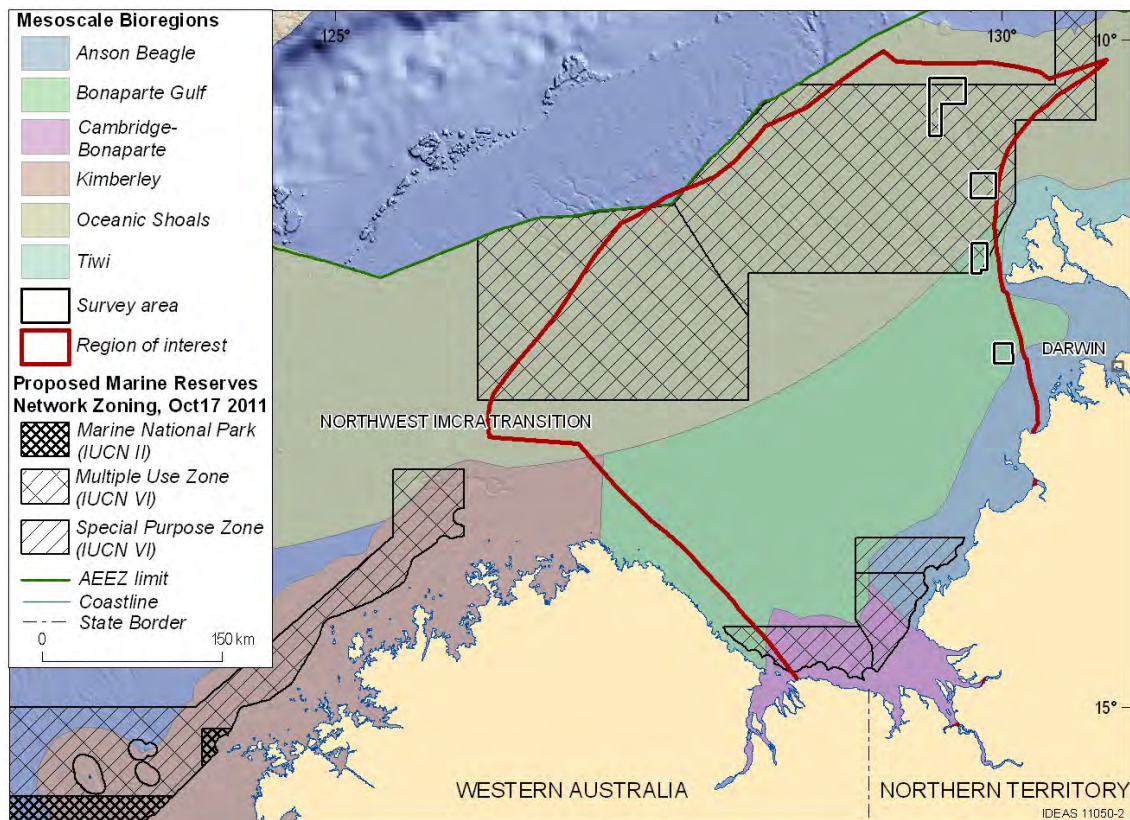


Figure 1.2: Marine protected area interest in the Joseph Bonaparte Gulf and Timor Sea region. Bioregionalisations are based on IMCRA 4.0; capital letters denote the provincial bioregion.

1.2 DEFINITION OF REGION OF INTEREST

The region of interest in the JBG-TS was restricted to three geologically distinct structures: the Petrel sub-basin, Darwin Shelf, and Malita Graben (Figure 1.3). The Petrel sub-basin was included because it encompasses most of the JBG and adjacent Timor Sea, and the Malita Graben and Darwin Shelf were chosen because they encompass the areas of the two main surveys used in this report. Geological structures were used to delineate the region of interest for the following reasons: 1) Clear boundaries were objectively identified. In contrast, the boundaries would have been subjective due to poor data coverage if we had used biological communities or habitats to define our region of interest (e.g., based on *Halimeda* beds or coral reefs as per Heyward et al. (1997)); 2) The boundaries as specified above all lie within Australia's exclusive economic zone (EEZ) and do not include the Joint Petroleum Development Area shared with Timor-Leste; 3) The region of interest includes a range of geomorphic features, thereby allowing for the inclusion of representative habitats; and 4) The boundaries seem to segregate based on the known differences in biological communities from the *Halimeda* and coral dominated banks for the west (Heyward et al. 1997) to the sponge dominated banks of the east (Anderson et al. 2011a; Heap et al. 2010).

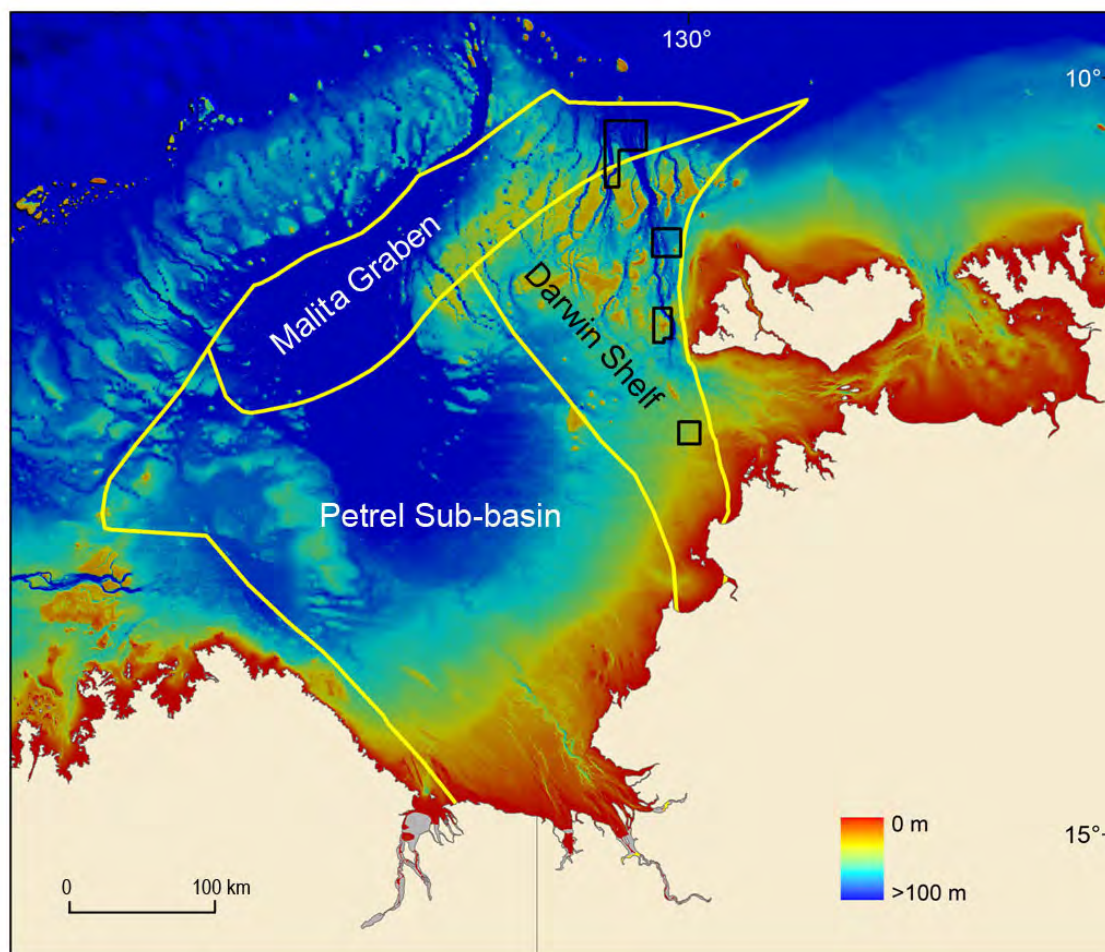


Figure 1.3: The main geological basins used to define the region of interest in this report overlaid on regional-scale bathymetry. . Yellow lines indicate basin boundaries, and black lines show GA-322 and GA-325 survey areas.

1.3 OBJECTIVES & DATA SOURCES

The objectives of this report are to identify and describe significant habitats, communities, and potential geohazards using available environmental data. This includes data from publications, industry and Geoscience Australia’s marine surveys. As part of the Australian Government’s program of collecting pre-competitive regional information on seabed habitats, Geoscience Australia recently collaborated with the Australian Institute of Marine Science to conduct two surveys within four study areas along a representative valley of the Van Diemen Rise in the Joseph Bonaparte Gulf: GA-0322 in 2009 (Heap et al. 2010) and GA-0325 in 2010 (Anderson et al. 2011a). A range of methods was used to collect physical and biological data including multibeam sonar, towed underwater video, oceanographic moorings, sediment sampling, and epibenthic sampling ([Appendix A](#)). At the time of writing, data were not available directly from industry for inclusion in this report. Nonetheless, some industry data has been publicly released in reports ([Appendix A](#)), and these are used wherever possible in conjunction with survey data to provide a regional context.

The main body of this report includes summarised findings related to the overall aim of synthesising environmental data for the JBG-TS. Detailed methods and analyses underlying these results can be found in discipline-specific appendices at the end of the report. Unless otherwise stated, all analyses are based on data from marine surveys GA-0322 and GA-0325 in the northeastern JBG-TS.

An assessment of the environmental impacts of specific industry activities is outside the scope of this report. Lavering (1994) provides some discussion of the potential for environmental disturbance due to ongoing petroleum exploration and infrastructure development in the JBG. In addition, this report focuses on offshore areas of the JBG-TS. Information on subtidal, intertidal, mangrove, and estuarine habitats can be found in Clarke et al. (2001), Metcalfe and Glasby (2008), Smit et al. (2000) and WEL (2004).

2. Habitats & Communities

2.1 REGIONAL SUMMARY OF HABITATS & COMMUNITIES

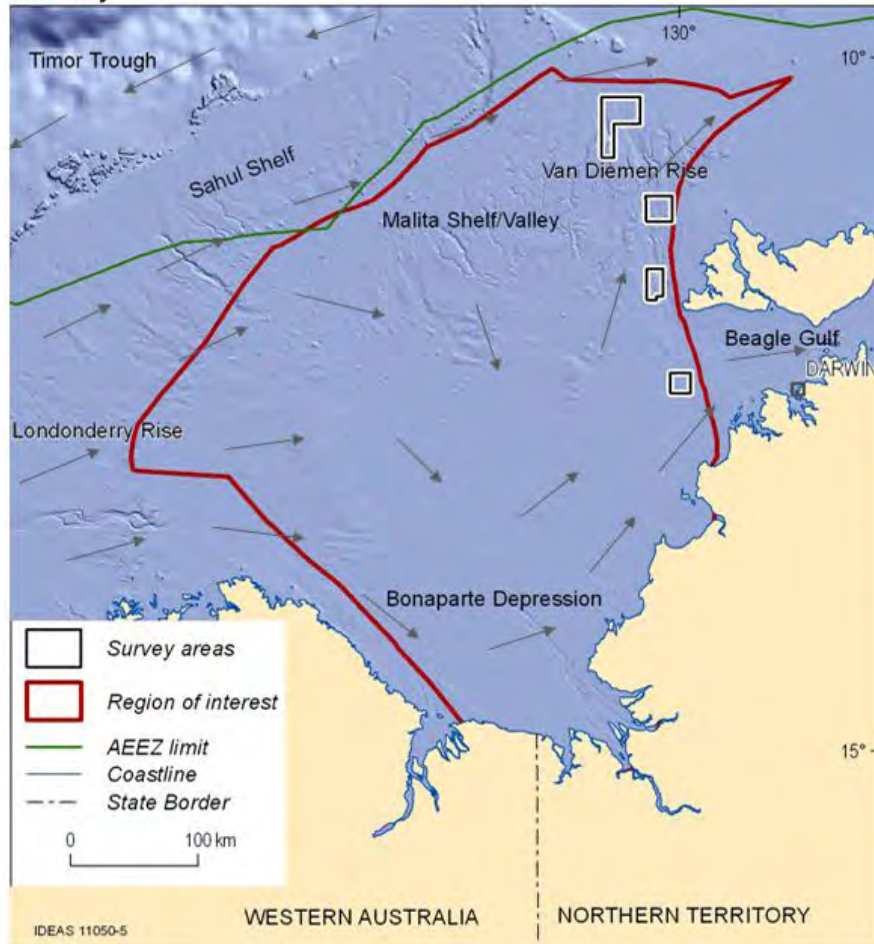
Several detailed studies have been conducted on seabed habitats and biological communities of regions to the northwest of JBG-TS (e.g., Big Banks in Heyward et al. (1997), Sahul Shelf in Wienberg et al. (2010)) and the east (e.g., Gulf of Carpentaria in Post (2008), Arafura Sea in Wilson (2006)). In contrast, very little is known about biodiversity patterns and habitat types for most of the JBG-TS, and this region has been recognised as an area of limited biological data (Hooper & Ekins 2004; Last et al. 2005; WEL 2001). Nevertheless, some regional trends of habitat availability and biodiversity can be inferred from existing studies.

The Joseph Bonaparte Gulf is an extensive, shallow (generally < 100 m) carbonate-dominated margin adjacent to the Sahul Shelf. The platform is one of the widest in the world, measuring 1,170 km from the southern shorelines of the gulf to the edge of the shelf (Lees 1992). The northwestern margin of the shelf/slope drops off into the Timor Trough (~3,000 m). The western boundary of the Gulf joins with the Indian Ocean, while the northern boundary joins with the Timor Sea. The Joseph Bonaparte Gulf receives significant loads of sediment from the numerous rivers in the region (Lees 1992), and is dominated by tidal and wind-driven currents according to the season (Figure 2.1).

The JBG is an area of soft substrate expanses with localised rocky outcrops, gravel deposits, and raised features (URS 2009; WEL 2001). Some areas contain high densities of pockmarks and sand waves, and calcarenite subcrops occur in the far northwest in an 11 km wide palaeo-channel (URS 2009). Benthic communities are exposed to strong tidal currents, high turbidity, and substantial sediment mobility, with disturbance decreasing offshore. High turbidity exists in the inner JBG, particularly during the wet season, with peak turbidity recorded 3 km from the coast, and much lower levels recorded ~ 30 km offshore (WEL 2004). The area also has high tidal variation year-round, with currents as high as 1.4 ms^{-1} predicted in 18 m water depth during severe cyclone conditions (WNI 2004 cited in WEL (2004)).

The epibenthos over most of the JBG is sparse (URS 2009; WEL 2004), although rocky outcrops in the far northwest support high abundances of epibenthic fauna, particularly crinoids (URS 2009). Although some scattered islands, reefs and other raised features in the inner JBG may support corals, macroalgae, and seagrass (e.g. King Shoals, Medusa Banks, Howland Shoals, Emu Reefs) (RPS 2009), the occurrence of these communities is much sparser than the dense assemblages of sessile invertebrates recorded in the far northwestern JBG (URS 2009) and neighbouring areas (e.g., Big Banks in Heyward et al. (1997), Sahul Shelf in Wienberg et al. (2010)). Previous surveys in the JBG have returned no seagrass or macroalgae beyond coastal habitats and only isolated hard corals (ENI 2005; LDM 1994; WEL 2004). Seabed sediments support these findings, with an absence of colonial corals, *Halimeda*, large foraminifera or coralline algae (Clarke et al. 2001). Similarly, species composition of bycatch from the prawn fishery is distinctly different from that of other tropical regions in northern Australia (Tonks et al. 2008), indicating that the biota in the inner JBG differs from the biota from other areas in the Timor Sea (Heyward et al. 1997; Van Andel & Veevers 1967). Prawns represent one of the dominant epifauna of the soft sediment expanses, while diverse infaunal communities are dominated by polychaetes and other crustaceans (WEL 2001).

January



July

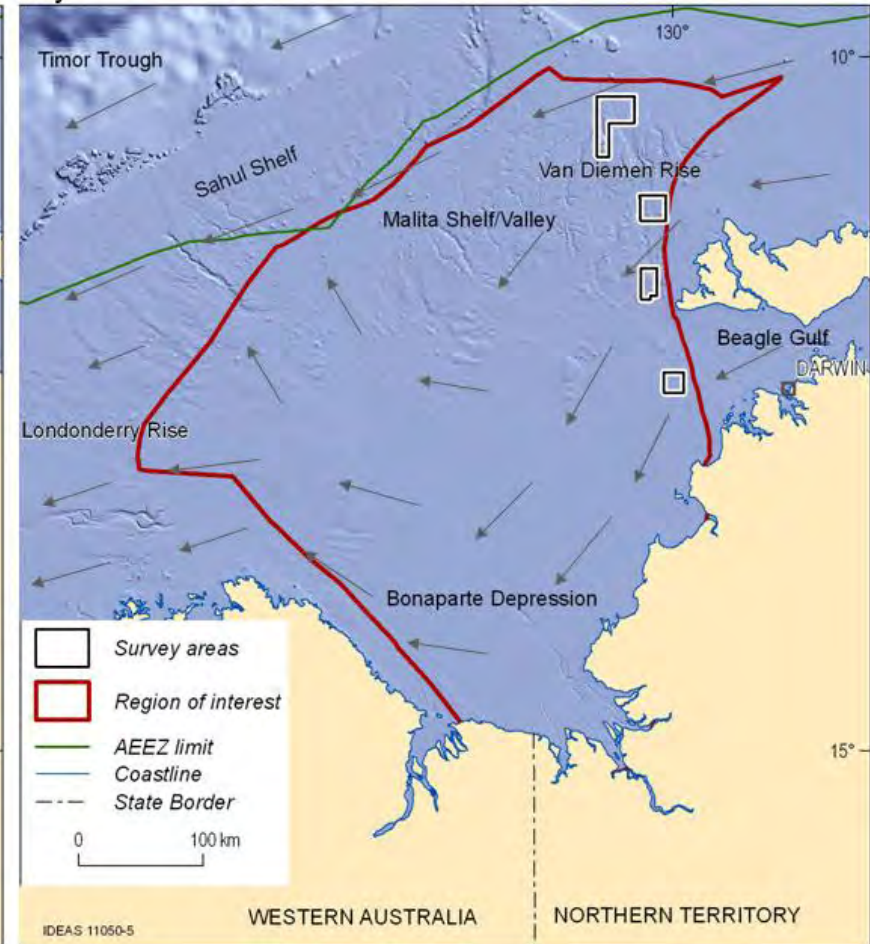


Figure 2.1: Key broadscale geomorphic features and ocean circulation patterns within the JBG-TS and adjacent region for wet (January) and dry (July) seasons. Arrows represent indicative wind-driven circulation and only show direction not magnitude of currents (after Condie, 2011).

Outside of the gulf in the northwest JBG-TS, elongate palaeoreefs rise from the surrounding flat seabed (~ 20 – 35 metres above surrounding seabed), the largest recorded of which is approximately 1.2 km² (George & Cauquill 2010). The palaeoreefs are covered with a layer of unconsolidated sediment and are no longer actively growing, with gorgonians being the main sessile organism (George & Cauquill 2010). Epifaunal diversity is highest at the summit of palaeoreefs, with little observed elsewhere. Available bathymetric data indicate that palaeoreefs are more abundant further offshore.

In the northeast JBG-TS, the carbonate banks and associated valleys of the Van Diemen Rise provide more habitat heterogeneity than the proper JBG. Epifaunal diversity is therefore much higher here than in the JBG. Recent marine surveys GA-322 and GA-325 have provided additional information on biophysical patterns in this part of the region, and this is explored in more detail in [Sections 2.4 – 2.5](#).

2.2 HABITAT CLASSIFICATIONS

The JBG-TS region has been included in several continental-scale habitat classifications. The most recent Commonwealth bioregionalisation (IMCRA 4.0) places most of the JBG into a single provincial bioregion called the Northwest IMCRA Transition (Commonwealth of Australia 2005) ([Figure 1.2](#)), indicating that the JBG is a distinctive region at a continental scale. IMCRA Transition provinces are regions of overlap between core centres of demersal fish endemism (Last et al. 2005). As such the JBG and surrounding region may provide an important habitat for both northwest and northern taxa. IMCRA further classifies Australia's marine region into smaller meso-scale bioregions, of which five overlap the JBG-TS ([Figure 1.2](#)).

Maps exist that provide measures of biodiversity of demersal fish (Dunstan & Foster 2010; Last et al. 2005), sponges (Hooper & Ekins 2004), and brittlestars (O'Hara 2008) ([Figure 2.2](#)). A potential hotspot of sponge biodiversity occurs near the far northwest of the JBG-TS near the Tiwi Islands (Hooper & Ekins 2004) ([Figure 2.2c](#)). However based on demersal fish data, most areas in the JBG-TS represent assemblages of the most common species richness and evenness measures in the Northern Marine Region (Dunstan & Foster 2010) ([Figure 2.2d](#)). Although valuable at a regional scale (100s km), the limited biological data for much of the region has precluded interpolations at a finer resolution, which is needed to identify potentially significant habitats and communities at a local scale (10s km).

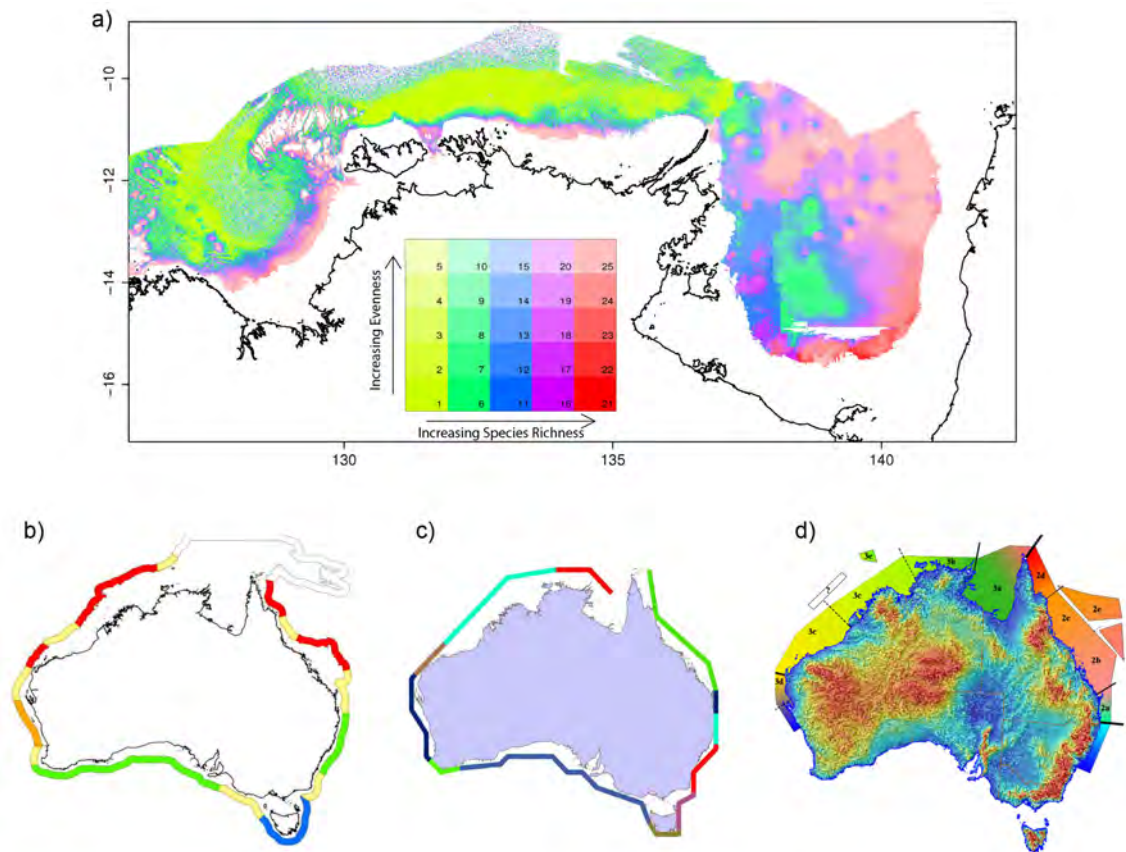


Figure 2.2: Maps of biodiversity have been developed for Australia based on data from (a-b) demersal fish, (c) brittlestars, and (d) tropical and sub-tropical sponges. Each colour denotes a distinct measure of biodiversity based on the associated data. The thickness of the lines in (d) represents uncertainty in differentiation between zones, with solid lines denoting high confidence and dotted lines denoting high uncertainty. Numbers in (d) indicate provinces, and letters indicate transitions within a province. Maps are from Dunstan and Foster 2010, Last et al. 2005, O'Hara 2008, and Hooper and Ekins, 2004, respectively.

Seascapes

Geoscience Australia derived a regional-scale habitat classification in which interpolated environmental variables were combined to produce seascapes, each of which represents a distinct benthic habitat within the JBG-TS (methods detailed in Heap et al. (2011)). The seascapes classification has been undertaken at the regional scale only because a number of the key datasets are available only at a large cell size (0.01 decimal degrees) which precludes derivation of seascapes at the local scale of surveys GA-322 and GA-325. The seascape classification used here includes several updated data layers compared to previous seascape classifications (Heap et al. 2011): new interpolations of seabed exposure (parameter R in Hughes et al. (2010)), mud content, and gravel content (details in Li et al. (2010), [Appendix B](#)), all of which are available in [Appendix H](#). This regional-scale seascape derivation yielded five classes, each of which represents discrete benthic environments ([Figure 2.3a](#)):

- Seascape 1 is characterized by comparatively deep cool waters and very low exposure;
- Seascape 2 is characterized by comparatively low exposure;
- Seascape 3 is characterized by comparatively moderate conditions;
- Seascape 4 is characterized by comparatively high exposure and high primary production;

- Seascape 5 is characterized by comparatively shallow warm waters, gravelly sediments, very high exposure and very high primary production.

Seascapes show an offshore gradient, with Seascape 1 furthest offshore in deeper water and Seascape 5 closest to shore (Figure 2.3a). An exception to this is the northeastern part of the JBG-TS which showed more similarity to nearshore areas, likely due to the proximity of the Tiwi Islands (Figure 2.3a).

Based on the number of different seascapes within a 25-cell radius, a focal variety index was derived to map the habitat complexity in the region. The eastern JBG-TS has a higher habitat heterogeneity than the western JBG-TS, and highest levels of habitat heterogeneity occur along the Van Diemen Rise and along the coast southwest of Darwin (Figure 2.3b).

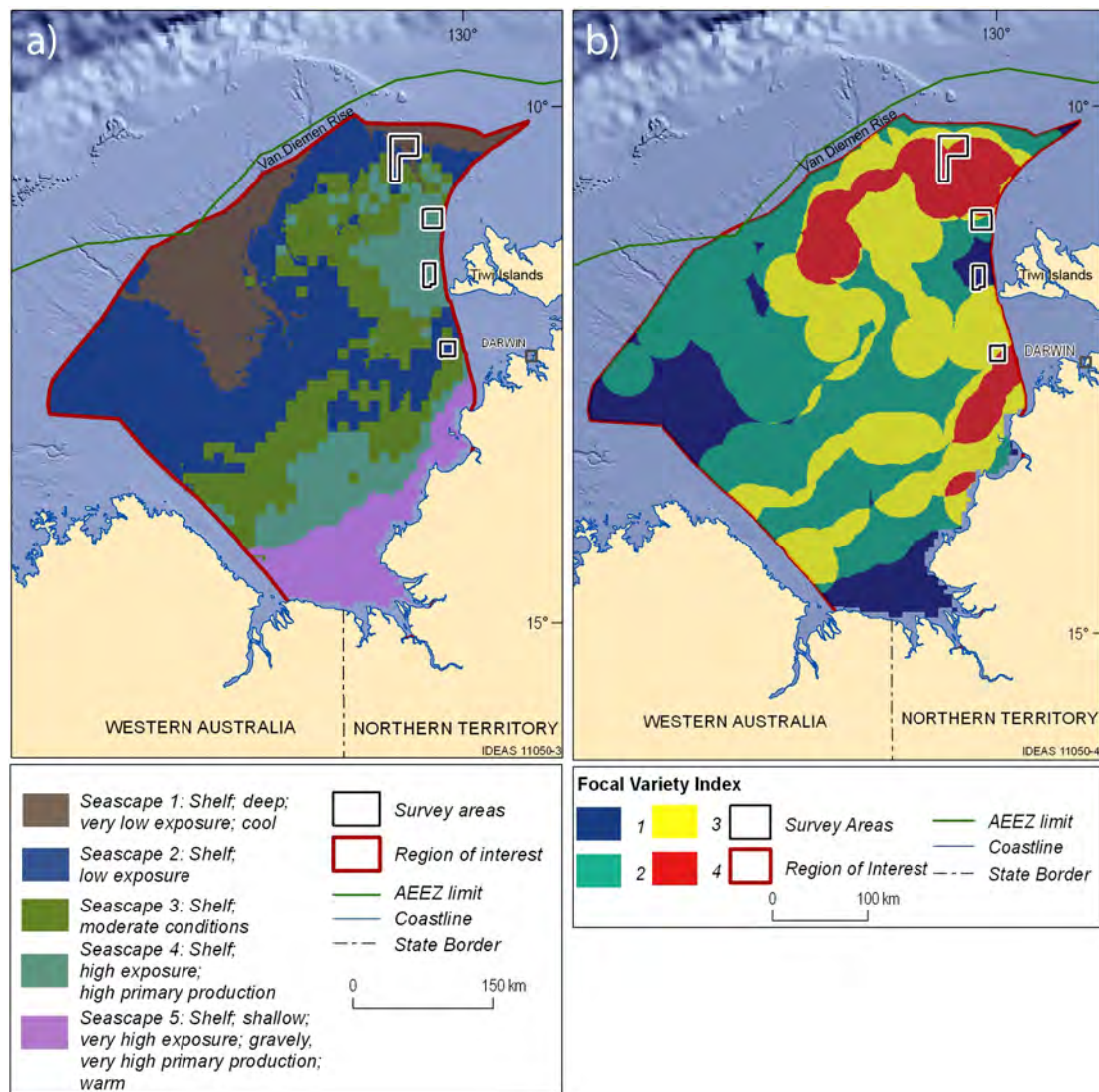


Figure 2.3: A habitat classification system based on regional-scale derivations of seascapes from combined interpolation of seven environmental factors in the JBG-TS: a) Each of the five seascapes in the JBG- represents a distinct habitat. The pronounced pixelation in the southern and eastern JBG-TS is due to the influence of seabed exposure which was available at a coarser resolution than other data layers and exerted more influence in this part of the JBG-TS; b) A focal variety index derived from the seascape map indicates habitat heterogeneity. Increasing numbers indicate increasing habitat heterogeneity.

In order to determine whether these seascapes reflect biological patterns at the local scale (10s km), seascapes were compared with biological data from surveys GA-322 and GA-325. Seascapes were associated with different levels of species richness and species composition. Specifically, Seascape 1 had the lowest infaunal species richness, and Seascape 4 had the highest epifaunal species richness (NB: Seascape 5 was not included in this analysis, as survey stations did not include this classification). See [Appendix C](#) for details. These results indicate that these regional-scale seascapes reflect biological patterns at a local scale, but the strength of these relationships varies according to individual seascapes and biological data, as has previously been found (Heap et al. 2011; Przeslawski et al. 2011).

2.3 REGIONAL-SCALE GEOMORPHOLOGY

The geomorphology of the JBG-TS has been influenced by sea level rise on a geological timescale. The modern bathymetry of the JBG-TS can be used to model inundation due to sea-level rise since the last glacial maximum approximately 18,000 years ago. At this time, the region was characterized by a semi-enclosed body of brackish water located in the current outer JBG, a region currently known as the Bonaparte Depression ([Figure 2.4](#)) (Yokoyama et al. 2001). As the sea level rose, the JBG opened to the Timor Sea, and a peninsula formed approximately 12,000 years ago where the Van Diemen Rise currently exists ([Figure 2.4](#)). Further sea level rise resulted in inundation of most parts of the JBG-TS, until the present sea level approximately 6000 years ago ([Figure 2.4](#)). The rising sea level likely drowned existing coral reefs, as confirmed by large quantities of coral rubble collected from survey GA-325 at 90 m (See [section 2.7](#) and [Figure 2.21](#)). These drowned reefs now provide habitat for the modern biota of the JBG-TS.

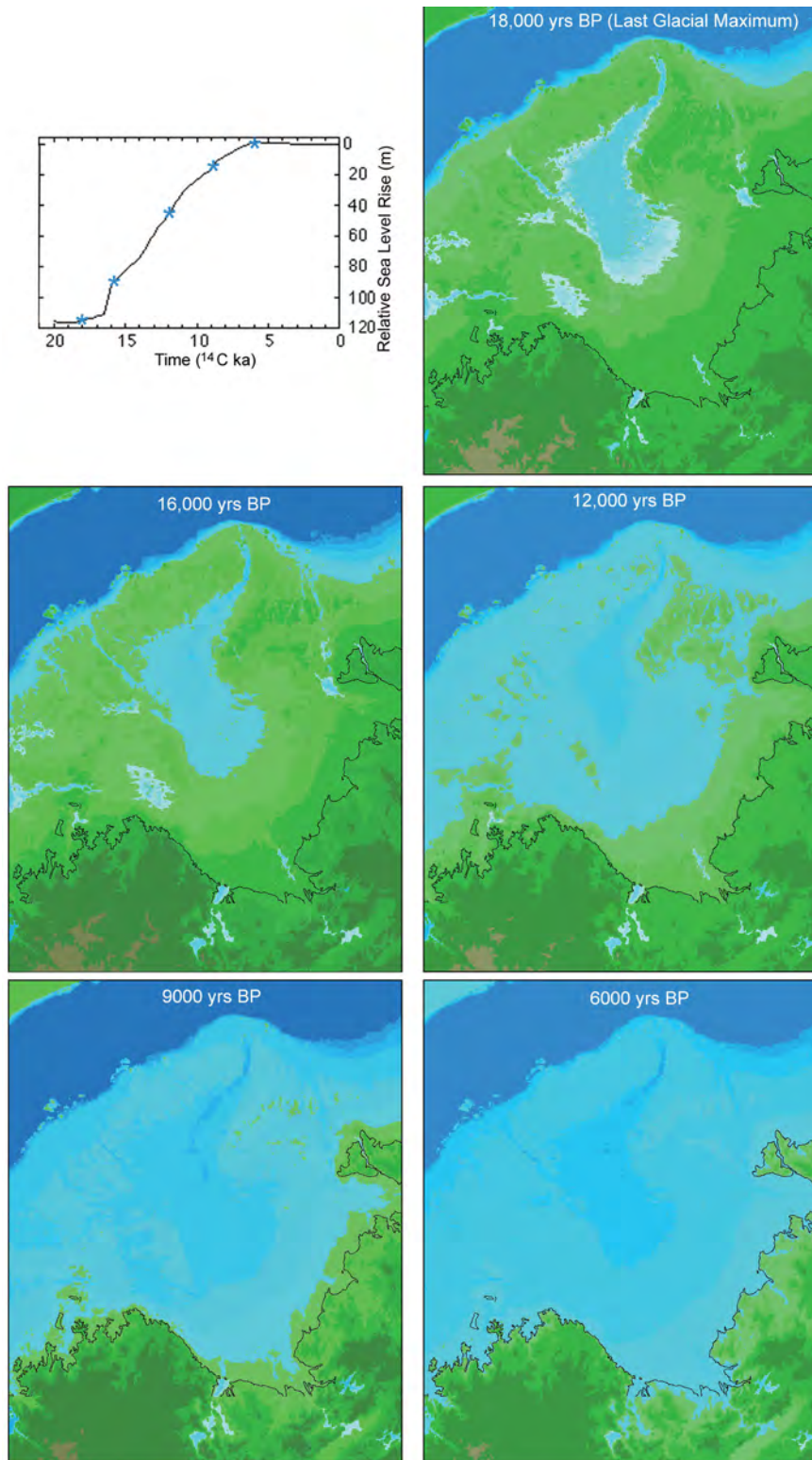


Figure 2.4: Palaeo-shoreline maps from the JBG-TS, with time series indicated on the line graph. The thin black line indicates the modern coastline. Ages are approximated based on radioactive carbon dating (^{14}C year BP). This figure is modified from (Yokoyama et al. 2001) and used with permission from Y. Yokohama.

The geomorphology of the JBG region is complex and consists of rises, depressions, banks, terraces and channels (Van Andel & Veevers 1967) (Table 2.1). Of particular interest are the submerged carbonate banks which may have developed over active hydrocarbon seeps (Heyward et al. 1997; Hovland et al. 1994; O'Brien & Glenn 2005). These banks flank the Bonaparte Depression and the Malita Valley. The banks are generally <10 km² in area with flat tops and contain steep slopes of up to 33° (Van Andel & Veevers 1967).

Table 2.1: Key geomorphic features in the vicinity of the JBG-TS. Refer to Figure 2.1 for the location of these features.

GEOMORPHIC FEATURE		
NAME	TYPE	REFERENCE
Bonaparte Depression	Valley	Lees (1992); van Andel & Veevers (1967)
Timor Trough	Trench	Veevers et al., (1978)
Malita Shelf/Valley	Valley	Lees (1992); van Andel & Veevers (1967)
Londonderry Rise	Bank	van Andel & Veevers (1967)
Sahul Shelf	Shelf	van Andel & Veevers (1967)
Van Diemen Rise	Bank	van Andel & Veevers (1967)

Based on a national-scale geomorphic classification of the Australian EEZ (Harris et al. 2005), the JBG-TS includes 10 geomorphic features, with the inner JBG comprising mostly shelf, the outer JBG comprising basin, and the outer JBG-TS comprising banks and terraces separated by deep/hole/valley features (Figure 2.5). See Appendix D for comparative areas of each feature in the JBG-TS. Each geomorphic feature is associated with particular environmental factors (e.g., depth, substrate) (Heap & Harris 2008). As such, geomorphology may be a suitable surrogate for biological communities (Anderson et al. 2011b). This premise is explored further in Section 2.5.

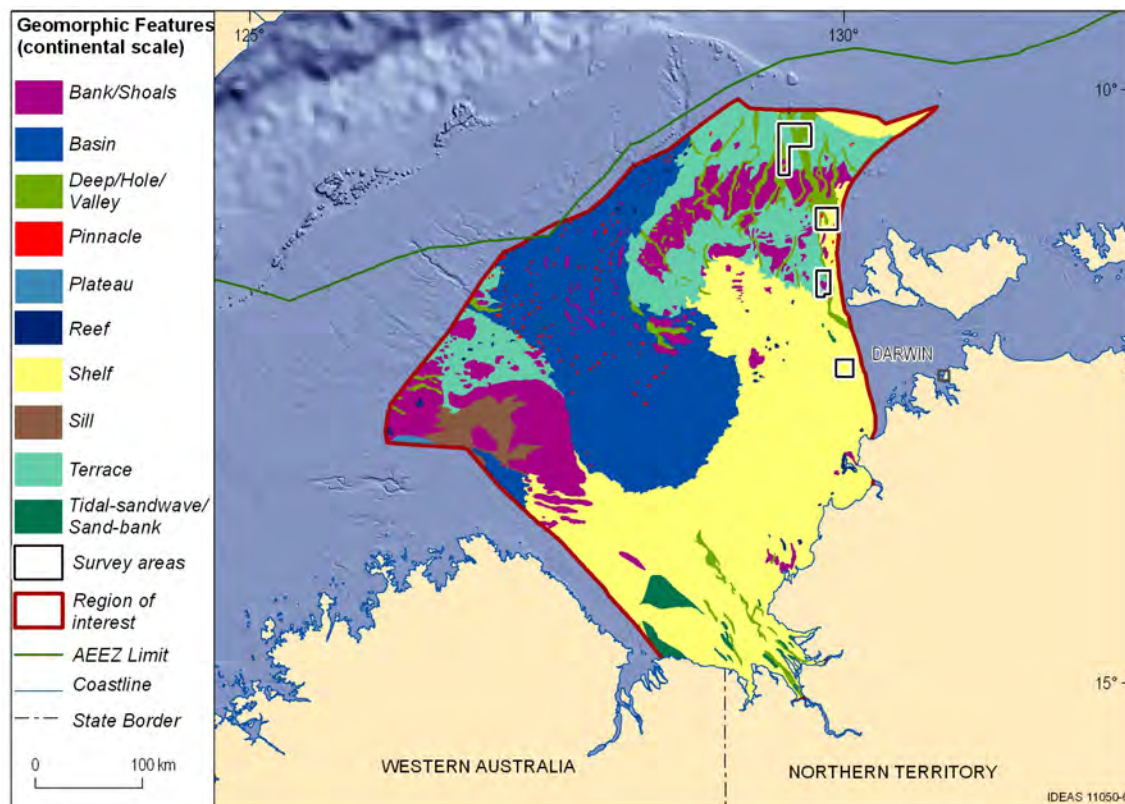


Figure 2.5: Map of JBG-TS geomorphology in the region of interest based on Harris et al (2005) and Heap and Harris (2008).

2.4 LOCAL-SCALE GEOMORPHOLOGY

High-resolution bathymetric grids were obtained from surveys GA-0322 and GA-0325 in four study areas (A, B, C, and D). Using this data, geomorphic features in the northwest JBG-TS were mapped at a local scale to provide a more detailed understanding of geomorphology in the area ([Figure 2.6](#); [Appendix D](#)). Within the four survey areas, six geomorphic features were observed based on definitions from Heap and Harris (2008): 1) Banks - local or regional areas of elevated seafloor with one or more steep sides; 2) Terraces - relatively flat or gently sloping seafloor with a moderately steep rise on one side and a moderately steep drop on the other side; 3) Plains - extensive, flat, gently sloping or nearly level; 4) Valleys - tapered depressions on the shelf characterised by laterally converging contours of increasing depth; 5) Ridges - long, narrow elevation with steep sides; and 6) Scarps - elongated and comparatively steep slope separating more gently sloping areas.

All four survey areas are consistent with the regional geomorphology; for example, numerous banks and terraces are dissected by deep channels on the outer shelf of the Van Diemen Rise in Area A ([Figure 2.6](#)). The inner shelf of Area D differs from the other three areas by having comparatively little relief (~20 m overall), with shallow channels eroded into an extensive plain ([Figure 2.10](#)). The other three survey areas are characterised by deeply incised valleys and considerably high relief (up to 100 m). Pockmarks occur in areas A, C, and D, most extensively in A and D ([Figure 2.7](#), [Figure 2.9](#), [Figure 2.10](#)). They occur generally in the valleys and plains where sediments have accumulated (i.e., away from hard substrates and scour zones). See [Section 3.2](#) for further information on pockmarks.

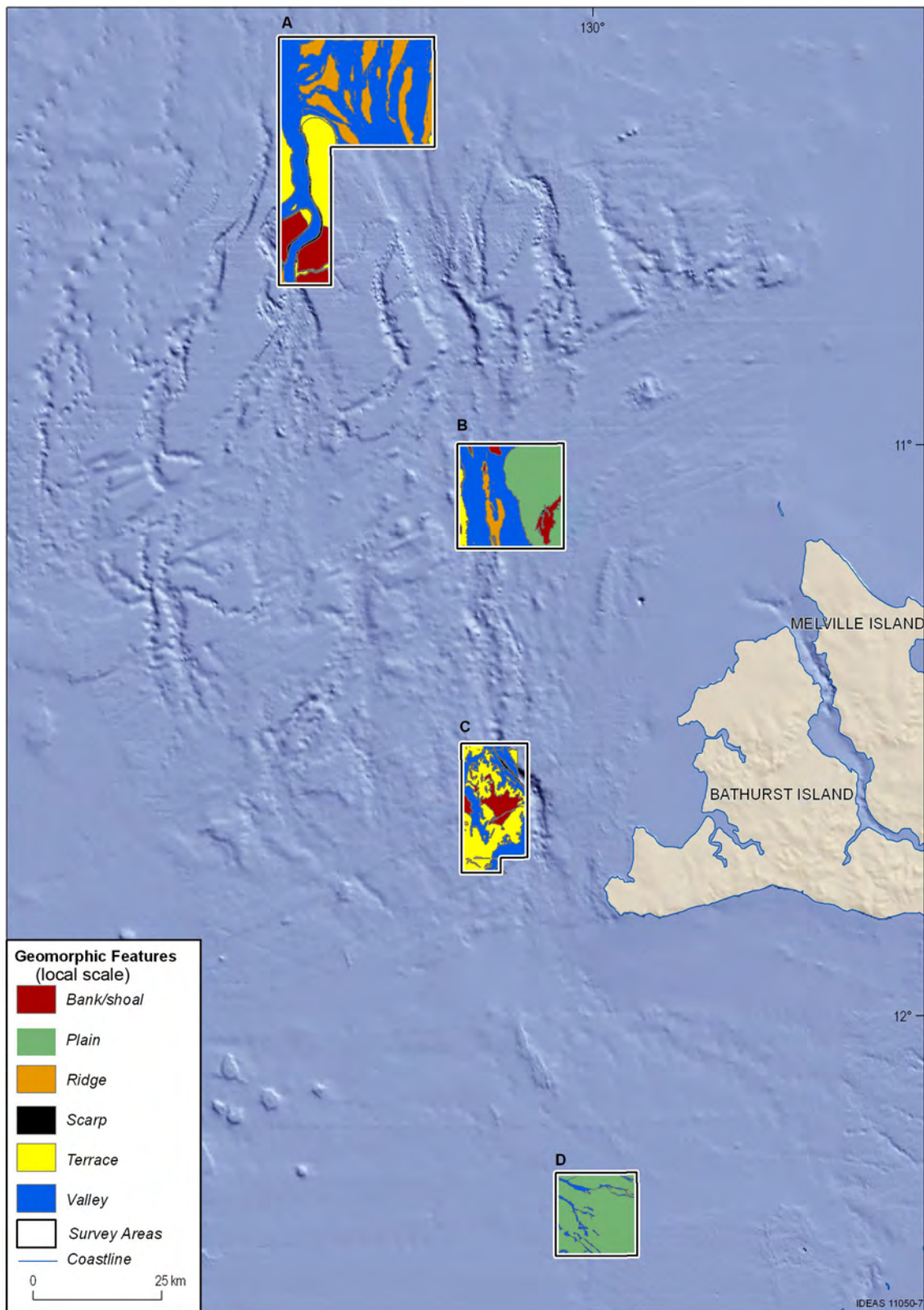


Figure 2.6: Geomorphic features from GA-0322 and GA-0325 survey areas. Letters indicate study areas. The underlying image is a 250 m bathymetric grid detailed in Whiteway (2009).

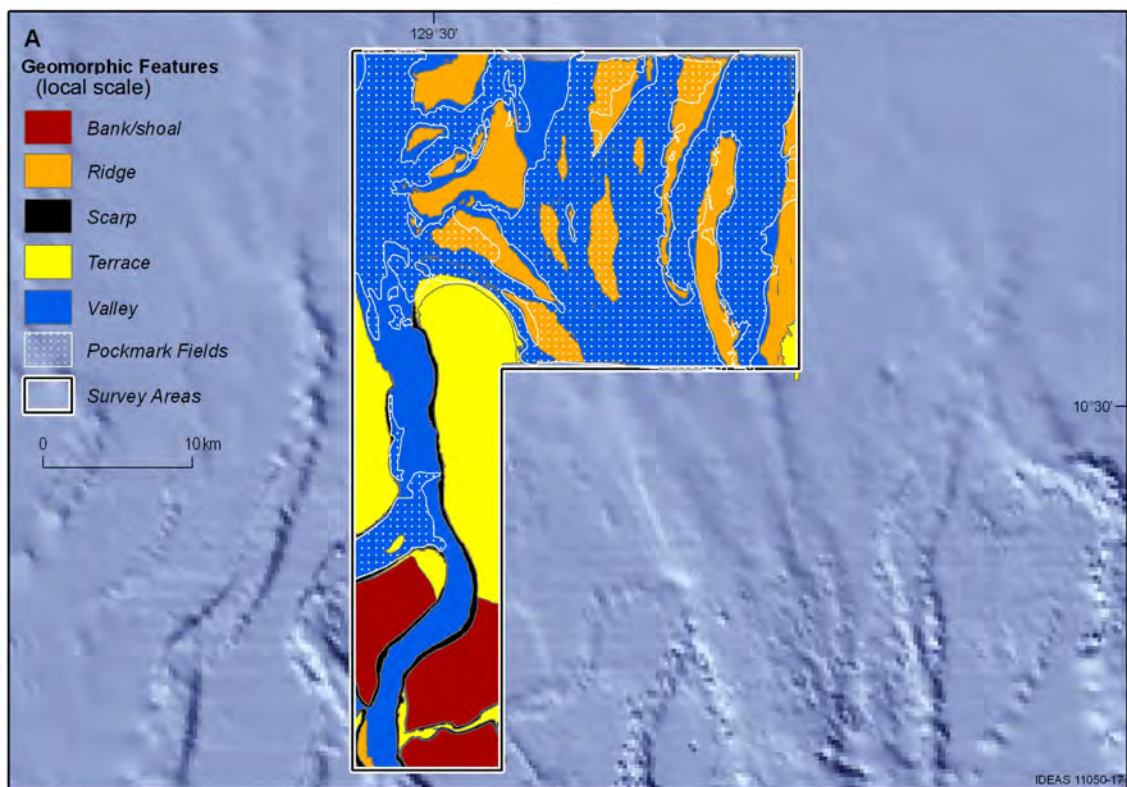


Figure 2.7: Geomorphic features from GA-0322 and GA-0325 survey area A.

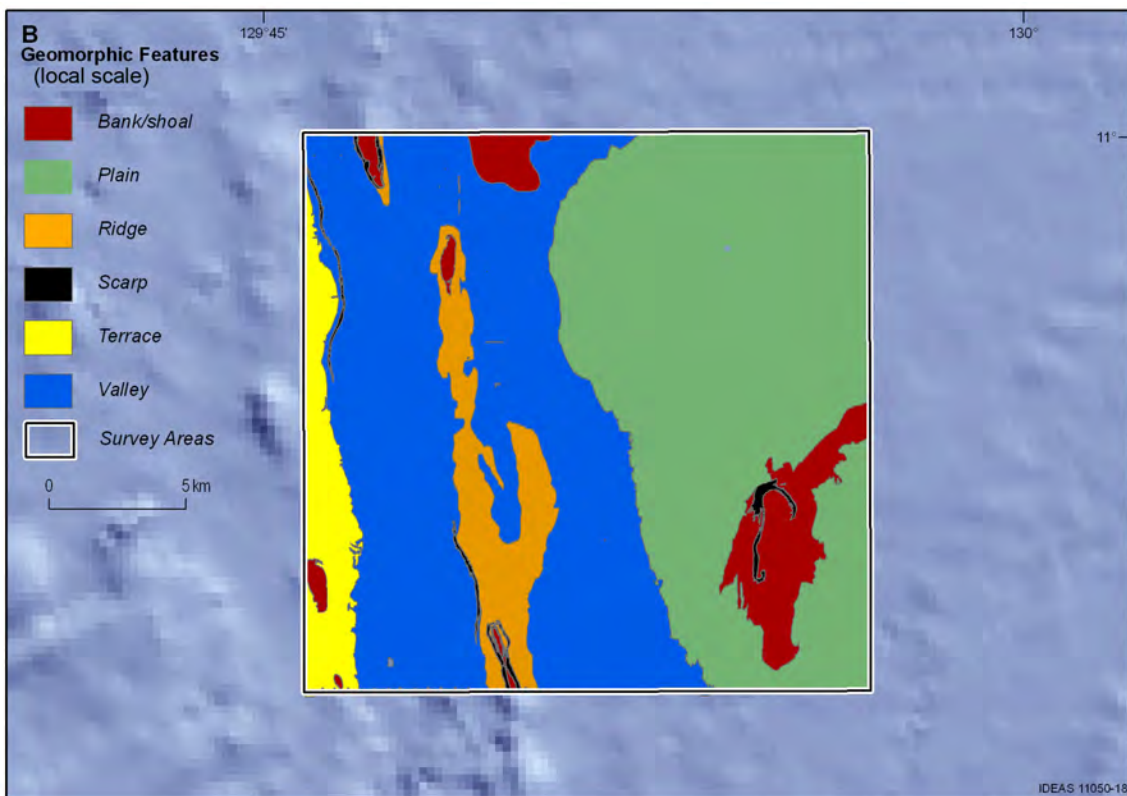


Figure 2.8: Geomorphic features from GA-0322 and GA-0325 survey area B.

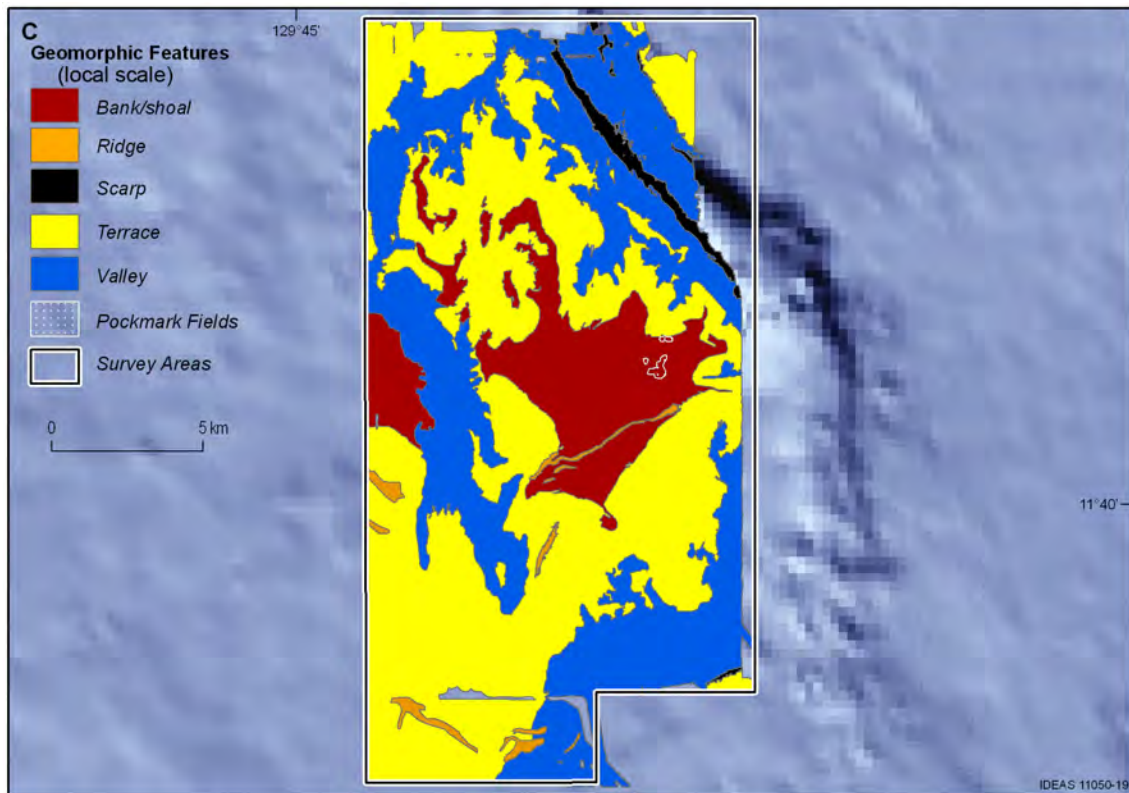


Figure 2.9: Geomorphic features from GA-0322 and GA-0325 survey area C.



Figure 2.10: Geomorphic features from GA-0322 and GA-0325 survey area D.

2.5 BIOPHYSICAL CHARACTERISATION OF GEOMORPHIC FEATURES

In this section, we use a range of datasets collected from the recent seabed mapping surveys to the northeastern JBG-TS to characterise the local-scale geomorphic features based on biophysical parameters. Scarps are excluded from our analyses as there are no samples from these environments. Several key environmental and biological factors varied by geomorphic type ([Table 2.2](#)). For example, rocky outcrops were more abundant and more homogeneous on banks, common but patchy on terraces and ridges, sparse and isolated in valleys, and absent on plains ([Appendix C](#)). Similarly, biological communities and species richness were also different among geomorphic features ([Figure 2.11](#), [Appendix C](#)). Integrated geological, oceanographic, and biological processes for these geomorphic features are presented in conceptual models in [Section 4](#).

Table 2.2: Summary of key biophysical variables used to characterise geomorphic features identified from the GA-0322 and GA-0325 seabed mapping surveys. Calculations are based on the values recorded at sampling stations. SR = species richness (number of species).

	BANKS	TERRACES	RIDGES	PLAINS	VALLEYS
Depth Range (m)	20-60	27-67	69-95	34-79	40-201
Mean Depth (\pm stdev)	28 \pm 6	45 \pm 15	81 \pm 9	44 \pm 13	98 \pm 44
Dominant substrate	Hard	Soft w/patches of rock outcrops	Soft w/patches of rock outcrops	Soft	Soft with isolated rock outcrops
Backscatter (dB)	-15 \pm 4	-20 \pm 3	-26 \pm 2	-21 \pm 2	-28 \pm 5
Mud (%) (\pm stdev)	16 \pm 20	15 \pm 16	14 \pm 6	20 \pm 9	19 \pm 10
Gravel (%) (\pm stdev)	26 \pm 23	15 \pm 10	9 \pm 9	8 \pm 4	8 \pm 13
Carbonate (%) (\pm stdev)	82 \pm 13	82 \pm 11	60 \pm 13	56 \pm 11	62 \pm 5
Epibenthic SR ¹	High	Moderate	Moderate	Low	Low
Infaunal SR ¹	Moderate	Low	Low	High	Moderate
Dominant Fauna ¹	Sponges, octocorals, hard corals	Sponges, octocorals	Sponges (e.g., <i>Cinachyrella</i>), octocorals	Polychaetes, amphipods, isopods	Polychaetes, amphipods
Terrestrial elements in sediments ²	Low	Low- moderate	Moderate	High	Moderate - high
Reactive organic matter in sediments ²	High	Moderate - high	Moderate	Low- moderate	Low

¹ Results are relative to other geomorphic features and are detailed in [Appendix C](#).

² Results are relative to other geomorphic features and based on a discriminant functions analysis detailed in [Appendix E](#).

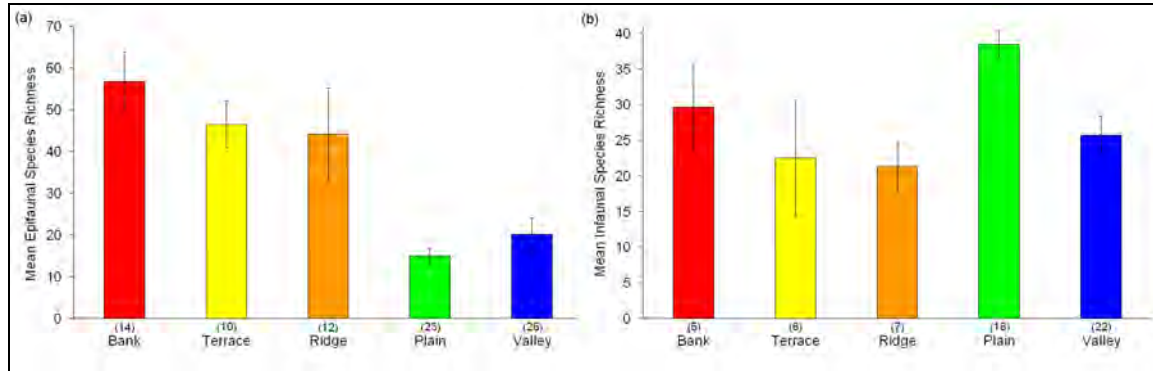


Figure 2.11: The number of (a) epifaunal and (b) infaunal species collected from the survey areas, classified by geomorphic feature type. Epifaunal species richness is based on onboard estimates from both surveys. Infaunal species richness is based on operational taxonomic units assigned from sorted GA-0322 samples only. Bars are standard error means.

2.5.1 Banks

Banks are elevated features with a relatively high proportion of hard substrate (Appendices C, F) (Figure 2.12). Sediments on banks have high average gravel and carbonate concentrations (Table 2.2). Banks are also characterised by having the lowest concentrations of terrestrial elements and the highest reactive organic matter concentrations (Table 2.2; Appendix E). The high organic matter reactivity is due in part to the shallowness of banks and the associated lack of time for organic matter to break-down as it descends through the water column. Interestingly, pore water salinity is extremely low (24 psu) at a station with high backscatter (Stn. 56B; -12.8 dB), possibly due to groundwater discharge.

The generally hard substrate of the banks support patches of moderately dense octocoral and sponge gardens which in turn provide habitat for other epifauna and cryptofauna. As such, banks are home to the highest number of epifaunal species (56.7 ± 26.7 species per ~ 100 m sled tow, mean \pm S.D.). Infaunal species richness is moderately high in bank sediments (29 ± 13.3 species per grab) (Figure 2.11). Very few macroalgae (including *Halimeda*) or reef-forming hard corals (Section 2.7) were recorded, in stark contrast to *Halimeda* and coral communities at similar depths in areas to the west of Van Diemen Rise (Heyward et al. 1997; Wienberg et al. 2010).

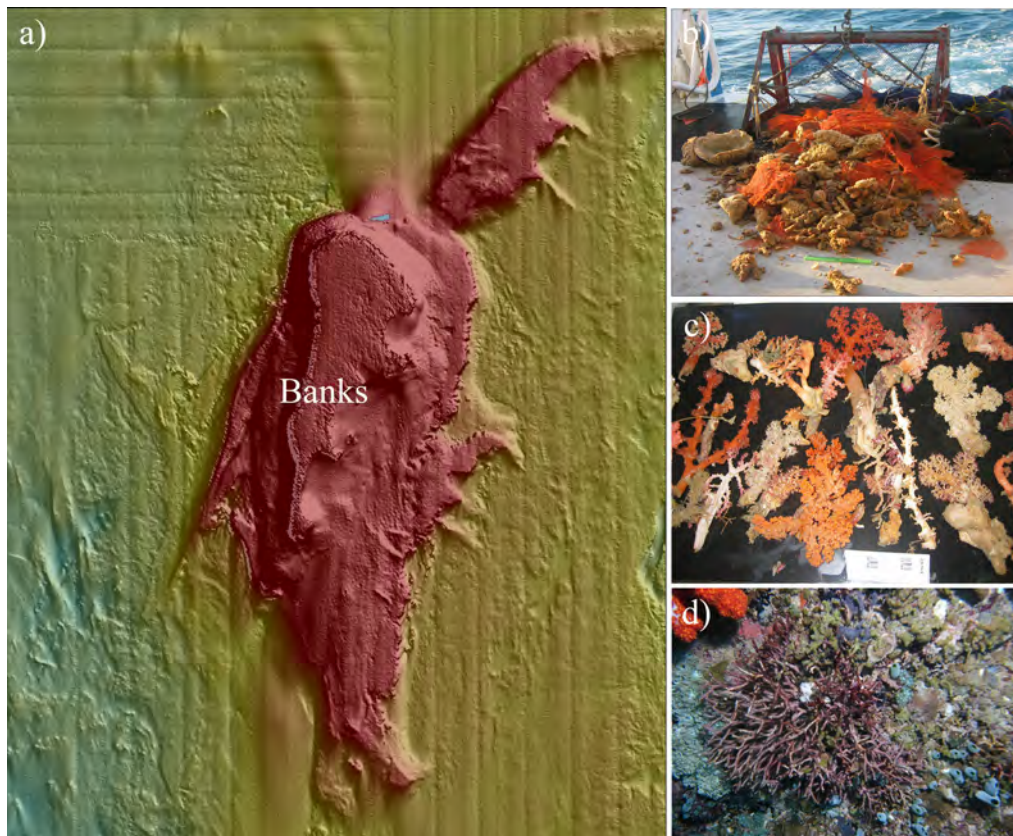


Figure 2.12: Representative images of banks. a) False colour bathymetry of Moss Shoal; b) epibenthic sled with an octocoral-and sponge-dominated catch from a transect spanning a bank and ridge (23A, 55 m); c) common soft corals found in bank environments (22A, 54 m); d) still photographs of hard coral environments with ascidians and soft corals (72B, 16 m). Depths are averages across sled and video transects.

2.5.2 Terraces

Terraces comprise relatively hard substrata, carbonate-rich unconsolidated sediments with variable grain-size distributions, high reactive organic matter concentrations, and low abundances of terrestrial elements ([Appendix E, Table 2.2](#)). Terraces occur in relatively intermediate water depths and have a diverse array of bedform types, including sand ripples and rocky outcrops ([Appendix C, Figure 2.13](#)).

Terraces support epifaunal communities with moderate numbers of species (46.4 ± 17.5 species per tow). Sponge and octocoral gardens occur at some stations, but their presence is not consistent among terrace stations. Sand ripples are observed at some terraces (e.g., Stations 30 from GA-322), as well as immediately adjacent to terraces (e.g., Stations 35 and 38 from GA-322). At these stations, epifaunal (22.5 ± 10.6 species per ~ 100 m sled tow) and infaunal species richness (8.0 ± 9.5 species per grab) are low which is indicative of a high disturbance environment. Like ridges, terraces have a low number of infaunal species (22.5 ± 19.8 species per grab) ([Figure 2.11](#)).

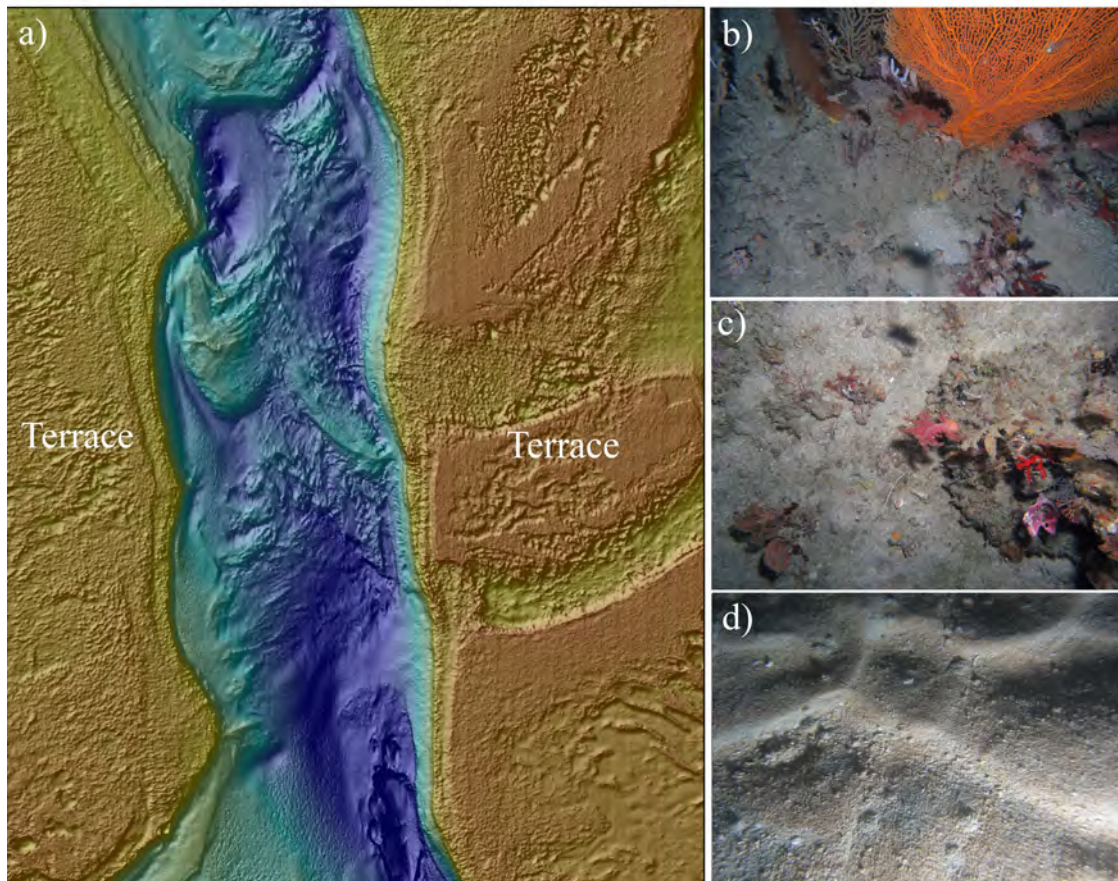


Figure 2.13: Representative images of terraces. a) false-colour bathymetry of terraces in Area A1; b) terraces with large gorgonian fans and branching octocorals (35B, 54 m); c) patchy soft corals and branching octocorals (35B, 54 m); d) rippled areas found in terraces (30A, 105 m).

2.5.3 Ridges

Ridges are characterised by soft sediments with relatively diverse relief and bedform types (Appendix C, Figure 2.14). Seabed sediments on ridges contain moderate proportions of mud (similar to terraces and banks) and low proportions of gravel and carbonate (similar to plains and valleys) (Table 2.2). The geochemical character of ridge sediments is intermediate regarding the amounts of reactive organic matter and terrestrial element concentrations (Appendix E)

Ridges have the highest variation among epifaunal species richness of any geomorphic feature (Figure 2.11), making them difficult to biologically characterise. Sponge and octocoral gardens occur at several stations. *Cinachyrella* sp., a small spherical sponge partially buried in sediment, may be a characteristic species of ridges, as large numbers of them were only recorded from ridges or immediately adjacent to them (Figure 2.14d). This species is common in soft sediments adjacent to patchy rock outcrops, and this type of environment is common for ridges. Ridges have a low number of infaunal species (21.3 ± 8.9 species per grab) (Figure 2.11).

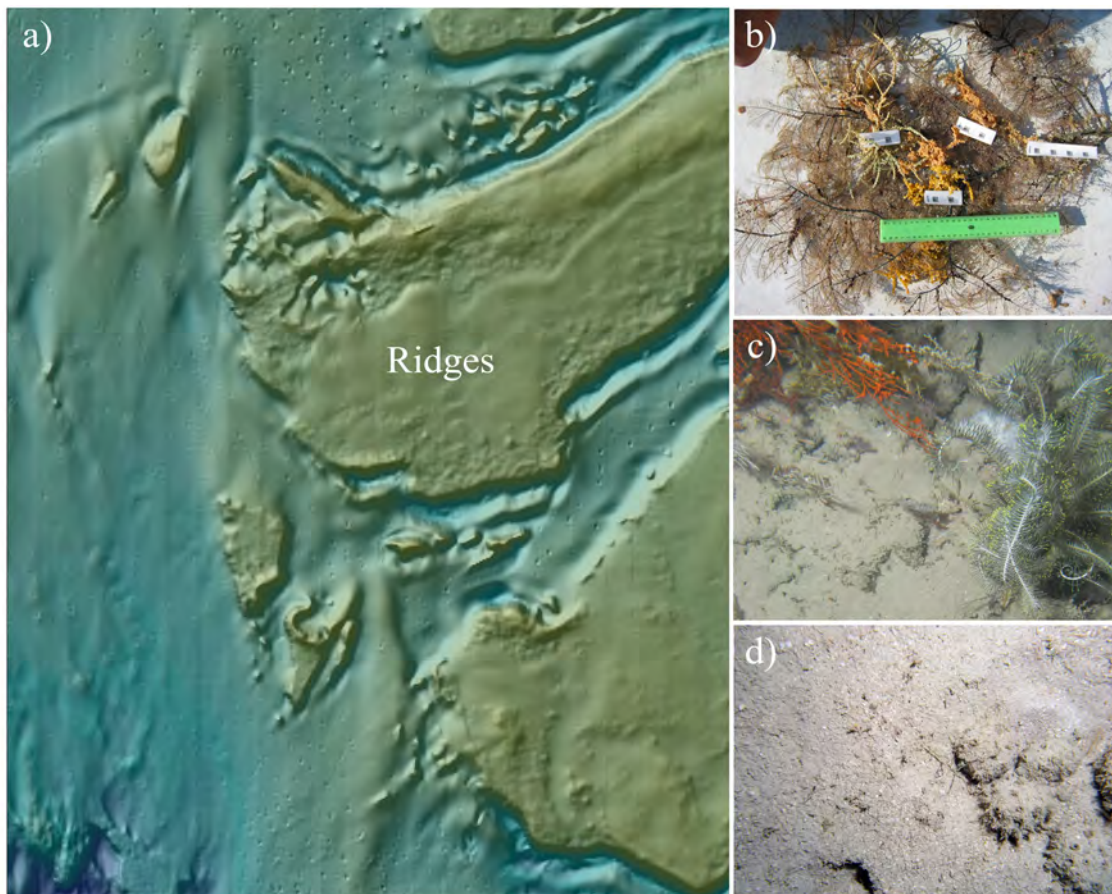


Figure 2.14: Representative images of ridges. a) False colour bathymetry of ridges in Area A1; b) epibenthic sled catch with abundant black coral (25A, 48 m); c) patchy gorgonians and sponges (23A, 68 m); d) *Cinachyrella* fields commonly found in ridges (24B, 72 m).

2.5.4 Plains

Plains are the shallowest and least complex geomorphic feature regarding bedform and relief, with ~99% of plains comprising homogenous flat soft-sediments (Appendix C, Figure 2.15). Similarly, the grain-size distribution of plain sediments is the most uniform of the geomorphic features, consisting mainly of very poorly-sorted gravelly-muddy sands (Appendix E). The physical uniformity of these sediments is also apparent in the backscatter measurements, for the plains have the narrowest range of acoustic returns (-18.6 to -24.2 dB). Sediments on plains are distinguished amongst the features in having the overall highest concentrations of terrestrial elements and the lowest median bulk carbonate contents (Appendix E, Table 2.2).

Plains have the lowest number of epifauna (14.9 ± 8.6 species per ~100 m sled tow). In contrast to other geomorphic features, large vulnerable growth forms of sponges and octocorals are extremely rare (<0.01% occurrence), suggesting either unsuitable substrate or a high disturbance environment. In contrast, infaunal species richness is highest in the plains (38.4 ± 7.9 species collected per grab; Figure 2.11).

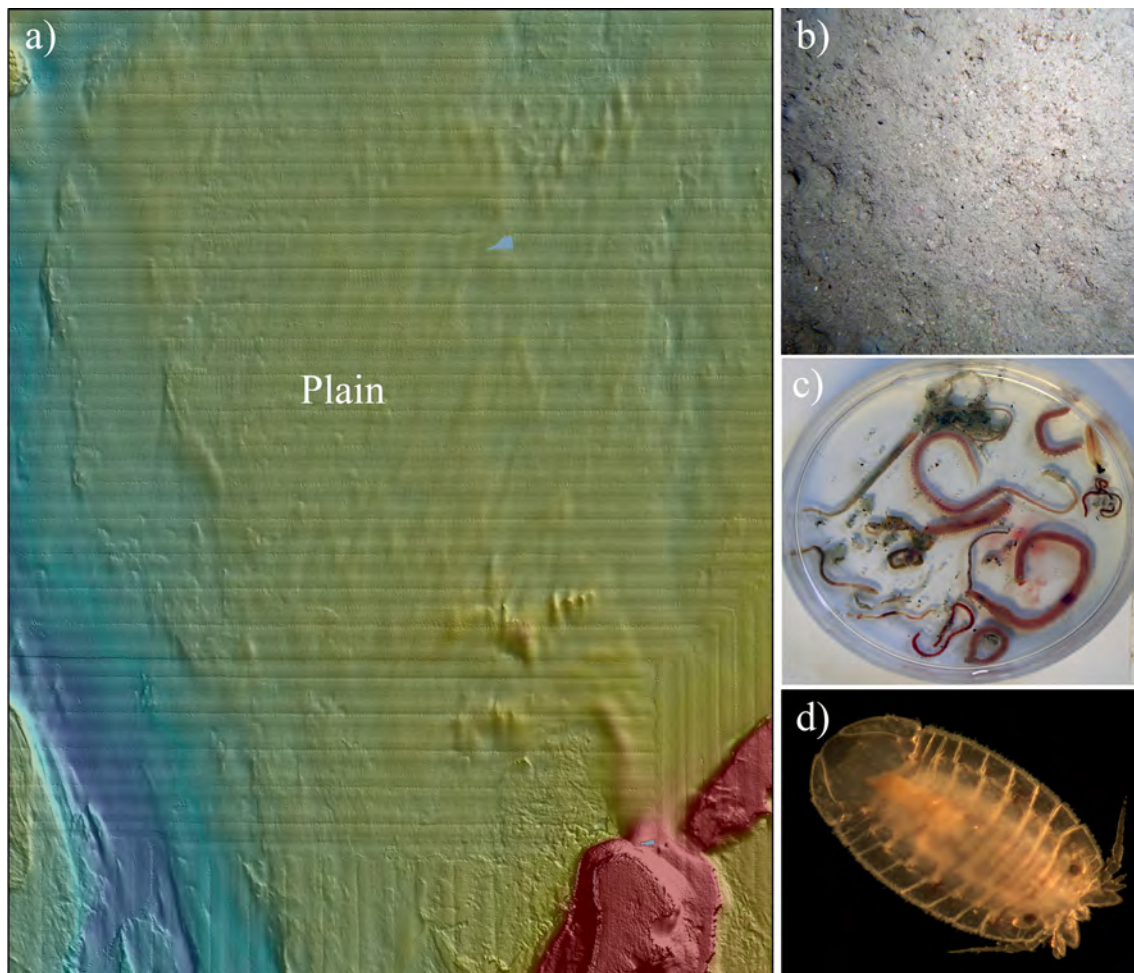


Figure 2.15: Representative images of plains. a) False colour bathymetry of plains in Area B; b) flat and sandy sediments found in plain environments (18B, 44 m); c) common polychaetes found in bank environments (59A, 38 m); d) isopod sp 2

2.5.5 Valleys

Valleys are dominated by flat soft sediment expanses (Appendix C, Figure 2.16), although they have the greatest range in backscatter values indicating high variation in substratum types (Table 2.2). Sediments with gravel contents <1% characterise approximately a quarter of valleys, although a wide-range of grain sizes are found among other valleys (Appendix E). The sediments of valleys comprise a range of geochemical compositions and are either quartz-dominated or carbonate-dominated (Appendix E). Sand ripples occur at some stations, although usually these features are observed at valley stations that border terraces (e.g., Stations 35A and 38A).

Valleys support low-moderate numbers of epifaunal species (20.1 ± 19.9 species per 100 m tow). Valleys include many debris-swept channels, which in places expose small patches of underlying rock that support moderate densities of sessile animals. However, these higher levels of disturbance may inhibit the ability of large and more vulnerable growth forms to colonise or grow. As with plains, valleys are not obviously dominated by any epifaunal taxa. Interestingly, scattered branched corals (possibly *Stylophora pistillata*) were found at either end of a single valley-plain feature in Area D (Station 53A, Station 13B), as well as other locations in or near shallow valleys in Area D (Figure 2.21d). This finding is unusual because of the high turbidity observed at these locations in the video transects. Infaunal species richness among deep/valley/hole features is moderate (25.6 ± 12.4 species per grab) (Figure 2.11), and bioturbation is the highest of all geomorphic features as evidenced by tracks, trails and similar features recorded from video transects (Appendix C, Figure 2.16b).

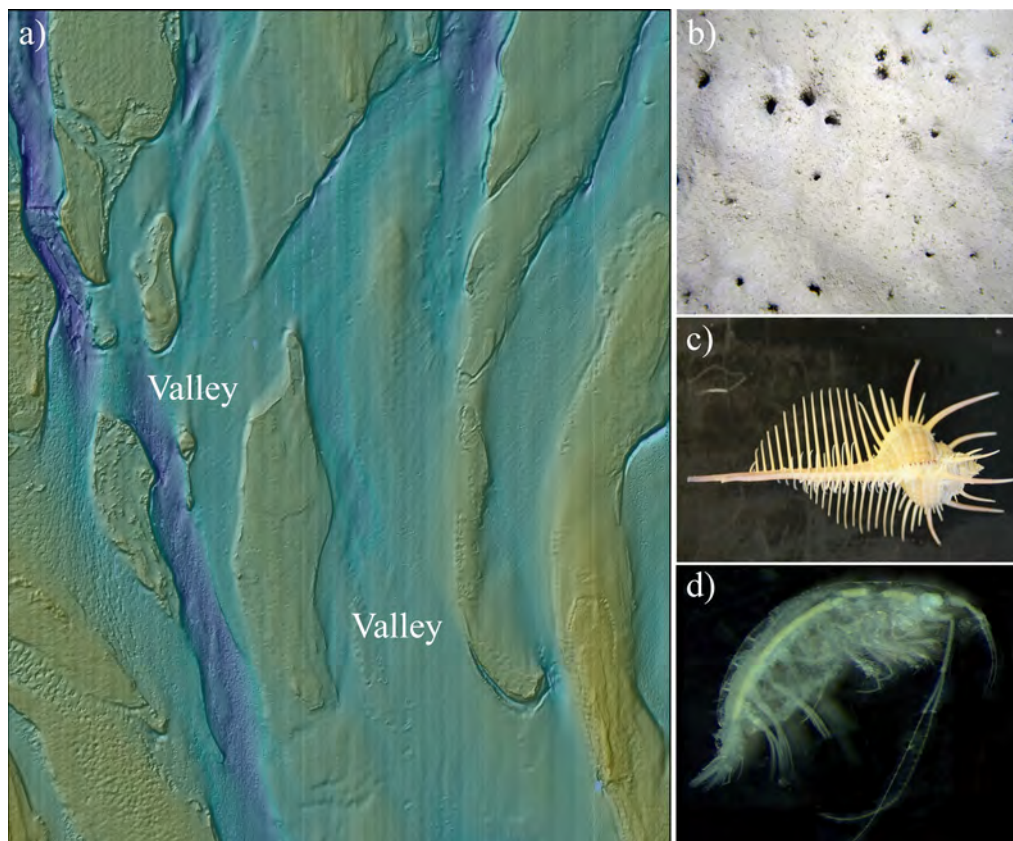


Figure 2.16: Representative images of valleys. a) False colour bathymetry of valleys in Area A; b) bioturbated sediments from valleys (41B, 103 m); c) *Murex soelae* (6A, 88 m); d) gammarid sp 7

2.6 DISTINCTIVE HABITATS & COMMUNITIES

An understanding of the distinctiveness of biological communities among locations is critical for marine zone management. In this section, species identifications of scleractinian corals, sponges and infauna are examined to determine whether biological communities are distinctive within and among geomorphic features and pockmarks (see [Appendix C](#) for details). For the purpose of this report, a distinctive habitat or community is defined as one in which a large proportion of species occur nowhere else at the scale of 1-10s of kilometres in area of data coverage. Importantly, the detection of new species and distribution records even among relatively well-studied taxa (e.g., echinoderms, molluscs) highlight how little is known about the distribution of species and biodiversity patterns in the JBG-TS ([Appendix C](#)). The following analyses are therefore preliminary, and the acquisition of more biological data in the region will contribute to a better understanding of the occurrence and distribution of unique species and communities.

2.6.1 Sponge, infaunal, and coral communities

On the northeastern margin of the JBG-TS, biological communities are more distinctive among geomorphic features than within them, although this trend varies according to taxa and geomorphic features. For example, sponge communities within a given geomorphic feature were more similar than sponge communities between features. Of the diagnostic species identified in [Appendix C](#), all stations at banks and terraces with mixed gardens support the giant barrel sponge *Xestospongia testudinaria*; but this sponge was not found in valley gardens. The two banks (Moss Shoal in Area B and unnamed bank in Area C) were separated by approximately 58 km and shared 19.2% of sponge species. This is roughly similar to the distinctiveness of sponge communities found on Sahul Shelf, in which three reefs were separated by 35, 40, and 50 km and shared 13%, 24%, and 9% of species, respectively (Hooper 1994). Importantly, large percentages (23-66%) of species collected from sled trawls were found at no other feature during survey GA-0322. These results indicate that at the local scale (10s km), sponges can form distinctive communities with locally endemic species on banks and reefs (Hooper 1994). However, such observations must be cautiously interpreted since sampling effort was unequal among banks and undersampling was extremely likely ([Appendix C](#)).

Geomorphic features are also related to the distinctiveness of infaunal communities, but unlike sponges, these differences only applied between plains and other features; infaunal communities were not statistically different among banks, terraces and valleys. Infaunal communities in Area A were distinct from communities in the other three study areas. A final analysis of the distinctiveness of communities within geomorphic features is pending identification of sponges and infauna collected on survey GA-0325.

At a regional scale, the hard corals from the carbonate banks on the Van Diemen Rise are distinct from coral reefs in other regions of northern Australia. While the coral reefs of Big Bank Shoals are dominated by *Acropora* and *Porites* (Heyward et al. 1997), these genera were not collected on the Van Diemen Rise, although they were observed in video transects. Instead *Fungia*, *Turbinaria* and *Stylophora* species dominated collected specimens. There is some suggestion that the reefs of the Van Diemen Rise include mesophotic species (e.g., *Stylophora pistillata*) able to adapt to low light levels in deeper or turbid waters (Falkowski & Dubinsky 1981; Mass et al. 2007; Mass et al. 2010). Such species are important due to their potential ability to recolonise a disturbed reef after environmental stress from comparatively deep refugia.

2.6.2 Pockmark communities

Pockmarks may be indicative of fluid/gas seepage which can provide habitat to abundant or distinctive benthic fauna (Wasmund et al. 2009). They are widely distributed throughout the JBG-TS (George & Cauquill 2010).

During surveys GA-322 and GA-325, pockmarks were identified from the acoustic data and compared with physical and biological samples. Sediments in pockmarks are different than non-pockmarked sediments based on 18 environmental variables (Area A, [Appendix E](#)). Pockmarked sediments in valleys have lower gravel content, smaller mean grain sizes, and higher mud content than the surrounding sediments. Most indicators of organic matter freshness point to higher reactivity in the non-pockmarked sediments ([Appendix E](#)). Despite these differences in environmental variables, infaunal communities at pockmarks are not clearly different from those at non-pockmark sites ([Appendix C](#)), although further analysis including the GA-0325 data is needed to confirm this trend.

2.7 SIGNIFICANT HABITATS & COMMUNITIES

For the purpose of this report, significant communities are defined as those that are habitat-forming, long-lived, aesthetically valuable, or otherwise contain species of interest (e.g., potential indicator species, threatened species).

Sponges and octocorals are major habitat-forming taxa on the seafloor, providing structure to otherwise flat environments and sheltering a range of animals on and near the seafloor, some of which are exclusive to particular sponge or octocoral species (Buhl-Mortensen et al. 2010) ([Figure 2.17](#)). Many large species of sponges and octocorals are long-lived and slow-growing, making them potentially vulnerable to anthropogenic and natural disturbance (Linares et al. 2007; Probert et al. 1997). Where sponges and octocorals occur in dense gardens, the number of other animals is often also high ([Appendix C](#)). Thus, sponge and octocoral gardens can be indicative of high biodiversity. In fact, octocorals have been suggested as a keystone group for highly diverse benthic habitats in the Arafura Sea (Wilson 2010).

Sponges represent the highest biomass and species richness recorded of all taxa from the GA-0322 and GA-0325 surveys ([Appendix C](#)). A rock probability index derived from backscatter signals and video groundtruthing revealed patterns of sponge garden distribution in relation to substrate (details in [Appendix F](#)). Mixed sponge and octocoral gardens were commonly found on rocky outcrops and patchy rock habitats, regardless of the geomorphic feature ([Figure 2.17](#), [Appendix C](#)), with the exception of Area A in which half of the gardens were identified from areas of the seafloor less likely to be rocky ([Figure 2.21](#)). Importantly, not all raised features had gardens. A few gardens were identified in valleys in Area A, and one mixed garden station was identified from a small area of rocky substrate in the plains of Area D based on sled samples (Station 6B) ([Figure 2.21](#)). Among stations with mixed gardens shown in [Figure 2.21](#), the proportion of octocorals in relation to sponges seems to increase with distance from the coast ([Appendix C](#)).

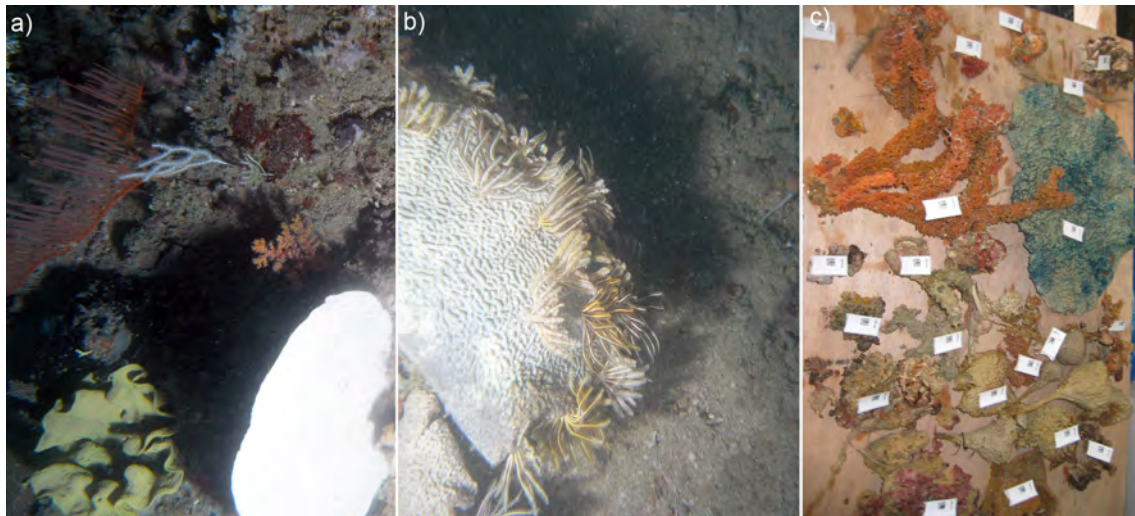


Figure 2.17: Sponge and octocoral gardens occurred along raised features of the JBG-TS: (a) Underwater still image (Station 34A, ~27 m), (b) Habitat-forming *Lanthella* sponge supporting crinoids (31A, ~27 m), and (c) Representative sponge species collected from a sled transect (Station 21A, ~21 m).

Scleractinians (hard corals) include small solitary corals as well as the more familiar reef-forming corals. As the latter grow, they leave behind their calcareous skeletons, providing a raised hard substrate that becomes an important habitat for a range of reef-associated species (Bennett 1971). Reef-forming corals are not only important ecosystem engineers, they are also aesthetically valuable due to their association with high levels of biodiversity, media attention, and tourism (Moberg & Folke 1999).

No reef-forming corals have previously been found in the JBG proper, apart from small patches located near intertidal rock platforms (Clarke et al. 2001; ENI 2005; LeProvost Dames & Moore 1994; Smit et al. 2000; WEL 2004). On the Van Diemen Rise, reef-forming corals were found on several shallow banks in Areas A and B (10-54 m depth), notably the north side of Moss Shoal and the shallow southeast banks of Area A (Figure 2.21). These corals were often diverse and locally dense (up to 90% cover), but overall cover on banks was very low (<1%). Based on collected samples, reef-forming corals were dominated by *Turbinaria*, *Fungia*, and *Stylophora* species, although additional taxa are common in underwater video from station 72B (Appendix C) (Figure 2.18). Several species were listed on the IUCN Red List, discussed further below. Branched coral rubble (possibly *Acropora*) was collected in the sled at a terrace in Area A (Station 48B, 90 m depth), likely reflecting coral reefs that occurred here approximately 18,000 years before present when the sea level stood at 120 m below present level before gradually rising to inundate these reefs (Yokoyama et al. 2001, George & Cauquill 2010). In addition, isolated small living hard corals (possibly *Stylophora pistillata*) were recorded from five stations in Area D (Stations 53 – 56A, 13B) (Figure 2.18d). These inshore areas are mostly soft-sediment and highly turbid compared to other study areas, but it appears that limited coral growth is possible for mesophotic species (Falkowski & Dubinsky 1981; Mass et al. 2007; Mass et al. 2010). No records of reef-forming corals were found elsewhere in the JBG-TS based on online database searches (www.ala.org.au, www.iobis.org), suggesting either that areas outside the survey area do not support corals or, more likely, that sampling has been insufficient in other regions of the JBG-TS.

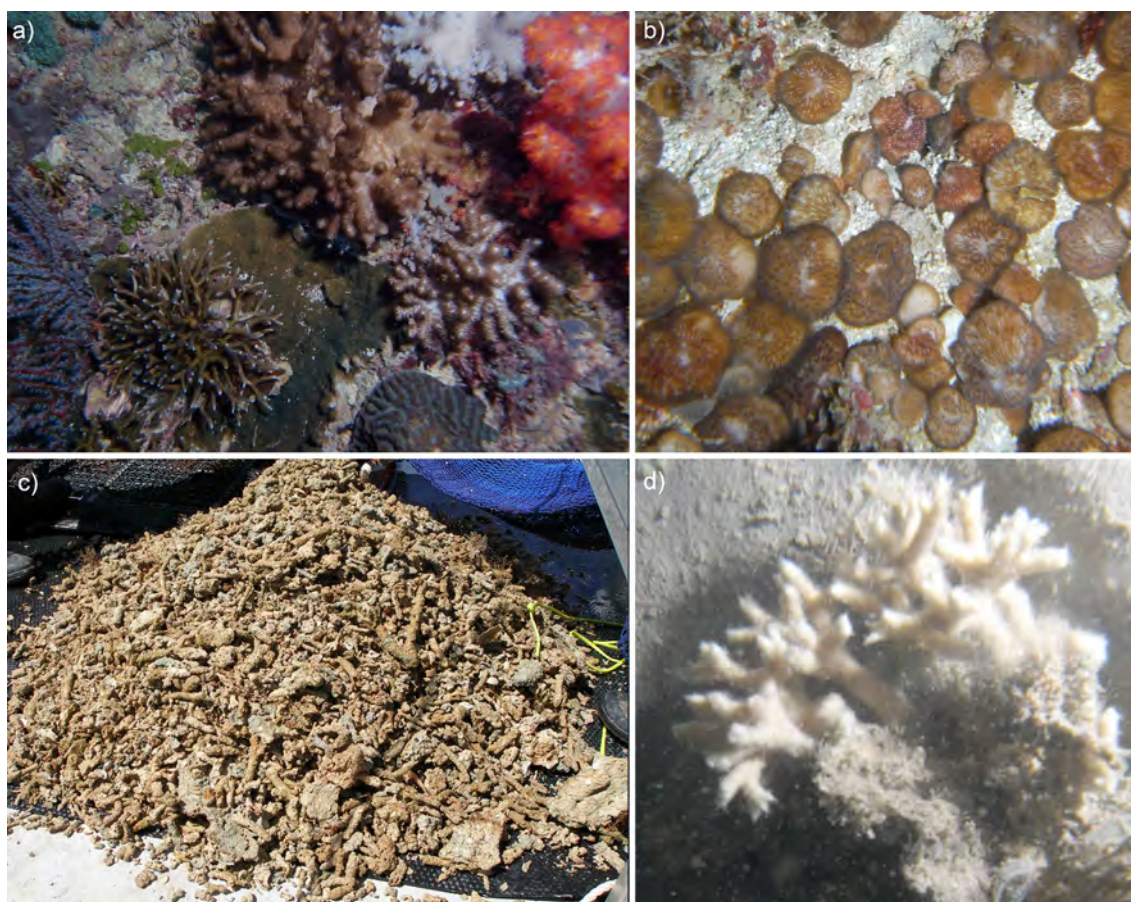




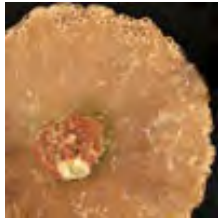

Figure 2.18: Scleractinian (reef-forming) corals were recorded from several stations on the GA-322 and GA-325 survey: a) Mixed coral community including *Stylophora pistillata* and *Cyphastrea serailia* (Station 72B at 13 m), b) mushroom coral *Fungia fragilis* (Station 52B at 28 m), c) branched coral rubble (Station 48B at 90 m), and d) branching mesophotic coral, possibly *S. pistillata*, (Station 53A at 53 m).

Indicator species are particular taxa associated with habitats of interests (e.g. hydrocarbon seeps or hydrothermal vents in Fisher et al (2000) and Harkantra (2006)). For example, siboglinids are a family of polychaetes sometimes referred to as ‘seep worms’, and they occur buried in sediment in association with seeps from a range of sources (Lösekann et al., 2008). There are no known records of siboglinids or any other potential indicator species recorded from the JBG-TS. However, the life history of many species are currently unknown so potential indicator species may still exist in current biological collections.

Vulnerable species are defined by the IUCN red list (www.iucnredlist.org) based on conservation status. A search of online biological databases (www.ala.org.au (ALA), www.iobis.org (OBIS)) show records for two Near Threatened dolphins (*Orcaella heinsohni*, *Sousa chinensis*), the Vulnerable sperm whale (*Physeter macrocephalus*), the Vulnerable olive ridley turtle (*Lepidochelys olivacea*), and the Endangered loggerhead turtle (*Caretta caretta*). Other vulnerable species also likely occur in the area but were not listed in the online databases searched. All of these species are pelagic migrants, and their distribution in the JBG is therefore dynamic and unpredictable.

Five species of hard coral recorded from the carbonate banks of the Van Diemen Rise are on the IUCN Red List as near threatened, vulnerable, or endangered (Table 2.3) (Figure 2.18). These species were collected from Area A at two stations. Unidentified coral specimens from Area D may be *Stylophora pistillata* (Figure 2.18d).

Table 2.3: Species identifications of reef-forming corals collected from GA-325 which are included on the IUCN Red List. Depth at Station 52 = 28.5 m and Station 55 = 31.4 m.

	SPECIES	FAMILY	STATION	IUCN STATUS
	<i>Stylophora pistillata</i>	Pocilloporidae	55B	Near Threatened
	<i>Turbinaria reniformis</i>	Dendrophyllidae	52B, 55B	Vulnerable
	<i>Turbinaria patula</i>	Dendrophyllidae	55B	Vulnerable
	<i>cf Caulastrea sp.</i>	Faviidae	55B	Vulnerable Near Threatened ¹
	<i>Cantharellus cf noumeae</i>	Fungiidae	55B	Endangered

¹ *Caulastrea curvata* and *C. echinulata* in northern Australia are listed as Vulnerable; *C. tumida* is listed as Near Threatened.

Listed marine species are protected by the *EPBC Act 1999* and include seasnakes, seals, crocodiles, dugongs, sea turtles, sea birds, and syngnathids (pipefish and seahorses). In addition, all cetaceans are protected under the *EPBC Act 1999*. Dugongs are not abundant in the JBG-TS due to lack of seagrass, but there have been some populations recorded near seagrass patches along the eastern coast of the JBG (WEL 2004). A few individuals may also migrate through the JBG (WEL 2001). The distribution of a variety of seabirds extends into the JBG, with breeding colonies typically located on offshore island or mainland beaches. No seabirds were recorded during an offshore environmental survey in May 2004 (WEL 2004). Public database records indicate that 12 species of cetacean, three species of sea turtle, 14 species of seasnake, and 12 species of syngnathids have been recorded from the JBG (Full list in [Appendix C](#)). These taxa are likely much more widely distributed throughout the JBG and adjacent regions than the sporadic records from databases may suggest.

Sea snakes are expected to be very common in JBG, although exact distributions and species present are unknown. At least 15 species of seasnake occur in the NT (Storr et al 1986 cited in WEL 2004), and at least two individuals were recorded from GA-0322 and GA-0325.

Six species of sea turtle have distributions that overlap the JBG-TS and may occur in the area. The low number of reefs, seagrass and macroalgae are thought to limit the numbers of green turtles (*Chelonia mydas*) (Woodside 2003 cited in WEL 2004), although this species has been found migrating through the JBG (ENI 2005) and feeding habitats for juveniles may occur around Grose Islands (Smit et al. 2000). Flatback turtles are the only species from which nests have been recorded along JBG-TS beaches (TOTAL E&P 2007; WEL 2004), although the Hawksbill and Olive Ridley may also use the region for nesting (LDM 1994).

Sharks & fish include five open water species that are protected under the *EPBC Act 1999* due to their status as migratory species: great white shark (*Carcharodon carcharias*), whale shark (*Rhincodon typus*), shortfin mako (*Isurus oxyrinchus*), longfin mako (*I. paucus*), and porbeagle (*Lamna nasus*). The porbeagle does not occur in northern Australian waters, and while the other species' ranges extend into the JBG-TS, there are very limited records. According to public database records (ALA and OBIS), the longfin mako has been recorded from the JBG-TS, but there are no records of the other migratory species. Similarly, none of these species were recorded in a tagging and recapture study which found that more sharks may occur along the edges of the JBG than in more open waters, although lower sampling effort in open waters makes this difficult to determine (Stevens et al. 2000).

2.8 RELATIONSHIP BETWEEN BIOLOGY AND THE ENVIRONMENT

Strong environmental and biological relationships may reveal environmental factors, termed 'surrogates', which can then be used to develop predictions for areas in which there are no biological data (McArthur et al. 2010). Since the biology of much of the JBG remains unknown, such surrogates may be particularly useful for this region. Previous studies have found that sediment grain size and distance offshore were moderately correlated to infaunal communities in the region (Metcalf & Glasby 2008; URS 2009; WEL 2004), although this may be an artefact of sampling as smaller species that are not retained during collection protocols may be relatively abundant in fine sediments (Wilson 2006). Another survey in the comparatively shallow waters of the Beagle Gulf (Figure 2.1) found no correlation between species richness and depth or sediment characteristics, although sediment grain size did differentiate benthic communities (Smit et al. 2000). Predictive models indicate that species richness decreases with depth and distance offshore in water > 50 m deep in the northwest marine region (Dunstan & Foster 2010).

Co-located physical and biological data from the GA-0322 and GA-0325 surveys were used to analyse the relationships between environmental factors and various biological factors including standard univariate (species richness, biomass) and multivariate (community structure) factors, as well as coarser levels of biological information (video habitat classification, occurrence of coral/mixed gardens).

There were no environmental variables identified as strong predictors of species richness, biomass, or community structure along the Van Diemen Rise (linear analysis only). Although these biotic factors were significantly correlated with several abiotic factors, the relationships were extremely weak (Table 2.4, Appendix C). Previous studies on the Van Diemen Rise revealed that species assemblages are gradational or patchy and not necessarily limited to specific depth ranges or seabed features (Lavering 1994); similar trends have been noted for the Beagle Gulf (Smit et al. 2000) and the Gulf of Carpentaria (Long & Poiner 1994). This could explain in part the few clear relationships between abiotic and biotic factors detected in the present study.

Alternatively, the relationships between the biotic and abiotic factors measured in this study were obscured by stronger environmental regulators. For example, algal blooms, likely the cyanobacteria *Trichodesmium*, occur throughout the JBG-TS region, particularly during austral spring months when waters are calm (Heap et al. 2010; WEL 2004). As they decay and sink to the seafloor, these algae likely influence the nutrient availability and dissolved oxygen content, thereby seasonally affecting the associated benthic communities (Burford et al. 2009).

Table 2.4: List of abiotic factors that were significantly related to biological factors. Full details of statistical tests and results are in [Appendix C](#), and details of abiotic factors are in [Appendix E](#).

BIOTIC FACTOR	ABIOTIC FACTOR(S)	ANALYSIS	STATISTICAL VALUE	P
Species richness (epifauna)	Gravel	Multiple regression	$R^2 = 0.0583$	0.0447
Species richness (epifauna)	Pheophytin	Multiple regression	$R^2 = 0.1145$	0.0069
Biomass (epifauna)	Gravel	Multiple regression	$R^2 = 0.0871$	0.0049
Biomass (epifauna)	Total reactive chlorin	Multiple regression	$R^2 = 0.0410$	0.0329
Biomass (epifauna)	Depth	Multiple regression	$R^2 = 0.0077$	0.0469
Species richness (infauna)	Nitrogen isotope ($\delta^{15}\text{N}$)	Multiple regression	$R^2 = 0.0397$	0.0017
Species richness (infauna)	Iron	Multiple regression	$R^2 = 0.0033$	0.0197
Community structure (sponge)	Depth, $\delta^{15}\text{N}$, Si/Al, Aluminium, Manganese	BIO-ENV	$\rho = 0.343$	0.120
Community structure (infauna)	Depth, Gravel, Pheophytin, %S-FeSAI	BIO-ENV	$\rho = 0.592$	0.010

Despite no strong relationships to individual environmental factors, species richness showed a weak spatial pattern in the northeastern JBG-TS, with epifaunal species richness slightly increasing away from the coast ([Figure 2.19a](#)) and infaunal species richness increasing towards the coast ([Figure 2.19b](#)). This could reflect larger expanses of soft sediment habitat for infauna on the inner shelf and more banks and other raised rocky features for epifauna on the outer shelf. Alternatively, the high turbidity and disturbance on the inner shelf may preclude sessile epifaunal animals. Benthic disturbance is greater nearshore due to continuous action from surface waves as well as strong tidal currents ([Appendix G](#)). Such high disturbance may limit the epibenthos able to settle and grow in nearshore environments. Anthropogenic disturbance may be higher towards the shore due to increased fishing, onshore urban development, and industry activity which may similarly limit the establishment of many epibenthic species.

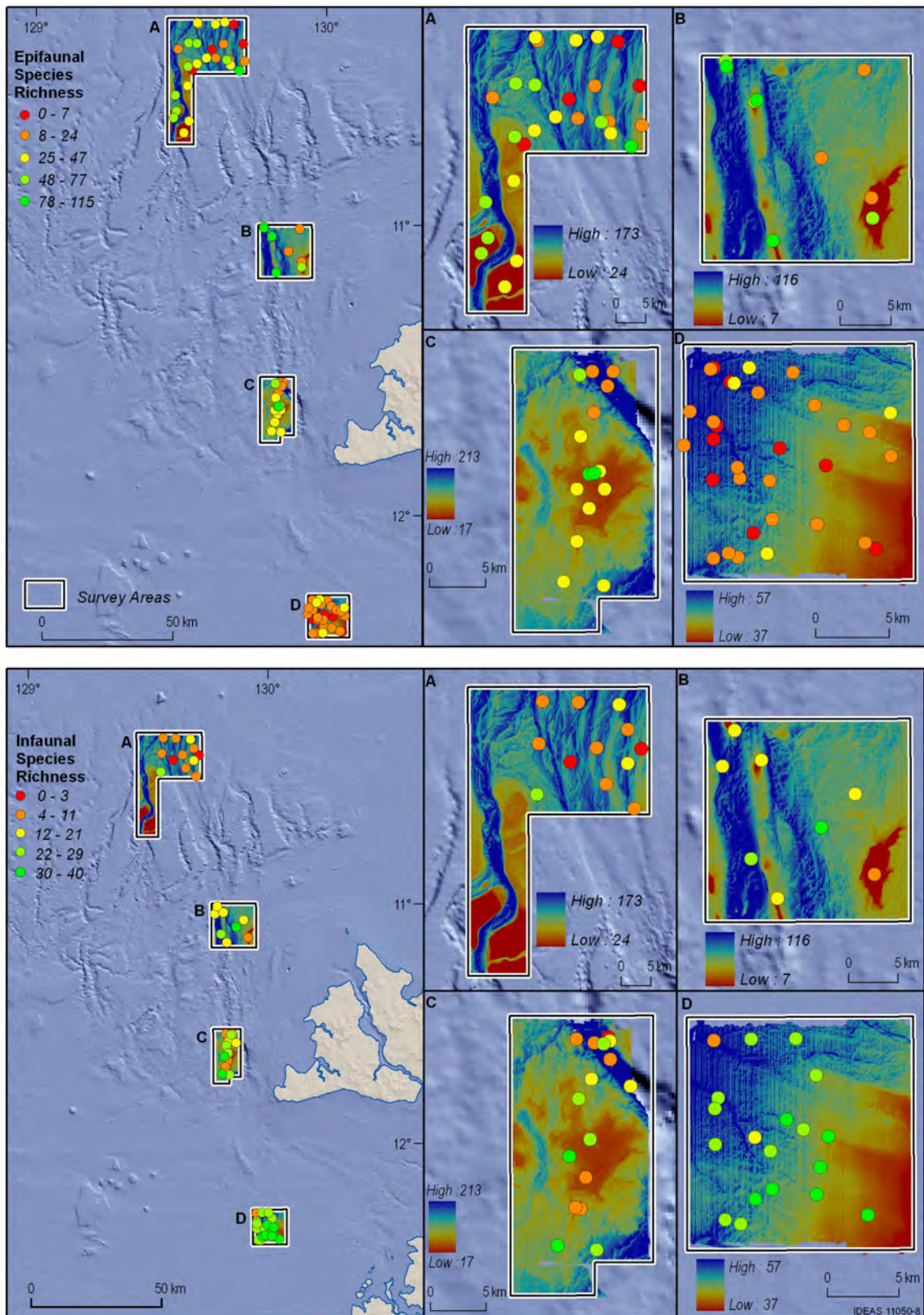


Figure 2.19: Map of GA-0322 and GA-0325 survey areas including bathymetric depth overlaid with species richness of (a) epifauna and (b) infauna.

Despite the absence of strong relationships between biological and environmental factors, predictions of biodiversity in the JBG may still be possible if the measures of biodiversity are coarse, rather than using standard variables such as species richness, abundance, biomass, or community structure. To that end, habitats were broadly classified based on video observations into the following categories which generally increase in epifaunal diversity:

1. *Barren*: sediment is flat and unmarked with infaunal or epifaunal activity,
2. *Bioturbated*: sediment shows at least moderate level of infaunal and epifaunal activity with characteristic trails and burrows (*lebensspuren*) but few epifauna,
3. *Mixed patches*: Patchy rocky outcrops supporting diverse and locally abundant patches of octocoral and sponge gardens interspersed with areas of low epibenthos,
4. *Mixed gardens*: Rocky outcrops comprising diverse and locally abundant octocoral and sponge gardens with no reef-forming hard coral,
5. *Mixed gardens with hard corals*: Rocky outcrops supporting diverse and abundant octocoral and sponge gardens with instances of reef-forming hard coral.

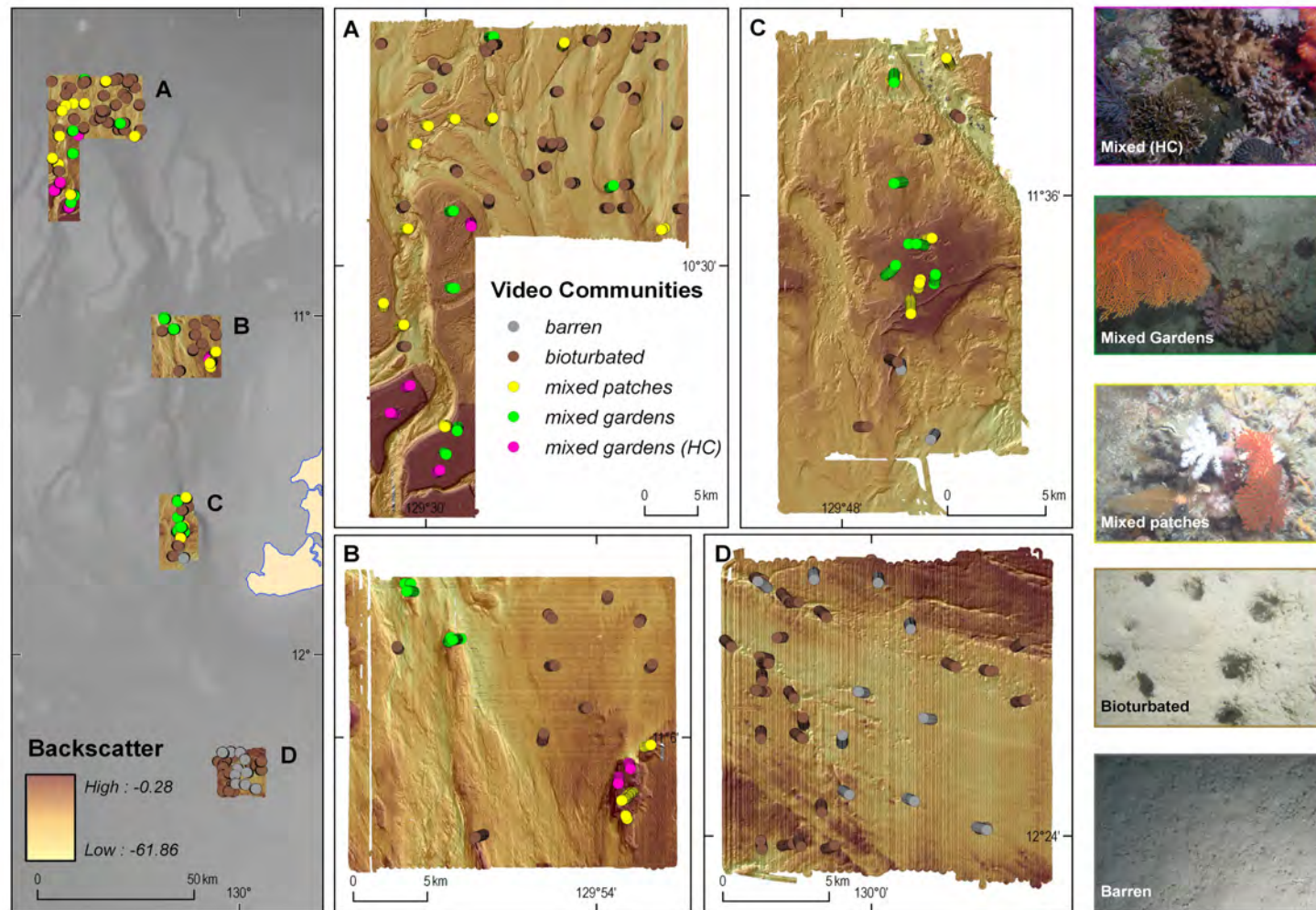


Figure 2.20: Backscatter image of areas A, B, C, and D. Video habitat classifications (coloured dots) shown are overlaid on backscatter. Still photographs from the five video habitats found: Mixed gardens with hard coral (HC), mixed gardens, mixed patches, bioturbated, and barren communities.

Barren and bioturbated habitats characterise expansive areas in Area D, while mixed gardens with reef-forming hard corals only occurred in Areas A and B (Figure 2.20). These video-based habitats are related to geochemical characterisations, with each video-based habitat grouping together according to similar geochemical characteristics (Appendix E). Specifically, barren and bioturbated habitats differ from mixed patches and mixed gardens due to higher terrestrial element concentrations in sediments (principally Si), while mixed gardens with hard corals and barren habitats differ from the other habitats due to more reactive organic matter (Appendix E).

Selected abiotic variables were also compared with the presence of mixed gardens and hard corals to identify environmental conditions that may be driving the distribution of these communities. Backscatter strength is significantly related to the presence of mixed gardens (and possibly hard corals, although there are not enough stations with reef-forming hard corals to statistically test this) (Appendix C).

A rock probability index that indicates the likelihood of rocky substrate is useful for predicting the occurrence of gardens of sponges, octocorals, and hard corals (see Appendix F). Rocky substrate is predicted at all sites at which reef-forming corals occur (Figure 2.21). The probability index performs worse in the prediction of mixed sponge and octocoral gardens, although more mixed gardens occurred on predicted rocky substrate than soft (Figure 2.21). However, in Area D the rock probability index performed well, showing relatively uniform bathymetry but highly varied rock probability. The single mixed garden and hard corals recorded from this area are located at sites with a high probability of rocky substrate (Figure 2.21). These results indicate that the rock probability index may be used to identify target features for video or sampling to determine hard coral and mixed garden occurrence, particularly in areas of uniform bathymetry. In addition, substrate has a particularly strong effect on composition of benthic invertebrates (McArthur et al 2010), but substrate type can vary at small spatial scales (metres) which are often much smaller than the size of cells used in interpolations and associated habitat mapping. The rock probability index provides an indication of substrate and associated biological communities at a finer scale (metres) than normally available using habitat maps.

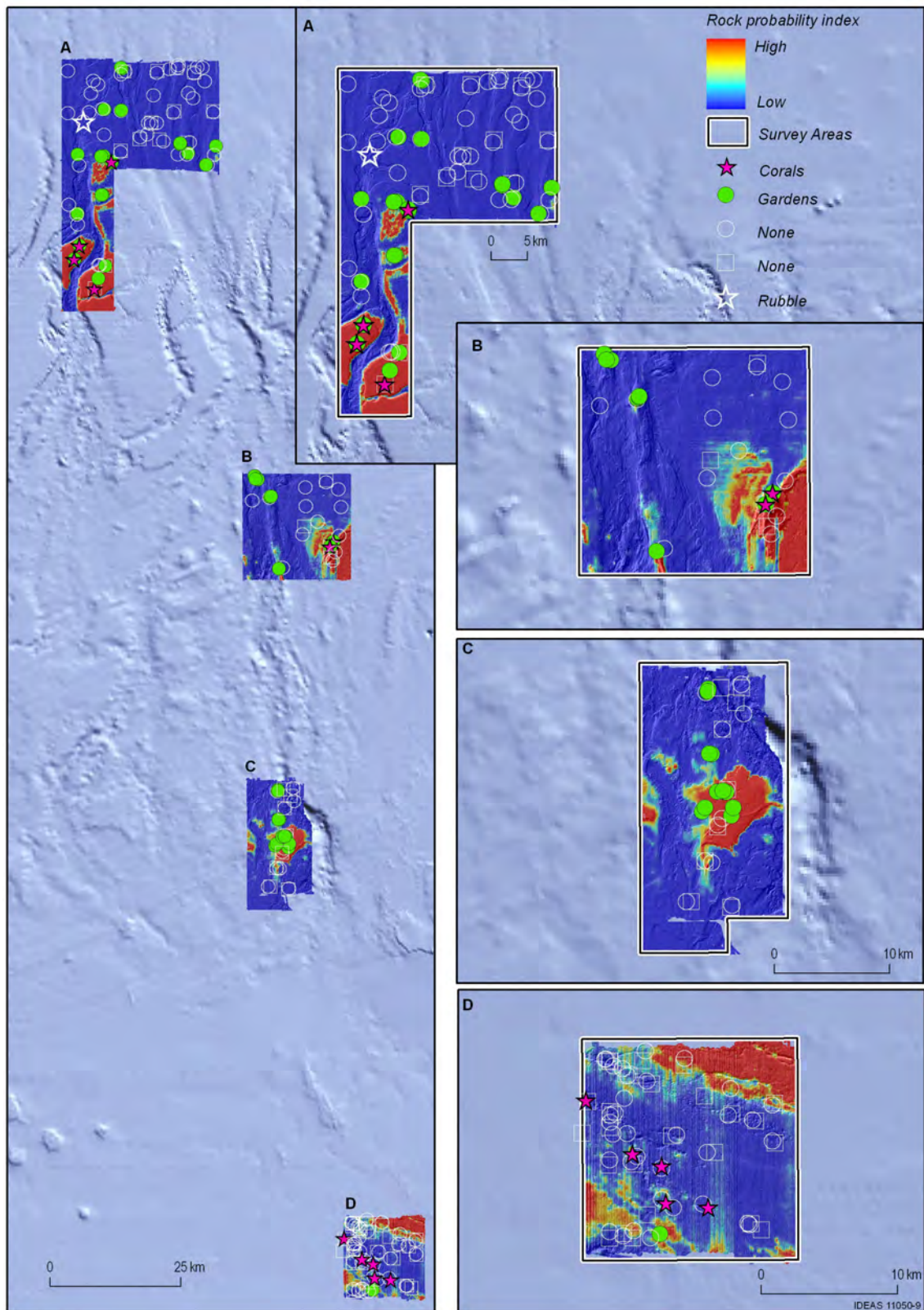


Figure 2.21: The locations of sponge and octocoral gardens and reef-forming hard corals found during surveys GA-322 and GA-325. The locations are overlaid on maps of rock probability based on an index described in [Appendix F](#). Letters indicate study areas.

3. Potential Hazards

The variability and complexity of seabed morphology and processes pose a range of engineering challenges to the construction, installation, and maintenance of seabed structures (Prior & Hooper 1999). Site-specific engineering on the seafloor requires a variety of basic geomorphological and geological information, including water depth, bottom slope and roughness, sediment properties, sub-bottom sediment geometries, rates of sedimentation, process assessments, and ages of seafloor and subsurface features (Hough et al. 2011). Surveying is directed towards identifying the possible occurrence of potentially hazardous processes such as erosion, faulting, fluid expulsion, and submarine landslides. Accumulation of shallow gas and fluids poses a range of hazards to the development of infrastructure such as undermining foundations and the potential ‘blow out’ during drilling (Sills & Wheeler 1992). In addition, wave hazards at the sea surface may pose a risk to vessel operations.

A review of scientific literature indicates that geohazards in the Joseph Bonaparte Gulf are not commonly documented despite the region being an area of active petroleum exploration for a number of decades. This indicates that the overall risk from geohazards in the region is likely to be low. The descriptions of potential geological and oceanographic hazards for the Bonaparte Basin region presented in this section are based on available literature and pre-existing survey datasets. Geophysical data from four surveys are used to identify evidence for fluid expulsion and slope failures (details in [Appendix A](#)), and sub-bottom profile data allows identification of potential geohazards from GA-322 and GA-325 survey areas ([Figure 3.1](#)). Oceanographic datasets and published literature are used to determine evidence for sediment mobility and to assess wave hazards at the sea surface.

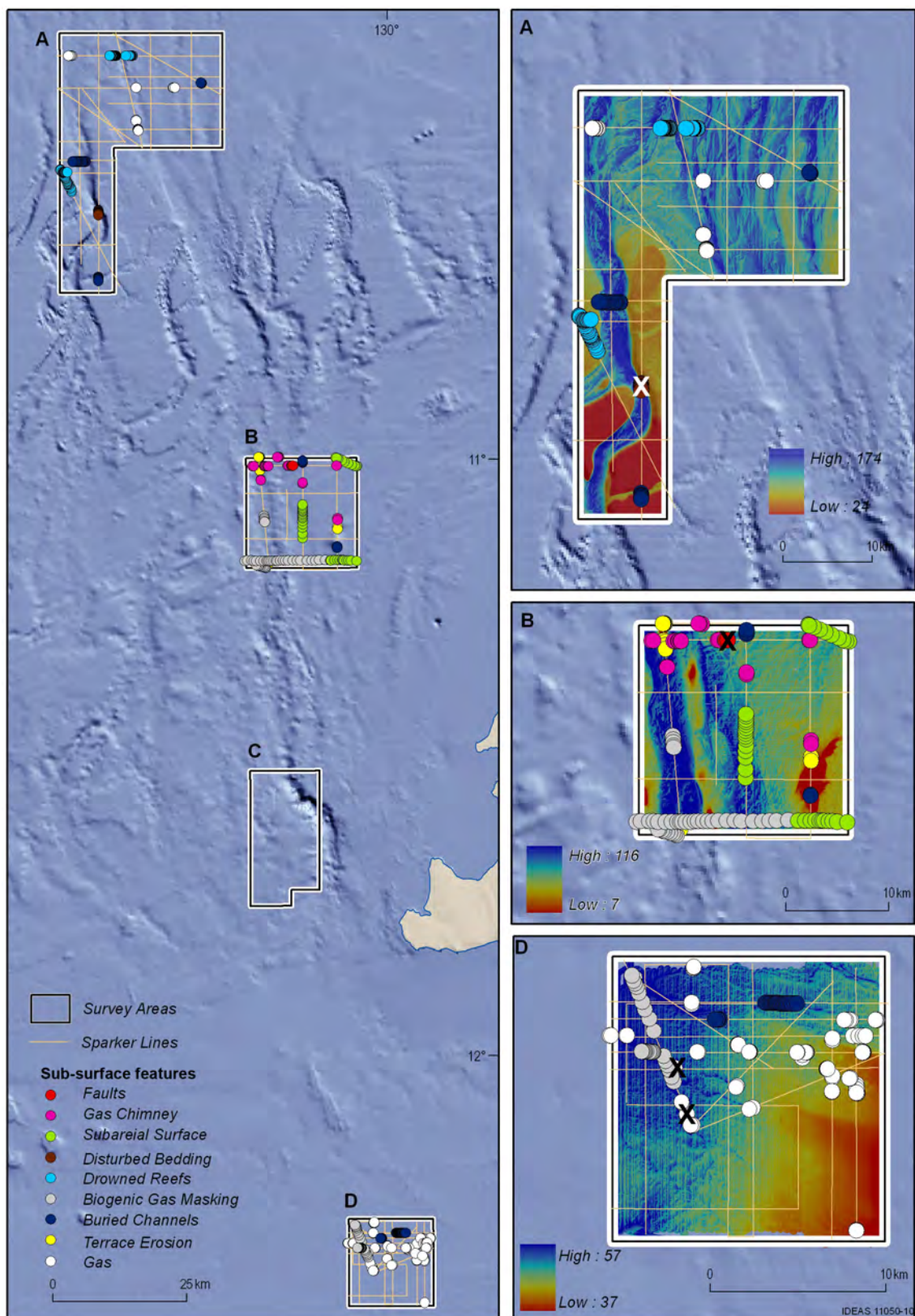


Figure 3.1: Map of potential geohazards and other sub-surface features as identified from sub-bottom profiles (SBPs) collected from surveys GA-322 and GA-325. Letters indicate study areas. An 'X' indicates the location of a SBP presented in Figures 3.3, Figure 3.4, or Figure 3.6

3.1 SLOPE INSTABILITY

Seabed sediment deposits can become unstable due to earthquakes and crustal movements, rapid sediment deposition, over-steepening, gas and fluid expulsion, and, in shallow water, ocean currents during severe storms (Prior & Hooper 1999). These unstable slopes fail when the down-slope component of stress (gravity and other factors) exceeds the resisting stress. Hazards generated by slope failure include changes in bottom morphology, removal or deposition of sediments leading to changes in foundation conditions, and burial of seabed infrastructure within depositional areas (Prior & Hooper 1999).

Slope failure is characterised by slides, slumps, and sediment gravity flows. Slides and slumps are the transport of materials along a discrete shear plane, with slides being translational and slumps rotational (Kennett 1982). Generally, they are common on slopes with gradients between 3-9 degrees, although they may form on slopes of less than 1 degree where sedimentation rates are especially high. Sediment gravity flows occur when the sediments in a slope failure can flow (Kennett 1982). Sediment gravity flows may occur in carbonate-dominated shelves, such as the Joseph Bonaparte Gulf, where over-steepening of carbonate slopes may lead to slope failure (Hampton & Locat 1996).

The risks associated with slope failure in much of the JBG-TS are minimal. At a regional-scale, most of the JBG-TS is flat with slope gradients commonly less than 2° (Figure 3.2a). Locally, however, steeper gradients of up to 20° occur within valleys located between the carbonate banks, terraces and ridges of the Van Diemen Rise (Anderson et al. 2011a; Heap et al. 2010) (Figure 3.2b). In an area mapped by high resolution multibeam sonar, the terraces and banks that flank the valleys display evidence of tidal scour and, in many areas, a moat at the base of the terrace. In addition, sub-bottom profile data across the steep slopes of the terrace sides show evidence of possible slope instability, in the form of slumping (e.g., Figure 3.3).

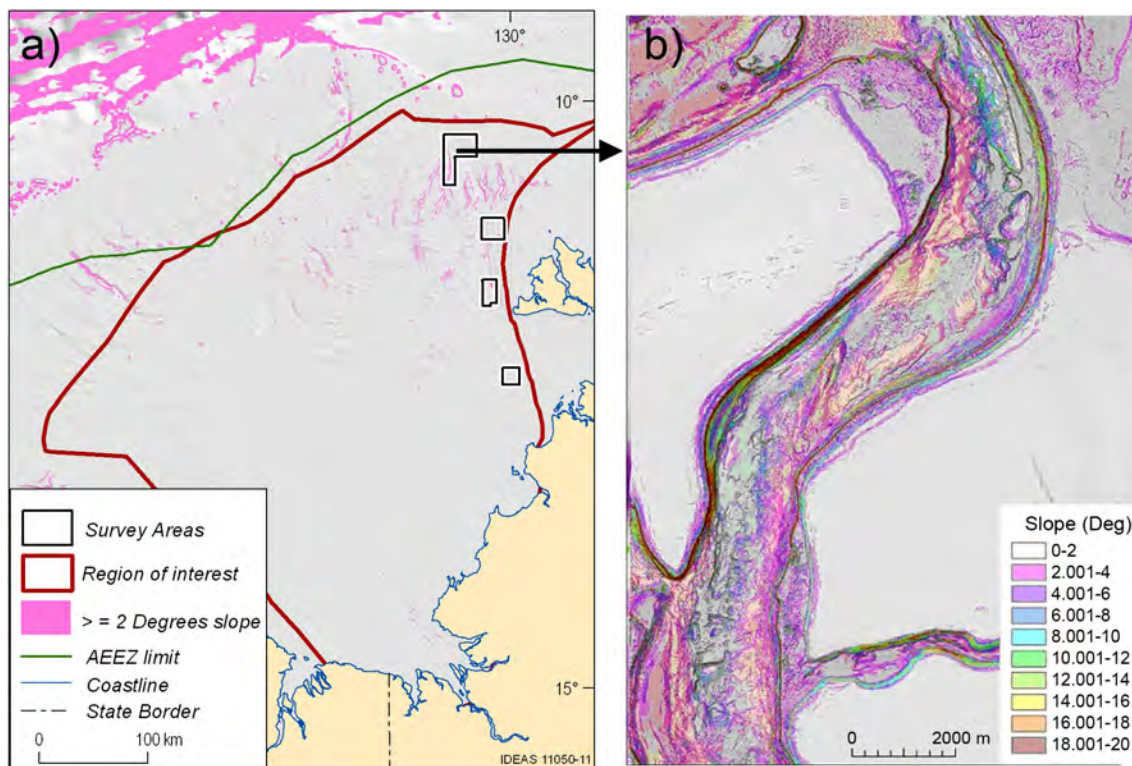


Figure 3.2: Slope map of the Joseph Bonaparte Gulf at: (a) a regional scale based on the 250 m Bathymetry grid of Australia (Whiteway 2009) and (b) a local scale based on multibeam bathymetry of the eastern JBG carbonate banks from surveys GA-0322 and GA-0325.

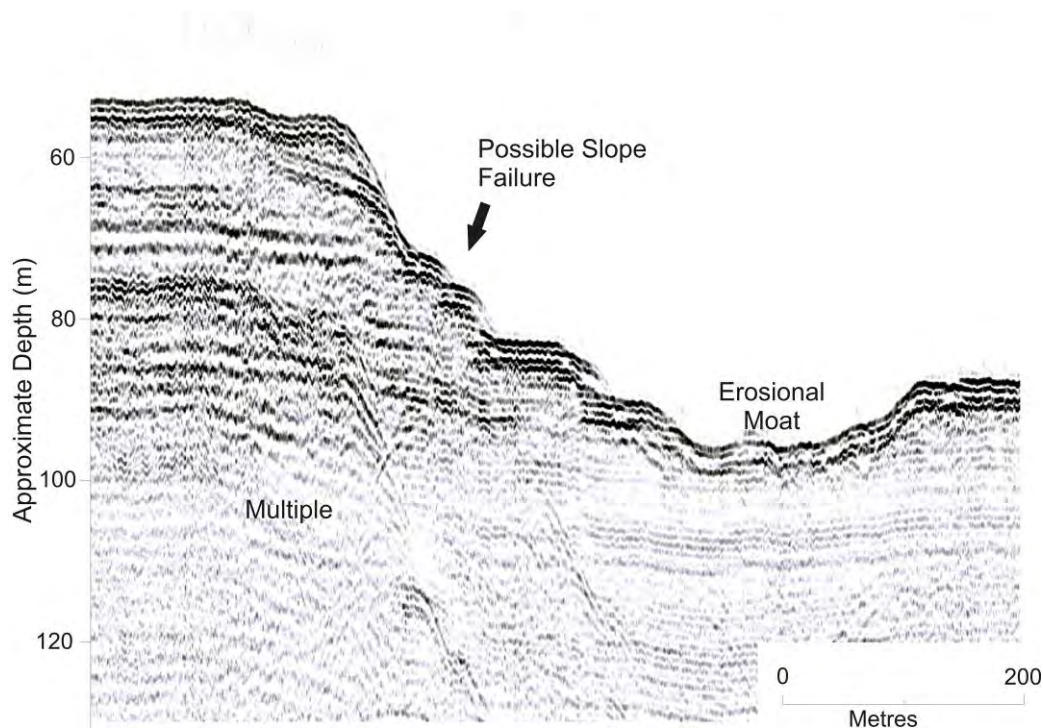


Figure 3.3: Sub-bottom profile from Geoscience Australia survey GA-0325 (Area A) showing possible slope failures on the flank of a terrace located on the outer shelf of JBG-TS. See [Figure 3.1](#) for location of SBP.

3.2 FLUID AND GAS EXPULSION

Submarine fluid and gas seepage can be a result of sediment overlying shallow gas deposits or breached hydrocarbon traps. On the northwest shelf, the Late Tertiary collision of the Australian and Eurasian plates has generated a compressional regime resulting in widespread extensional reactivation of existing faults in the Timor Sea area (Etheridge et al. 1991; Keep et al. 2002; O'Brien et al. 1999a). These faults are typically located at depths greater than 500 m below the seabed and are considered the major cause for numerous breached hydrocarbon traps in the region (O'Brien et al. 1996; 1999a; 1999b). Similar processes have resulted in active seepage on the Yampi Shelf to the southwest of the Joseph Bonaparte Gulf (Rollet et al, 2006). Many of the carbonate bank systems within the Timor Sea may have developed over active hydrocarbon seeps (Hovland et al., 1994; Heyward et al., 1997; Lavering and Jones, 2001; O'Brien and Glenn, 2005). The distribution of these reefs and banks in the Bonaparte region are found in [Figure 2.5](#). Little is known about the connectivity and flow between these faults and the seabed in the JBG. Sub-bottom profiler data, where available, may aid the identification of locations where faults and gas chimneys extend to within the upper 100-200 m of the region's sediment deposits ([Figure 3.4](#)).

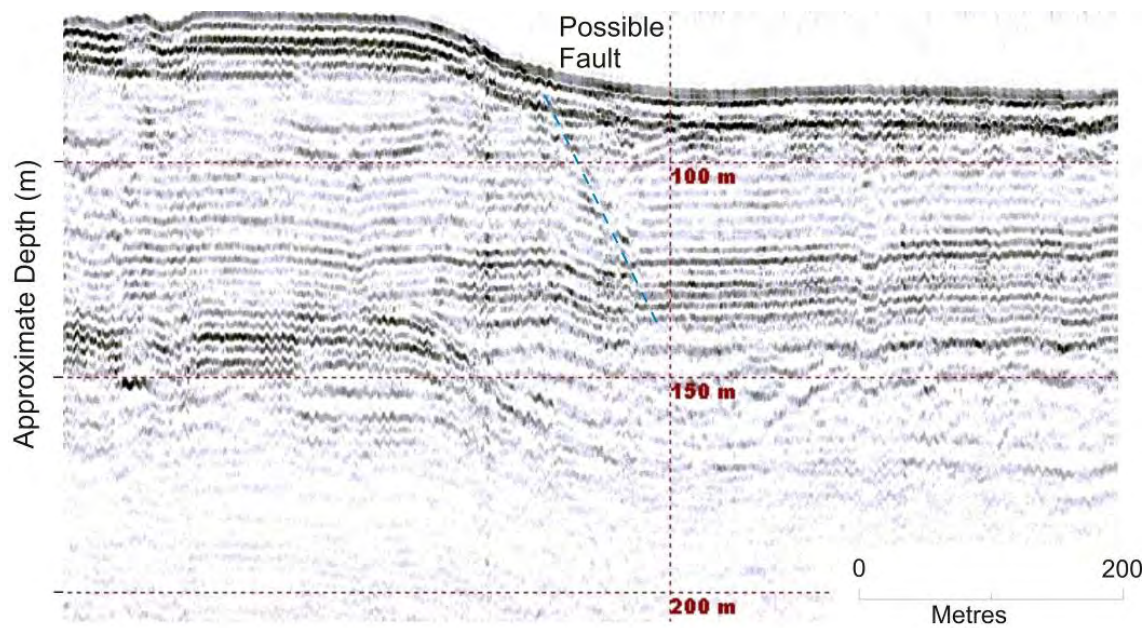


Figure 3.4: Sub-bottom profile from Geoscience Australia survey GA-0325 (Area B) showing possible faulting adjacent to the edge of a carbonate bank on the outer shelf of JBG-TS. See [Figure 3.1](#) for location of SBP.

Fluid and gas escape is commonly indicated by pockmarks, gas chimneys, hard grounds, domes, mud diapirs, plumes, and bioherms (Dando & Hovland 1992; Rollet et al, 2006). Pockmarks are depressions which are believed to have been formed by a rapid expulsion of fluid through the seabed causing the displacement of fine-grained sediment (Hovland & Judd 1988). They are typically found in basins containing fine-grained soft sediments which overlie shallow gas deposits. The depressions are frequently elongated in the direction of the prevailing currents and typically lack a rim (Hovland & Judd 1988; King & MacLean 1970). Gas chimneys are sub-surface expressions of gas leakage or expulsion. They cause the surrounding rock and sediments to have low sound velocities and are visible in seismic or sub-bottom profile data as ‘push-downs’ or areas of poor data. Numerous other techniques can be used to identify regions of expulsion from geochemical profiler and satellite imagery (reviewed in Logan et al. (2010).

The geomorphic expression of fluid and gas expulsion is commonly mapped by multibeam sonar, sub-bottom profiler, and sidescan sonar. Pockmarks in the JBG-TS are limited to sediment covered areas away from carbonate bank and reefs. They are common throughout the central Bonaparte Depression and in sediment covered channels and valleys, between carbonate banks, terraces and palaeoreefs (Anderson et al. 2011a; George & Cauquill 2010; Heap et al. 2010; WEL 2004) ([Figure 3.5](#)). They can occur in close aggregates with up to 100 per km² ([Figure 3.5](#)), although lower densities have been recorded from the northern JBG (URS, 2009). The pockmarks typically have sizes from 10-20 m diameter with some exceeding 4 m deep; many are elongated indicating locally-active bedload transport. Heap et al. (2010) presented limited evidence that these seeps are currently active for a pockmark field in Area D. In this area, scattering of the acoustic signal in the water column above a pockmark is interpreted as the product of gas bubbles providing a strong impedance contrast to the surrounding seawater.

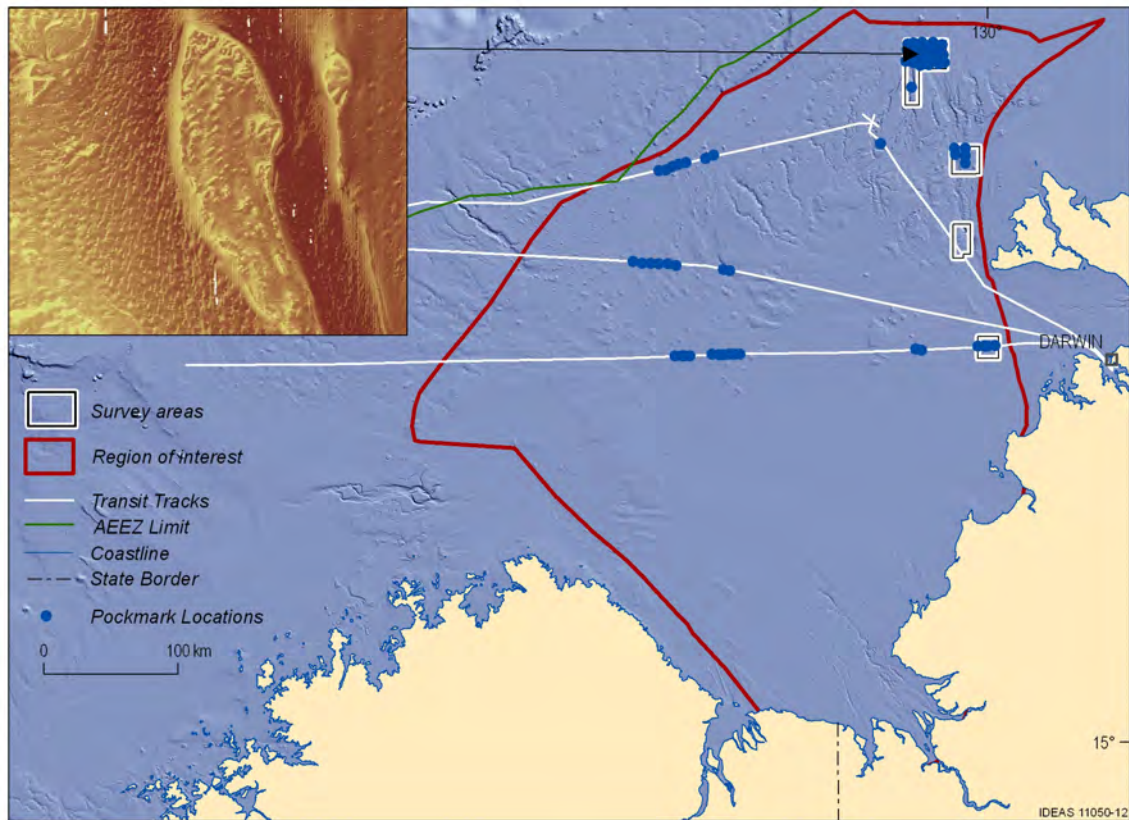


Figure 3.5: Locations of pockmarks in the JBG-TS from multibeam sonar surveys. Locations of pockmarks are shown in blue, vessel tracks are pink. The inset map shows pockmarks from eastern JBG-TS that are limited to areas in between banks.

The gas chimneys in the JBG-TS are commonly associated with buried channels located 50 – 70 m below the seabed and extend through the entire profile cutting through multiple stratigraphic units (Figure 3.1, Figure 3.6). Since the gas is derived from depth, the source may be thermogenic.

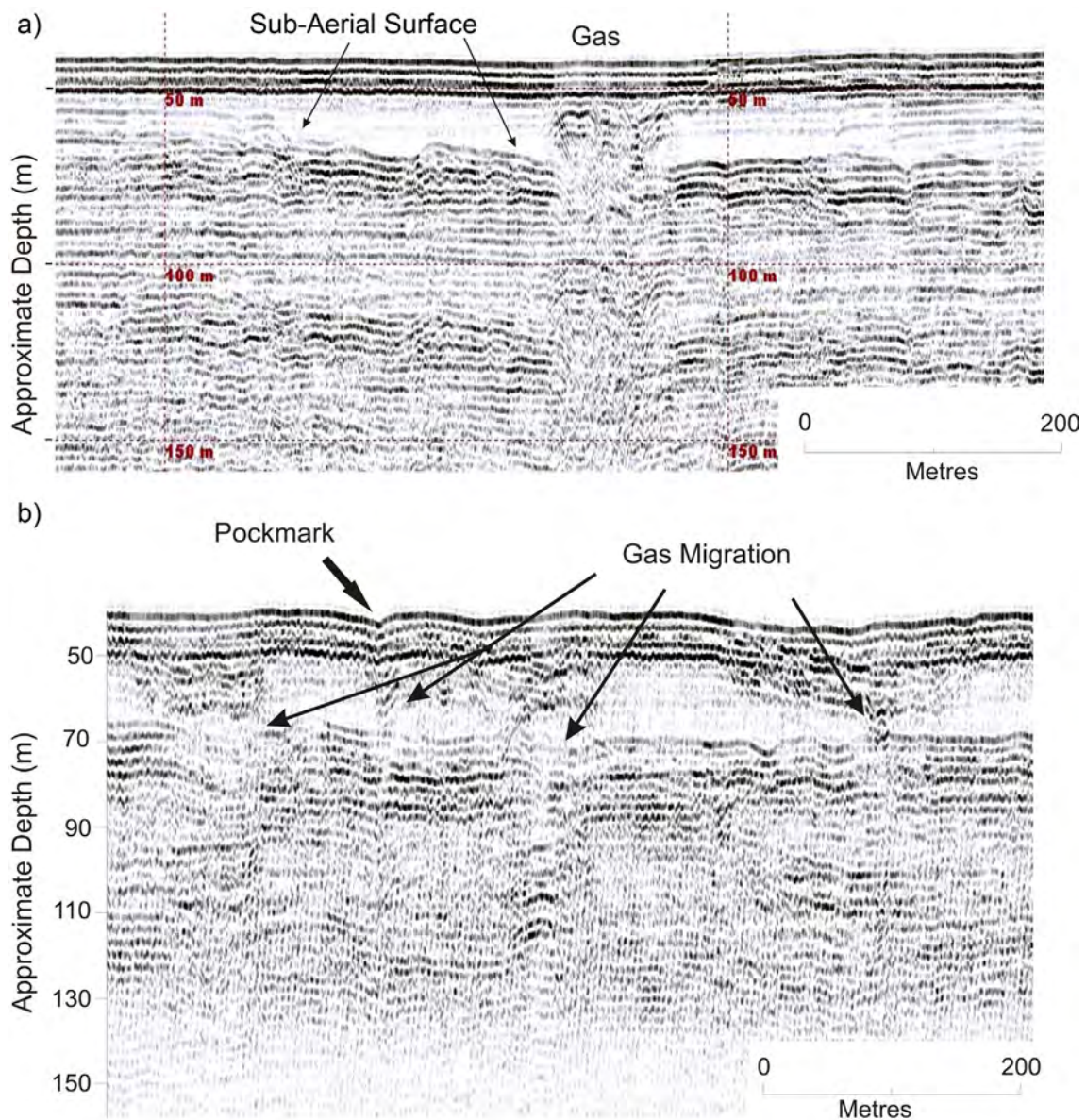


Figure 3.6: Sub-bottom profiles from Geoscience Australia survey GA-0325 (Area D) showing: (a) gas chimneys extending through the full profile, and; (b) pockmarks located above areas of gas migration on the inner shelf of JBG. See [Figure 3.1](#) for location of SBPs.

3.3 ELEVATED FEATURES / HARD GROUND

Elevated geomorphic features such as banks, shoals and reefs have been mapped at a regional-scale in the JBG-TS ([Figure 2.5](#)). Detailed multibeam surveys have mapped carbonate banks and shoals (of up to 25 m relief) that are not evident from the Australian 250 m bathymetry grid (George & Cauquill 2010) ([Figure 2.6](#)). For example, palaeoreefs have been mapped in the northern Bonaparte Basin, ranging between 80 – 1500 m in length and rising up to 35 m below sea level. As a result, the known distributions of carbonate banks and shoals are limited by resolution of regional-scale bathymetric data. Thus, it is likely that the presence of elevated features is likely to be more extensive than current bathymetric data indicate. Sub-bottom profiler data have also revealed

extensive, subsurface palaeoreefs within the JBG-TS (George & Cauquill 2010) (Figure 3.1). These reefs exist beneath a layer of unconsolidated sediments and may pose issues for dredging or ploughing in the region.

Extensive areas of hard ground (Area D from Solander surveys) and scour zones (Lees 1992) also occur within the JBG-TS. These zones are commonly limited to shallow regions that are subject to highest rates offshore directed bedload transport.

3.4 EROSION AT THE SEABED

The JBG-TS region is macro-tidal, and the average spring tide range is >7 m (Lees 1992). The large tidal range generates strong currents, with current velocities of up to 3.0 ms^{-1} measured at the Cambridge Gulf (Coleman & Wright 1978) (Figure 3.7). These strong tidal currents scour the inner shelf and transport seabed sediments towards the deeper part of the shelf. In the marine environment, three common types of sediment accumulations form as a result of tidally driven flows: ripples, dunes and sand banks (Ashley, 1990). Lees (1992) mapped the distributions of bedforms in part of the inner JBG (Figure 3.7) from scour zones to areas of sand dunes and ripples, revealing that sediment mobility associated with bedforms (e.g. sand dunes, sand banks) is highest near the coast. The bedload transport Shields parameter shows similar high levels of sediment mobility in the inner JBG and also reveals high mobility along the Van Diemen Rise (Figure 3.8).

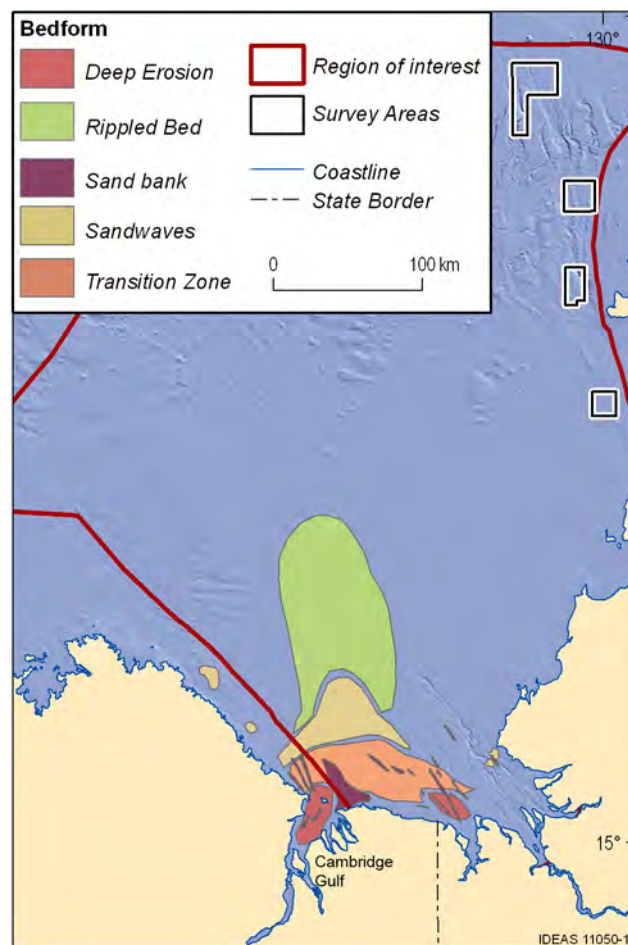


Figure 3.7: Map of bedforms distributions from Lees (1992) and modified using additional data from Royal Australian Navy charts 316 and 318

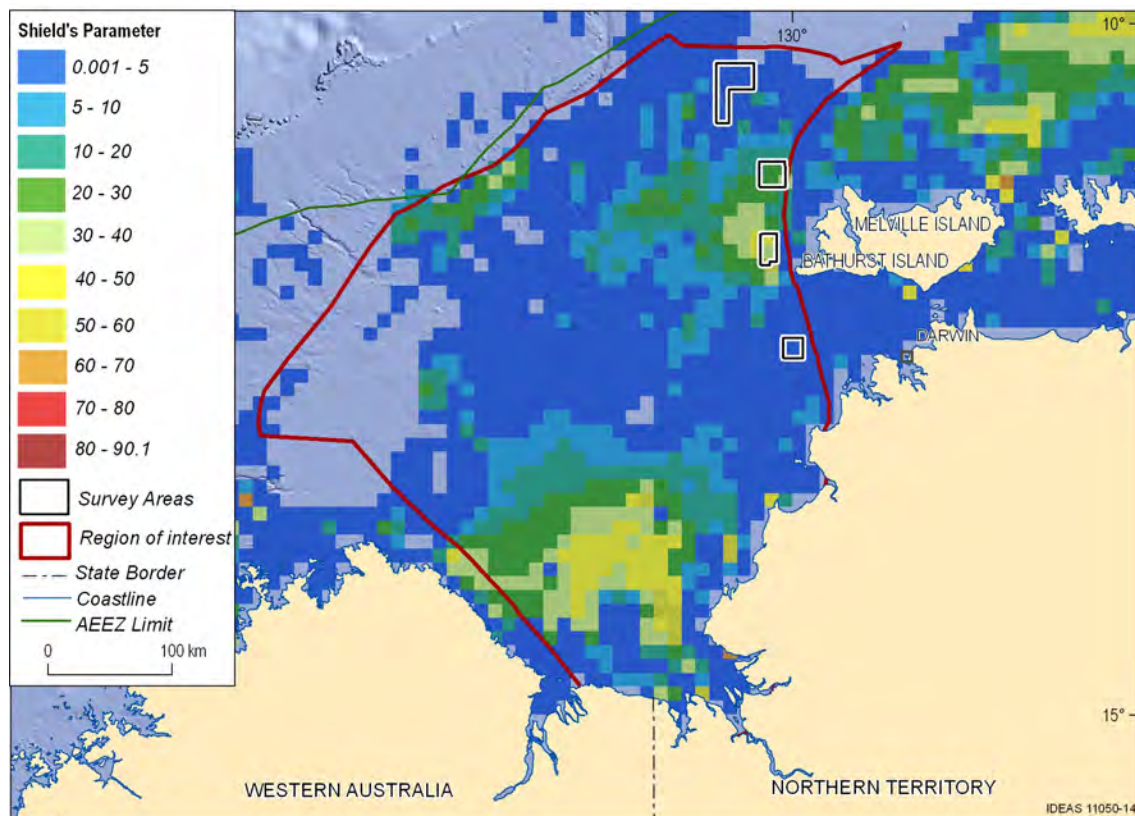


Figure 3.8: Map of bedload transport Shield's parameter

In deeper water (>100 m) a repeat bathymetric survey of an area of ridges and valleys in the northeastern JBG-TS did not detect any change in seabed morphology between 2009 and 2010 (Area A in Anderson et al. (2011)). This suggests that even across potentially higher-risk areas, the seabed in the JPB-TS is stable over annual time scales. However, no major cyclones in the area during this time thus their potential impacts remain unknown.

3.5 OCEANOGRAPHIC HAZARDS AT THE SEA SURFACE

This section presents model hindcast data on wave conditions across the Joseph Bonaparte Gulf to assist informed assessment of hazards due to surface waves. No long term wave measurements were available to verify the hindcast data, but some measurements are available from short deployments during surveys GA-322 and GA-325. A description of the oceanographic models and detailed interpretation can be found in [Appendix G](#).

The pattern of wave heights across the JBG-TS reveals broadly shore-parallel bands of increasing wave height in an offshore direction ([Figure 3.9](#)). This is true for all the percentiles shown and reflects the greater impact of wave diffraction and frictional dissipation in shallow water depths. It also reflects the greater fetch distances available offshore. The eastern JBG-TS tends to be less energetic than the western JBG-TS, because it is the lee shore for the wind regime primarily responsible for larger waves (i.e. SE Trades). Mean and 50th percentile values for H_s inside the gulf are typically <1 m. The 95th percentile values inside the gulf range up to 2 m, and up to 2.5 m further offshore ([Figure 3.9](#)).

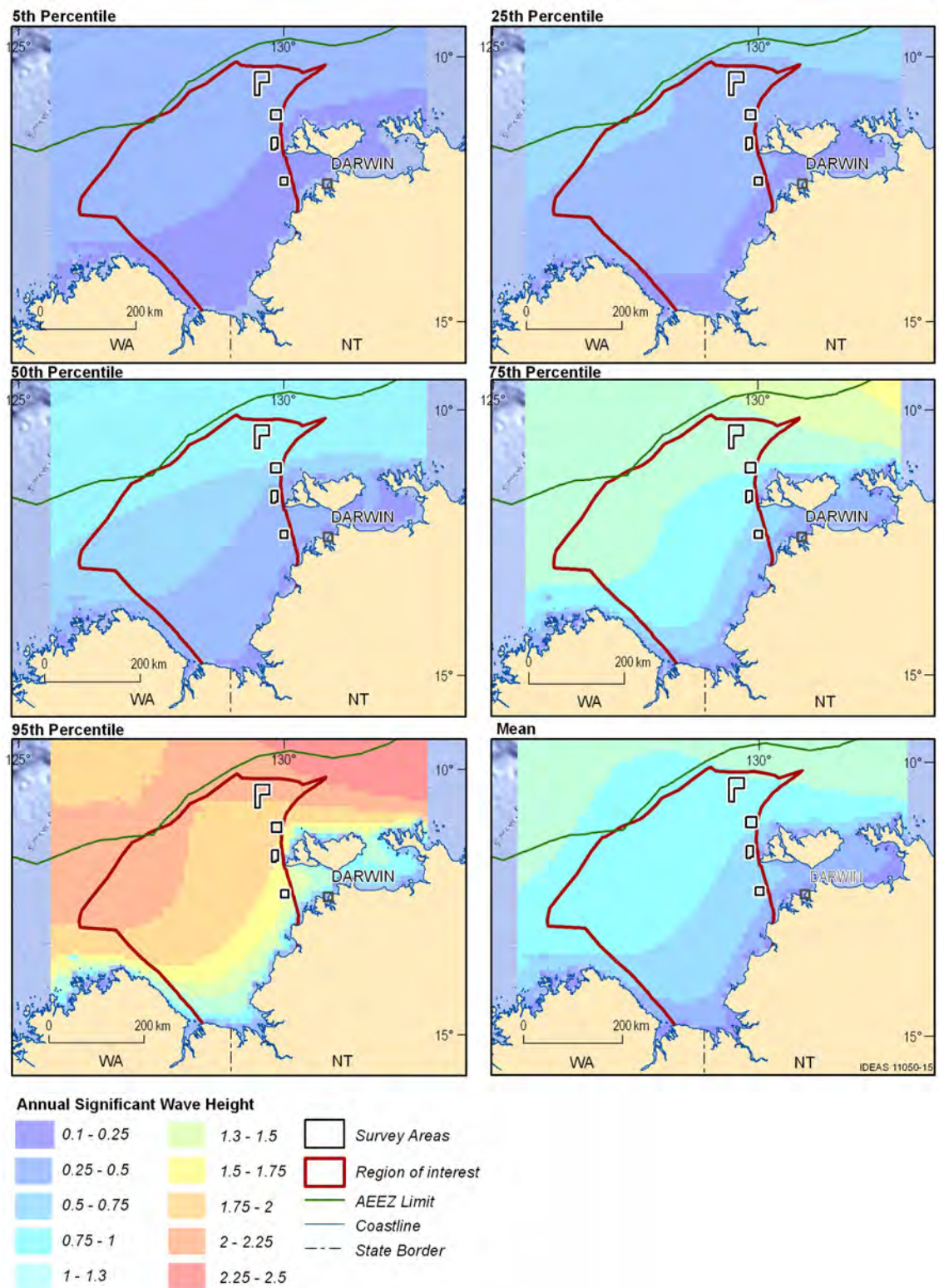


Figure 3.9: Statistics for annual significant wave height, H_s in metres at difference percentiles and mean.

The most energetic seasons with respect to significant wave height are centred on January and July (Figure 3.10) due to monsoon and trade wind seasons, respectively. While the largest waves in the region occur in July, they mostly occur outside of the Gulf waters. Significant wave heights inside Gulf waters are restricted to <1 m, due to the short fetch distance associated with the southeasterly

wind regime at this time of year. The northwesterly wind regime during January results in relatively smaller waves across the region overall, but waves up to 1.2 m penetrate into gulf waters, due to the favourable fetch (Figure 3.10). The small wave heights, <0.8 m, that persist across the entire region outside the monsoon and trade wind seasons demonstrates that the wave climate is dominated by locally-generated sea; very little swell penetrates the region.

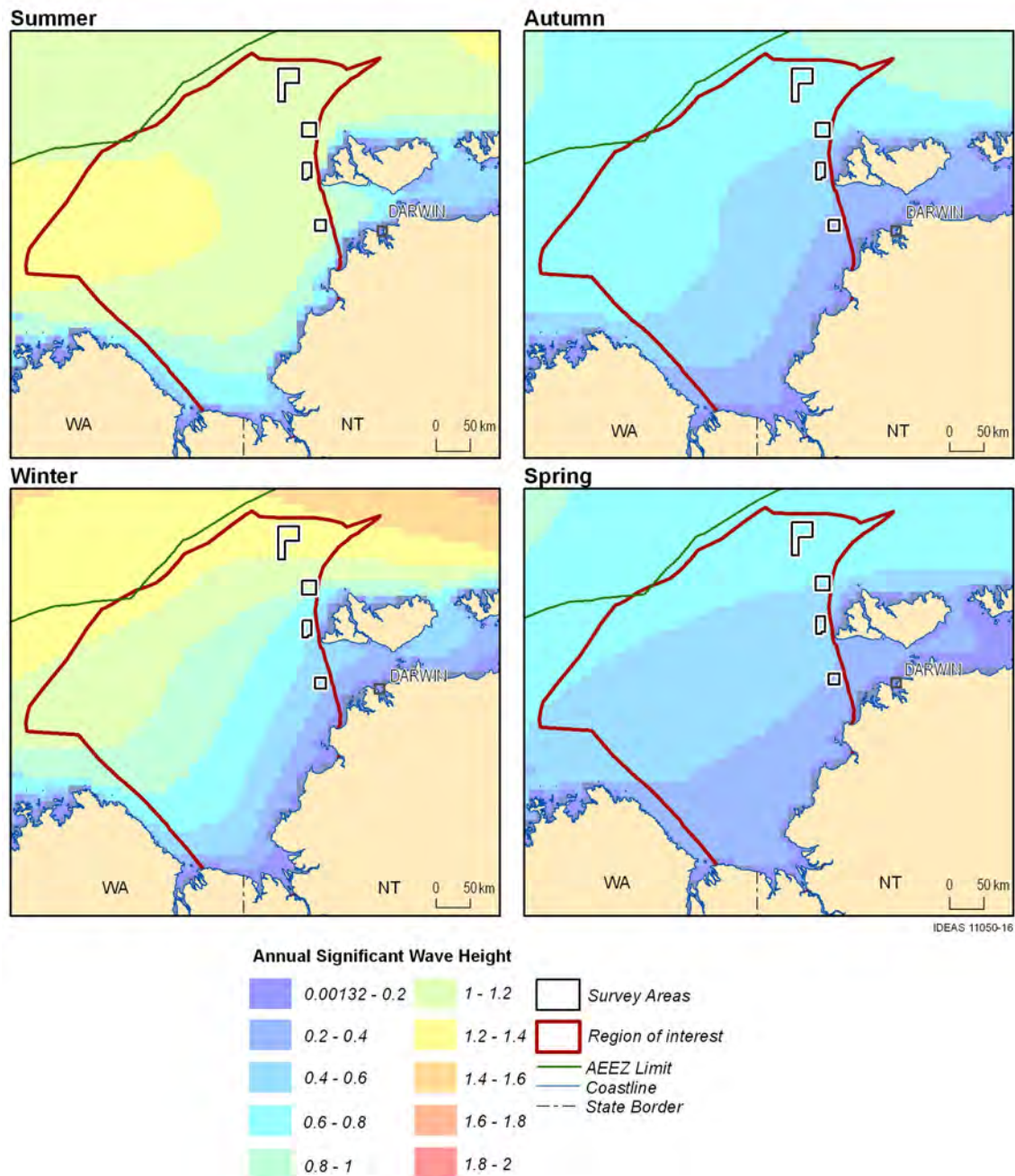


Figure 3.10: Statistics for annual significant wave height, H_s in metres, for different seasons.

A hindcast time series from the central JBG shows that a mean wave period of 5-6 s is typical of the local sea conditions (Figure 3.11). The mean wave period reaches 10 s during short-lived events. The raw time series and the box-and-whisker summary plots reiterate that, on average, the largest wave heights occur during January and June-July. Figure 3.11c shows, however, that extreme wave heights of up to 8 m can occur between December and March associated with tropical cyclones. The

four largest events in the record shown in Figure 3.11a occurred in December 1998, March 2004 and 2005, and January 2008. The tropical cyclones responsible for these events are listed in Table 3.1 and their tracks are shown in Appendix G.

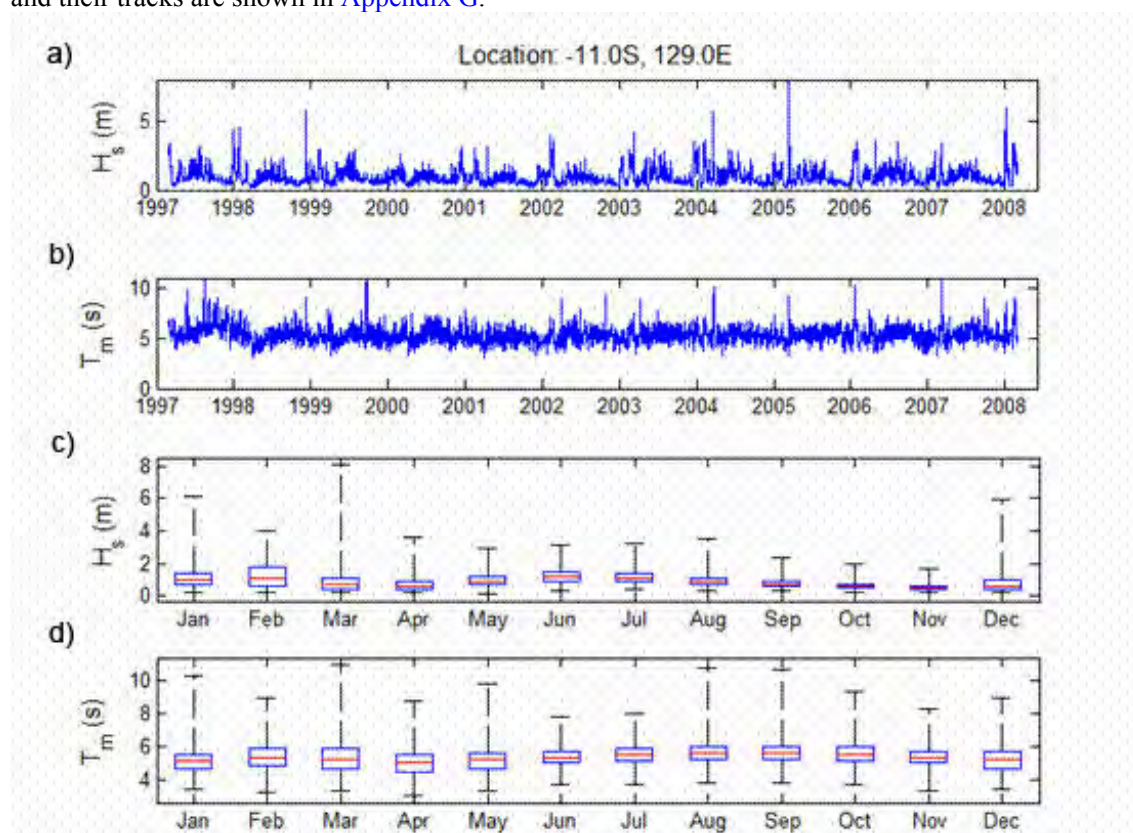


Figure 3.11: Example 11-year time series showing wave conditions from a location in the outer Gulf; 11° S, 129° E: (a) time series of significant wave height H_s in metres; (b) mean wave period T_m in seconds; (c) box-and-whisker plot of H_s ; and (d) box-and-whisker plot of T_m . The horizontal red line shows the median value, the vertical extent of the blue box shows the inter-quartile range and the vertical dashed line shows the entire data range.

Table 3.1: A listing of cyclones between 1997 and 2008 that produced significant wave heights larger than 5 m in gulf waters. LCP = lowest central pressure (hPa); LWS = largest wind speed (10-minute average; knots). Information was compiled from the Australian Bureau of Meteorology and the Joint Typhoon warning Centre.

NAME	DATE IN JBG-TS	CATEGORY	LCP ²	LWS ³
TC Thelma	8-10 Dec 1998	5	925	120
TC Fay	16-18 Mar 2004	3	970	70
TC Ingrid	14-16 Mar 2005	5	935	110
TC Helen	3-4 Jan 2008	2	975	50

The largest significant wave height at the location presented in Figure 3.11 of approximately 8 m was associated with the second most intense cyclone, TC Ingrid. Category 2 and 3 cyclones TC Helen and TC Fay produced similar wave heights to those generated by the most intense cyclone, TC Thelma. The wave heights at a specific location depend not only on the wind speed, but the track of the cyclone, which affects the fetch distance. It appears that all cyclone categories are therefore capable of producing significant wave heights of over 5 m in the outer JBG-TS.

4. Conceptual Models

In this chapter, conceptual models and a generalized habitat map are presented to provide an integrated summary of the key biophysical processes operating in the JBG-TS. The models and map capture local-scale spatial patterns and relationships as observed in survey areas and regional-scale trends related to broad bathymetric and oceanographic influences on seabed habitats, biological communities and potential geohazards.

Limited biological data in the JBG-TS region precludes the development of a regional habitat map based on empirical methods (e.g. Robinson et al. 2011), but the generalized map in [Figure 4.1](#) nonetheless broadly indicates the likely distribution of general habitats and biological communities in the JBG-TS. In this map, similar regional-scale geomorphic features are combined and characterized according to available biological data ([Appendix A](#)). For example, both basin and shelf features include low-relief expanses of unconsolidated sediment, and the available biological data suggests that these habitats are dominated by infauna with limited epifauna irrespective of geomorphic feature ([Appendix C](#); URS 2009). The majority of the JBG-TS is likely characterized by infaunal plains, with some localized reefs and outcrops supporting sponge gardens ([Figure 4.1](#)). Large expanses of barren sand banks are likely to occur in the inner Gulf due to sediment mobility. The outer JBG-TS is characterized by sponge gardens and epifaunal terraces interspersed with deep valley communities and is thus a more heterogeneous area than the inner JBG-TS.

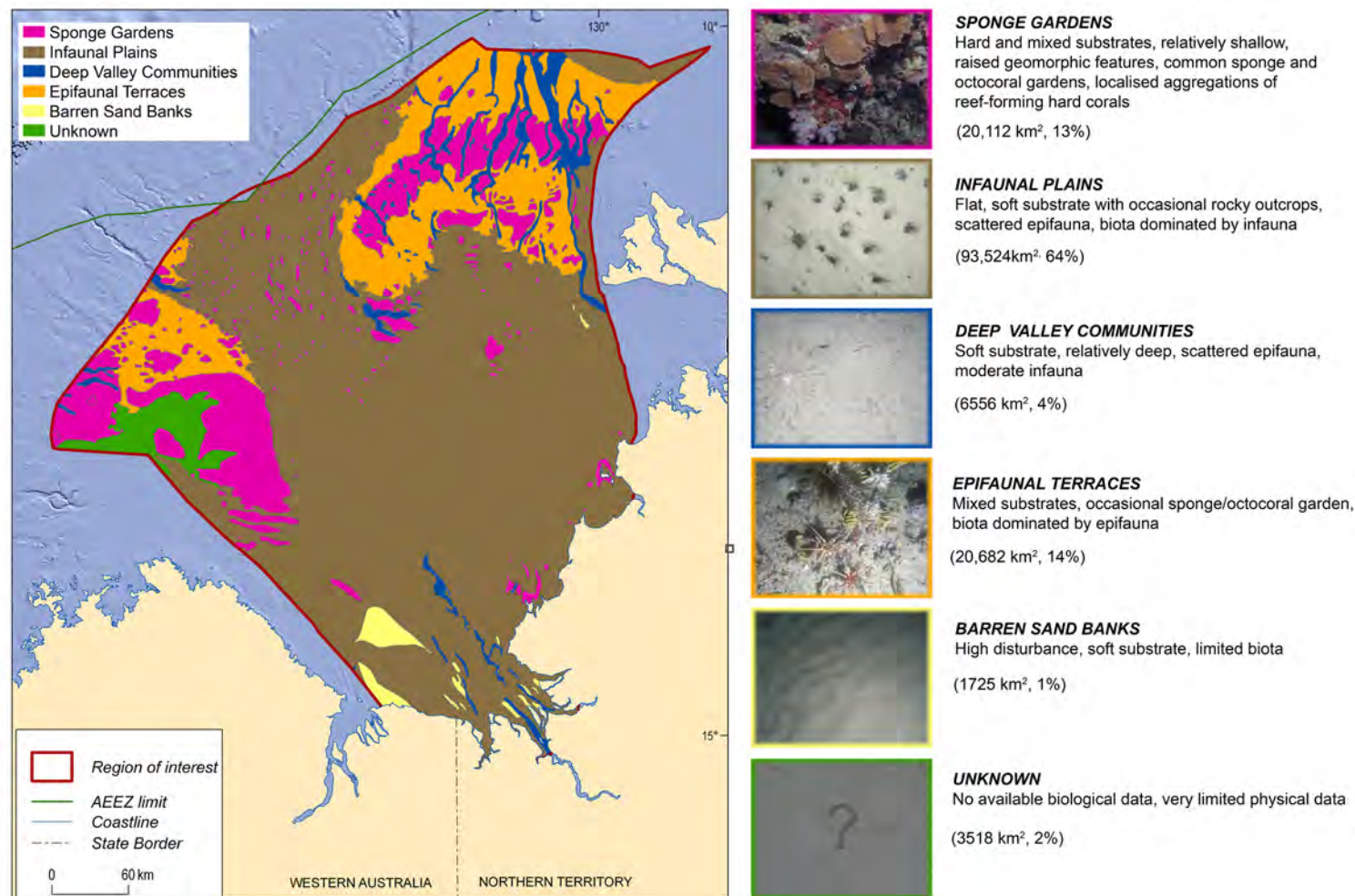


Figure 4.1: A generalised habitat map showing the potential distribution of habitats and biological communities in the JBG-TS. Habitats are based on the combination and characterisation of regional-scale geomorphic features according to available biological data. Parentheses indicate area of coverage for each habitat with percentages expressed as total area of the region of interest.

Cross-shelf and along-shelf patterns in the distribution of seabed habitats and associated biophysical processes are represented by the conceptual models shown in [Figure 4.2](#) and [4.3](#).

In the cross-shelf model, the inner part of JBG-TS encompasses extensive sediment plains that are swept by strong tidal currents and are subject to large influxes of suspended sediment and freshwater, particularly during the wet season. The region is also affected by cyclones on an approximate frequency of once every 3 years. These events generate waves of sufficient size to disturb the seabed of the inner JBG-TS, with all parts of this low gradient seabed potentially impacted. Together, these oceanographic and bathymetric conditions result in benthic habitats characterised by regular re-suspension of fine-grained sediments leading to reduced light availability. Algae and photosymbiotic animals are therefore limited in their ability to photosynthesise. Sessile epifauna generally occur only as isolated individuals on scattered rocky outcrops and on consolidated sediments located on the edge of shallow channels. In turn, these organisms support other animals (e.g. crustaceans and echinoderms) but in low overall abundance.

The sediment plains are not biologically barren zones, however, as they support diverse infaunal communities ([Figure 4.4](#)). These communities play a key ecological role by contributing to nutrient cycling and sediment turnover (bioturbation) at the local scale. The richness of these infaunal communities is likely driven by nutrients from decaying phytoplankton, (e.g. *Trichodesmium*) and, to a lesser extent, sediment-bound organic matter. Soft sediment habitats of the inner JBG-TS are also characterised by numerous shallow pockmarks. These distinctive seabed features provide evidence for connectivity to sub-bottom diagenetic processes, with release of biogenic gas or fluids from shallow (< 50 m) sedimentary deposits a likely cause.

The mid to outer parts of the JBG-TS, including the Van Diemen Rise, incorporate a mix of low relief and raised geomorphic features ([Figures 4.5, 4.6, 4.7](#)). Low relief features include plains and channel floors characterised by sediments that support rich infaunal communities but sparse epifauna. In contrast, raised features (banks, ridges, terraces) support diverse epifaunal communities, including sponge and octocoral gardens. Again, these epifaunal assemblages provide habitat for other species. The richness of epifauna is clearly due to the greater availability of hard substrata and light on these raised features, relative to the deeper valleys and plains. In addition, the influence of tides and associated turbidity on biota is less in these waters due to increased distance from the coast.

Localised variability in epifaunal assemblages is observed between banks and terraces across the mid to outer Gulf. For example, Moss Shoals (Area B) is a bank that is dominated by the octocoral *Tubipora musica* (pipe organ coral) which has a hard skeleton that contributes to the reef structure on this bank. No other banks were found to have the same dominance of this particular coral species. Similarly, dense patches of reef-forming corals occur on the outer banks (Area A) but not on any other bank surveyed in this study. It is not known if these differences in species distribution are regulated by water quality (e.g. turbidity, food availability), anthropogenic factors (e.g. historical fishing activity) or geological factors (e.g. substrata, sediments), or some combination of these.

The raised geomorphic features of the mid to outer JBG-TS are also associated with a range of potential geohazards related to stability of the seabed. Stratigraphic evidence for slumps and faults is observed in sub-bottom profiles across some valley walls and ridges of the mid to outer Gulf. However, whether these slumps and faults are active is not known. Repeat mapping of a ridge and channel network in the outer Gulf did not detect any change in the form or position of these features, suggesting that regular tidal processes do not drive large scale morphological change at these depths (50 – 130 m). However, this does not preclude episodic change due to cyclone-generated waves and currents.

In addition to cross-shelf variability, the seabed morphology, oceanography, and biota of the JBG-TS is characterised by along-shelf variation due to the Bonaparte Depression ([Figure 4.3](#)). The along-shelf profile of the Gulf ranges from shallow (<40 m) coarse-grained, tidal sandbanks and

dune fields in the southwest (e.g. Medusa Bank and King Shoals) to silt to clayey sands in the deeper and low-energy Bonaparte Depression. This transition also involves a change from coarse siliciclastic-dominated sediments derived from rivers to fine calcareous-dominated sediments in the deeper areas. The habitat complexity in the areas influenced by strong tidal currents and high turbidity is likely to be limited. Palaeoreefs and relict channels are observed in regional-scale bathymetric data from the Bonaparte Depression. High-resolution bathymetry data also indicates that parts of the Bonaparte Depression have extensive pockmark fields. Habitat complexity in these areas will be limited by water depth (commonly 80-90 m) which limits photosynthesis, although palaeoreefs may provide hardground for sessile epifaunal communities. Toward the northeast, the along-shelf profile of JBG transitions to the carbonate-dominated, bank and ridge morphology of the Van Diemen Rise (described above).

In addition to the spatial patterns in habitats captured by the conceptual models presented here, temporal variations in environmental processes occur over seasonal to inter-annual timescales. In particular, primary productivity and turbidity are highest during the wet season, with variability most evident in the inner Gulf and decreasing with distance from the coast. During the wet season, cyclones occur, with magnitude and duration varying from year to year. Cyclones can cause mechanical damage to communities in shallow waters (e.g. banks), as well as increasing bank erosion and the risk of slope failure.

These conceptual models and generalized map provide an important overview of the key processes and linkages that affect the distribution of significant habitats, communities and geohazards in the JBG-TS. An understanding of these processes will further inform marine management and development in the region by identifying potential drivers of habitat and hazard distribution and facilitating predictive models.

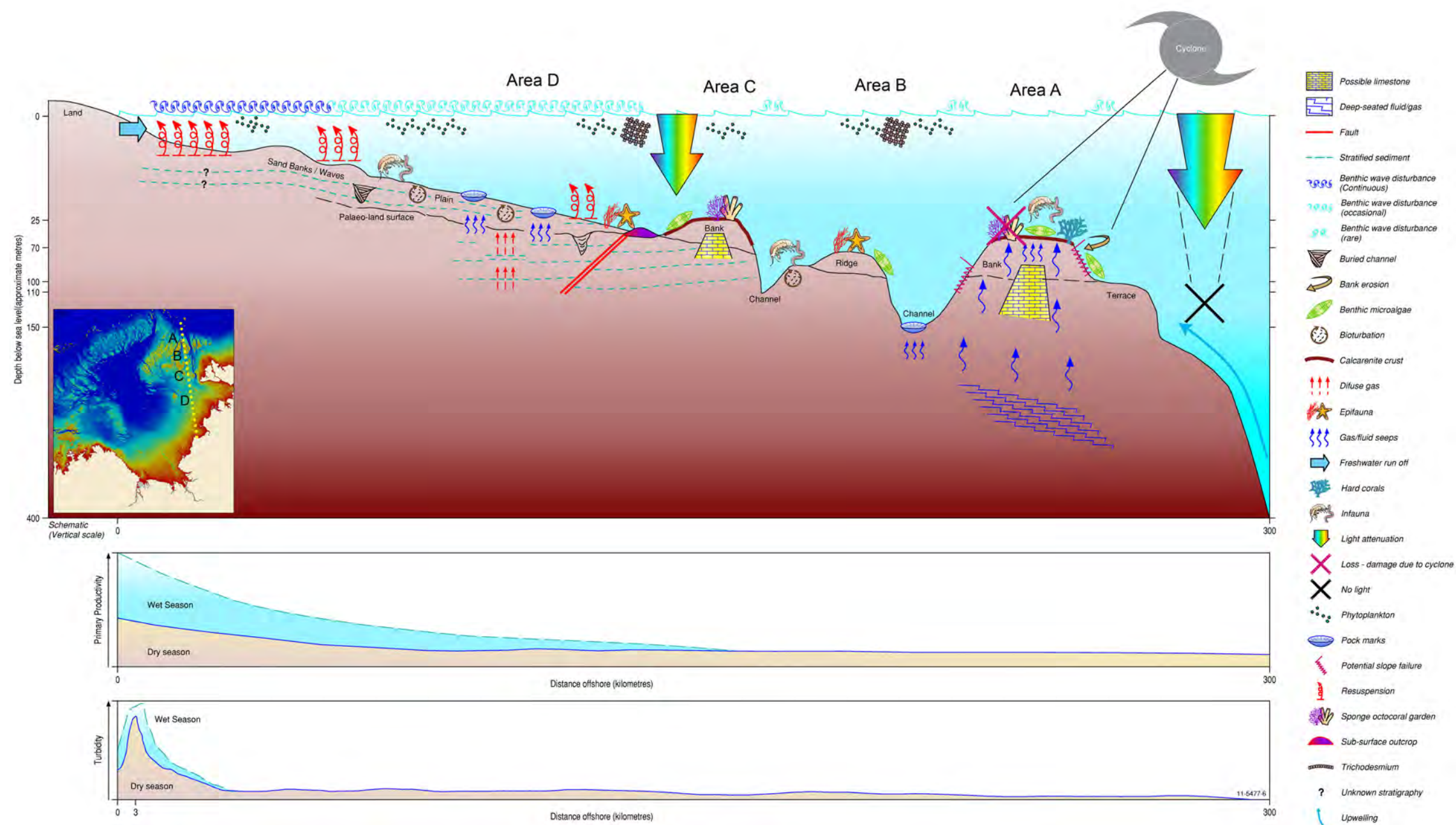


Figure 4.2: A conceptual model showing the biophysical processes operating in the eastern JBG-TS across the shelf in a S to N transect marked by the inset map (approximate survey areas marked with letters in inset map and on top of conceptual model). The nearshore environment (S) is shallower, flatter, dominated by soft sediments and associated taxa, with scattered rocky reefs near sand banks (Areas D). Further offshore (N), the environment is deeper, steeper and dotted with palaeoreefs and banks/ridges/terraces separated by valleys (Areas C, B, A).

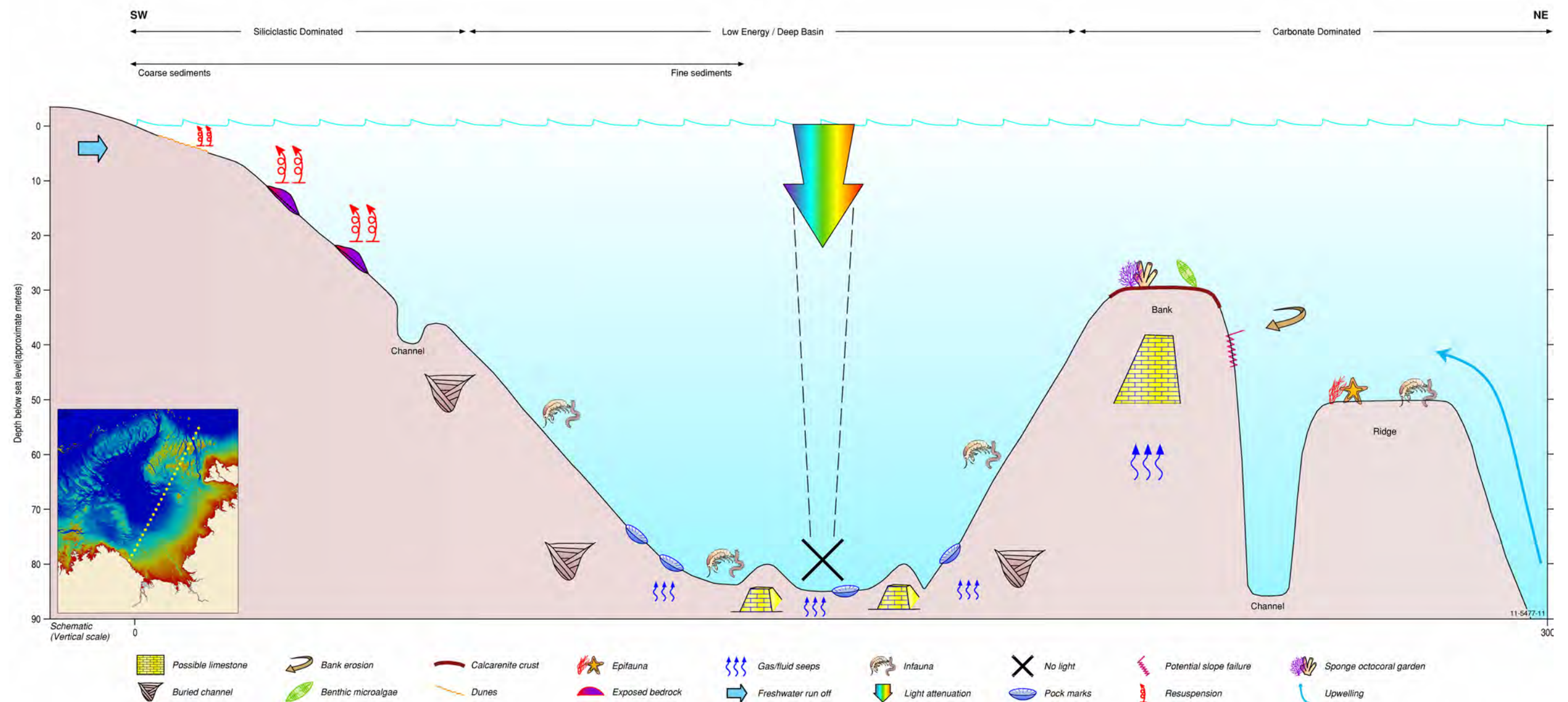


Figure 4.3: A conceptual model showing the biophysical processes operating in the JBG-TS along the shelf in a SW to NE transect marked by the inset map. The SW shelf adjacent to the basin gently slopes to deeper water and flat soft sediment ecosystem of the basin, interspersed with pockmarks and buried palaeoreefs. To the NE of the basin, the environment is steeper with comparatively complex topography, including banks/ridges/terraces separated by valleys..

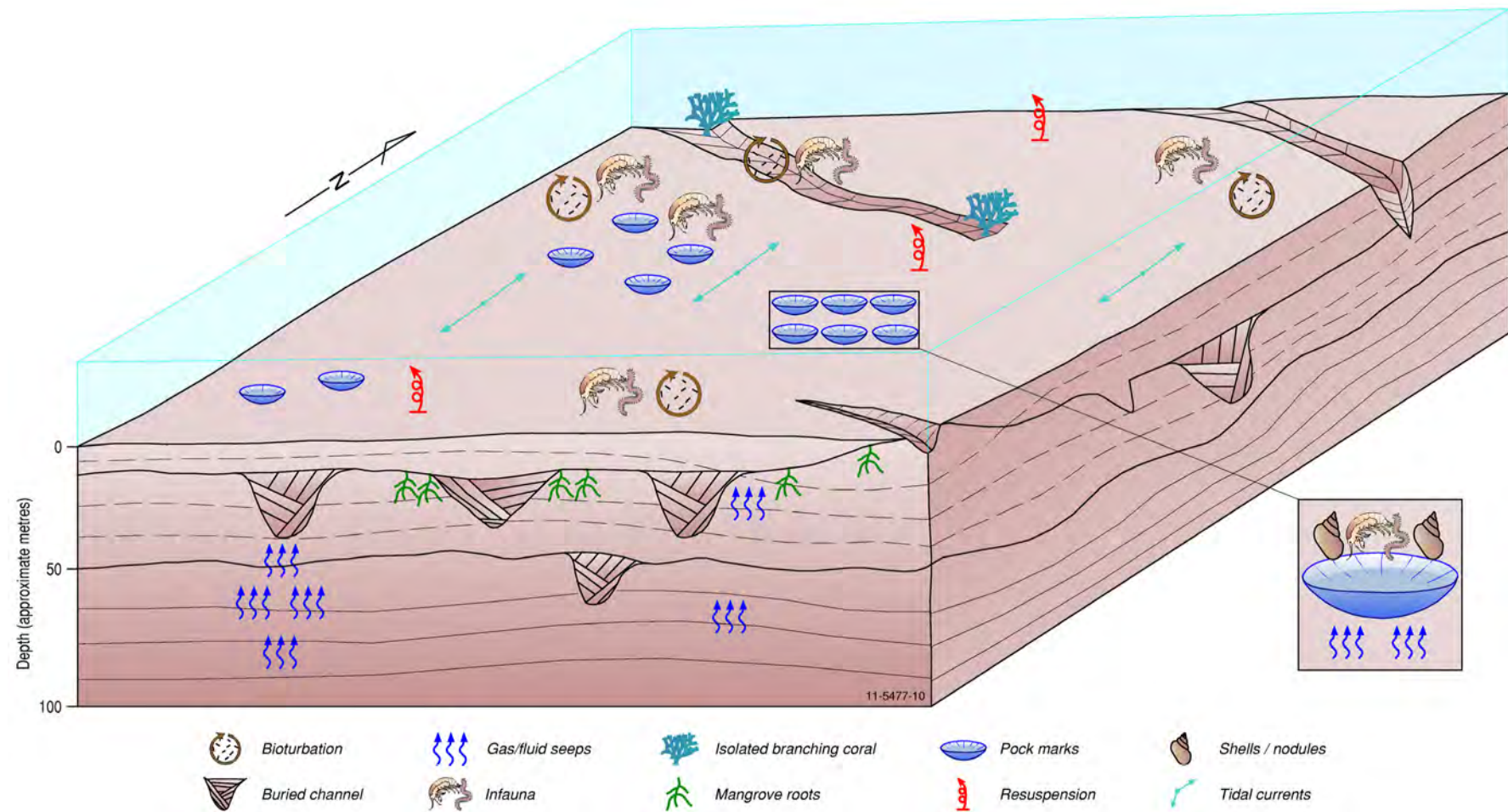


Figure 4.4: A conceptual model showing the biophysical processes operating in Area D.

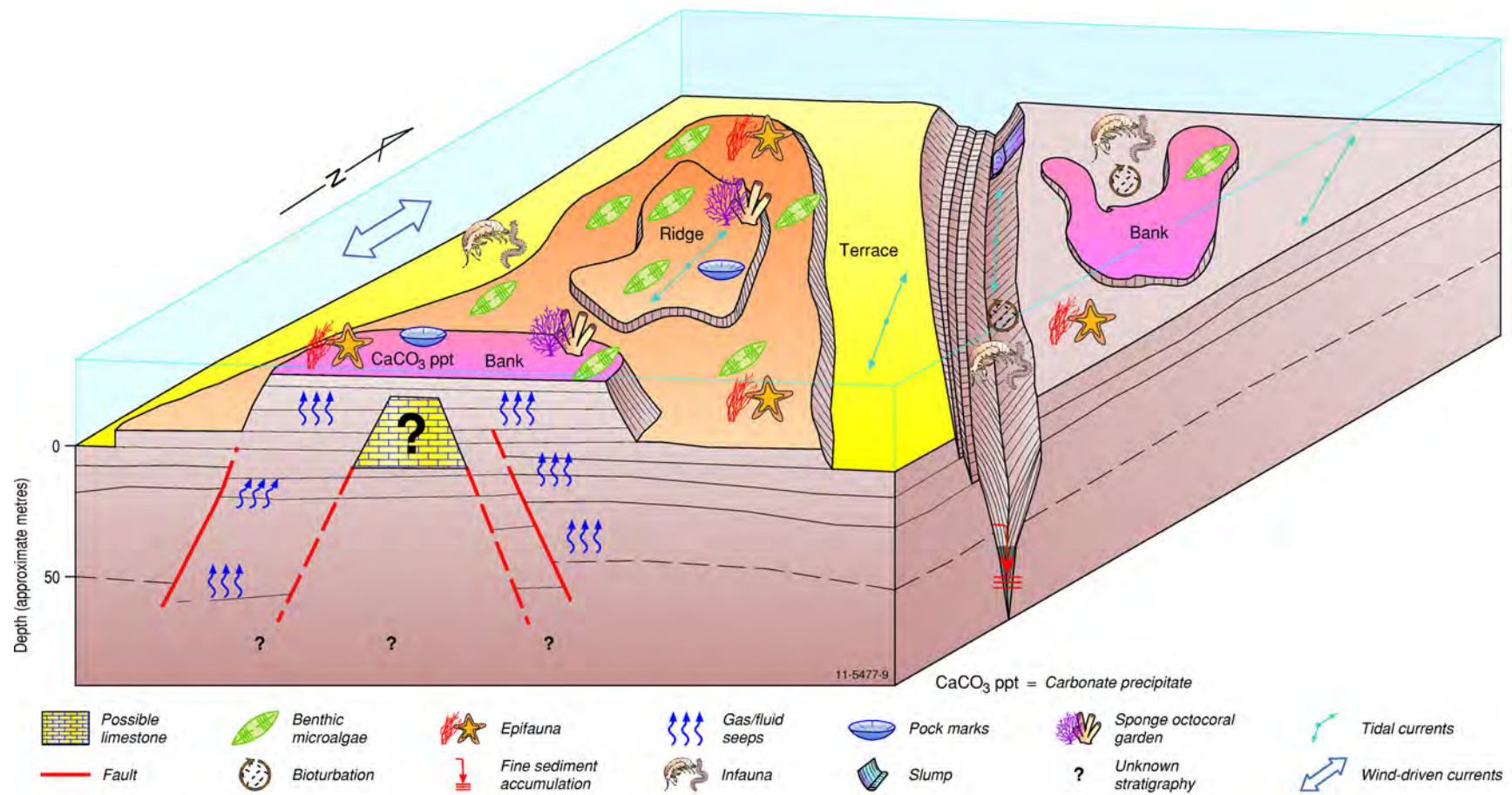


Figure 4.5: A conceptual model showing the biophysical processes operating in Area C

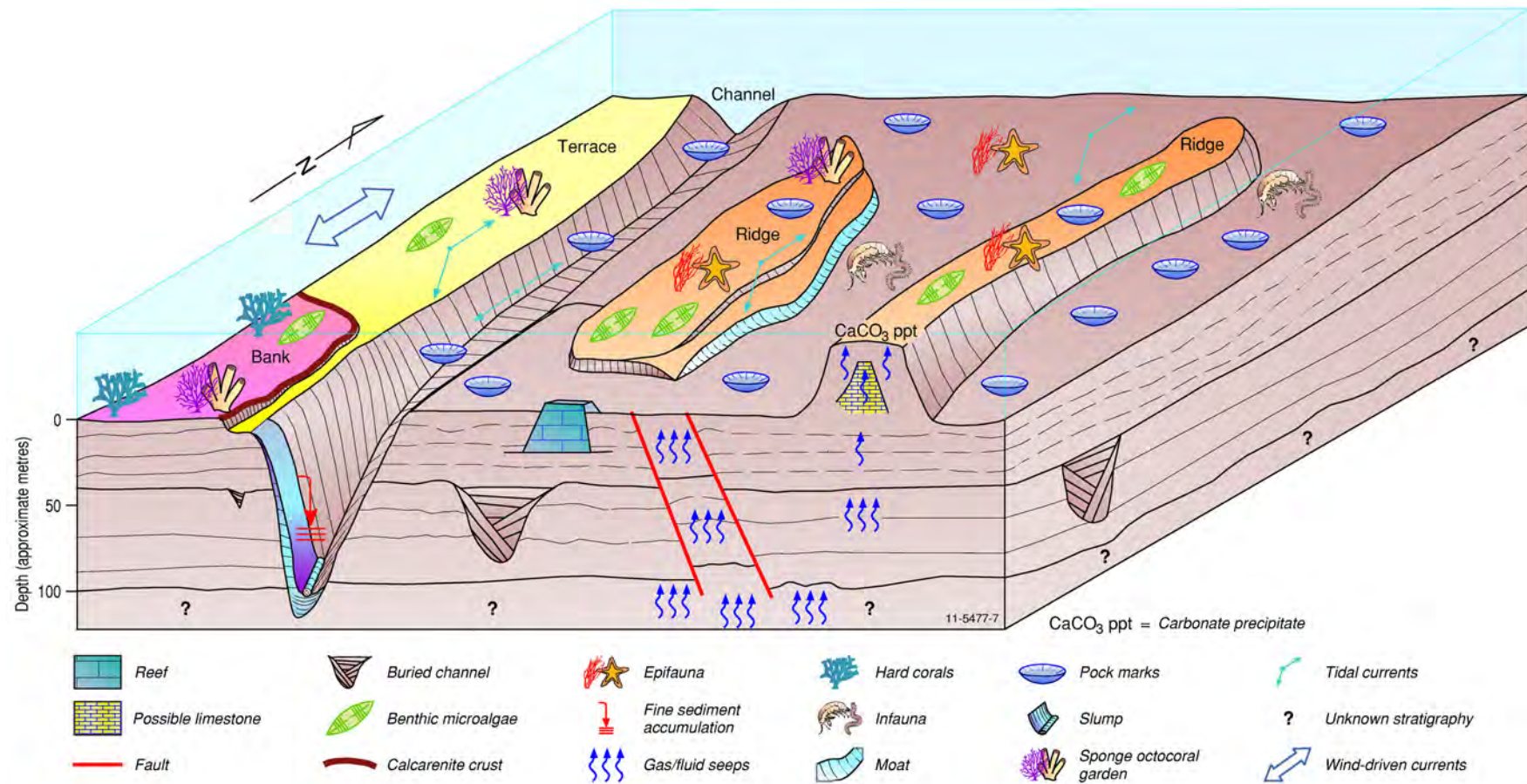


Figure 4.7: A conceptual model showing the biophysical processes operating in Area A

5. Conclusions

This report has identified and mapped significant habitats, communities and hazards in the Joseph Bonaparte Gulf and Timor Sea region to provide pre-competitive data for industry. In addition, information in this report will assist in the characterisation of new marine reserves and provide a baseline for future marine monitoring programs.

The main outputs of this report are new maps showing the distribution of geomorphic features, seascapes, significant biological communities, and hazards in the region. In addition, we have investigated relationships between significant habitats and hazards and the environment to facilitate prediction of their location in areas of the JBG-TS for which data are limited.

Major findings in the JBG-TS are as follows:

- The inner JBG is flat and dominated by soft sediments and associated taxa, with isolated rocky reefs occurring near some headlands and sand banks scattered throughout the inner JBG. The outer JBG and Timor Sea are dotted with banks and palaeoreefs which provide habitat for sessile invertebrates and fish. The Van Diemen Rise comprises a system of carbonate banks and valleys.
- Offshore gradients exist in habitat complexity and species richness.
- Raised geomorphic features support sponge and octocoral gardens which provide habitat to other epifauna.
- Reef-forming hard corals are rare throughout the JBG-TS region; however some locally dense hard corals were found on the banks of the Van Diemen Rise. Corals here are diverse and contain near threatened, vulnerable and endangered species. The few samples identified suggest that coral communities on the Van Diemen Rise are distinct from those elsewhere in northern Australia.
- Habitats and communities were related to several environmental factors (geomorphic features, seascapes, terrestrial elements, organic matter, rock probability index and the backscatter signal from which it was derived). These environmental factors may therefore be suitable surrogates for certain biological measures by facilitating the prediction of significant habitats and communities in areas where there is limited biological data.
- Risks associated with slope failure are minimal throughout the JBG-TS but increase on the flanks of carbonate banks, terraces and ridges of the Van Diemen Rise.
- Fluid or gas escape is evident throughout the JBG-TS, with pockmarks and gas chimneys most common in the soft sediments of valleys and plains.
- The macro-tidal conditions of JBG-TS contribute to potential erosion and sediment mobility. These types of geohazards are greatest in the inner JBG where bedload transport is highest and bedforms such as sand dunes are common.
- Oceanographic hazards associated with wave conditions show an offshore gradient, with higher waves occurring offshore. The highest waves occur in January and July; however wave heights can reach up to 8 m in the outer JBG-TS during cyclone season (Dec - March).
- The distribution of significant habitats, communities and geohazards in the JBG-TS is regulated by complex associations between oceanographic, geological, and biological processes. The suite of processes operating at a given location is affected by distance from the coast and geomorphologic features present.

Many of the observations in the current report relate to broad spatial patterns identified from regional-scale data (e.g., regional-scale geomorphology, seascapes, wave heights) which allows the

offshore petroleum industry to put proposed developmental plans in a regional context in relation to environmental compliance. However, marine management generally occurs at the local scale (10s km) and ideally requires data coverage and analysis at the same scale (Stevens 2002; Stevens & Connolly 2005). Importantly, results from surveys GA-322 and GA-325 indicate that significant habitats, communities, and hazards exist at a scale too small to be detected in regional-scale analysis. For example, the reef-forming hard corals and sponge and octocoral gardens that occur on the shallow banks of the Van Diemen Rise are unique on a regional scale but would not have been identified without sampling at a local scale. Similarly, potential hazards such as buried palaeoreefs and gas expulsions are identified using sub-bottom profiles collected from transects of 1-2 kilometers. These results highlight the continued importance of acquiring high-resolution geophysical data and robust biogeophysical sampling to allow the identification of significant habitats and communities that may otherwise remain undetected.

6. References

- *Anderson, T.J., Cochrane, G.R., Roberts, D.A., Chezar, H. & Hatcher, G. (2008). A rapid method to characterize seabed habitats and associated macro-organisms, *in* Todd, B.J. and Greene, H.G., eds., Mapping the Seafloor for Habitat Characterization: Geological Association of Canada, Special Paper 47, 71-79.
- Anderson, T. J., Nichol, S., Radke, L. C., Heap, A. D., Battershill, C., Hughes, M. G., Siwabessy, P. J. W., Barrie, V., Alvarez de Glasby, B., Tran, M., & Daniell, J. (2011a). *Seabed Environments of the Eastern Joseph Bonaparte Gulf, Northern Australia: GA0325/SOL5117 - Post Survey Report*. Canberra, Geoscience Australia. GA Record 2011/08.
- Anderson, T. J., Nichol, S. L., Syms, C., Przeslawski, R., & Harris, P. T. (2011b). Deep-sea biophysical variables as surrogates for biological assemblages, an example from the Lord Howe Rise. *Deep Sea Research II*, 58, 979-991.
- *Anonymous (2009). *Australian National Tide Tables*. Australian Hydrographic Office.
- Ashley, G.M. (1990). Classification of large-scale subaqueous bedforms: a new look at an old problem, *Journal of Sedimentary Petrology* 60, 160–172.
- *Bear, J. (1972). *Dynamics of fluids in porous media*. Elsevier, New York.
- Bennett, I. (1971). *The Great Barrier Reef*. Melbourne: Lansdowne Press.
- Bishop, M. G. (1999). *Total Petroleum Systems of the Bonaparte Gulf Basin Area, Australia: Jurassic, Early Cretaceous-Mesozoic; Keyling, Hyland Bay-Permian; Milligans-Carboniferous, Permian*. United States Geological Survey. Open File Report 99-50-P.
- Borthwick, D. (2010). *Report of the Montara Commission of Inquiry*. Commonwealth of Australia: Canberra.
- *Breiman L., 2001. Random forests. *Machine Learning* 45: 5-32.
- *Breiman L., Friedman J.H., Olshen R.A., Stone C.J., 1984. Classification and regression trees. Wadsworth: Belmont.
- *Brunskill, G.J. (2005). *Voyage Summary SS06/2005*. CSIRO.
- Buhl-Mortensen, L., Vanreusel, A., Gooday, A. J., Levin, L. A., Priede, I. G., Buhl-Mortensen, P., Gheerardyn, H., King, N. J., & Raes, M. (2010). Biological structures as a source of habitat heterogeneity and biodiversity on the deep ocean margins. *Marine Ecology*, 31(1), 21-50.
- Burford, M. A., Rothlisberg, P. C., & Revill, A. T. (2009). Sources of nutrients driving production in the Gulf of Carpentaria, Australia: a shallow tropical shelf system. *Marine and Freshwater Research*, 60, 1044-1053.
- Clark, K.R., & Warwick, R.M. (2001). *Change in Marine Communities: An Approach to Statistical Analysis and Interpretation*, 2nd Edition. PRIMER-E: Plymouth.

Clarke, J. D. A., Bone, Y., Cann, J. H., Davies, M., MacPhail, M. K., & Wells, F. (2001). Post-glacial biota from the inner part of southwest Joseph Bonaparte Gulf. *Australian Journal of Earth Sciences*, 48(1), 63-79.

*Clarke, J.D.A. (1997). *Geology and Interpreted Geophysical Data from Diamond Exploration in Joseph Bonaparte Gulf*. WMC. K3749/97

Coleman, J. M., & Wright, L. D. (1978). Sedimentation in an arid macrotidal alluvial river system; Ord River, Western Australia. *Journal of Geology*, 86, 621-642.

*Condie, S.A. (2011). Modelling seasonal circulation, upwelling and tidal mixing in the Arafura and Timor Seas. *Continental Shelf Research*, doi:10.1016/j.csr.2011.06.005

Commonwealth of Australia (2005). *National Marine Bioregionalisation of Australia. Summary*. Canberra, Department of Environment and Heritage.

*Currie, D.R., Sorokin, S.J., & Ward, T.M. (2009). Infaunal macroinvertebrate assemblages of the eastern Great Australian Bight: effectiveness of a marine protected area in representing the region's benthic biodiversity. *Marine and Freshwater Research*, 60, 459-474.

Dando, P. R., & Hovland, M. (1992). Environmental effects of submarine seeping natural gas. *Continental Shelf Research*, 12, 1197-1207.

*Daniel, J., Jorgensen, D.C. et al. (2009). *Frontier Basins of the West Australian Continental Margin: Post-survey Report of Marine Reconnaissance and Geological Sampling Survey GA2476*. GA Record 2009/38. Geoscience Australia: Canberra.

DEH (2005) *National Marine Bioregionalisation of Australia*. Department of the Environment and Heritage: Canberra.

DEWHA (2009). *Description of Areas for Further Assessment in the North Marine Region*. Department of Environment Water Heritage and the Arts.

DEWHA (2010). *Description of Areas for Further Assessment in the Northwest Marine Region*. Department of Environment Water Heritage and the Arts.

Dunstan, P. D., & Foster, S. D. (2010). *Predicted patterns of seabed biodiversity in the Northern Marine Region (NMR)*. Canberra, Department of Environment, Water, Heritage and the Arts (Environmental Resources Information Network).

*Edgar, G.J. (2000). *Australian Marine Life Revised Edition*. Reed New Holland: Sydney.

ENI (2005). *Proposal to Undertake 2-D Seismic Survey in TP/22 and WA-280-P, Published EPBC Referral*. Canberra, Department of Environment and Heritage.

Etheridge, M., McQueen, H., & Lambeck, K. (1991). The role of intraplate stress in Tertiary (and Mesozoic) deformation of the Australian continent and its margins: a key factor in petroleum trap formation. *Exploration Geophysics*, 22, 123-128.

Falkowski, P. G., & Dubinsky, Z. (1981). Light-shade adaptation of *Stylophora pistillata*, a hermatypic coral from the Gulf of Eilat. *Nature*, 289(5794), 172-174.

Fisher, C. R., MacDonald, I. R., Sassen, R., Young, C. M., Macko, S. A., Hourdez, S., Carney, R. S., Joye, S., & McMullin, E. (2000). Methane ice worms: *Hesiocaeca methanicola* colonizing fossil fuel reserves. *Naturwissenschaften*, 87, 184-187.

Folk, R.L. (1954). The distinction between grain size and mineral composition in sedimentary rock nomenclature. *Journal of Geology*, 62, 344-359.

GA (2010). *Regional Geology of the Bonaparte Basin, Offshore Petroleum Exploration Acreage Release*. Canberra, Geoscience Australia.

*Garilov, A.N., Duncan, A.J., McCauley, R.D., Parnum, I.M., Penrose, J.D., Siwabessy, P.J. W., Woods, A.J., & Tseng, Y-T. (2005). Characterisation of the seafloor in Australia's coastal zone using acoustic techniques. *Proceedings of Underwater Acoustic Measurements Conference*. Heraklion, Crete, Greece, June 2005.

George, T., & Cauquill, E. (2010). A multi-disciplinary site investigation for the assessment of drilling geohazards and environmental impact within the northern Bonaparte Basin. *Preview*, 148, 41-44.

*Gingele, F.X., De Deckker, P., & Hillenbrand, C-D. (2001). Clay mineral distribution in surface sediments between Indonesia and NW Australia – source and transport by ocean currents. *Marine Geology*, 179, 135-146.

*Glenn, K., & O'Brien, G.W. (2002). Coral reefs & hydrocarbon seeps. *AusGeoNews*, 68, 4–7.

*Greenslade, D.J.M. (2001). The assimilation of ERS-2 significant wave height data in the Australian region. *Journal of Marine Systems*, 28, 141-160.

Hampton, M. A., & Locat, J. (1996). Submarine landslides. *Review of Geophysics*, 34, 33-59.

Harkantra, S. N., & Nagvenkar, S. S. (2006). Do gas seepage sites support distinct macrofaunal communities? *Current Science*, 91(2), 217-221.

Harkantra, S.N., Nagvenkar, S.S. (2006). Do gas seepage sites support distinct macrofaunal communities? *Current Science* 91, 217-221.

Harris, P. T., Heap, A., Passlow, V., Hughes, M., Daniell, J., Hemer, M., & Anderson, O. (2005). Tidally incised valleys on tropical carbonate shelves: an example from the northern Great Barrier Reef. *Marine Geology*, 220, 181-204.

Harris, P., Heap, A., Passlow, V., Sbaffi, L. Fellows, M., Porter-Smith, R., Buchanan, C., & Daniell, J. (2005). *Geomorphic Features of the Continental Margin of Australia*. GA Record 2003/30. Geoscience Australia: Canberra, 142pp.

*Hasselmann, S., Hasselmann, K., Bauer, E., Janssen, P.A.E.M., Komen, G.J., belotti, L., Lionello, P. Guillaume, A., Cardone, V.C., Greenwood, J.A., REistad, M., Zambresky, L., Ewing, J.A. (1988). The WAM model – a third generation ocean wave prediction model. *Journal of Physical Oceanography*. 18, 1775-1810.

Hawke, A. (2009). *The Australian Environment Act - Report of the Independent Review of the Environment Protection and Biodiversity Act 1999*. Department of Environment Water Heritage and the Arts; Canberra.

- Heap, A., Anderson, T. J., Falkner, I., Przeslawski, R., Whiteway, T., & Harris, P. T. (2011). *Seascapes for the Australian Margin and Adjacent Seabed*. Canberra, Geoscience Australia. GA Record 2011/06.
- Heap, A. D., & Harris, P. T. (2008). Geomorphology of the Australian margin and adjacent seafloor. *Australian Journal of Earth Sciences*, 55, 555-585.
- Heap, A. D., Przeslawski, R., Radke, L. C., Trafford, J., & Battershill, C. (2010). *Seabed Environments of the Eastern Joseph Bonaparte Gulf, Northern Australia: SOL4934 - Post Survey Report*. Canberra, Geoscience Australia. GA Record 2010/09.
- *Hughes, M.G., Heap, A.D. (2010) National-scale wave energy resource assessment for Australia. *Renewable Energy* 35, 1783-1791.
- Heyward, A., Pinceratto, E., & Smith, L. (1997). *Big Bank Shoals of the Timor Sea: An Environmental Resource Atlas*. Melbourne: BHP Petroleum.
- Hooper, J.N.A. (1994). Coral reef sponges of the Sahul Shelf - a case for habitat preservation. *Memoirs of the Queensland Museum*, 36, 93-106.
- Hooper, J. N. A., & Ekins, M. (2004). *Collation and Validation of Museum Collection Databases Related to the Distribution of Marine Sponges in Northern Australia*. Canberra, Department of Environment and Heritage. Contract National Oceans Office C2004/020.
- Hough, G., Green, J., Fish, P., Mills, A., & Moore, R. (2011). A geomorphical mapping approach for the assessment of seabed geohazards and risk. *Marine Geophysical Research*. DOI: 10.1007/s11001-010-9111-z
- Hovland, M., Croker, P. F., & Martin, M. (1994). Fault-associated seabed mounds (carbonate knolls?) off western Ireland and North-west Australia. *Marine and Petroleum Geology* 11, 232-246.
- Hovland, M., & Judd, A. G. (1988). *Seabed Pockmarks and Seepage*. London: Graham and Trotman.
- Hughes, M. G., Harris, P. T., & Brooke, B. P. (2010). *Seabed exposure and ecological disturbance on Australia's continental shelf: Potential surrogates for marine biodiversity*. Canberra, Geoscience Australia. 2010/43.
- Hughes, M.G., Heap, A.D. (2010) National-scale wave energy resource assessment for Australia. *Renewable Energy* 35, 1783-1791.
- *Jones, A.T., Logan, G.A., Kennard, J.M., O'Brien, P.E., Rollet, N., Sexton, M., & Glenn, K.C. (2005). *Testing Natural Hydrocarbon Seepage Detection Tools on the Yampi Shelf, Northwestern Australia*. GA Record 2005/15. Geoscience Australia: Canberra.
- Keep, M., Clough, M., & Langhi, L. (2002). Neogene tectonic and structural evolution of the Timor Sea region, NW Australia. *WABS*, 3, 342-353.
- Kennett, J. (1982). *Marine Geology*. New Jersey: Prentice-Hall Inc.
- King, L. H., & MacLean, B. (1970). Pockmarks on the Scotian Shelf. *Geological Society of America Bulletin*, 81, 3141-3148.

- Last, P., Lyne, V., Yearsley, G., Gledhill, D., Gomon, M., Rees, T., & White, W. (2005). *Validation of National Demersal Fish Datasets for the Regionalisation of the Australian Continental Slope and Outer Shelf (> 40 m)*. Hobart, National Oceans Office.
- Lavering, I. H. (1994). Gradational quaternary benthic marine communities on the Van Diemen Rise, Timor Sea, Northern Australia. *Palaeogeography Palaeoclimatology Palaeoecology*, 110(1-2), 167-178.
- Lavering, I. & Jones, A. (2001). Carbonate shoals and hydrocarbons in the western Timor Sea. *PESA News*, Dec/Jan 2001/02.
- Lees, B. G. (1992). Recent terrigenous sedimentation in Joseph Bonaparte Gulf, northwestern Australia. *Marine Geology*, 103, 199-213.
- LeProvost Dames & Moore (1994). *Exploration Drilling, EP32 and EP57 Joseph Bonaparte Gulf, Northern Territory, Environmental Review Report*. Tokyo, Teikoku Oil (Bonaparte Gulf) Co Ltd.
- *Li J., Heap A., 2008. A Review of Spatial Interpolation Methods for Environmental Scientists. Geoscience Australia: Canberra; 137.
- *Li J., Heap A., Potter A., Daniell J.J., 2011. Predicting Seabed Mud Content across the Australian Margin II: Performance of Machine Learning Methods and Their Combination with Ordinary Kriging and Inverse Distance Squared. Geoscience Australia: Canberra; 69.
- Li, J., Potter, A., Huang, Z., Daniell, J. J., & Heap, A. (2010). *Predicting Seabed Mud Content across the Australian Margin: Comparison of Statistical and Mathematical Techniques Using a Simulation Experiment*. Canberra, Geoscience Australia. GA Record 2010/11.
- *Liaw A., Wiener M., 2002. Classification and regression by randomForest. *R News* 2: 18-22.
- Linares, C., Doak, D. F., Coma, R., D'Áz, D., & Zabala, M. (2007). Life history and viability of a long-lived marine invertebrate: the octocoral *Paramuricea clavata* *Ecology*, 88(4), 918-928.
- Logan, G. A., Jones, A. T., Kennard, J. M., Ryan, G. J., & Rollet, N. (2010). Australian offshore natural hydrocarbon seepage studies, a review and re-evaluation. *Marine and Petroleum Geology*, 27(1), 26-45.
- Long, B. G., & Poiner, I. R. (1994). Infaunal benthic community structure and function in the Gulf of Carpentaria, Northern Australia. *Australian Journal of Marine and Freshwater Research*, 45(3), 293-316.
- Lösekann, T., Robador, A., Niemann, H., Knittel, K., Boetius, A., & Dubilier, N. (2008). Endosymbioses between bacteria and deep-sea siboglinid tubeworms from an Arctic Cold Seep (Haakon Mosby Mud Volcano, Barents Sea). *Environmental Microbiology*, 10, 3237-3254.
- *Louis, J.P., Radok, J.R.M. (1975). Propagation of tidal waves in the Joseph Bonaparte Gulf. *Journal of Geophysical Research*. 80, 1689-1690.
- Mass, T., Einbinder, S., Brokovich, E., Shashar, N., Vago, R., Erez, J., & Dubinsky, Z. (2007). Photoacclimation of *Stylophora pistillata* to light extremes: metabolism and calcification. *Marine Ecology Progress Series*, 334, 93-102.

- Mass, T., Kline, D. I., Roopin, M., Veal, C. J., Cohen, S., Iluz, D., & Levy, O. (2010). The spectral quality of light is a key driver of photosynthesis and photoadaptation in *Stylophora pistillata* colonies from different depths in the Red Sea. *Journal of Experimental Biology*, 213, 4084-4091.
- McArthur, M., Brooke, B., Przeslawski, R., Ryan, D. A., Lucieer, V., Nichol, S., McCallum, A. W., Mellin, C., Cresswell, I. D., & Radke, L. C. (2010). On the use of abiotic surrogates to describe marine benthic biodiversity *Estuarine Coastal and Shelf Science*, 88, 21-32.
- Metcalf, K. N., & Glasby, C. J. (2008). Diversity of polychaeta (Annelida) and other worm taxa in mangrove habitats of Darwin Harbour, northern Australia. *Journal of Sea Research*, 59(1-2), 70-82.
- Moberg, F., & Folke, C. (1999). Ecological goods and services of coral reef ecosystems. *Ecological Economics*, 29(2), 215-233.
- O'Hara, T. (2008). *Bioregionalisation of Australian waters using brittlestars (Echinodermata: Ophiuroidea), a major group of marine benthic invertebrates*. Canberra, Department of the Environment, Water, Heritage and Arts.
- O'Brien, G. W., & Glenn, K. C. (2005). Natural hydrocarbon seepage, sub-seafloor geology and eustatic sea-level variations as key determiners on the nature and distribution of carbonate build-ups and other benthic habitats in the Timor Sea, Australia. . In: B. C. Russel, H. K. Larson, C. J. Glasby, R. C. Willan, & J. Martin, *The Beagle, Records of the Museums and Art Galleries of the Northern Territory. Supplement 1. Understanding the Cultural and Natural Heritage Values and Management Challenges of the Ashmore Region* (pp. 31-42). Darwin: MAGNT.
- O'Brien, G. W., Higgins, R., Symonds, P., Quaife, P., Colwell, J., & Blevin, J. (1996). Basement control on the development of extensional systems in Australia's Timor Sea: an example of hybrid hard linked/soft linked faulting. *APPEA Journal*, 36, 161-201.
- O'Brien, G. W., Lisk, M., Duddy, I. R., Hamilton, J., Woods, P., & Cowley, R. (1999a). Plate convergence, foreland development and fault reactivation: primary controls on brine migration, thermal histories and trap breach in the Timor Sea, Australia. *Marine and Petroleum Geology*, 16, 533-560.
- O'Brien, G. W., Morse, M., Wilson, D., Quaife, P., Colwell, J., Higgins, R., & Foster, C. B. (1999b). Margin-scale, basement-involved compartmentalisation of Australia's North-West Shelf: a primary control on basin-scale rift, depositional and reactivation histories. *APPEA Journal*, 39, 40-63.
- *Pebesma E.J., 2004. Multivariable geostatistics in S: the gstat package. *Computer & Geosciences* 30: 683-691.
- Post, A. L. (2008). The application of physical surrogates to predict the distribution of marine benthic organisms. *Ocean & Coastal Management*, 51(2), 161-179.
- Prior, D. B., & Hooper, J. R. (1999). Sea floor engineering geomorphology: recent achievements and future direction. *Geomorphology*, 31, 411-439.
- Probert, P. K., McKnight, D. G., & Grove, S. L. (1997). Benthic invertebrate bycatch from a deep-water trawl fishery, Chatham Rise, New Zealand. *Aquatic Conservation: Marine and Freshwater Ecosystems*, 7, 27-40.
- Productivity Commission. (2009). *Review of Regulatory Burden on the Upstream Petroleum (Oil and Gas) Sector*. Research Report: Melbourne.

Przeslawski, R., Althaus, R., Currie, D., Sorokin, S., Ward, T., & Williams, A. (2011). Utility of a spatial habitat classification system as a surrogate of marine benthic community structure for the Australian margin. *ICES Journal of Marine Science*, 68, 1954-1962.

*Radke, L.C., Heap, A.D., Douglas, G., Nichol, S., Trafford, J., Li, J., & Przeslawski, R. (2011). A geochemical characterization of deep-sea floor sediments of the northern Lord Howe Rise. *Deep Sea Research II*, 58, 909-921.

Robinson, K.A., Ramsay, K., Lindenbaum, C., Frost, N., Moore, J., Wright, A.P., & Petrey, D. (2011). Predicting the distribution of seabed biotopes in the southern Irish Sea. *Continental Shelf Research*, 31(2) Supplement, S120-S131.

Rollet, N., Logan, G.A., Kennard, J.M., O'Brien, P., Jones, A.T., & Sexton, M. (2006). Characterisation and correlation of active hydrocarbon seepage using geophysical data sets: an example from the tropical, carbonate Yampi Shelf, Northwest Australia. *Marine and Petroleum Geology*, 23, 145-164.

RPS (2009). *Environment Plan: PGS 2D Seismic Survey: Bonaparte Gulf, Timor and Arafura Seas*. West Perth, Petroleum Geoservices.

Sills, G. C., & Wheeler, S. J. (1992). The significance of gas for offshore operations. *Continental Shelf Research*, 12, 1239-1250.

Smit, N., Billyard, R., & Ferns, L. (2000). *Beagle Gulf Benthic Survey: Characterisation of soft substrates*. Darwin, Parks and Wildlife Commission of the Northern Territory. Technical Report No. 66.

Stevens, J. D., West, G. J., & McLoughlin, K. J. (2000). Movements, recapture patterns, and factors affecting the return rate of carcharhinid and other sharks tagged off northern Australia. *Marine and Freshwater Research*, 51(2), 127-141.

Stevens, T. (2002). Rigor and representativeness in marine protected area design. *Coastal Management*, 30, 237-248.

Stevens, T., & Connolly, R. M. (2005). Local-scale mapping of benthic habitats to assess representation in a marine protected area. *Marine and Freshwater Research*, 56(1), 111-123.

*Thurman, H.V., Trujillo, A.P. (2004). *Introductory Oceanography*, 10th edition. Prentice Hall: New Jersey. 624 pp.

Tonks, M. L., Griffiths, S. P., Heales, D. S., Brewer, D. T., & Dell, Q. (2008). Species composition and temporal variation of prawn trawl bycatch in the Joseph Bonaparte Gulf, northwestern Australia. *Fisheries Research*, 89(3), 276-293.

TOTAL E&P Australia (2007). *Proposal for 3D Seismic Survey in WA-402-P and WA-403-P, Published EPBC Referral*. Canberra, Department of Environment Heritage and the Arts.

URS Australia Pty Ltd (2009). *Ichthys Gas Field Development Project: studies of the offshore marine environment*. Perth, INPEX Browse Ltd.

Van Andel, T. H., & Veevers, J. J. (1967). Morphology and sediments of the Timor Sea. *Bureau of Mineral Resources, Geology and Geophysics: Bulletin*, 83, 173.

Veevers, J. J., Falvey, D.A., & Robins, S. (1978). Timor Trough and Australia; facies show topographic wave migrated 80 km during the past 3 m.y. *Tectonophysics*, 45, 217-227.

Wasmund, K., Kurtboke, D. I., Burns, K. A., & Bourne, D. G. (2009). Microbial diversity in sediments associated with a shallow methane seep in the tropical Timor Sea of Australia reveals a novel aerobic methanotroph diversity. *Fems Microbiology Ecology*, 68(2), 142-151.

Webster, I.T., Brinkman, R., Parslow, J.S., Prange, J., Steven A.D.L., Waterhouse, J. (2008) *Review and Gap Analysis of Receiving-Water Water Quality Monitoring in the Great Barrier Reef: Report to the Department of Environment, Water, Heritage and the Arts*. CSIRO: Canberra.

WEL Woodside Energy Limited (2001). *Proposal to Drill an Exploration (Thresher-1) in Permit Area WA-280-P in Joseph Bonaparte Gulf, Published EPBC Referral Form*. Canberra, Department of the Environment and Heritage.

WEL Woodside Energy Limited (2004). Existing Marine Environment. *Blacktip Draft Environmental Impact Statement*: Woodside

Whiteway, T. (2009). *Australian Bathymetry and Topography Grid*. Canberra, Geoscience Australia. GA Record 2009/21.

Wienberg, C., Westphal, H., Kwohl, E., & Hebbeln, D. (2010). An isolated carbonate knoll in the Timor Sea (Sahul Shelf, NW Australia): facies zonation and sediment composition. *Facies*, 56(2), 179-193.

*Williams, A. Kloser, R. (2007). *Voyage Summary SS05/2007*. CSIRO.

Wilson, G. D. F. (2006). *Arafura Sea Biological Survey, Report on RV Southern Surveyor Expedition 05/2005, 28 April - 28 May 2005*. Canberra, Department of the Environment and Heritage.

Wilson, G. D. F. (2010). *Taxonomic Results: Arafura Sea Biological Survey*. Sydney, Australian Museum.

Yokoyama, Y., Purcell, A., Lambeck, K., & Johnston, P. (2001). Shore-line reconstruction around Australia during the Last Glacial Maximum and Late Glacial Stage. *Quaternary International*, 83-85, 9-18.

Zabanbark, A. (2010). The structural features and petroleum resource potential of basins in the western and northwestern Australian margins. *Oceanology*, 50(2), 268-280.

* References present in Appendices only

APPENDICES

Appendix A: Data Sources

Table A1. List of data sources used in this report from the JBG-TS.

SOURCE	REGION (VESSEL)	YEAR ACQUIRED	DATA TYPE	DATA DETAILS	REFERENCE
Atlas of Living Australia	JBG-TS	Accessed 2011	Species presence	1546 species	www.ala.org.au
Ocean Biogeographic Information System	JBG-TS	Accessed 2011	Species presence	1039 occurrences of 385 species	www.iobis.org
GA-0325 / SOL5117	Van Diemen Rise (RV Solander)	2010	Underwater video, still images Sled specimens (epifauna) Grab specimens (infauna, geochemistry) Multibeam bathymetry Grab specimens (sedimentology) SBP Cores Oceanography	17hrs 33min from 79 transects, 8294 still images from 77 stations ~ 760 specimens from 40 stations Sediment samples from 77 stations 1154km ² 76 sediment samples 595 km 22 cores from 14 stations 3 moorings	Anderson et al 2011
GA-0322 / SOL4934	Van Diemen Rise (RV Solander)	2009	Underwater video, still images Sled specimens (epifauna) Grab specimens (infauna, geochemistry) Multibeam bathymetry Grab specimens (sedimentology) SBP Cores Oceanography	11hr 38min from 47 transects, 7659 still images from 45 stations ~ 950 specimens from 44 stations Sediment samples from 55 stations 1154km ² 59 sediment samples 340 km 15 cores from 15 stations 4 moorings	Heap et al 2010
Ichthys EIS	Northern JBG	2008	Drop camera characterisations	Characterisations from 13 stations	URS 2009
GA-2437 / SS052007	Northwest (RV Southern Surveyor)	2007	Multibeam bathymetry, SBP	Various in transit	Williams and Kloser 2007
GA-2375 / SS062005	Cornea Cartier (RV Southern Surveyor)	2005	Multibeam bathymetry, SBP	Various in transit	Brunskill 2005

Blacktip EIS	JBG (MV Island Explorer)	2004	Grab specimens (infauna, geochemistry)	Sediment samples from 37 stations (including inshore)	WEL 2004
GA-267 (Seeps & Signatures Survey)	Yampi Shelf (Parmelia K)	2004	Dredge, grab and gravity core samples (sedimentology)	185 samples ¹	Jones et al 2005
Western Mining Corporation Bonaparte Gulf Diamond Exploration	Joseph Bonaparte Gulf (unknown)	1997	Core samples (sedimentology)	60 samples ¹	Clarke 1997
Beagle Gulf Benthic Survey	Beagle Gulf (Kunnunyah)	1993	Dredge samples (sedimentology)	54 samples ¹	Smit et al 2000
Western Australia and Northern Territory Surveys (CSIRO)	WA/NT (Small vessel - name not available)	1989	Grab samples (sedimentology)	4 samples ¹	
Holocene sedimentation in an epicontinental sea	Joseph Bonaparte Gulf (Small vessel - name not available)	1979	Dredge samples (sedimentology)	34 samples ¹	Lees 1992
GA-142	Arafura Sea (San Pedro Sound/ Yamato)	1969	Dredge samples (sedimentology)	15 samples ¹	
GA-69, GA-70	Timor Sea (Matila/Stranger)	1960-61	Dredge, grab and gravity core samples (sedimentology)	163 samples ¹	

¹ Sample quantities include all those collected from the survey, including those outside of the JBG-TS region. Data was obtained from the Marine Sediments (MARS) database at Geoscience Australia (www.ga.gov.au/oracle/mars)

Appendix B: Spatial interpolation of gravel and mud content in the JBG-TS

Spatially continuous layers of seabed sediments (i.e., gravel and mud) were required to produce seascape in the Bonaparte region. Data on mud and gravel content are only available in point samples. Therefore, spatial interpolation methods were required to produce spatially continuous information of the sediments. In this appendix, we briefly introduce the methods used for spatial interpolation of gravel and mud content. Detailed information on selecting and developing these methods for mud content is reported in Li et al. (2010, 2011) and for sand content will be available in a future Geoscience Record.

B1. Datasets of sediments and secondary information

Samples that were available from the Marine Samples database (MARS) and from survey GA-325 were quality controlled and used. The quality control process is similar to those reported by Li et al. (2010).

Bathymetry, slope, distance to the coast, relief, latitude and longitude at 0.01 degree were used for developing predictive models.

B2. Spatial interpolation methods

The methods used for spatial interpolation were developed for a study predicting the seabed sediments across Australian margin at Geoscience Australia. These methods involve random forest (RF), ordinary kriging (OK) and inverse distance squared (IDS) (Li and Heap, 2011).

B2.1. Random forest

Random forest is an ensemble method that combines many individual classification and regression trees (Breiman et al., 1984). In standard trees, each node is split using the best split among all variables. In a RF, each node is split using the best predictor among a subset of predictors randomly selected at that node. From the complete forest the status of the response variable is predicted as an average of the predictions of all individual trees (Breiman, 2001).

Random forest was applied to the samples of seabed sediments to develop a predictive model for each of gravel and mud content. The following secondary information was used in the model development for mud content:

1. Bathymetry and its second and third order;
2. Distance to coast and its second and third order;
3. Slope and its second and third order;
4. Latitude and its second and third order;
5. Longitude and its second and third order;
6. Interaction of latitude with longitude and its second order; and
7. Interaction of longitude with the second order of latitude.

For gravel content, relief and its second and third order were also used as secondary information.

These RF predictive models have taken into account the global trend of sediments in the Bonaparte region. The predictive models were then used to predict the spatial distribution of gravel and mud content in the Bonaparte region.

Ordinary kriging and IDS were then applied to the residuals of the RF predictive models for gravel and mud content to develop predictive models for spatial variation at local scales.

B3. Predictions of mud and gravel content

For mud content, the predictions were produced using RFOK (Li et al., 2011). This method is a combined method of RF and OK. The predictions of RFOK were the sum of the predictions of RF and the predictions of OK.

For gravel content, the predictions were the average of the predictions of RF, RFOK and RFIDS; RFIDS is combined method of RF and IDS (Li et al., 2011). The predictions of RFIDS were the sum of the predictions of RF and the predictions of IDS.

All the modelling work was conducted in R using randomForest (Liaw and Wiener, 2002) and gstat (Pebesma, 2004).

The final predictions of mud and gravel content were scaled along with the predictions of sand content to ensure their sum equalled 100% at each location. This scaling was done using the root mean square error (RMSE) associated with each of the sediments as a weight. This scaling ensured that the predictions of the sediment with small predictive error were less affected during the scaling process.

The spatial distributions of mud and gravel content can be found in [Appendix D](#), along with a brief description of associated patterns.

Appendix C: Ecology

In this appendix, we provide a detailed account of the ecological data and analyses that were used to generate some of the trends in the Joseph Bonaparte Gulf –Timor Sea region (JBG-TS) that are summarised in the main report. The ecological data is divided into three major types: 1) Online public databases used to determine species presence, 2) Underwater video used to characterise the seafloor habitat and broad biological communities, and 3) Biological specimens from sleds and grabs used to characterise the diversity of epifauna and infauna.

C1. PUBLIC DATABASES

C1.1 Methods

The Atlas of Living Australia (ALA) (www.ala.org.au) was searched using a location grid centred on the Joseph Bonaparte Gulf (11.5°S – 15.0°S; 126.5°E - 131°E). Results included all species recorded in this grid, including terrestrial species. All terrestrial and known freshwater species were excluded from analyses, although due to the sheer volume of species a thorough investigation of habitat was unable to be conducted. The Ocean Biogeographic Information System (OBIS) (www.iobis.org) allowed a more spatially explicit search; species lists were compiled from 1 degree grids throughout the region of interest. Organisms for which family was unknown were excluded from both databases. Database searches were conducted in March 2011.

C1.2 Results

A total of 1546 marine species were compiled from the ALA. Of these, the majority were fish, sharks and rays (64%), although molluscs were also well-represented (23%) (Figure C1). OBIS returned 1039 records of 385 species in the JBG-TS region. There was an even higher percentage of fish, sharks and rays (88%) than that found in the ALA, with molluscs only representing 6% of all records. These results almost certainly reflect the increased effort collecting and identifying vertebrates, rather than a true disproportionate abundance of fish in the region.

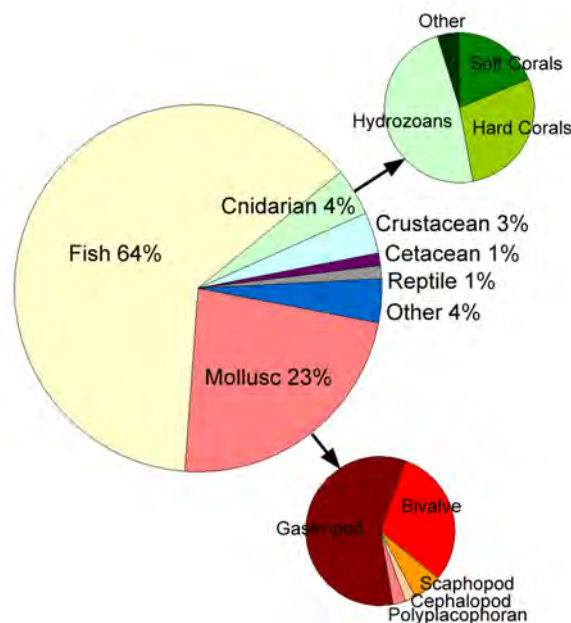


Figure C1: The proportion of major taxonomic groups recorded in the Joseph Bonaparte Gulf according to the Atlas of Living Australia.

There were no reef-forming species of hard coral recorded from ALA or OBIS. Of the remaining solitary corals, there were no obvious patterns of distribution, with several species found in four 1-degree quadrats throughout the gulf (14-15°E/128-129°S; 13-14°E/129-130°S; 12-13°E/128-130°S).

We targeted several groups under potential threat (hard corals, cetaceans, reptiles) by searching the IUCN Red List of Threatened Species (www.iucnredlist.org). Several species recorded from the ALA and OBIS were on the Red List and are therefore significant for conservation reasons (Table C1). In addition, several species recorded in the ALA and OBIS are protected as Listed Marine Species under the *EPBC Act 1999*, including sea snakes, sea turtles, and syngnathids (sea horses and pipefish) (Table C1). All cetaceans are also protected under the *EPBC Act 1999*.

Table C1. A list of species recorded from the JBG-TS based on ALA and OBIS records that are protected through inclusion on the IUCN Red List or the Listed Marine Species of the *EPBC Act 1999*. Importantly, this list is not exhaustive, and there are likely other species that occur in the region not included here.

GROUP	SPECIES	COMMON NAME	EPBC ACT PROTECTION	IUCN RED LIST STATUS	SOURCE
Cetacean					
	<i>Mesoplodon</i>	Beaked whale	All cetaceans protected	Data deficient	ALA
	<i>Grampus griseus</i>	Risso's Dolphin		Least concern	ALA
	<i>Orcaella heinsohni</i>	Australian Snubfin Dolphin	All cetaceans protected	Near threatened	ALA
	<i>Peponocephala electra</i>	Melon-headed Whale		Least concern	ALA, OBIS
	<i>Pseudorca crassidens</i>	False Killer Whale	All cetaceans protected	Data deficient	ALA
	<i>Sousa chinensis</i>	Indo-pacific Hump-backed Dolphin	All cetaceans protected	Near threatened	ALA
	<i>Stenella attenuata</i>	Pantropical Spotted Dolphin		Least concern	ALA
	<i>Stenella longirostris</i>	Long-snouted Spinner Dolphin	All cetaceans protected	Data deficient	ALA
	<i>Tursiops aduncus</i>	Bottlenose Dolphin	All cetaceans protected	Data deficient	ALA
	<i>Megaptera novaeangliae</i>	Humpback Whale		Least concern	OBIS
	<i>Kogia simus</i>	Dwarf Sperm Whale	All cetaceans protected	Data deficient	ALA
	<i>Physeter macrocephalus</i>	Sperm Whale	All cetaceans protected	Vulnerable	ALA
Sea Turtle					
	<i>Lepidochelys olivacea</i>	Olive ridley turtle	Listed marine species	Vulnerable	OBIS
	<i>Caretta caretta</i>	Loggerhead turtle	Listed marine species	Endangered	OBIS
	<i>Natator depressa</i>	Flatback turtle	Listed marine species	Not listed	OBIS
Seasnake					
	<i>Acalyptophis peronii</i>	Horned Seasnake	Listed marine species	Least concern	ALA
	<i>Aipysurus eydouxii</i>	Eydoux's Seasnake	Listed marine species	Least concern	ALA
	<i>Astrotia stokesii</i>	Stokes's Seasnake	Listed marine species	Least concern	ALA
	<i>Disteira kingii</i>	Spectacled Seasnake	Listed marine species	Least concern	ALA
	<i>Disteira major</i>	Olive-headed Seasnake	Listed marine species	Least concern	ALA
	<i>Enhydrina schistosa</i>	Beaked Seasnake	Listed marine species	Least concern	ALA

<i>Hydrophis atriceps</i>	Black-headed Seasnake	Listed marine species	Least concern	ALA
<i>Hydrophis elegans</i>	Elegant Sea Snake	Listed marine species	Least concern	ALA
<i>Hydrophis fasciatus</i>		Listed marine species	Least concern	ALA
<i>Hydrophis macdowellii</i>	Small-headed Seasnake	Listed marine species	Least concern	ALA
<i>Lapemis curtus</i>	Spine-bellied Seasnake	Listed marine species	Least concern	ALA
<i>Lapemis hardwickii</i>		Listed marine species	Least concern	ALA
<i>Parahydrophis mertoni</i>	Northern Mangrove Seasnake	Listed marine species	Data Deficient	ALA
<i>Pelamis platurus</i>	Yellow-bellied Seasnake	Listed marine species	Least concern	ALA
Seahorses & Pipefish				
<i>Campichthys</i> sp.		Listed marine species	Not listed	ALA
<i>Choeroichthys brachysoma</i>	Pacific Short-bodied Pipefish	Listed marine species	Not listed	ALA
<i>Festucalex</i> sp.		Listed marine species	Not listed	ALA
<i>Halicampus</i> sp.		Listed marine species	Not listed	ALA
<i>Haliichthys taeniophorus</i>	Ribboned Pipefish	Listed marine species	Not listed	ALA
<i>Hippichthys parvicarinatus</i>	Short-keel Pipefish	Listed marine species	Not listed	ALA
<i>Hippichthys penicillus</i>	Beady Pipefish	Listed marine species	Not listed	ALA
<i>Hippocampus angustus</i>	Narrow-bellied Seahorse	Listed marine species	Data Deficient	ALA
<i>Hippocampus taeniopterus</i>	Common Seahorse	Listed marine species	Not listed	ALA
<i>Micrognathus</i> sp.		Listed marine species	Not listed	ALA
<i>Parasyngnathus</i> sp.		Listed marine species	Not listed	ALA
<i>Trachyrhamphus bicoarctatus</i>	Bend Stick Pipefish	Listed marine species	Not listed	ALA

C2. UNDERWATER VIDEO

In this section, we describe and map seabed habitats and assemblages across the Van Diemen Rise using underwater towed-video observations from two surveys (GA-322 and GA-325). C-BED (Characterization of the Benthos and Ecological Diversity) observations were recorded along each video transect to characterise the composition and structure of the seabed (substrata, relief and bedforms) and the associated epibenthic assemblages (presence of epifauna and the percent cover of dominant sessile invertebrates). The combination of towed-video surveys and C-BED characterisations meant that the seabed could be quantified at multiple spatial scales, from fine (cm) to broad (kms) spatial scales, which has important implications for resource management and conservation. For the purpose of this report, data are presented relative to the four preliminary geomorphic features that were described for the region immediately after each survey: banks, terraces, plains, deep/hole/valleys. Final classification of geomorphic features was not available at the time of video analysis. See [Table C2](#) for comparison between preliminary and final geomorphic classifications.

Table C2. Comparison of preliminary and final geomorphic classifications for all stations from which grab, sled, video or core samples were taken on GA-322 (denoted by ‘A’) or GA-325 (denoted by ‘B’). Video analyses were undertaken on preliminary classifications. B = Bank; T = Terrace; R = Ridge; P = Plain; V = Valley.

STATION	PRELIM	FINAL	STATION	PRELIM	FINAL	STATION	PRELIM	FINAL	STATION	PRELIM	FINAL
1A	B	B	38A	T	V	12B	V	V	49B	V	V
2A	B	B	39A	V	V	13B	V	V	50B	B	B
3A	T	T	40A	V	V	14B	V	V	51B	B	B
4A	T	V	41A	B	B	15B	P	P	52B	B	B
5A	T	R	42A	P	P	16B	P	P	53B	T	T
6A	V	R	43A	V	V	17B	P	P	54B	V	V
7A	V	V	44A	V	V	18B	P	P	55B	B	B
8A	T	V	45A	P	P	19B	P	P	56B	B	B
9A	T	R	46A	P	P	20B	V	V	57B	V	B
10A	V	V	47A	V	V	21B	T	R	58B	V	V
11A	T	V	48A	P	P	22B	V	V	59B	T	T
12A	V	V	49A	P	P	23B	T	R	60B	V	V
13A	T	V	50A	P	P	24B	T	R	61B	V	V
14A	T	R	51A	V	V	25B	T	R	62B	V	V
15A	V	V	52A	P	P	26B	V	V	63B	V	V
16A	V	V	53A	V	P	27B	T	R	64B	B	B
17A	T	R	54A	P	P	28B	T	R	65B	B	B
18A	V	V	55A	V	V	29B	V	V	66B	P	P
19A	V	V	56A	P	P	30B	V	V	67B	P	P
20A	T	R	57A	P	P	31B	V	V	68B	P	P
21A	B	B	58A	P	P	32B	V	V	69B	P	P
22A	B	R	59A	P	P	33B	V	V	70B	P	P
23A	B	R	60A	P	P	34B	T	R	71B	P	P
24A	V	V	61A	P	P	35B	T	T	72B	B	B
25A	R	R	62A	P	P	36B	V	V	73B	B	B
26A	V	P	63A	T	T	37B	T	R	74B	B	B
27A	P	P	1B	P	P	38B	V	V	75B	B	B
28A	V	V	2B	B	B	39B	V	V	76B	P	P

29A	T	T	3B	V	V	40B	V	V	77B	P	P
30A	T	T	4B	P	P	41B	V	V	78B	P	P
31A	B	T	5B	P	P	42B	V	V	79B	P	P
32A	T	T	6B	P	P	43B	V	V	80B	P	P
33A	B	B	7B	P	P	44B	T	T	81B	B	B
34A	B	B	8B	V	V	45B	T	T	82B	T	T
35A	T	V	9B	P	P	46B	V	V	83B	V	V
36A	V	V	10B	V	V	47B	T	R			
37A	V	V	11B	V	V	48B	T	R			

C2.1 Methods

To characterize the physical structure of the seabed and associated biota within each of the four survey areas, a single towed-video transect was undertaken at each station using the AIMS's towed-video system. At each station, the towed-video system was deployed from the stern of the *RV Solander* and towed at 0.5 to 1.5 knots at an altitude of 0.5 - 2 m above the seabed for a distance of approximately 500 m (full details provided in Heap et al., 2009 and Anderson et al., 2011). Seabed habitats and biota were characterized in real-time using the 3-tiered real-time C-BED characterisation scheme (Anderson et al., 2008), and validated post-survey from spatially-referenced video footage. High-resolution still photographs (recorded five seconds along each towed-video transect) were used in conjunction with the video footage to assist identification of biota. Real-time C-BED characterisations recorded substratum composition (rock, boulders, cobble, mud, sand, etc.), bedform-relief (e.g. sediment ripples, waves, or vertical 'relief' of hard substrata), and presence of macro-biota at approximately 30 second intervals along each transect (see Anderson et al., 2011). To characterise the structural cover of key habitat-forming organisms, percentage cover of sponges, octocorals, and combined invertebrates (e.g. bryozoan and ascidians) were recorded post-survey to 5% precision. The growth morphology of sponges (e.g. massive, barrel, and fan) and octocorals (e.g. fan, branching and whips) were also recorded during the 2010 survey to characterise the morphological diversity of these habitats (details in: Anderson et al., 2011). Video characterisations from the two surveys were then combined for regional examination. In addition, for stations where hard corals were recorded on video or collected in sleds, all living and dead hard corals were classified by growth form and either systematically counted (e.g. isolated cup corals) or estimated as percent cover (most growth forms) from the high resolution (12-megapixel) still images. This more detailed sampling approach (still images captured every 5 seconds) was used for hard corals because of their low numbers and localised distributions and to ensure that small sized corals (e.g. small cup corals only a few cms in size), which are difficult to see in video footage, were also adequately recorded. Error rates were then systematically assessed for 15% of the dataset. Error rates calculated for the combined CBED characterisations were less than 3% for all substratum, relief, biota presence, and % cover variables.

Analyses

Bathymetry and backscatter data, along with geomorphology categories, were acquired in ArcGIS (ESRI v.9.2) for all video characterisations along each transect. Data were processed and analysed using SAS (Statistic Analysis System, SAS Institute Inc., 2001 v.9.1). To examine the relationship between physical variables and geomorphic features, means and standard errors, along with upper quartiles and ranges were calculated for each physical variable. Percent occurrence estimates were calculated for substrata, relief and bedform categories, epifauna and growth morphologies as the number of 30-sec points (Frame of View) where each category type was recorded as a function of

the total number of points sampled per geomorphic feature. Similarly, means and standard errors were then calculated for the percent cover estimates of each key taxa (octocorals, sponges, other sessiles).

C2.2 Results

Seabed Environments

Four geomorphic features (banks, terraces, valleys and plains) were preliminarily identified within the four study regions. Over 29 hours of video footage and 15,953 still photographs were acquired during the combination of these two surveys, in which an estimated 58 line-km of seabed was surveyed. A total of 2,703 real-time seabed characterizations (C-BED) were recorded from a total of 124 stations (22 stations were surveyed in banks, 29 in terraces, 45 in valleys and 28 in plains) (Table C3). The Van Diemen Rise was dominated by soft sediments (86% of all locations), as combinations of muddy sands and sandy mud. These soft-sediments were mostly flat (92% of all locations), with rare occurrences of sediment waves, ripples, and hummocky bedforms (2% each). Conversely, hard substrata in the form of rocky outcrops were much rarer (13%) and were comprised of mostly low, flat or moderate relief (42%, 29% and 27% respectively) with only negligible amounts of high relief (2%). Hard substratum occurred in all four geomorphic features, but amounts varied significantly (Figure C2). Banks had the most hard substrata (Mean $55.8\% \pm 1.7$ SE; range 0-100%) as well as more homogenous outcrops. Terraces had significantly less hard substrata (mean $14.2\% \pm 1.2$ SE; range 0-100%) which occurred mostly as small patches of mixed rock and sediment. Valleys had small isolated patches of hard substrata (Mean $5.7\% \pm 0.7$ SE; range 0-100%), while plains only had very small and isolated patches of hard substrata (Mean $0.13\% \pm 0.08$ SE; range 0-29%). Assemblages varied by geomorphic feature, although all four features were dominated by high occurrences of octocorals and sponges, and bioturbation (Figure C3). High % cover of sessile filter-feeders (termed ‘Mixed Gardens’) reflected the availability of hard substrata, with the highest % cover of mixed gardens recorded in banks, where living hard corals were also often present (Table C4). Terraces and valleys supported locally high densities of sessile filter-feeders, but overall means were low. Conversely bioturbation increased relative to the availability of soft-sediments, with the exceptions of plains (see below). Large (>30 cm) and vulnerable sponges (e.g. barrels, vases and fans) were also most common on banks and terraces, reflecting stable environments for their colonisation and growth.

Table C3. Summary information on the locations surveyed and data types collected within each geomorphic feature during surveys GA-322 and GA-325. Geomorphic features are based on preliminary classifications done immediately after each survey (see Table C2)

GEOMORPHIC FEATURE	SURVEY AREAS	NO. OF STATIONS	DEPTH (M) MEAN & RANGE	BACKSCATTER MEAN & RANGE	NO. OF CBED CHARACT.	NO. OF STILL IMAGES
bank	A, B and C	22	34.6 m (10.6 – 60.0)	-15.2 (-5.6 to -46.8)	434	2867
terrace	A and C	29	74.4 m (23.7 – 100.8)	-11.6 (-24.0 to -36.6)	689	4077
valley	A, B, C, D	45	83.2 m (44.7 – 204.7)	-11.7 (-26.3 to -46.8)	931	4872
plain	B and D	28	50.0 m (40.6 – 79.3)	-15.8 (-20.9 to -28.9)	649	3702

NB: Two transects (GA-322: stn22cam12 and stn23cam13) extended beyond the targeted geomorphic feature, over a deeper adjacent geomorphic feature. Here the dominant and targeted geomorphic type only is included in analyses.

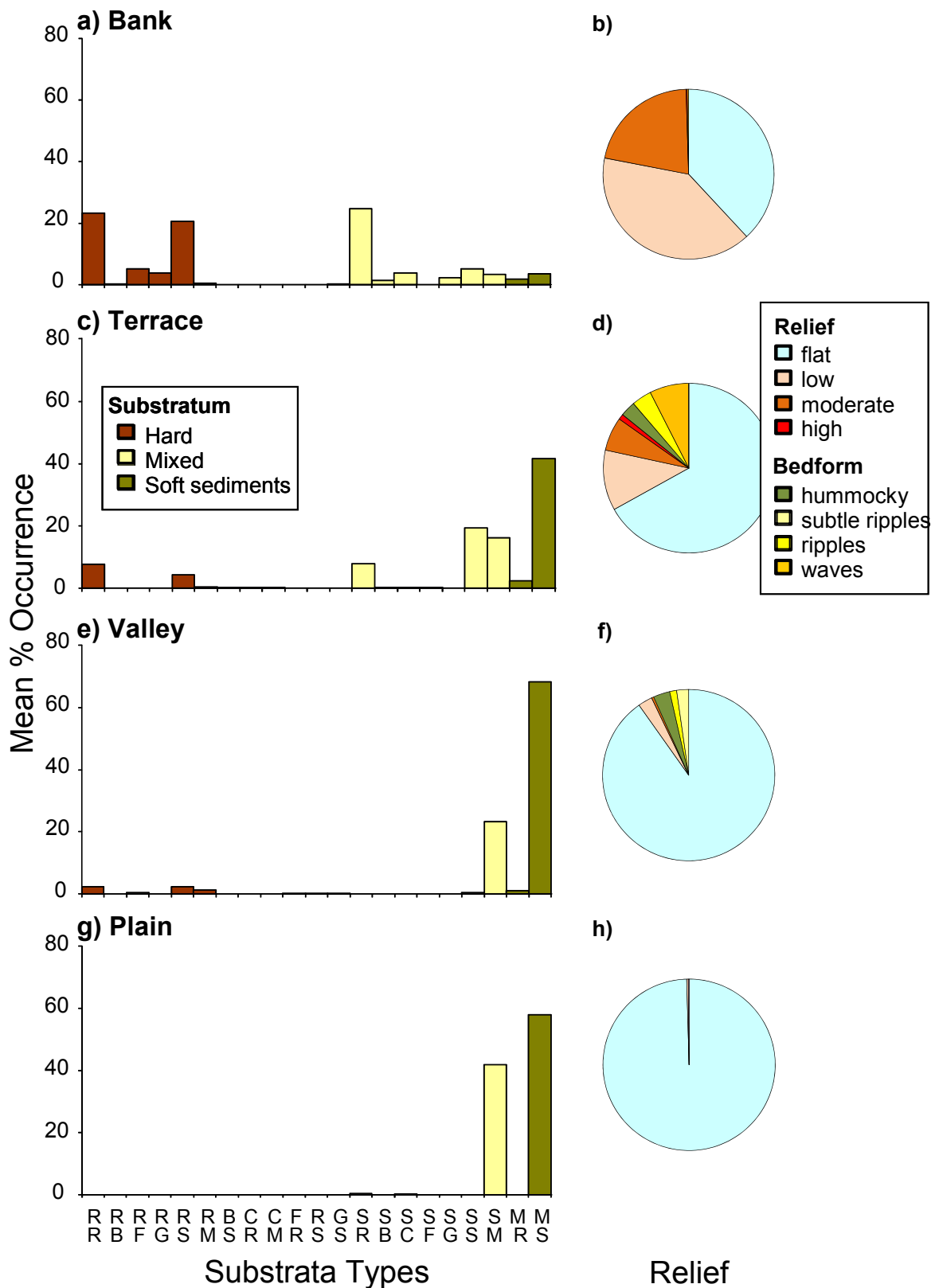


Figure C2: C-BED characterizations from geomorphic features of the Van Diemen Rise based on towed-video observations. Percent occurrence of: primary (1st letter) and secondary substratum (2nd letter), R=rock, B= boulder, C=cobble, F=fragments, G=gravel, S=sand, M=mud and substratum relief of a-b) banks; c-d) terraces; e-f) valleys; g-h) plains. Geomorphic features are based on preliminary classifications done immediately after each survey (see [Table C2](#))

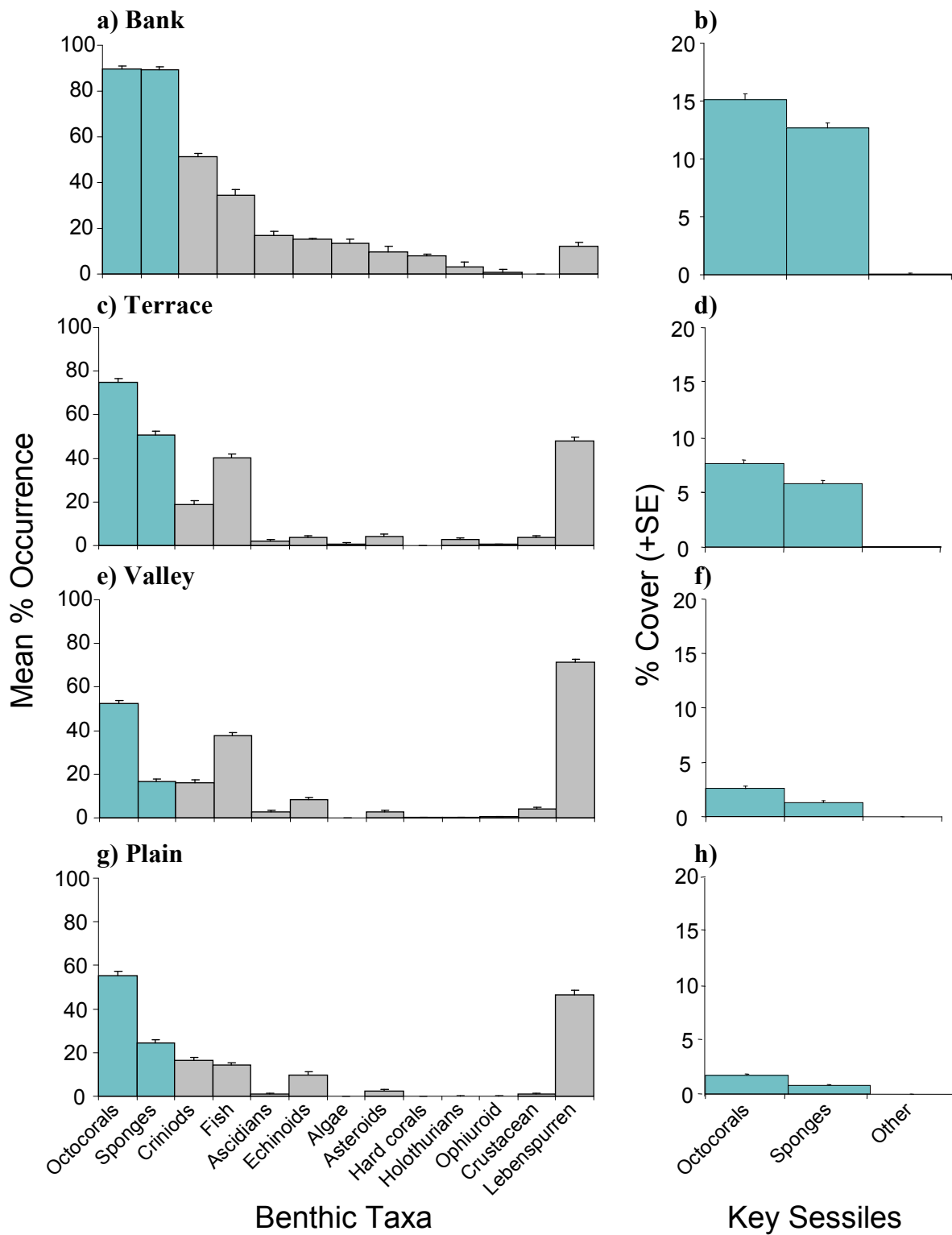


Figure C3: Percent occurrence of key biota types and mean percent cover of octocorals and sponges within geomorphic features (+SE) using C-BED characterizations in the Joseph Bonaparte Gulf from two surveys; GA-322 and GA-325. a-b) Banks; c-d) terraces; e-f) valleys; and g-h) plains. Geomorphic features are based on preliminary classifications done immediately after each survey (see Table C2)

Table C4. Summary information on the relative occurrence and abundance (number individuals or percent cover) of hard corals (HC) recorded in video characterisations (Frame of View every 30-sec) and still images (Frame of View every 15-sec) from video transects surveyed across the Van Diemen Rise. G=Geomorphic features (V=Valley, B=Bank, T=Terrace, P=Plain); Mean depth and depth range – bracketed value; Video characterisations and still images with hard corals are presented as number of occurrences and % of total frames – bracketed value. Geomorphic features are based on preliminary classifications done immediately after each survey (see [Table C2](#))

SURVEY	STN	AREA	MEAN LAT.	MEAN LONG.	MEAN DEPTH (RANGE) (M)	G	VIDEO W/ HC	STILLS W/ HC	VIDEO HABITAT CLASS	DESCRIPTION
GA-325	72	B	-11.1181	129.9204	13 (10-25)	B	11 (85%)	94 (78%)	Mixed gardens (HC) Moderate-relief reef with dense sessile assemblages, including hard corals	Mixed coral assemblage (dense) - Branching (mean=51%; range 0-95% cover) - Plating (<i>Turbinaria</i>) (mean=22%; range 0-75%) - Encrusting (mean=18%; range 0-80%) - Pocilloporidae (mean=16%; range 0-40%) - Fungiids (mean=6%; range 0-10%, 0-1 indiv.)
GA-325	73	B	-11.1279	129.9136	24 (23-25)	B	2 (14%)	13 (10%)	Mixed gardens (HC) Low-relief reef (patchy) with sponge and octocoral gardens, and some hard corals	Mixed coral assemblage (sparse) - Encrusting (mean=16%; range 0-70%) - Fungiids (mean=4%; range 0-5%, 0-1 indiv.)
GA-325	2	C	-11.6423	129.8353	24 (23-24)	B	2 (11%)	28 (25%)	Mixed patches Flat reef (patchy) with sponges, octocorals, and hard corals	Some isolated corals (sparse) - Solitary cup corals (mean=2; range, 0-3 indiv.) - Encrusting red coral (mean=13%; range 0-35%).
GA-325	52	A	-10.6291	129.4721	28 (26-29)	B	11 (69%)	149 (96%)	Mixed gardens (HC) Low-relief reef with dense sessile assemblages, including hard corals	Mixed coral assemblage (common) - Solitary cup corals (mean=4; range, 0-24 indiv.) - Fungiids (mean=19%; range 0-90%, 0-288 indiv.) - Plating (mean=8%; range 0-10%) - Encrusting (mean=14%; range 0-50%) - Branching/Pocillopora (mean=18%; range 0-40%) - <i>Euphyllia</i> sp. or similar (mean=7%; range 0-15% cover) - <i>Goniopora</i> sp. or similar (mean=5%; range 0-5% cover)
GA-325	55	A	-10.6054	129.4846	33 (31-35)	B	6 (43%)	111 (92%)	Mixed gardens (HC) Low relief reef, with diverse hard corals, and large octocorals and sponges	Mixed coral assemblage (common) - Solitary cup corals (mean=14; range, 0-110 indiv.) - Plating (<i>Turbinaria</i>) (mean=23%; range 0-30%) - Fungiids (mean=5%; range 1-25%, 0-20 indiv.) - Encrusting (mean=4%; range 0-5%) - <i>Euphyllia</i> sp. or similar (mean=4%; range 0-5%) - <i>Goniopora</i> sp. or similar (mean=40%; range 0-40%)
GA-325	50	A	-10.6790	129.5114	34 (33-34)	B	2 (14%)	69 (59%)	Mixed gardens (HC) Low-relief reef with sponge and sponge and octocoral gardens, and some hard corals	Mixed coral assemblage (common) - Solitary cup corals (mean=4; range, 0-18 indiv.) <i>Heteropsammia</i> & <i>Heterocyathus</i> spp. or similar - Fungiids (mean=2%, range 0-2%, 0-1 indiv.)

SURVEY	STN	AREA	MEAN LAT.	MEAN LONG.	MEAN DEPTH (RANGE) (M)	G	VIDEO W/ HC	STILLS W/ HC	VIDEO HABITAT CLASS	DESCRIPTION
GA-325	13	D	-12.3166	129.9399	52 (51-54)	V	1 (3%)	0	Bioturbated Flat sediment, few epifauna	Isolated coral (rare) 1x small branched coral
GA-322	53	D	-12.3492	129.9712	53 (50-54)	V	2 (6%)	1 (0.5%)	Bioturbated Flat sediment, few epifauna	Isolated coral (rare) 1x small branched coral
GA-325	35	A	-10.4636	129.5384	55 (54-55)	T	0	8 (8%)	Mixed gardens HC Low-relief reef, (patchy) with sponges, octocorals, and some hard corals	Some isolated corals (sparse) - Encrusting coral (mean=9%; range 0-15%) - Fungiid (mean=7%; range 0-10%, 0-2 individuals)
GA-325	48	A	-12.3492	129.9712	90 (84-93)	T	-	-	Mixed Patches Low-relief reef (patchy) with sponges and octocorals.	No living corals in video or stills NB: Dead branched coral (400 kg collected in sled)
GA-325	36	A	-10.4204	129.5866	115 (114-118)	V	-	-	Bioturbated Flat sediment, few epifauna	No living corals in video or stills NB: Dead hexacorals (some live?) in sled.

Banks

Banks were the shallowest (mean 33 m, range 11 to 60 m) and most complex geomorphic feature recorded (Table C3; Figure C2a,b) and supported the most diverse and abundant epibenthic assemblages (Figure C3a,b). Banks contained the highest amount of hard substrata, but this comprised combinations of mixed hard and soft substrata (e.g. sand-rock [SR], rock-sand [RS], and rock-fragment [RF], etc.; totalling 65% of area surveyed) and homogeneous rock (23%), with some homogeneous soft-sediments (12%) (Figure C2a). Banks also supported more complex relief than all other geomorphic features (Figure C2b). Banks were dominated by low (40%) and moderate (21%) relief outcrops (61% total), with most of the remaining seabed characterised by flat relief (38%), with only very rare occurrences of high relief (0.2%; Figure C2b). Rocky outcrops were highly patchy across banks interspersed by sediment. However where rock outcrops occurred they supported moderately-dense mixed gardens (up to 75% cover), comprised of mostly octocorals ($\leq 50\%$ cover) and sponges ($\leq 40\%$ cover), and often included living hard corals (termed 'mixed garden HC') (Table C4). In contrast to dense aggregations on rocky outcrops, the soft-sediments that interspersed these rock outcrops supported only low numbers of sponges and octocorals, along with low levels of bioturbation ($<10\%$ occurrence) (Figure C3a). Consequently, although banks supported the highest cover of sponges and octocorals compared to all other geomorphic features, overall mean % cover was still generally low (28% total sessiles, with 15% octocorals and 13% sponges; Figure C3b).

Mixed gardens also comprised other sessile invertebrates, such as bryozoans (18% occurrence), ascidians (17% occurrence), macroalgae (14% occurrence) and hard corals (8%) but their total % cover across the entire bank was negligible (Figure C3a,b). Importantly, hard corals on the banks were diverse and included small solitary cup corals (possibly *Heteropsammia*, *Heterocyathus*), mushroom corals (Fungiids), as well as reef building corals, such as branching (Pocilloporid) and plating (*Turbinaria* spp.) forms (Table C4). While some of these coral forms were uncommon (e.g. plating *Turbinaria* spp.), others were often locally dense. For example, mushroom corals covered substantial amounts (up to 80%) of the seabed at station 52, but were only found in lower numbers ($<20\%$) at four other stations (Table C4). In other locations, such as station 72, coral cover was high but reflected an assortment of coral species (Table C4). While reef-building corals were present at many stations (23% of all bank stations), the most numerically dominant corals were small solitary cup corals (overall mean 1.0 ± 0.67 SE, range 0-17 individuals) and mushroom corals (overall mean 1.1 ± 0.80 SE, range 0-288 individuals). In total, hard corals occurred in 6 of the 22 (27%) bank stations, but only 17% of all still images from all bank locations. Importantly, while a few locations supported high % cover of hard corals (up to 90% cover), overall mean % cover of hard corals on banks was extremely low (total mean 0.74 ± 0.25 SE, range 0-95 % cover).

Banks, particularly mixed gardens, also supported a diverse array of associated motile fauna, such as crinoids (51% occurrence), urchins (15%), starfish (10%), brittlestars (Figure C3a), as well as a diverse range of octocoral and sponge growth morphologies, including vulnerable growth forms. Octocorals were comprised of hydroids (61%), whips (37%), soft corals (including Nephthediidae; 35%), branching (including harp gorgonian *Ctenocella*; 25%), and gorgonian fans (18%), while sponges were comprised of digitate (24%), fan (25%), branching (18%) and giant barrels (*Xestospongia* 15%). In addition, nearly two thirds (64%) of all large sponges ($>30\text{cm}$) collected during these two surveys ($n=1046$ from GA-322 and GA-325) were found in bank habitats. Sponges, like corals, are often slow growing and can be very long lived (Garrahou and Zabala, 2001) with large sponges and vulnerable growth forms (e.g. barrel, branching and fans) often indicative of stable environments where disturbances regimes are low (i.e. natural hazards, storms, cyclones) (McMurray et al., 2008).

Terraces

Terraces were generally deeper (mean 74 m, range 24-101 m) and contained less hard (only 22%), and patchier substrata than banks, but where present these outcrops also supported diverse and complex mixed gardens, although no living hard corals were found (Table C4). Substrata within terraces were dominated by homogenous soft sediments (e.g. mud-sand [MS], sand-sand [SS], sand-mud [SM], mud-mud [MM], totalling 77% of area surveyed), interspersed with patchy rocky outcrops of mixed hard and soft substrata (SR, RS, mud-rock [MR], rock-mud [RM]), 14.5% of area surveyed) and homogenous rock (8%). Terraces had more diverse relief and bedform types than banks, but less complex reef structure (Figure C2d). The

seabed in terraces was generally flat (66%), with rarer occurrences of low and moderate relief (11% and 6%, respectively), and the addition of sand waves, sand ripples and hummocky bedforms (7%, 4% and 3%, respectively) (Figure C2d). The spatial patchiness of the seabed was reflected in the spatial patchiness of the epibenthic assemblages (Figure C3c,d). The availability of more intervening sediments equated to higher occurrences of bioturbation activity (48% total occurrence), characterised by infaunal activity of burrows (34%), craters (21%) and mounds (20%), with only negligible occurrences of epifaunal tracks (3%). Where present, small rocky outcrops also supported moderately-dense (up to 75% cover) mixed gardens of octocorals ($\leq 50\%$ cover) and sponges ($\leq 40\%$ cover).

Octocorals and sponges also occurred in the majority of terrace locations (75% and 51% occurrence, respectively), however, the reduced availability of rocky outcrops with their locally high densities, resulted in a significantly lower mean % cover (14% total sessiles, with 8% octocorals and 6% sponges) (Figure C3c,d). However, terraces also contained the highest numbers of *Cinachyrella* sp., a small spherical sponge that is often partially buried in sediment, with a total of 899 individuals (90% of total *Cinachyrella* recorded). This particular sponge was common (up to 32 individuals p/30m²) in soft sediments adjacent to patchy rock outcrops, a habitat which was prevalent in terraces. Other sessile epifauna, such as bryozoans (4% occurrence) and ascidians (2%) were also present, but % cover was low (Figure C3d).

Terraces also supported a diverse array of other motile biota, but other than fish (40% occurrence) and crinoids (19%) overall occurrence of these taxa were low (e.g. crustaceans (4%) and starfish (4%)) (Figure C3b). Terraces also supported a diverse range of octocoral and sponge growth forms, including vulnerable growth forms, such as large branching, fan-shaped and barrel-like sponges. Octocorals were comprised of whips (44%), hydroids (35%) and soft corals (26%), while sponges comprised mostly digitate (20%), branching (11%), fan (8%), vase (5%) and barrel (3%) forms. While most large sponges (64%) were found on banks, many large sponges (31%) were also recorded on terraces. Large vulnerable growth forms indicate that terraces like banks, may be relatively stable low-disturbance environments.

Valleys

Valleys were the deepest geomorphic feature found within the Joseph Bonaparte Gulf (mean 83 m; range: 45 - 205 m), contained significantly less rocky habitats, and supported significantly less epibenthos compared to banks and terraces (Table C3). Valleys were dominated by homogenous soft-sediments (e.g. sandy mud (SM) and muddy sand (MS) totalling 91% of area surveyed), with only rare amounts of mixed hard and soft substrata (e.g. RS, SR, RM 4% of area surveyed), or homogeneous rock (2%) (Figure C2e). Although diverse relief and bedform structures were found in valleys, these were dominated by flat relief (90%), with only rare occurrences of other relief/bedforms, such as low relief outcrops (3%), and hummocky or subtle rippled bedforms (3% and 2%, respectively) (Figure C2f). The flat soft sediments of the valleys supported the highest occurrences of bioturbation (71%) of all geomorphic features (Figure C3g). Infaunal activity was the highest, characterised by burrows (59%), craters (33%), mounds (28%) and pits (17%), while epifaunal tracks were infrequent (7%). Importantly, although rock patches were rarer and smaller than in banks or terraces, where present these outcrops also supported moderately dense mixed gardens (up to 65% cover), comprising octocorals ($\leq 50\%$ cover) and sponges ($\leq 25\%$ cover). However, due to the rarity of these habitats, overall mean % cover was very low (4% total, with 3% octocorals and 1% sponges, Figure C3e,f). *Cinachyrella* sp. were also recorded in valleys (76 individuals: 8% of all *Cinachyrella* sp. recorded), with high local densities at the interface between soft sediments and patchy rock outcrops (up to 19 individuals p/30m²), but overall occurrences and abundance was very low (1.8% occurrence; mean 0.08 individuals p/30 m²). Bryozoans (2% occurrence) and ascidians (3%) were also present, but their total % cover was negligible (Figure C3e,f), while occurrence of motile epifauna were comparable to banks and terraces (e.g. fish (38%), crinoids (16%), urchins (8%), crustaceans (4%), and ascidians (3%)) (Figure C3e). In addition, several small living hard corals (possibly *Stylophora pistillata*.) were recorded from two stations at either end of a single valley feature in the Area D (13B - depth 52 m, and Station 53A - depth 53 m). Although these inshore areas are mostly soft-sediment and highly turbid, it appears that some limited coral growth is possible.

Although the % cover of octocorals and sponges was very low, occurrences were still relatively high, with valleys supporting similar growth forms to those recorded in banks and terraces (e.g. whips [24%

occurrence], hydroids [16%] and branching gorgonians [7%]; along with digitate [8%] and branching [4%] sponges). However large sponges (4.7% occurrence; 0.05 individuals p/30 m²) and vulnerable growth forms, such as barrels, vases, and fans (0.4%, 1.4% and 1.6% respectively) were rare or absent from these assemblages. Valleys included many debris-swept channels, which in places exposed small patches of underlying rocky substrata that supported moderately-dense sessile assemblages. However, these higher levels of disturbance may inhibit the ability of large and more vulnerable growth forms to either colonise and/or grow.

Plains

Plains were the shallowest (mean 50 m, range 41-79 m) and least complex geomorphic feature recorded (Table C3; Figure C2g-h), and supported the lowest occurrence and abundance of sessile epifauna (Fig.C3g-h). Of all geomorphic features, plains comprised the highest amount of homogenous soft-sediments (e.g. 99% MS and SM; Fig.C2g) with only rare amount of hard substrata (<1%). Soft-sediments had flat relief (99%), with rare occurrences of hummocky bedforms and low relief (<1% each; Fig C2h). Although plains supported expansive soft-sediments, the seabed was characterised by only moderate occurrences of bioturbation (47%), mostly from infaunal activity, resulting in burrows (36%) and craters (15%), with little to no epifaunal activity (e.g. tracks <1%). In areas where sediment had been excavated by faunal activities, large amounts of broken shell were revealed directly beneath the surface sediments. Sled collections in plains also returned large volumes of shell material (Anderson et al., 2011). The presence of shell material may inhibit bioturbation activities, and explain why higher levels of bioturbation were not recorded. Like the other geomorphic features, plains also supported regular occurrences of octocorals (55%) and sponges (24%), but numbers of these sessile epifauna were generally very low (est. 1-2 individuals p/30 m²; mean total sessiles 2%) with only very rare occurrences of low (~25% cover) and dense (~75% cover) assemblages (<2% and <1%, respectively) (Figure C3h). Other sessile epifauna, such as bryozoan and ascidians, were rare (both <1% occurrence) with negligible % cover (Figure C3h), yet motile epifauna, such as crinoids (17% occurrence), fish (14%), pencil and heart urchins (10%) and seastars (2%) were frequently recorded. Growth forms were still diverse, with octocorals comprised of whips (14% occurrence), soft corals (11%), branching gorgonians (10%) and hydroids (8%), while sponge morphologies were mostly digitate (12% occurrence), with rarer occurrences of other forms (<5%). However, in contrast to other geomorphic features, large vulnerable growth forms were extremely rare (<0.01% occurrence).

C3. BIOLOGICAL SAMPLES

In this section, we present results for the major taxonomic groups collected in the sled and grabs from GA-322 and GA-325 (sponges, octocorals, echinoderms, molluscs, infauna). In addition, the relationships between environmental and biological factors are examined, with the specific aim of identifying potential abiotic surrogates for marine biodiversity.

C3.1 Methods

Organisms were collected from benthic sleds and Smith-McIntyre grabs as per methods described in Heap *et al.* (2010) and Anderson *et al.* (2011).

For all benthic sleds, estimates of epifaunal species richness and biomass were made onboard, and specimens of selected taxonomic groups were later identified to species or lowest OTU (operational taxonomic units) by various experts (Table C5). For all Smith-Mac grabs, animals were sorted at GA according to taxonomic group and sent to experts wherever possible (Table C5). Infaunal species richness and abundance were calculated using these identifications as well as in-house classifications of OTUs. All identified specimens are lodged at the Museum and Art Gallery of the Northern Territory, with the exception of echinoderms (Museum of Victoria), hard corals (Museum of Tropical Queensland), and infauna from taxonomic groups not listed in Table C5 (Australian Museum).

Table C5. Animals from GA-322 and GA-325 that have been identified to species level as of August 2011. MAGNT = Museum and Art Gallery of Northern Territory; MTQ = Museum of Tropical Queensland; MV = Museum of Victoria; JCU = James Cook University.

TAXA	GA-322	GA-325	TAXONOMISTS	COMMENTS
Sponges	Completed	Pending	Dr Belinda Glasby (MAGNT)	Identified from spicule preparations and hand sections
Hard corals ¹	n/a	Completed	Dr Carden Wallace, Dr Paul Muir (MTQ), Marcelo Kitahara (JCU)	
Polychaetes & other worms	Completed	Pending	Dr Chris Glasby, Charlotte Watson (MAGNT)	
Molluscs	Completed ²	Completed ³	Dr Richard Willan (MAGNT)	
Crinoids	Completed	Completed ³	Kate Naughton (MV)	
Ophiuroids	Completed	Completed ³	Dr Tim O'Hara (MV)	
Infauna from other groups	Completed	Pending	Dr Rachel Przeslawski (GA)	Lowest OTUs only; identified by non-taxonomist

¹ Does not include GA-322; these samples have yet to be identified

² Approximately half of the molluscs from GA-322 are still unidentified, pending separation from other taxa

³ Excluding grabs which were being processed at the time of writing this report

Stations with sponge and octocoral gardens were identified based on > 5kg sponges or octocorals collected in the sled or expanses of dense octocorals or sponges observed in the video.

In order to identify the key environmental drivers of biological communities, multiple regressions were performed on species richness and biomass; and multivariate analyses were conducted on species-level data from sponges and infauna (GA-322 only). For the multivariate datasets, there were a large number of species that occurred only once or twice, thereby making it difficult to obtain meaningful interpretations. We therefore used reduced datasets that included only those species contributing at least 4% to the total abundance (Clarke and Warwick, 2001). These reduced datasets were square-root transformed to further limit the effects of rare species (Clarke and Warwick, 2001). The BIO-ENV procedure was then performed to identify the best combination of abiotic data driving the biological patterns, limited to a combination of three variables.

Environmental data were chosen based on their potential as useful surrogates (McArthur et al., 2010) and expert consultation (L. Radke, pers. comm.), with a total of 17 variables analysed. Where environmental data were missing, the average among all other stations was used. For multivariate analyses, environmental data were normalised to give each variable equal weighting (Clarke and Warwick, 2001).

Univariate analyses were performed in the R statistical platform (v. 2.7.2), and multivariate analyses were conducted in PRIMER (v.6).

C3.2 Results

To date, over 654 species have been identified from sponges and infauna from GA-322. The actual number of species collected from both surveys almost certainly exceeds 2000 but many groups have not been identified and species-level data is not yet available for GA-325 specimens. Furthermore, species rarefaction curves of sponges and infauna do not show any signs of levelling, thus indicating that the species richness is underestimated (Figure C4).

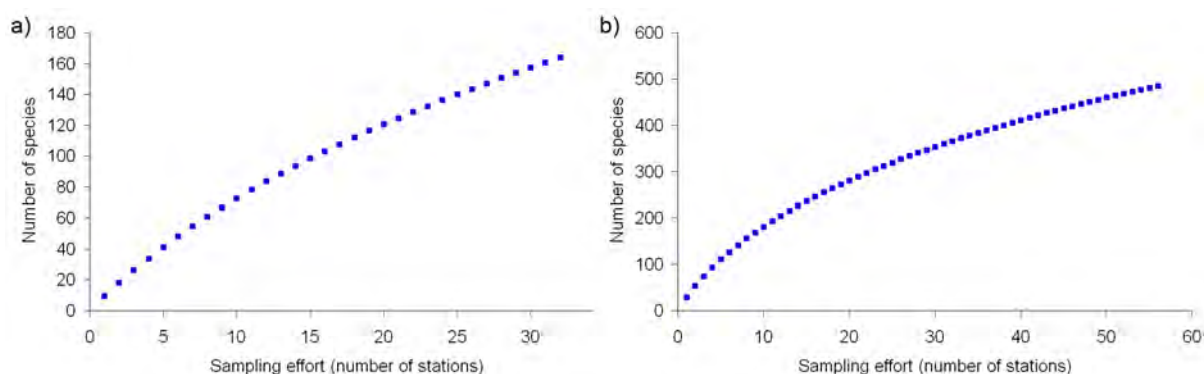


Figure C4: Species rarefaction curves of (a) sponges and (b) infauna collected from GA-322. Neither curve flattens, thus indicating that new species are continuing to be collected at each new station and species richness is likely underestimated.

Sponges

Sponges represent one of the major habitat-forming taxa on the seafloor, providing structure to otherwise flat environments (Buhl-Mortensen et al. 2010). As such, their distribution can be an indicator of overall biodiversity. A bioregionalisation of sponges in tropical Australian waters comprises 3 major provinces with smaller transitions within these. Northern and western fauna are included in a single province, along with several unresolved transitions (Hooper and Elkins 2004). The sponge communities in northern bioregions (including Gulf of Carpentaria) are more similar to west bioregions than east, suggesting biogeography is more important in structuring sponge communities than geographic proximity (Hooper and Elkins 2004). A previous survey in the Beagle Gulf recorded a rich sponge fauna in the soft sediments of the JBG (Smit et al 2000).

Sponges represented the highest biomass and richness recorded of all taxa collected from the GA-322 and GA-325 surveys, with over 150 species from 41 families currently identified from the GA-322 survey. These include several new species and records for the area of Northern Australia. Most widespread species were comparatively large (*Xestospongia tesudinaria*, *Ianthella flabelliformis*), with many cryptofauna such as brittlestars and decapods inhabiting these specimens (Figure C5). The highest species richness (16.7 ± 10.8 species) (mean \pm stdev) and biomass (23.3 ± 24.8 kg) were recorded from banks, although some terraces and ridges were also home to rich sponge gardens. As the number of sponge species increased, the number of species of other taxa also increased (Figure C6), highlighting the importance of sponges as habitat for a range of animals in northern Australia.

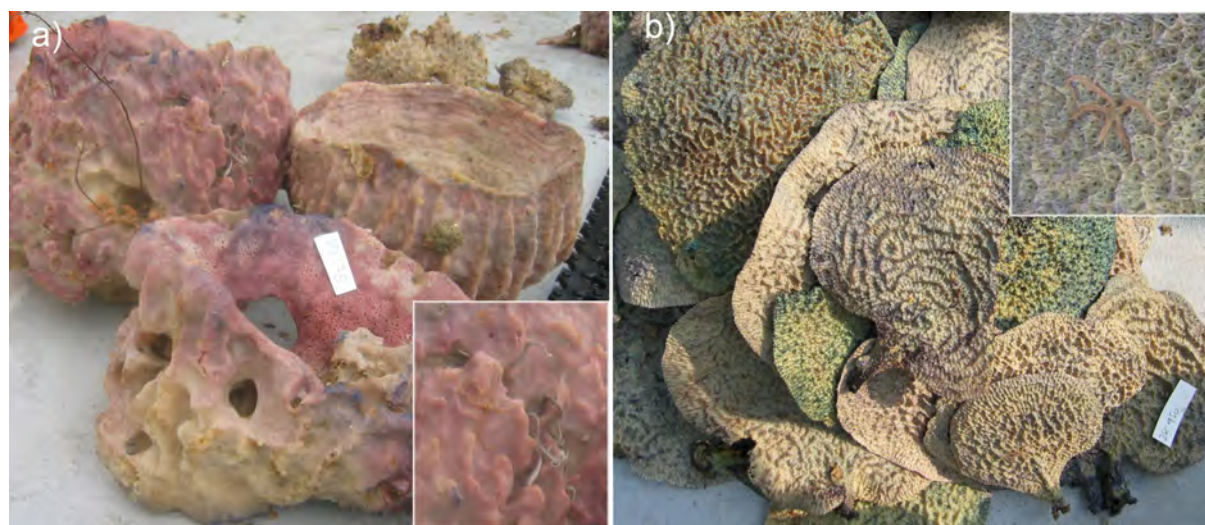


Figure C5: The most widespread sponge species collected on GA-322 were a) *Xestospongia tesudinaria* (station 41A) and b) *Ianthella flabelliformis* (station 32A). Insets show brittlestars inhabiting the sponges. Species identifications were undertaken by B. Glasby (MAGNT).

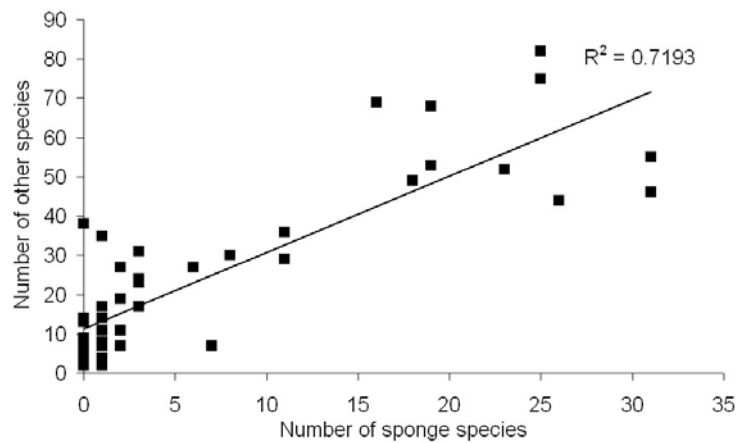


Figure C6: The relationship between species richness of sponges and other taxa collected from each sled tow on the GA-322 survey.

An understanding of the distinctiveness of biological communities among locations is critical for marine zone management. Here we use stations at which sponge gardens were identified based on sled trawls to investigate whether sponge communities are distinctive within and among geomorphic features (GA-322 only)). As identified by the BVSTEP procedure (Clarke and Warwick 2001), the following species were the main drivers of variation in sponge communities among these stations: *Echinodictyum mesenterinum*, *Ectyoplasia tabula*, *Ianthella flabelliformis*, *Ircinia irregularis*, *Leiodermatium* sp 4, *Oceanapia* sp 2, *Reniochalina* sp 2, *Scleritoderma* sp 1, *Suberea* sp 1, and *Xestospongia testudinaria*.

Among stations with mixed gardens, sponge communities within a geomorphic feature were more similar than sponge communities between features (Figure C7) (ANOSIM: $R = 0.486$, $p = 0.0019$). Of the driving species identified above, all stations at banks, ridges and terraces with mixed gardens were home to the giant barrel sponge *Xestospongia testudinaria* (Figure C5a); this sponge was not found in valley gardens. Within all stations at banks, all except Station 2A held *Echinodictyum mesenterinum* (Table C6). Two species were recorded at several stations on the bank in Area C (*Ircinia irregularis*, *Ectyoplasia tabula*), but found nowhere else on GA-322. The two banks surveyed (Moss Shoals in Area B and unnamed bank in Area C) were separated by approximately 58 km and shared 16.7% of sponge species. Similarly, the two groups of terraces surveyed in Area B and C were separated by similar distances and shared 12.1% of species. This is slightly less distinctive than sponge communities found among the Sahul Shelf, in which three reefs were separated by 35, 40, and 50 km and shared 13%, 24%, and 9% of species (Hooper and Ekin 2004). The majority of species (55%) identified from the 5 stations on the bank in Area C were collected from no other sponge garden, although results must be cautiously interpreted since sampling effort was unequal among banks (Figure C8). These findings indicate that sponge communities in the eastern JBG separated by tens of kilometres may be more distinct than those separated by kilometres. A final analysis of the distinctiveness of communities within geomorphic features is pending identification of GA-325 sponges.

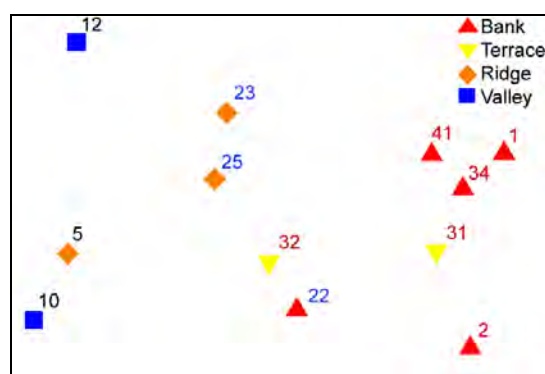


Figure C7: A non-metric multidimensional scaling plot of sponge communities from stations at which mixed gardens were identified from sled trawls. Each point represents the community of sponges at a given station based on presence/absence data. The distance between points denotes similarity between stations, with closer points representing stations with similar communities. Numbers are stations, with text colour indicative of study area (black = area A; blue = area B; red = area C). Data available only from GA-322. Stress = 0.08.

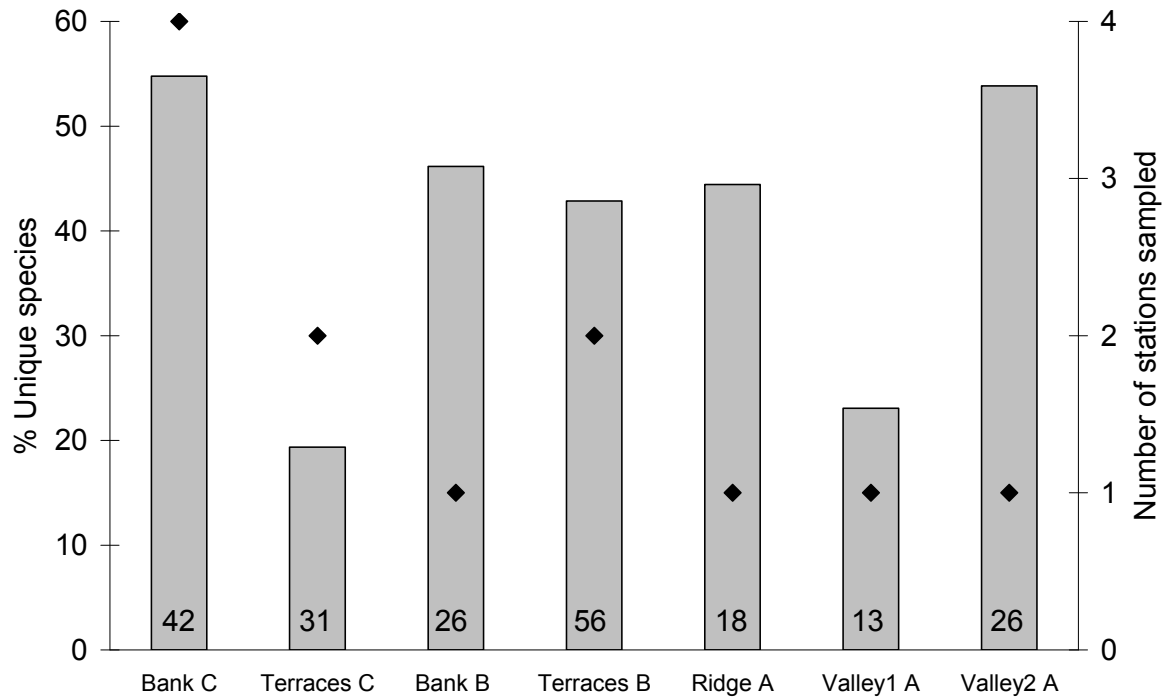


Figure C8: Unique sponge species identified from sled trawls over stations at which sponge gardens were found on GA-322. The bars represent percentage of unique species which was calculated by dividing the number of species found nowhere else by the total number of sponge species (indicated at bottom of bars). The diamonds represent sampling effort for each location feature and area. Features are listed on the x-axis with letters denoting the survey area (A, B, or C).

Table C6. Presence of key sponge species across all GA-322 bank stations at which sleds were deployed. Green indicates that the sponge was present at that station.

STATION	33	1	41	34	2	21	22
STUDY AREA	C	C	C	C	C	B	B
<i>Echinodictyum mesenterinum</i>							
<i>Ectyoplasia tabula</i>							
<i>Ianthella flabelliformis</i>							
<i>Ircinia irregularis</i>							
<i>Leiodermatium sp 4</i>							
<i>Oceanapia sp 2</i>							
<i>Reniochalina sp 2</i>							
<i>Scleritoderma sp 1</i>							
<i>Suberea sp 1</i>							
<i>Xestospongia testudinaria</i>							

Octocorals

Like sponges, octocorals (e.g. gorgonians, whips) provide habitat to a range of animals on the seafloor (Buhl-Mortensen et al 2011). In addition, octocorals can also be extremely long-lived and slow-growing (Linares et al 2007), making them potentially vulnerable to anthropogenic and natural disturbance (Probert et al. 1997). They have also been suggested as a key group for identifying high diversity in benthic habitats in the Arafura Sea (Wilson 2010). The most common octocoral along the Van Diemen Rise is the orange sea fan *Mopsella* sp. (Figure C9a) which is prevalent in sponge and octocoral gardens on ridges, banks and terraces, accounting for most of the biomass and abundance of octocorals. Ridges had the highest biomass (1.7 ± 3.4 kg) and species richness (10.2 ± 11.1 species) of habitat-forming octocorals (gorgonians, whips, black corals). The organ pipe coral *Tubipora musica* was found on the shallow banks of Moss Shoal.

Although a soft coral, this species is unique in that it secretes a hard skeleton which contributes to reef formation (Figure C9b,c).

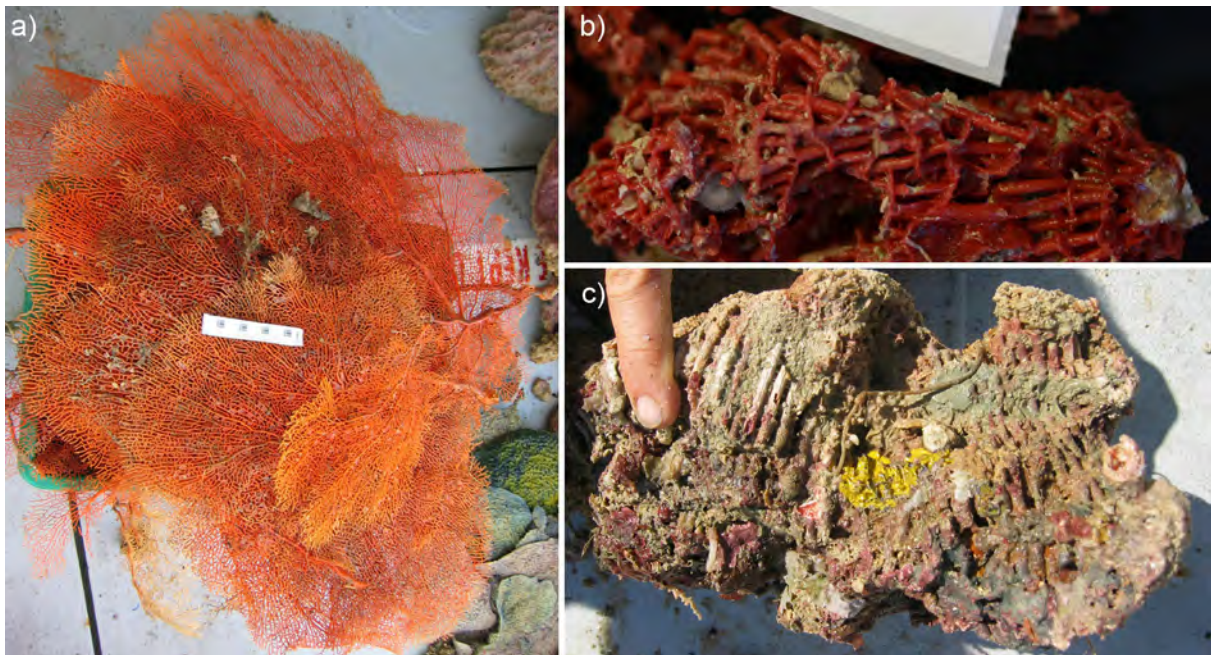


Figure C9: Several conspicuous species of octocoral were collected including a) the orange sea fan *Mopsella* sp., the most common gorgonian collected on GA-322 and GA-325 (specimens from bank at Station 25A, 42 m depth), and b) the organ pipe coral *Tubipora musica* that secretes a hard skeleton (specimen from Moss Shoal at Station 21A, 20 m depth) c) which contributes to reef formation (consolidated material from Moss Shoal at Station 21A, 20 m depth)

Among stations with sponge and octocoral gardens, the proportion of octocorals in relation to sponges seems to increase with distance from the coast (Figure C10). Although sponges still predominate the mixed gardens, octocorals may play an increasingly more important role in community structure as distance from the shore increases.

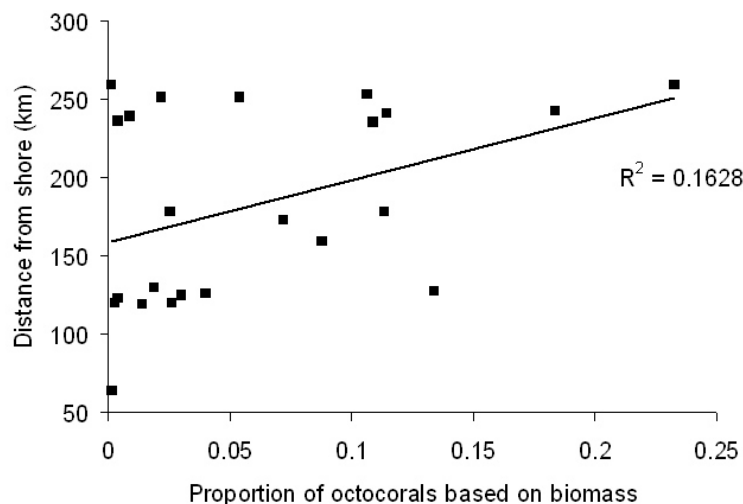


Figure C10: The relationship between distance from shore and proportion of octocorals that made up sponge and octocoral biomass from sled trawls.

Hard Corals

Scleractinian corals (i.e. hard corals) include solitary corals, as well as larger reef-forming corals. The latter can dramatically alter the available habitat in a region due to the continual growth and deposition of their carbonate skeletons. In addition to their ecological importance, coral reefs are also aesthetically valuable. Epifauna in the inner JBG are regulated by turbidity rather than temperature which suppresses macroalgae,

hard corals, and other photosynthetic benthic organisms, thereby allowing typically cool water biota such as molluscs and bryozoans to dominate (Clarke 2001). Indeed, surveys nearshore in the JBG revealed that scleractinian fauna was poor and consisted of mainly ahermatypic corals, with the solitary coral *Truncatoflabellum* dominating scleractinians from Beagle Gulf (Smit et al 2000).

Species identification from GA-325 revealed a range of families representing solitary corals, large polyp stony (LPS) corals, and large reef-building (i.e. hermatypic) corals (Table C7). Solitary corals occurred in low numbers with the exception of *Truncatoflabellum macroeschara* at Station 67B (Table C7) (Figure C11). Reef-building corals occurred at shallow depths of 28.5 – 33.4 m, while the solitary corals *Caryophyllia grayi* and *Truncatoflabellum* sp. were found at greater depths of up to 113 m (Figure C11). Most species of large reef-forming corals were collected only at a single location, with the exception of *Turbinaria reniformis*, a plate coral found at Stations 52B and 55B. Banks had the highest biomass (7.2 ± 26.0 kg) and species richness (1.2 ± 1.7 species) of all hard corals due to the fact that reef-forming corals were almost exclusively found on this geomorphic feature. The only exceptions were isolated branched corals, possibly the mesophotic *Stylophora pistillata* (Mass et al. 2007, 2010), which were found on the plains of Area D at Stations 53A and 13B. Several species were listed on the IUCN Red List, and further details are available in Section 2.7 of the main report.

Table C7. Species identifications of non reef-forming scleractinian corals from GA-325. Species identifications were undertaken by P. Muir, C. Wallace (MQT) and M. Kitahara (JCU). Refer to main report for images of large reef-forming corals.

AREA	STATION	DEPTH	FAMILY	SPECIES	TYPE	NUMBER	WT (G)
A	25B	75	Dendrophylliidae	<i>Balanophyllia gigas</i>	Solitary	1	
A	25B	75	Flabellidae	<i>Truncatoflabellum incrustatum</i>	Solitary	1	
A	036B	113	Caryophylliidae	<i>Caryophyllia grayi</i>	Solitary	3	10
A	036B	113	Flabellidae	<i>Truncatoflabellum</i> sp.	Solitary	3	10
A	050B	33.4	Caryophylliidae	<i>Heterocyathus aequicostatus</i>	Solitary	2	<100
A	050B	33.4	Fungiidae	<i>Cycloceris cf vaughani</i>	LPS	2	<100
A	052B	28.5	Fungiidae	<i>Fungia fragilis</i>	LPS	> 50	4000
A	052B	28.5	Dendrophyllidae	<i>Turbinaria reniformis</i>	Large hermatypic	Unknown ¹	
A	055B	31.4	Pocilloporidae	<i>Stylophora pistillata</i>	Large hermatypic	Unknown ¹	5800
A	055B	31.4	Dendrophyllidae	<i>Turbinaria reniformis</i>	Large hermatypic	Unknown ¹	100000
A	055B	31.4	Faviidae	cf <i>Caulastrea</i> sp	LPS	7	200
A	055B	31.4	Dendrophyllidae	<i>Turbinaria patula</i>	Large hermatypic	3	100
A	055B	31.4	Faviidae	<i>Cyphastrea serailia</i>	Large hermatypic	3	100
A	055B	31.4	Fungiidae	<i>Cantharellus cf noumeae</i>	LPS	3	100
B	65B	51	Dendrophyllidae	<i>Balanophyllia</i> sp.	Solitary	2	100
B	67B	78	Flabellidae	<i>Truncatoflabellum macroeschara</i>	Solitary	24	100

¹ Samples were broken during collection with the epibenthic sled so abundance was unable to be determined.

Although no live corals were recorded in the video from terraces, dead hard coral was recorded at one station (GA-325, Area A, station 48, 92 m water depth), with ~400 kg of dead branching coral rubble collected in the associated epibenthic sled. It is unclear however if these coral remnants are the result of *in situ* growth or transport from neighbouring areas.

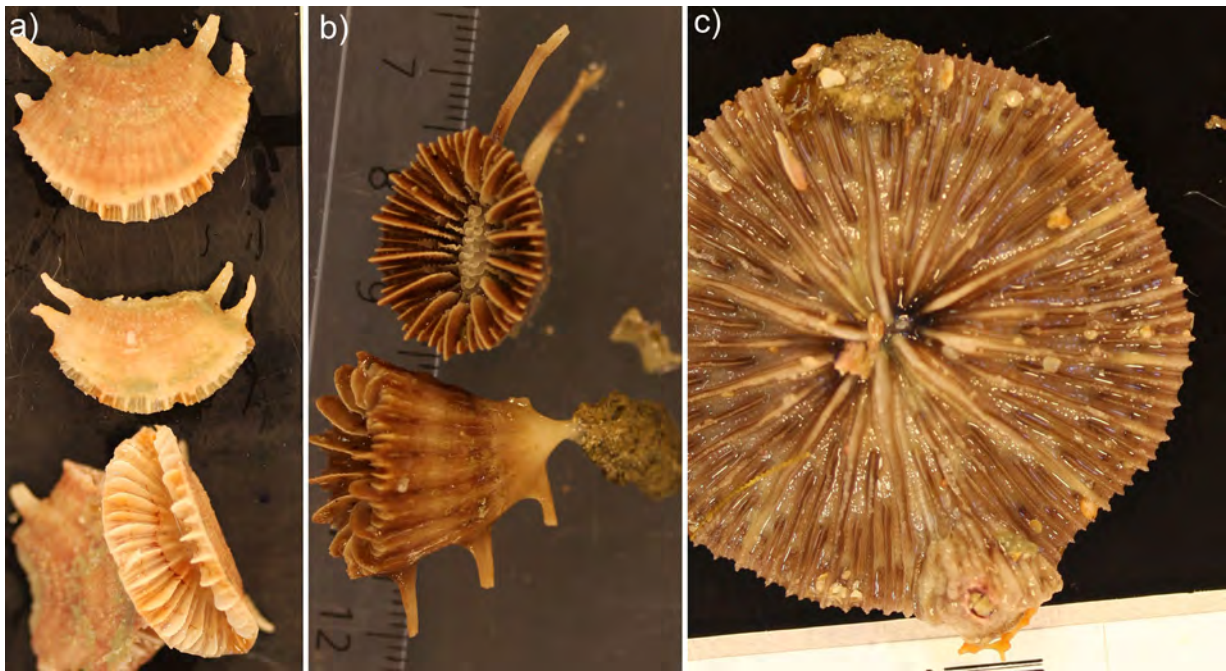


Figure C11: Solitary and LPS corals collected on GA-325: a) *Truncatoflabellum macroeschara*, b) *Truncatoflabellum* sp., and c) *Cycloceris cf vaughani*. Species were identified by P. Muir, C. Wallace (MQT) and M. Kitahara (JCU).

Echinoderms

Echinoderms include epifauna, infauna, and cryptofauna and comprise species from a range of habitats and trophic levels. In the current study species identifications were done for two classes of echinoderms: ophiuroids (brittlestars) and crinoids (featherstars). Ophiuroids are typically associated with soft sediments, and most species are deposit feeders (Edgar 2000) (Figure C12a). In contrast crinoids are more likely to occur on hard substrata and feed on drifting particles in the water column (Edgar 2000) (Figure C12b,c). Both crinoids and ophiuroids can also use larger taxa such as sponges, corals, or algae to provide substrate or habitat (Figure C5, Figure C12d). Brittlestar communities of northwest Australia including the JBG-TS show more variation than those in other regions (O'Hara 2008).

A total of 35 species of crinoids and 33 species of ophiuroids were collected from the sled from both surveys, with a further 16 species of ophiuroids collected from the grabs (GA-322 only). Of these, there were potentially four new ophiuroid species (*Ophiomyxid* sp., *Ophioplax* sp., *Asteromorpha* sp., and *Ophiarachna* sp.), as well as at least five new records for crinoids in Australia (*Amphimetra molleri*, *Himerometra bartschi*, *H. variipinna*, *H. martensi*, *Liparometra regalis*) and several range extensions. *Ophiochasma stellata* (Figure C12a) was the brittlestar that occurred at the most number of stations (21), and *Capillaster multiradiata* (Figure C12b) and *Cornatula pectinata* (Figure C12c) were the crinoid species that occurred at the most number of stations (22 and 23, respectively). Many animals were seen within sponges and wrapped around octocoral branches, and there was only a cursory attempt made to remove and catalogue these animals. Our estimates of echinoderm diversity in the survey area are therefore quite conservative.

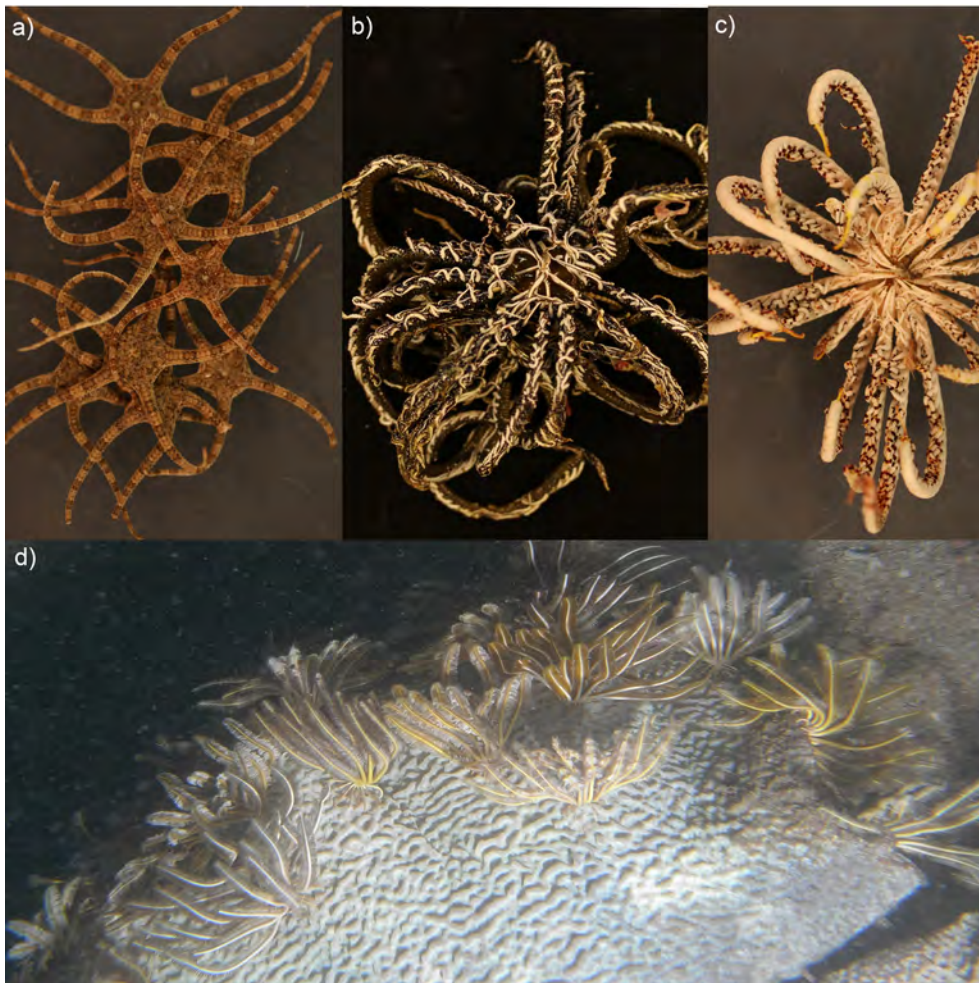


Figure C12: A range of echinoderms were collected on GA-322 and GA-325 including ophiuroids such as (a) *Ophiochasma stellata* and crinoids such as (b) *Cornatula pectinata* and (c) *Capillaster multiradiata*, both of which (d) use sponges as a key habitat provider. Species identifications were undertaken by T. O'Hara and K. Naughton (MV).

Molluscs

Like echinoderms, molluscs inhabit a range of environments and trophic guilds (Beesley *et al.* 1997). In addition, molluscs represent the 2nd largest animal phylum, and their shells can form an important component of biogenic sediments and the fossil record. Only 95 species from 40 families were identified (68 gastropods, 24 bivalves, 3 scaphopods) from the inner JBG, most of these small (<5mm) and fragmented (Clarke 2001). These numbers are similar to the 75 species of mollusc recorded from the Arafura Sea during a single survey (Wilson 2010) but far less than the 181 species recorded from the Beagle Gulf in which molluscs were the secondmost species rich phylum (Smit *et al.* 2000). Geographical ranges of many of these species are widespread throughout northern Australia or the Indo-Pacific (Clarke 2001).

A total of 59 species of live molluscs have been identified to date from sled transects from both GA-322 and GA-325, with a further 43 species collected from the grabs (GA-322 only) (Figure C13). Of these, at least four new species are likely (*Oliva* sp., *Eleutheromenia* sp., *Cuspidaria* sp., *Talabrica* sp., as well as at least one new record for Australia (*Obrussena moesimaensis*) and several range extensions. The most common mollusc from sled samples was *Bufonaria rana* which occurred at 6 stations; the most common mollusc from grab samples was *Notocorbula monilis* which occurred at 8 stations. In addition to live specimens, some empty shells were identified (Figure C13d), suggesting that species richness is actually far higher than suggested by our samples. In addition, despite low numbers of molluscs collected in both the sled and grabs, the detection of new species and distribution records indicate that much more intensive sampling is required to appropriately measure molluscan diversity in this region.

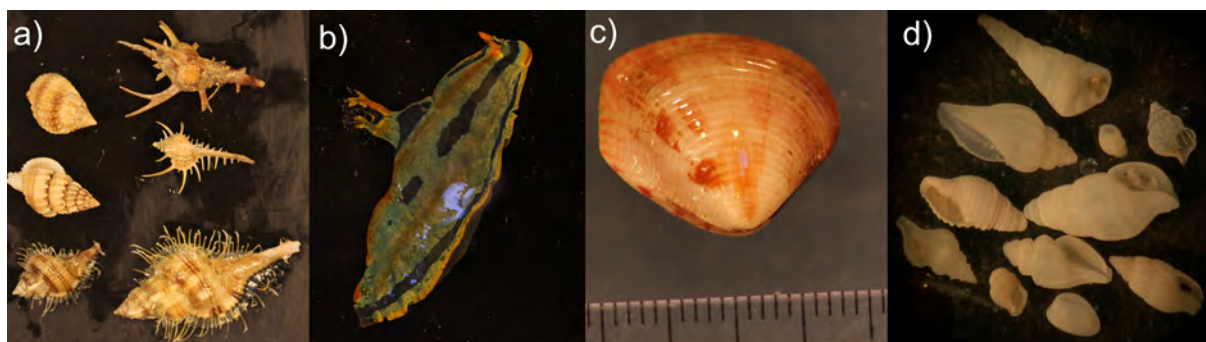


Figure C13: A small but diverse collection of mollusc was obtained from GA-322 and GA-325: (a) gastropods collected in the benthic sled, (b) a nudibranch *Tambja* sp., (c) a likely new species (*Talabrica* sp.), and (d) empty shells separated from grab samples. Species identifications were performed by R. Willan (MAGNT).

Other Epifauna

A large number of soft corals, hydroids, ascidians, bryozoans, crustaceans, and fish were also collected by the epibenthic sled (Figure C14). At the time of writing this report, no species have been identified, and data from these groups are only included in the current report as part of onboard estimates of overall species richness and biomass from sled transects.



Figure C14: Several taxonomic groups were commonly collected in the epifaunal sled but have not yet been identified: (a) hydroids and bryozoans, (b) ascidians, (c) crustaceans, (d) fish.

Infauna

Infauna live beneath the seafloor within the spaces created by grains of sediment. As such, they can be strongly associated with sediment and geochemical parameters (Mcarthur et al. 2010), although this is not always the case (Currie et al. 2009). In the lower JBG, 135 species were identified (WEL 2004), and 76 species of marine worms were identified in Darwin Harbour (Metcalf and Glasby 2008). This is similar to 117 species identified at the Ichthys Field to the northwest of our region of interest (URS 2009), but far less than the 684 species identified from the Gulf of Carpentaria in Long and Pointer (1994), most likely due to a much more intense sampling regime in the latter. JBG-TS infauna are dominated by polychaetes, with crustaceans also forming a major component (WEL2001), again similar to other studies in nearby regions (URS 2009, Long and Poiner 1994). The Beagle Gulf survey indicates that crustaceans, molluscs, and echinoderms are the dominant soft sediment taxa here (Smit et al 2000), and another survey found that crustaceans were much more prevalent than polychaetes in the soft sediments of the JBG (WEL 2004). However, these results may be a sampling artefact due to the large mesh size used (1 mm), whereby most of the polychaetes and smaller taxa were lost (Wilson 2006). In the southern JBG, crustaceans (tanaids, brachyurans, gammarid amphipods) and polychaetes were the most dominant taxa, followed by cnidarians (hydroids, alcyonarians), molluscs (bivalves), and echinoderms (urchins, brittlestars) (WEL 2001). Compared to marine sediments in other parts of the JBG-TS and neighbouring regions, sediments in the southern JBG have relatively depauperate infauna. However, closer to shore, higher species richness has been noted in the Beagle Gulf, with over 874 OTUs recorded and 1200 species predicted (Smit et al 2000). Infaunal diversity throughout the entire region is likely underestimated, as most surveys yielded only small

abundances of each taxon and species accumulation curves did not flatten (e.g. WEL2004, Wilson 2010). Annual and seasonal differences in species richness and abundance have been recorded for marine worms in the JBG; this is likely associated with monsoon intensity (Metcalf and Glasby 2008).

Based on a combination of expert taxonomic identification and identification using operational taxonomic units (Table C5), 490 species were identified from grabs deployed on GA-322. Infaunal communities were dominated by polychaetes and crustaceans, with ophiuroids, molluscs, and lancelets also common (Figure C15). Some epifaunal taxa were also collected (bryozoans, sponges, fish, cnidarians, molluscs), but there were few individuals in each grab.

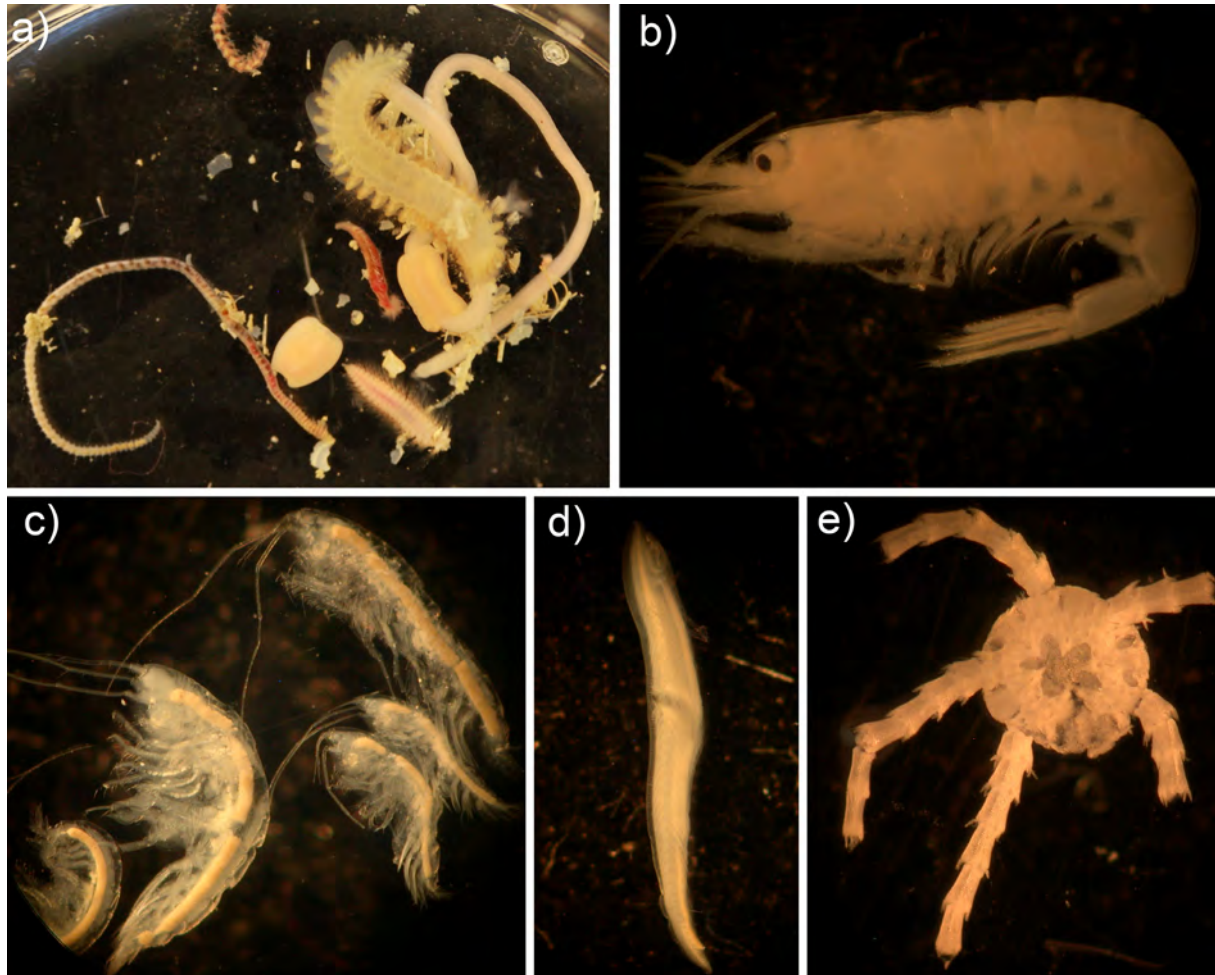


Figure C15: Infaunal communities were dominated by (a) polychaetes, (b) decapods (carid sp. 5) and (c) amphipods (gammarid sp. 7). Other taxa such as (d) lancelets and (e) ophiuroids (*Amphioplous* sp.) were also present.

Some geomorphic features were characterised by certain infaunal species: The most abundant taxon in the sediments from plains was gammarid sp. 7 (5.9 ± 3.0 individuals per grab) (Figure C15c). Plains were also characterised by more isopods than other geomorphic features, particularly isopods spp 2 and 8 (1.1 ± 1.9 , 0.4 ± 0.7 individuals per grab, respectively) Similarly, the most prevalent taxa in valleys were amphipods, particularly gammarid sp. 7 (Figure C15c), which had an average abundance of 2.3 ± 3.1 individuals per grab. The most characteristic species of valleys were carid sp. 5 (0.8 ± 1.2 individuals per grab) (Figure C15b), and the tube-dwelling tanaid sp 2 (0.6 ± 0.8), both of which also occurred in plain sediments. There were no infaunal species common enough to characterise ridges, banks or terraces.

As identified by the BVSTEP procedure (Clarke and Warwick 2001), the following species were the main drivers of variation in infaunal communities (GA-322 only): *Aglaophamus hedlandensis*, Capitellid sp. 4, Carid sp 1, Carid sp 23, Carid sp 5 (Figure C15b), Gammarid sp 2, Gammarid sp 3, Gammarid sp 4, Gammarid sp 6, Gammarid sp 7 (Figure C15c), Gammarid sp 9, *Harmothoe* sp. 1, *Micronephthys maryae*, Nebaliid sp 1, *Prionospio* cf *queenslandica/australiensis*, Tanaid sp 8, and *Trichobranchus bunnabus*.

Infaunal communities were significantly different among geomorphic features (ANOSIM: $R = 0.268$, $p < 0.001$). Communities within plains were more similar than infaunal communities among features, and similar but weaker trends existed among ridges. However, there was no clear separation of infaunal communities between banks, terraces, and valleys (Figure C16a). In addition, infaunal communities within plains were not distinctive from some communities from banks and valleys, as evidenced by the tight grouping of plain communities overlapping communities from the other features in the n-MDS (Figure C16a). Study area plays a more important role than geomorphic features in structuring infaunal communities (ANOSIM: $R = 0.322$, $p < 0.001$). Infaunal communities in Areas B, C, and D have some overlap, but the communities in Area A are distinct (Figure C16b). Area A infauna was characterised by species found nowhere else in the survey (e.g. carid sp. 23), and it was missing other species that were relatively widespread in other areas (e.g. *Micronephthys maryae*).

Infaunal communities at pockmarks were not clearly different from those at non-pockmark sites. Although there was some suggestion of similarity among pockmark communities in the n-MDS based on a possible grouping of pockmarked sites (Figure C16c), an ANOSIM revealed no significant differences ($R = -0.055$, $p = 0.729$). Incorporation of the GA-325 data may further confirm the lack of infaunal communities specific to pockmarks.

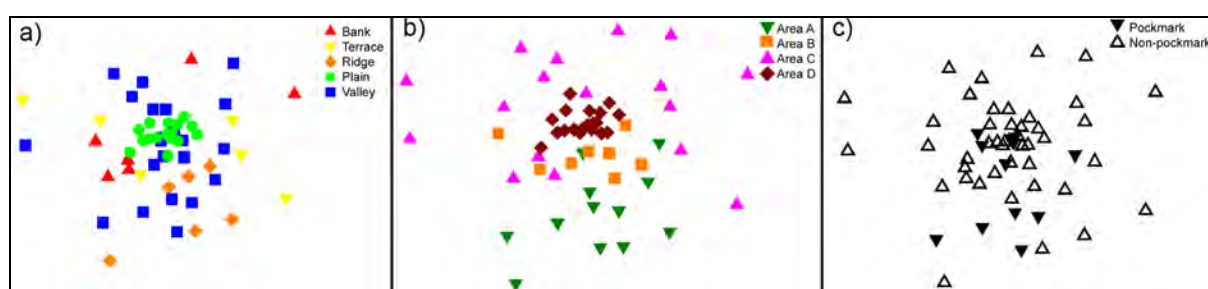


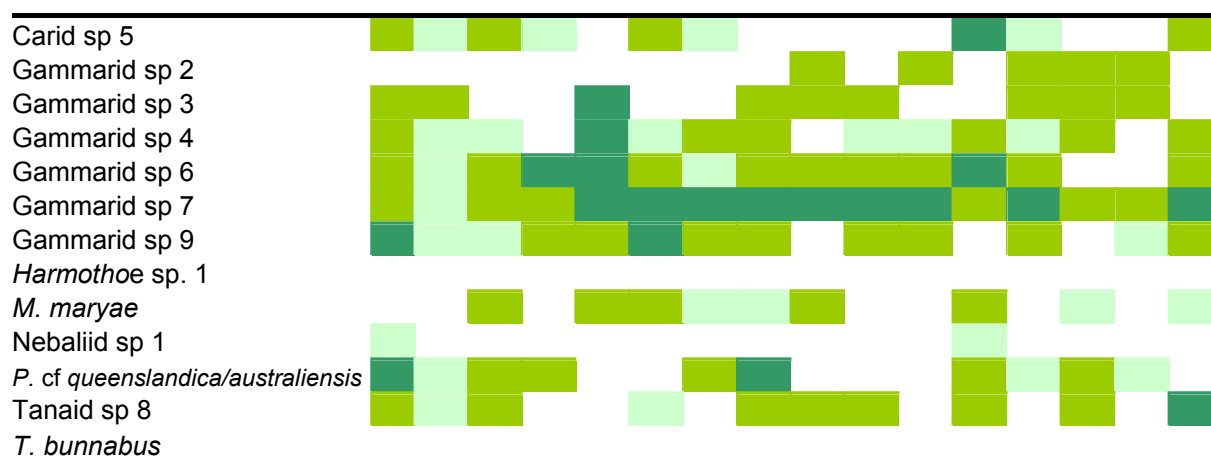
Figure C16: Non-metric multidimensional scaling plots of infaunal communities with potential differences based on (a) geomorphology, (b) study area, and (c) pockmarks. Each point represents the community of infauna at a given station based on square-root transformed abundance data. The distance between points denotes similarity between stations, with closer points representing stations with similar communities. Data available only from GA-322. Stress = 0.24.

Interestingly, 43 small transparent sipunculans (peanut worms) were collected at Station 43A (non-pockmark, valley, Area D). These worms were the most abundant organism collected at a single station and were found nowhere else on GA-322. This station was not characterised by any known exceptional environmental factors, although cluster analysis revealed that this station was geochemically similar to shallow pockmark stations ($< 60\text{m}$) (L Radke, unpublished data). The high abundance of these worms is likely due to localised recruitment, high micro-scale habitat heterogeneity, or environmental factors not considered here.

Of the driving species identified above, gammarid sp. 7 was the only ubiquitous species (Figure C15c), although several other species of gammarid amphipods occurred at most stations (Table C8). The two plain stations from Study Area B were home to infauna similar in species composition to those in Study Area D (Table C8). Thus, infaunal communities may be relatively similar across plains but with lower abundance as distance from shore increases. Unfortunately, most plain stations were in Study Area D (Table C8) so we are unable to validate this hypothesis with any degree of certainty. Future processing of infaunal communities from GA-325 will allow us to further investigate the distinctiveness of infaunal communities in the Joseph Bonaparte Gulf.

Table C8. Occurrence of key infaunal species across all GA-322 plain stations at which SM grabs were deployed. Light green indicates that 1 individual was collected at that station; green indicates that 2-4 individuals were collected; dark green indicates that 5 or more individuals were collected.

STATION	26	27	42	45	46	48	49	50	52	53	54	56	57	58	59	60
STUDY AREA	B	B	D	D	D	D	D	D	D	D	D	D	D	D	D	D
<i>A. hedlandensis</i>	Dark Green	Dark Green	Light Green			Dark Green	Dark Green	Dark Green	Dark Green		Dark Green	Dark Green	Dark Green	Dark Green	Dark Green	Dark Green
Capitellid sp 4	Dark Green	Dark Green				Dark Green	Dark Green		Light Green				Dark Green	Dark Green	Dark Green	Light Green
Carid sp 1			Dark Green	Dark Green	Dark Green					Light Green		Dark Green	Dark Green	Dark Green	Dark Green	Dark Green
Carid sp 23	Dark Green											Dark Green	Dark Green			



Environmental Drivers

Epifaunal species richness was significantly but weakly correlated with gravel content ($p = 0.0447$) and pheophytin ($p = 0.0069$), with number of species increasing as gravel content and pheophytin increased (Figure C17). Epifaunal biomass was significantly but weakly correlated with gravel content ($p = 0.0049$) and total reactive chlorin ($p = 0.0329$), with biomass increasing as gravel content and total reactive chlorin increased. As depth increased, biomass decreased, but although significant, this relationship was extremely weak, with depth explaining $< 1\%$ of the variation among sites ($p = 0.0469$) (Figure C18). Infaunal species richness was significantly and moderately correlated to $\delta^{15}\text{N} \text{‰ AIR}$ ($p = 0.0017$) and significantly but very weakly correlated to effective iron ($p = 0.0197$) (Figure C19).

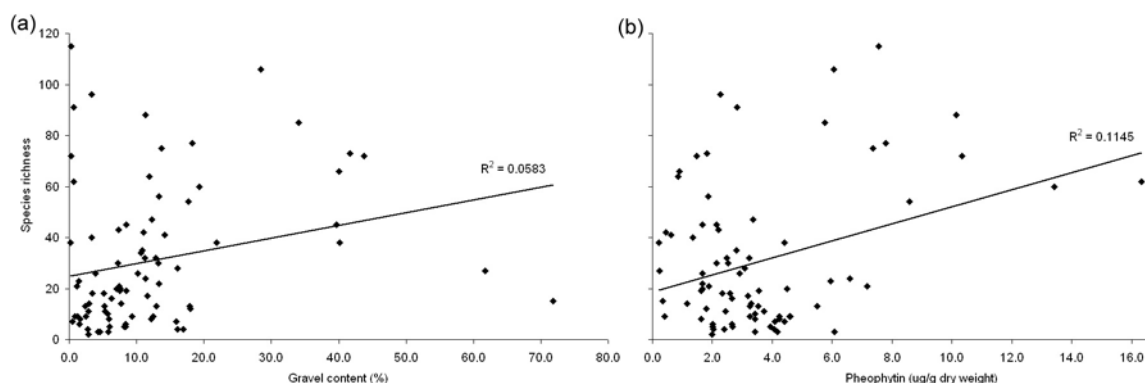


Figure C17: Epifaunal species richness was significantly but weakly correlated with (a) gravel content and (b) pheophytin. Data includes onboard estimated species richness from GA-322 and GA-325. Lines indicate best fit.

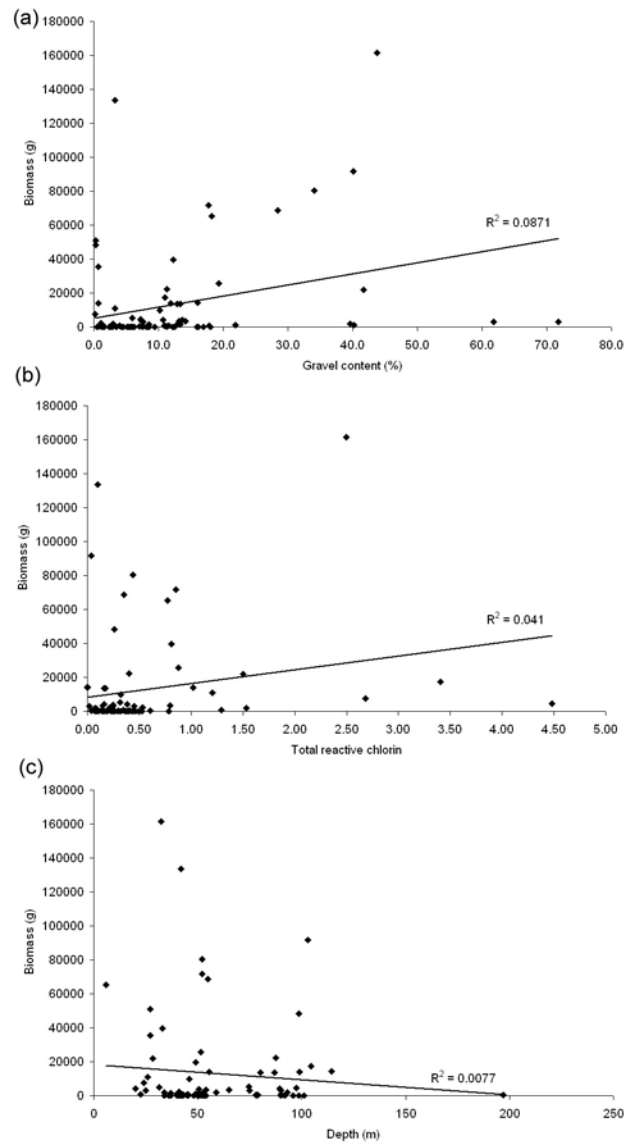


Figure C18: Epifaunal biomass was significantly but weakly correlated with (a) gravel content and (b) phaeophytin. Data includes onboard estimated biomass from GA-322 and GA-325. Lines indicate best fit.

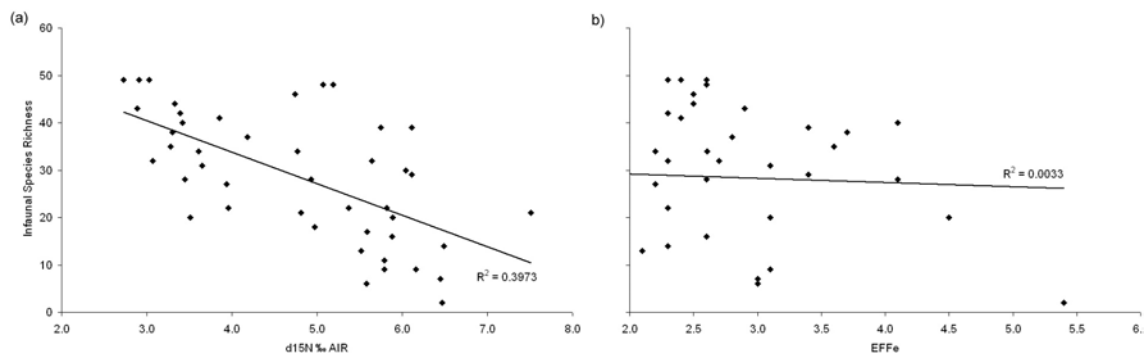


Figure C19: Infaunal species richness was significantly but weakly correlated with (a) d15N ‰ AIR and (b) effective iron. Lines indicate best fit.

The abiotic factors that best explained variation among sponge communities were a combination of depth, d15N% Air, Si/Al, aluminium, and manganese ($\rho = 0.343$). The abiotic factors that best explained variation

among infaunal communities were a combination of depth, gravel content, pheophytin, and %S-FeSAI ($p = 0.592$).

Backscatter signal was not correlated to species richness, biomass, or sponge community composition. However, backscatter signal was related to the presence of sponge gardens as identified from video and sled data (LDA, $F = 25.205$, $p < 0.0001$) (Figure C20a). Backscatter may also be related to the presence of hard corals (Figure C20b), but there were not enough stations with hard coral reefs to statistically test this hypothesis. Indeed, a probability index derived from backscatter and groundtruthing from video seems to have some predictive power for the occurrence of gardens of sponges, octocorals, and hard corals (Section 2.8 in main report).

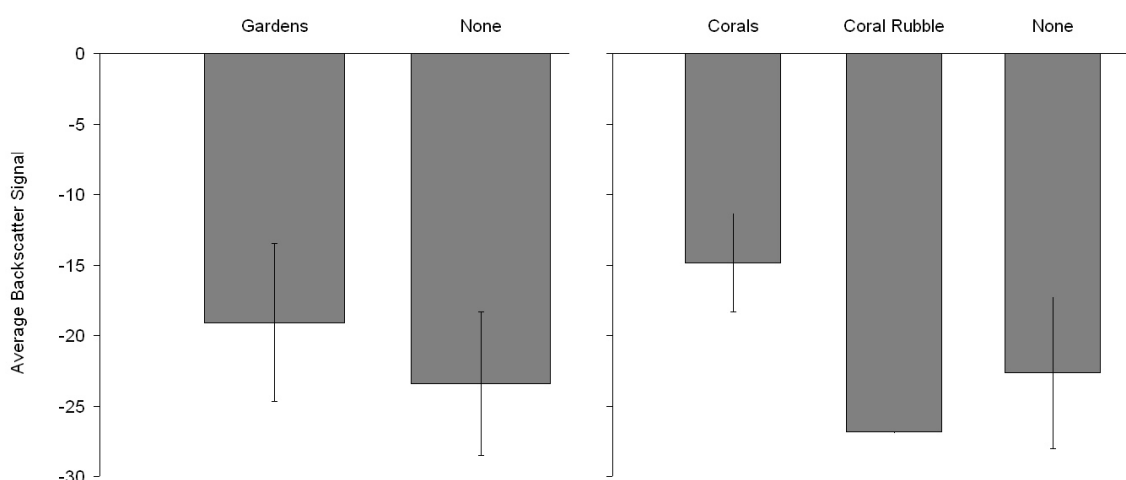


Figure C20: The relationship between backscatter signal and (a) presence of mixed gardens and (b) presence of hard coral reef. Biological data is based on both video and sleds from GA-322 and GA-325. Only one station returned was characterised by coral rubble (48B). Error bars are standard deviation.

Seascapes

Seascapes and associated focal variety indices were derived on a regional scale for the JBG-TS (Section 2.2 in main report). In order to determine whether these seascapes were biologically meaningful at the local scale, they were compared with species richness and species composition from GA-322 and GA-325. There was a difference among seascapes in both epifaunal ($F = 6.6692$, $p = 0.0004$) and infaunal species richness ($F = 0.9889$, $p = 0.0002$). Among epifauna, Seascape 4 had significantly higher epifaunal species than the other seascapes (Figure C21a). Among infauna, Seascape 1 had significantly lower infaunal species than Seascapes 2 and 4 (Figure C21b) (NB: Seascape 3 was unable to be statistically tested, as only one station from GA-322 occurred in this seascape). In contrast, there was only a very weak relationship between focal variety indices and epifaunal ($R^2 = 0.020$, $p < 0.0001$) and infaunal ($R^2 = 0.030$, $p < 0.0001$) species richness.

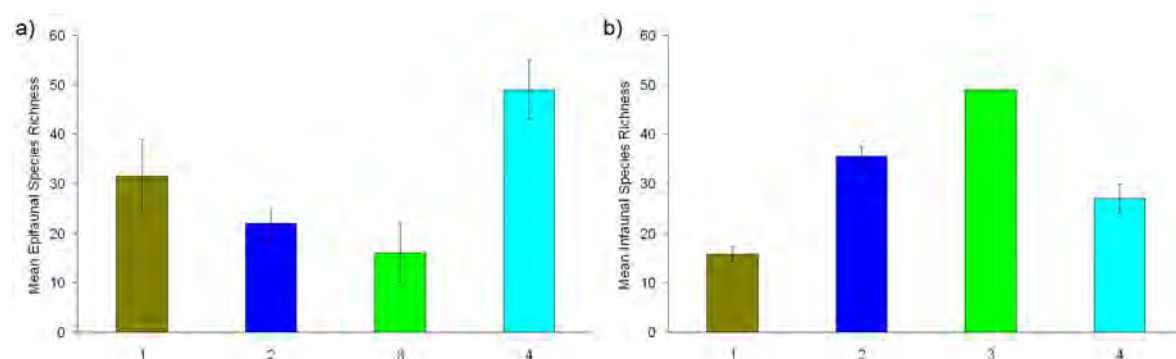


Figure C21: Species richness of (a) infauna and (b) epifauna among seascapes derived at a regional scale. Error bars are SEM.

Species composition of infauna and sponges was significantly different among seascapes (ANOSIM: $R = 0.275$, $p < 0.001$; $R = 0.22$, $p = 0.005$; respectively). However, the magnitude of differentiation varied among seascapes, with some classifications showing characteristic species composition and others showing little or no differentiation (Figure C22). These results support previous work which found that the biological utility of seascapes varied among individual classifications, spatial scales, and biological measures (Przeslawski et al. 2011).

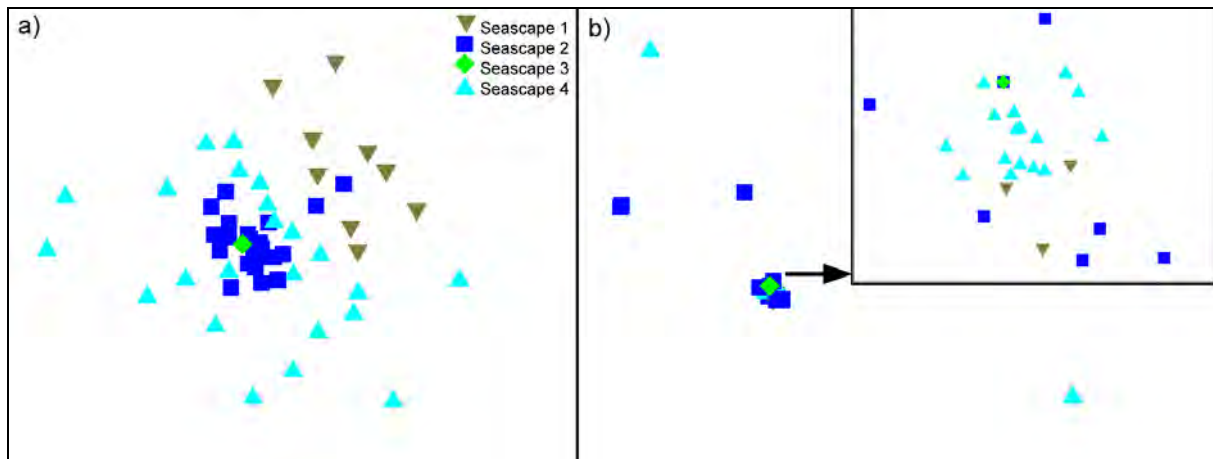


Figure C22: A non-metric multidimensional scaling plot of (a) infaunal and (b) sponge species according to regional scale seascape classifications for the JBG-TS. Each point represents the species composition at a given station based on abundance for infauna and presence/absence data for sponges. The distance between points denotes similarity between stations, with closer points representing stations with similar communities. The inset shows a magnified portion of the main sponge MDS. Data available only from GA-322. Stress = 0.24.

C4. Summary

- Several species of cetacean, hard corals and sea turtle that occur in the JBG-TS are endangered, threatened or vulnerable. In addition, several species recorded in the region are protected as Listed Marine Species, including sea snakes, sea turtles, and syngnathids (sea horses and pipefish).
- The availability of hard substrata varied by geomorphic type. Outcrops were more abundant and more homogeneous in banks, common but patchy in terraces and ridges, sparse and isolated in valleys, and absent in plains.
- Rocky outcrops and patchy rock habitats, regardless of the geomorphic feature, commonly supported mixed gardens (diverse assemblages of sessile invertebrates dominated by octocorals and sponges). Among stations with mixed gardens, the proportion of octocorals in relation to sponges seems to increase with distance from the coast
- Sponges represented the highest biomass and richness recorded of all taxa collected from the GA-322 and GA-325 surveys.
- Reef-forming living hard corals were identified from rocky outcrops on shallow banks and terraces (10-54 m depth). These corals were often diverse and locally dense (up to 90% cover), but overall % cover was very low (<1%). Two isolated branched corals were also recorded along a shallow valley in an inshore plain (Area D), indicating that highly turbid sediment plains can also support limited hard coral growth. These specimens may be mesophotic strains of *Stylophora pistillata*, a reef-forming coral able to adapt to limited light conditions. This species was found on the banks in Area A as well. There were no reef-forming species of hard coral recorded from ALA or OBIS, suggesting either that areas outside the survey area do not support corals or, more likely, that sampling has been insufficient in other regions of the JBG-TS.

- Banks, ridges and terraces may represent environments with comparatively less disturbance, as higher abundances and large vulnerable growth forms of octocorals and sponges were more common in these features.
- Sponge and infaunal communities were more similar within a geomorphic feature than between features.
- Species richness and species composition varied among seascapes derived at a regional scale. However the strength of these differences varied according to the biological data used and each seascape classification.
- Infaunal communities at pockmarks were not clearly different from those at non-pockmark sites.
- Bioturbation occurred in all geomorphic types, but overall occurrence generally increased with increased sediment availability. The exception to this was plains, where buried shell material appears to have limited bioturbation activity.
- There were no strong relationships between environmental variables and species richness, biomass, or sponge community structure. However, lower backscatter signal was associated with mixed gardens and reef-forming corals.
- Specimens collected included new species, range extensions, and records for Australia.
- No siboglinids or other species known to be indicative of seeps were found.

Appendix D: Geomorphology & Sedimentology

In this appendix, we provide a detailed account of the classification of geomorphic features in the study area, as well as their patterns of distribution and spatial coverage. We examine regional scale geomorphology (100s km) which includes our entire region of interest as defined in the main report. We then examine local scale geomorphology (10s km) which includes the survey areas from GA-322 and GA-325. This appendix also briefly summarises regional scale trends in sediment distribution.

D1. REGIONAL SCALE GEOMORPHOLOGY

Heap and Harris (2008) divide the Australian EEZ into four physiographic regions: the inner shelf; middle shelf; outer shelf/slope; and abyssal plain/deep ocean floor. These divisions are made on the basis of water depth and geomorphic features. The Joseph Bonaparte Gulf consists of only the inner and middle shelf regions. The inner shelf occurs in water depths of <30 m, the middle shelf includes water depths that range from 30 – 200 m. The Bonaparte Gulf receives significant loads of sediment from the numerous rivers in the region. Lees (1992) described the southern portion of the Bonaparte Gulf as “an excellent example of a macro-tidal carbonate/clastic transition”. The shallower, inner shelf, within the Joseph Bonaparte Gulf is dominated by recently deposited clastic sediments from these rivers. These sediments transition within increasing depth into relict clastic sediments and then into the carbonate dominated middle shelf.

The geomorphology of the JBG region is complex and consists of a series of rises, depressions, banks, terraces and channels (van Andel and Veevers, 1967 and summarised in [Section 2.3](#) of main report). The Bonaparte Depression is bound by the Londonderry, Sahul, and van Diemen Rises. The depression comprises a 45,000 km² basin that forms an epicontinental sea with a maximum water depth of 155 m (Lees, 1992). The eastern flank of the depression is steep, the western flank very gentle and the south merges into a broad, featureless plain (van Andel and Veevers, 1967). The floor of the depression is relatively flat and punctured by numerous pinnacles and subaqueous banks (Harris et al., 2003). The Matila Shelf Valley is a long, narrow, curved channel that connects the Bonaparte Depression with the Timor Trough (van Andel and Veevers, 1967).

Flanking the Bonaparte Depression and the Malita Valley are a series of submerged carbonate banks that are separated from one another by narrow sinuous channels of up to 150 km in depth (Harris et al., 2003). The banks are generally <10 km² in area with flat tops and developed both as terraces and benches and contain steep slopes of up to 33°, with an average of 20° (van Andel and Veevers, 1967). It has been proposed that many of the carbonate bank systems within the Timor Sea have developed over active hydrocarbon seeps (Hovland et al., 1994; Heyward et al., 1997; Lavering and Jones, 2001; Glenn and O’Brien, 2002; O’Brien and Glenn, 2005). The banks are interpreted by Lavering (1994) to be drowned carbonate platforms that were unable to keep pace with rising sea level during the Holocene.

Harris et al. (2005) provide a national-scale geomorphic classification of the Australian Exclusive Economic Zone (EEZ) based on published literature and an interpretation of the national 250m resolution bathymetric grid. This classification yielded 10 geomorphic features within the JBG-TS region of interest ([Fig. 2.5](#) in main report). The four dominant geomorphic classes in the JBG-TS were shelf (36.17%), basin (22.91%), terrace (13.07%), bank/shoal (11.99%) ([Table D1](#))

Table D1. Total areas represented by individual geomorphic features within the JBG based on Harris et al (2005) and Heap and Harris (2008).

FEATURE	AREA (KM)	AREA (%)
bank/shoals	18987.17	11.99
basin	36270.75	22.91
deep/hole/valley	6555.86	4.14
Land	12139.93	7.67
pinnacle	634.75	0.40
plateau	291.54	0.18
reef	490.89	0.31
shelf	57253.91	36.17
sill	3226.58	2.03
terrace	20682.31	13.07
tidal-sandwave/sand-bank	1725.04	1.09

D2. LOCAL SCALE GEOMORPHOLOGY

Within the GA-322 and GA-325 survey areas, six major geomorphic features were observed based on definitions from Heap and Harris (2008) (Tables D2-3): 1) Banks are local or regional areas of elevated seafloor with one or more steep sides; 2) Terraces are defined by a relatively flat or gently sloping seafloor with a moderately steep rise on one side and a moderately steep drop on the other side; 3) Plains are extensive, flat, gently sloping or nearly level region; 4) Valleys are tapered depressions on the shelf characterised by laterally converging contours of increasing depth; 5) Ridges are a long, narrow elevation with steep sides; 6) Scarps are elongated and comparatively steep slopes separating more gently sloping areas.

All four survey areas show features consistent with the regional geomorphology, i.e. numerous bank and terraces dissected by deep sinuous channels. Area D differs from the other three areas by having comparatively little relief (~20m overall), with shallow channels eroded into an extensive flat plain (Table D2). The other three survey areas are deeply incised by valleys and possess considerably high relief. These channels dissect terraces and banks, many of which presently support extensive hard substrate communities including living hard corals. The excessive depth (> 200m) and scoured appearance of the valleys indicates that incision by tidal processes during sea-level transgression may have shaped some of them. Valley systems from a tidally dominated environment with a similar morphology are documented from the northern Great Barrier Reef (Harris et al 2005).

Pockmarks occur in areas A, C, and D but are only found extensively in A and D. They are indicative of seepage of fluid or gas from the subsurface. Pockmarks generally occur in the valleys and plains where sediments have accumulated (i.e. away from hard substrates and scour zones) (Section 2.4 in main report).

Table D2. Summary of Geomorphic Features within the for Survey Areas (from surveys GA-322 and GA-325)

SURVEY	BANK/ SHOAL	PLAIN	RIDGE	SCARP	TERRACE	VALLEY
Area A km ²	78.78	-	158.47	20.42	130.62	490.19
Area A %	8.97	-	18.04	2.32	14.87	55.80
Area B km ²	25.26	166.91	26.46	3.4	22.40	165.86
Area B %	6.16	40.68	6.45	0.83	5.46	40.43
Area C km ²	38.53	-	3.29	4.20	137.47	91.39
Area C %	14.02	-	1.20	1.53	50.01	33.25
Area D km ²	-	207.26	-	-	-	26.33
Area D %	-	88.73	-	-	-	11.27
Total km²	168.9	374.17	188.22	28.02	290.49	747.44
Total %	9.40	20.82	10.47	1.56	16.16	41.59

Table D3. Depth ranges within survey areas.

	AREA A	AREA B	AREA C	AREA D
Depth Range (m)	24-174	7-116	16-214	37-57

Each sampling station was assigned a geomorphic classification based on the feature with which it overlapped. Several sled and camera transects crossed two geomorphic features. In these cases, the geomorphic feature over which the majority of the transect crossed was used. If the transect included roughly the same proportion of each feature, we assigned the station the geomorphic feature over which an associated grab was deployed.

D3. SEDIMENTOLOGY

Geoscience Australia's Marine Sediments Database (MARS) contains 357 grainsize data points occurring in the JBG-TS study region. These represent a range of point and transect samples including grabs, dredges and cores. Samples were sourced from 9 surveys conducted by GA and other organizations between 1960 and 2010 (Total available samples for each survey are listed in [Appendix A](#)). Weight % gravel, sand and mud assays were generated by GA and external laboratories using a sieve method. Additional assessments of physical properties (e.g. laser grainsize distributions, and interpretation of sorting and kurtosis) exist for some samples.

Samples provide sparse coverage of the entire region however, distribution is not uniform. Samples cover a water depth range of 10 - 175 metres and achieve coverage of 9 of the 10 regional scale geomorphic features identified in the study region. No samples are available for reefs. Samples provide coverage of all of the local scale geomorphic features identified in the survey areas.

Regional sediment distribution was predicted by interpolating available point sediment assays at a 0.01 decimal degree resolution using optimised interpolation methods ([Appendix B](#)). Accuracy of this dataset and ability to resolve fine scale trends in sediment distribution depend on distribution and density of point sample data used in modelling.

Interpolations of sand/gravel/mud content of sediment within the study region show that gravel generally forms between 1 and 20 % of sediment. Higher gravel contents are present locally in the south of the Joseph Bonaparte Gulf, in the northwest and north east of the JBG-TS associated with Banks and Shoals, and in a basin in the west. Gravel values predicted for these areas range from 20 - 60%, though higher concentrations of gravel may be present locally.

Mud occurs as a minor component of sediment across the entire basin area. Mud forms a substantial part of sediment across the entire study area. Lower mud values (<40%) are present near the coast in the south and south west of the Gulf. Sediments with >80% mud occur locally near shore in the south east of the gulf, and in the northeast associated with banks/shoals there.

The artefacts in the mud and gravel predictions reflect the impacts of latitude and longitude that were used as secondary information in the predictive models. For detailed discussion of this, please see Li et al. (2010, 2011).

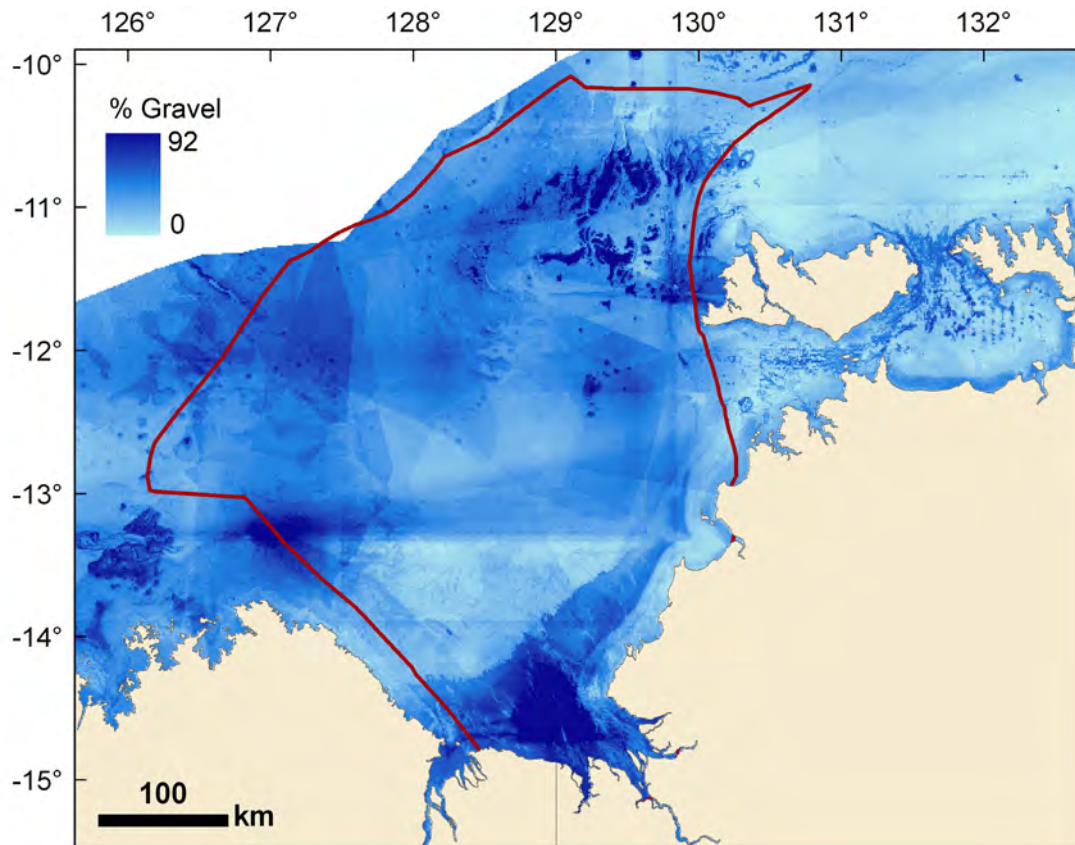


Figure D1: Spatial distribution of gravel content (%) in the JBG-TS based on interpolations described in [Appendix B](#). The red line indicates the region of interest in this report.

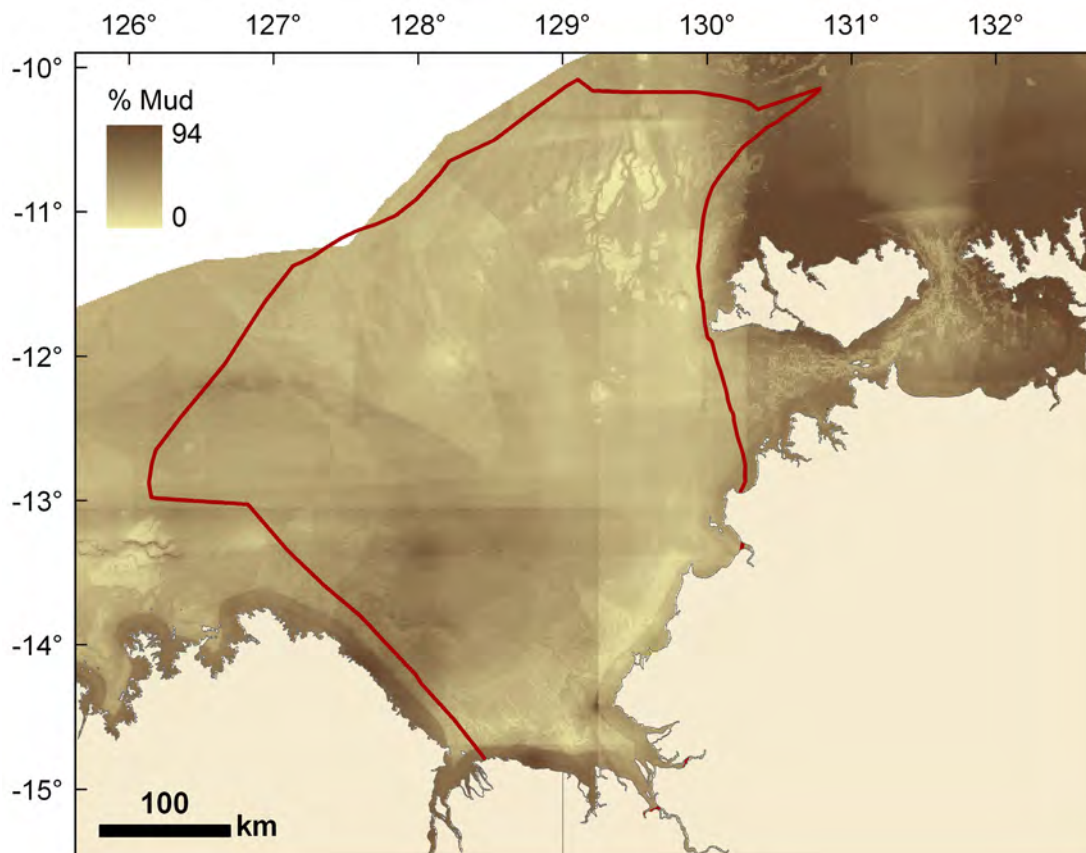


Figure D2: Spatial distribution of mud content (%) in the JBG-TS based on interpolations described in [Appendix B](#). The red line indicates the region of interest in this report.

Appendix E: Geochemistry

The principle aim of the geochemistry component of the study was to determine the geochemical composition of seabed sediments in order to develop a better understanding of the major sedimentary environments (including pockmarks and large-scale geomorphic features) and biodiversity patterns in the region. After providing a basic description of the sediments in terms of the main geochemical constituents and grain size distribution, we use Discriminant Function Analysis (DFA) to determine the geochemical/sedimentological variables that best discriminate between different: (i) geomorphic features and (ii) communities based on video-assessment. Geomorphic features are sometimes a useful surrogate of biodiversity (McArthur, et al. 2010; Anderson et al., 2011a), and we hypothesised that they may form the fundamental basis for extrapolating the results of our study areas to the wider Gulf. The main geomorphic features in the Joseph Bonaparte Gulf are plains, banks, terraces, deep holes/valleys (DHV) and ridges (Figure 2.5). The video-based communities are classified as being 'barren', 'bioturbated', 'mixed patches', 'mixed gardens' and 'mixed gardens with hard corals'. The sediments of pockmarks are also compared/contrasted to pools of remaining (non-pockmarked) DHV and plain sediments, and pore water TCO₂ concentrations are discussed in relation to the physical character of the sediments.

E1. DATA & METHODS

E1.1 Data

A range of geochemical/sedimentological variables were measured at each station on unconsolidated surface sediments that were collected using single grabs measuring 21 x 20 cm (10 cm deep; Shipek grab) or 0.1 m² (Smith-McIntyre grab). The variables included major, minor and trace elements, pigments, carbon and nitrogen concentrations and isotopes, pore water constituents (including pore water carbon dioxide), oxygen consumption and carbon dioxide production rates as well as a range of derived parameters (e.g. enrichment factors relative to average upper continental crust (UCC); chlorin indices etc). Summaries of the methods that pertain to the collection and analysis of the geochemical/sedimentological data are provided in Heap et al. (2010) and Anderson et al. (2011b). Radke et al. (2011) has provided a rationale for the use of most variables, as they pertain to benthic characterisation and biodiversity applications.

E1.2 Discriminant Function Analysis

Forward stepwise DFAs were undertaken on sub-sets of variables (Table E1) using STATISTICA[®] Release 6, with geomorphic features/video-based habitats as grouping variables and tolerance values set to default (0.01). The forward stepping procedure successively selects variables that make the most significant contribution to the separation of groups until the F-values of remaining variables are smaller than a user defined value. The default *F to enter* value of 1 was used for our purposes. Variables used in the analyses (Table E1) met the assumptions of DFA in having approximately normal distributions, approximate homogeneity of variances/covariances (based on Brown-Forsythe Test), and means that were not correlated to variances (before or after transformation and across the groups in all cases).

DFA derives a set of linear functions from multiple variables that maximise the separation of pre-defined groups. Therefore, we use the DFA classification functions to determine the classification efficiency in assigning individual stations to features on the premise that low error rates are required in order to extrapolate our results to other regions within the Gulf. *A priori* classification probabilities were made proportional to group sizes and errors were calculated manually by jackknifing to produce a 'new cases' e.g. a single case was left out (1/125), and the functions derived from DFA's on the remaining cases (123/124) were used to classify the 'new case'. The procedure was repeated until all cases (124 samples) were tested.

Table E1. Variables used in the discriminant function analysis and the transformations applied to these variables. The listed variables met the assumptions of DFA either before or after transformation.

	UNTRANSFORMED (USED IN ANALYSIS)	LOG ₁₀ TRANSFORMED (USED IN ANALYSIS)	SQUARE-ROOT TRANSFORMED (USED IN ANALYSIS)
Features	Al, Fe, Ti, Zn, EFe, CaCO ₃ , Pheophytin, Sediment Oxygen Demand (SOD), reaction coefficient (k), particle surface area (PSA), Ba, V, La _N , *K, δ ¹³ C	TOC:S, Chlorophyll-b (Chl- b), Chlorophyll-c (Chl-c), total reactive chlorins (TRC), Total chlorins, C:N, Si:Al, C m ² , N m ² , C:P, mean grain size, *Mg, La _N /Yt _N	Mn, Si, S, Co, %sand, %gravel, Chloroplastic Equivalents (CPE), TCO ₂ flux, δ ¹⁵ N.
Video-based Communities	*K, Ti, Co, %Mud, %CaCO ₃ , SOD, pH, δ ¹⁵ N, δ ¹³ C,	Mg, Si, Zn, EFMn, EFGc, EFCd, EFBa, EFAs, EFV, EFU, Eu, Fe/Al, TOC:TS, Total chlorins: pheophytin; TCO ₂ pool, TN (CFB), TOC (CFB), TOC, TN, Si/Al	Al, Fe, EFe, EFCo, Cr, Ce, %Gravel, Total chlorins, chlorin index, Total reactive chlorins, TCO ₂ flux, RCK, TOC:TN

1. The superscript * denotes that an element was corrected for seawater salts
2. EF refers to the enrichment factor of an element relative to the average for upper continental crust.
3. CFB refers to carbonate-free basis
4. The subscript 'N' on an element (La_N) indicates that the element was chondrite normalised.

E1.3 Statistical comparison of Means

Statistical tests were undertaken in STATISTICA[®] Release 6 to determine if there were differences in the mean values of sediment parameters between samples taken from pockmark regions and those belonging to the remaining pools of DHV (Area A) and plain (Area D) sediments. T-tests were used to compare variables for which the assumptions of approximate normality and equal variances were met (before or after square-root or Log₁₀ transformation). Mann Whitney U test were used on non-parametric data.

E2. RESULTS & DISCUSSION

E2.1 A general description of sediments

Chemical composition

Ca, Si, Mg and Al were the four main elements in the sediments of the eastern Bonaparte Gulf comprising ~95% of the sediments by weight. Examination of the interrelations between these elements in SiO₂-CaO+MgO-Al₂O₃ ternary space (Figure E1) reveals that the sediments were depleted in Al relative to upper continental crust (UCC), and that most major elements variation was along the CaO+MgO – SiO₂ dimension. The CaO-MgO end-member consisted of a mixed-carbonate assemblage comprising 26 ± 9.6% high-Mg calcite, 19.4 ± 6.4% low-Mg calcite and 24 ± 6% aragonite (based on SOL4934 data only). The SiO₂ end-member was composed mainly of quartz (24.5 ± 15.8%), but with small percentages of aluminosilicate. Clay percentages were small (5.4 ± 3.6%). Bank and terrace sediment were carbonate-dominated, plain sediments were mostly quartz-dominated, and DHV and ridge sediments could be either quartz or carbonate-dominated.

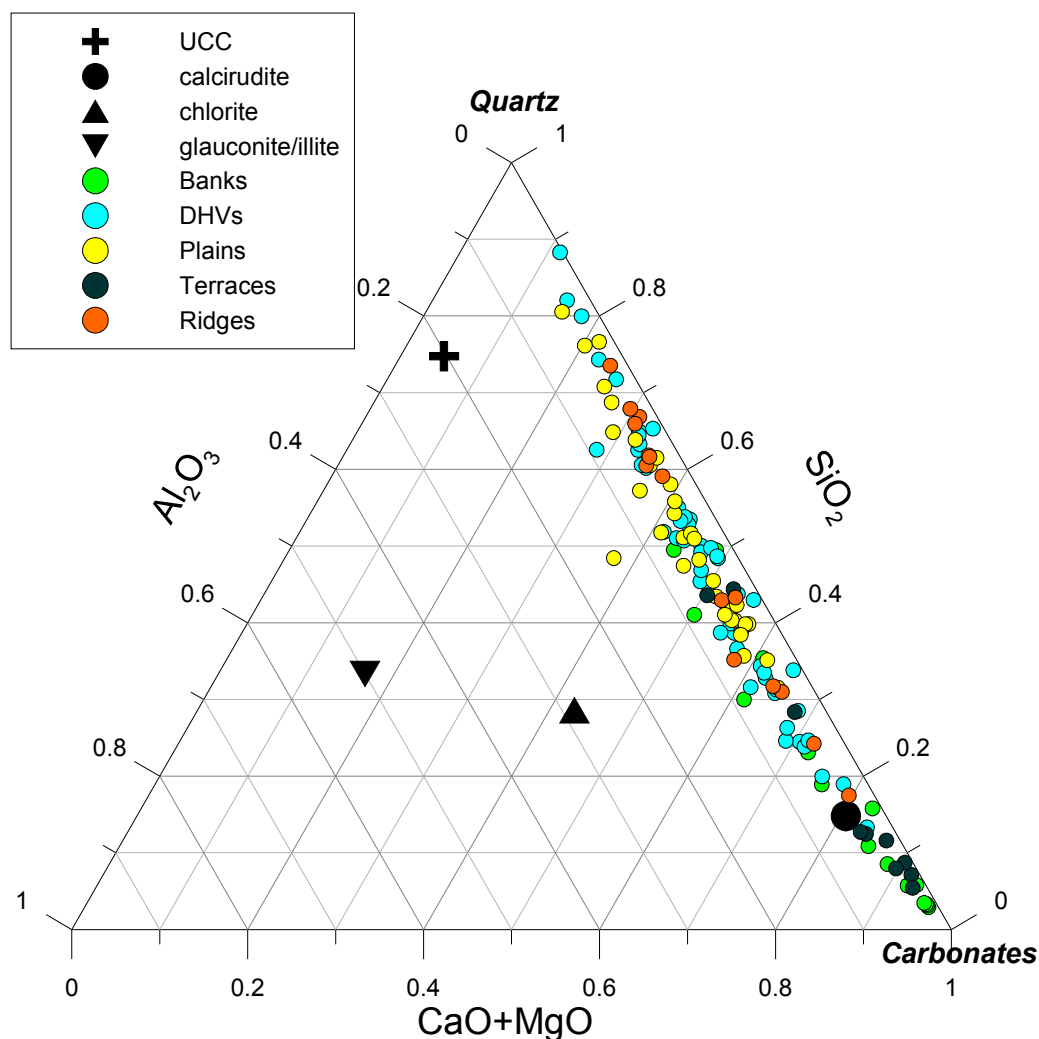


Figure E1: Trilinear diagram featuring the four main elements (mol %) found in the sediments of the study area. UCC refers to average upper continental crust. The positions of calcirudite (brown pellet group; Van Andel and Veevers, 1967), chlorite and illite/glaucouite are also shown because these minerals are known to occur in sediments in the region (Van Andel and Veevers, 1967; Gingeles et al., 2001). The calcirudite sample was collected from station 004 during SOL5117.

Grain Size Distribution and Sorting

With a few exceptions, sediment samples from the eastern Bonaparte Gulf were sand-dominated (>50% sand), and were described by eight Folk grain-size categories (Figure E2). Banks had lower median sand concentrations and higher median gravel concentrations than the other features, while plains had the most restricted range of grain size classes (mainly gravely muddy-sands). The sorting parameter for the sediments ranged from 1.5 to 13.5. However, the statistics for most samples were at the low end of the very poorly sorted range (4-6) (Figure E3). The widest range of sorting parameters and the most heterogeneous sediments were found on the banks.

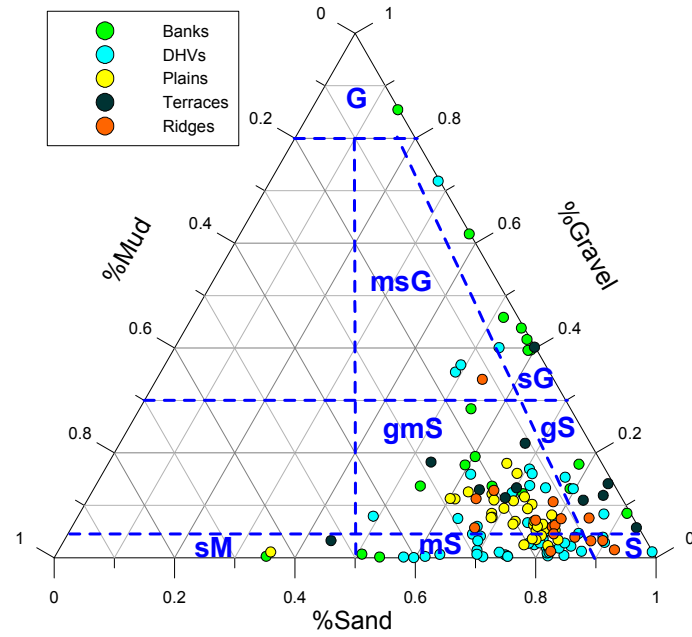


Figure E2: The relative percentages of sand, mud and gravel in the sediments of the study areas (simplified after Folk, 1954). The different classes include: sandy muds (sM), muddy sands (mS), sands (S), gravelly muddy sands (gmS), gravelly sands (gS), muddy sandy gravels (msG), sandy gravels and gravels.

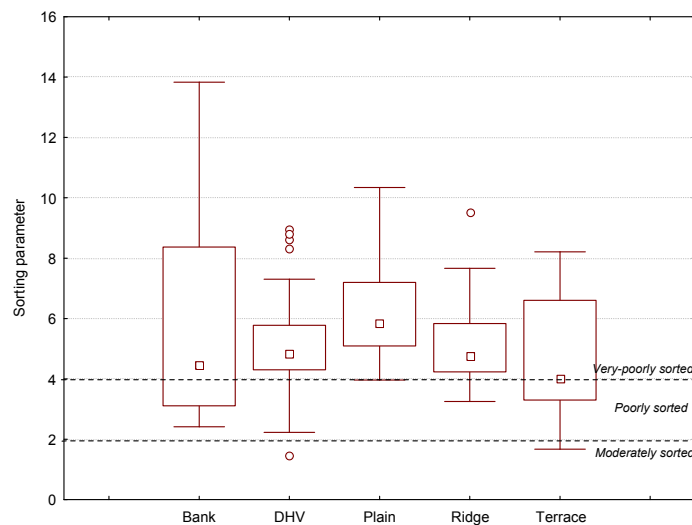


Figure E3: Box and whisker diagram showing sorting parameter statistics (median, 25th and 75th percentiles and maximum and minimum values) according to geomorphic feature.

B2.2 Geochemistry of Geomorphic Features

Four statistically-significant and independent (orthogonal) discriminant functions (canonical roots) were identified in a 25 parameter model. The first two functions accounted for 86.3% of the discriminatory power (Table E2) and, with the exception of some plains and DHVs, produced a good separation between the geomorphic features (Figure E4). Root 1 separates DHVs, plains and ridges from banks and terraces, with maximum separation between banks and plains. Root 2 has maximum discrimination between banks/terraces and ridges. Factor structure coefficients (Table E2) are correlations between variables and discriminant functions, and are a good basis for interpreting the roots. They show that the terrace/bank – DHV/plain/ridge differentiation on root 1 is due to higher relative CaCO_3 percentages and lower relative terrigenous element (Fe, Mn, Ti

and La_N) concentrations in the terraces and banks. Root 2 differentiated banks and terraces (and to a lesser extent plains) from ridges and valleys on the basis of higher Mg and reactive organic matter concentrations, and lower Si/Al ratios. The root 2 canonical scores correlated weakly but significantly with water depth (root 2 = - 0.02 * water depth - 1.7; $R^2 = 0.26$; $P < 0.001$). The sediments found in the shallower water environments (e.g. banks, terraces and shallow plains) had magnesium calcite concentrations (>35%) that were typically higher than the average for the data-set (e.g. ~25%; SOL4934 only). The higher organic matter reactivity is also due to the general shallowness of these environments, in part because there is not much time for organic matter to break-down as it descends through the water column, and because some terraces/banks likely support benthic micro-algae. Sediment anoxia may occur in bank and terrace sediments because these samples closely correspond with a mixing line from UCC to pyrite in $\text{FeS}_2\text{-SO}_3\text{-Al}_2\text{O}_3$ ternary space (Figure E5).

Table E2. Factor structure coefficients and allied statistics: DFA of features.

VARIABLE	ROOT 1	ROOT 2
Mn (mg kg ⁻¹)	-0.48	-0.24
La_N (mg kg ⁻¹)	-0.47	-0.27
Fe (mg kg ⁻¹)	-0.39	-0.18
Ti (mg kg ⁻¹)	-0.34	-0.09
Co (mg kg ⁻¹)	-0.31	-0.07
Si:Al (mol)	-0.26	0.22
C:N (mol)	-0.23	0.27
C:S (wt)	-0.16	0.03
C:P (mol)	-0.15	-0.18
%Sand	-0.12	0.16
$\text{La}_\text{N}/\text{Yt}_\text{N}$	-0.07	-0.03
Zn (mg kg ⁻¹)	-0.07	0.18
Chl-b (µg g ⁻¹ dwt)	-0.07	0.11
EFFe	-0.06	-0.05
CPE (µg g ⁻¹ dwt)	-0.05	-0.01
N (g m ² dwt)	-0.03	0.03
C (g m ² dwt)	-0.01	0.07
k (y ⁻¹)	0.01	-0.09
Total reactive chlorins (µg g ⁻¹ dwt)	0.11	-0.29
*Mg (mg kg ⁻¹)	0.19	-0.29
$\delta^{15}\text{N}$ ‰ Air	0.21	0.18
%Gravel	0.29	-0.23
$\delta^{13}\text{C}$ ‰ VPDB	0.30	-0.23
*S (mg kg ⁻¹)	0.36	-0.24
%CaCO ₃	0.37	-0.09
<i>Eigenvalue</i>	3.53	1.83
<i>Per cent variance</i>	56.9	29.4
<i>Canonical correlation</i>	0.80	0.57

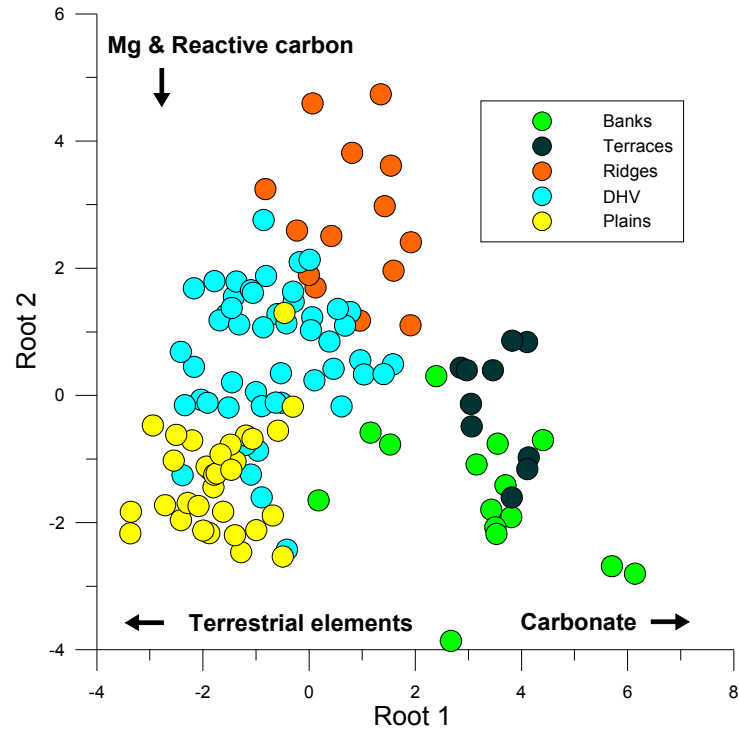


Figure E4: Scatterplot of DFA canonical scores for analysis on geomorphic features.

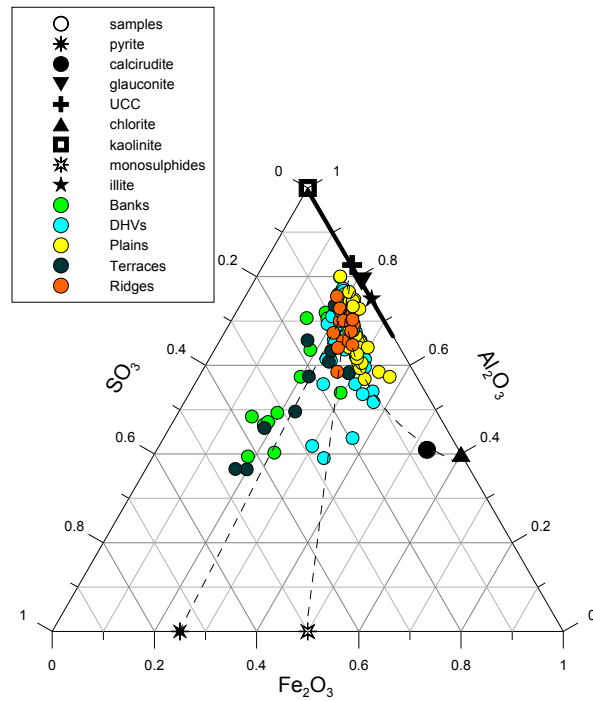


Figure E5: The interrelationships of SO_3 , Al_2O_3 and Fe_2O_3 in ternary space. UCC refers to average upper continental crust. The positions of calcirudite (brown pellet group; Van Andel and Veevers, 1967), chlorite and illite/glauconite are also shown because these minerals are known to occur in sediments in the region (Van Andel and Veevers, 1967; Gingeles et al., 2001). The calcirudite sample was collected from station 004 during SOL5117.

Table E3. Discriminant Function Analysis cross-validation classification rates (%) and sampling effort for different geomorphic classes. Values appearing in bold are the percentages of correctly classified samples for a given feature.

GEOMORPHIC CLASS	% CLASSIFIED AS:					
	Bank	DHV	Plain	Terrace	Ridge	No. stations
Bank	57.1	14.3	7.1	21.4		15
DHV		55.8	28.8	3.8	11.5	52
Plain	3.0	18.2	78.8			33
Terrace	50	10		30.0	10	10
Ridge	7.1	21.4			71.4	14

The accuracy of the DFA was 63.4% based on the cross-validation classification rates (Table E3), suggesting that the geochemical distinctness of the geomorphic features was moderate overall. Plains and ridges had the highest proportions of correctly classified samples. Misclassification rates were highest amongst terraces (Table E3): only 3 terraces were correctly classified.

Twenty-three DHVs were misclassified as plains (15), ridges (6) and terraces (2) (Table E3). There was a strong depth bias in these error rates. Approximately 75% of the misclassified DHVs were found at water depths <100 m, whereas most of the correctly classified samples were found at greater depths. The misclassified samples from water depths <100 m were all from Area D and were interpreted as plains. That the analysis differentiated poorly between plains and valleys is also evident in the strong degree of overlap between plains and DHVs in Figure E4, and in the misclassification rate data for plains. Six of seven of the misclassified plain samples were interpreted as DHV's.

The analysis always differentiated between plains and terraces/ridges, it seems because the terraces/ridges always had much smaller proportion of terrestrial elements than the plains. The analysis seldom misclassified banks for DHVs and visa versa which is due to the influence of water depth on the organic matter freshness indicators.

B2.3 Geochemistry of Video-habitats

Four statistically-significant and independent (orthogonal) discriminant functions (canonical roots) were identified in a 19 parameter model. The first two functions accounted for 82% of the discriminatory power (Table E4) and, with exception of the mixed patch samples, provided a good separation of the classes (Figure E6). As with the DFA on features, the first two functions can be interpreted as due to differences in terrestrial element and reactive organic matter concentrations. Barren and bioturbated sediments are differentiated from mixed patches and mixed gardens on the basis of higher terrestrial element concentrations, while mixed gardens with hard corals and barren sediments are noted for larger values for the reactive organic matter indicators. As with the DFA on features, the root 2 scores correlate weakly but significantly with water depth (root 2 = 0.02 *water depth -1.5; $R^2 = 0.19$; $p < 0.001$).

Table E4. Factor structure coefficients and allied statistics: DFA of video-habitats.

	ROOT 1	ROOT 2
Total reactive chlorins ($\mu\text{g g}^{-1}$ dwt)	0.41	-0.37
$\delta^{15}\text{N} \text{‰ Air}$	0.28	0.44
Si (mg kg^{-1})	-0.46	0.23
EFU	0.21	-0.21
%Gravel	0.33	-0.16
Zn (mg kg^{-1})	-0.14	0.29
EFV	0.16	-0.25

	ROOT 1	ROOT 2
Total chlorins/Pheophytin	0.14	-0.04
Total chlorines ($\mu\text{g g}^{-1}$ dwt)	0.22	-0.06
Cr (mg kg^{-1})	-0.07	-0.24
EFMn	-0.07	-0.28
EFEu	-0.14	-0.31
C:N (mol)	-0.20	0.12
Ti (mg kg^{-1})	-0.27	0.09
Chlorin Index	-0.30	0.38
RCK	0.03	-0.07
TCO ₂ flux ($\mu\text{mol g}^{-1} \text{d}^{-1}$)	0.09	-0.08
*K (mg kg^{-1})	-0.16	0.17
Al (mg kg^{-1})	-0.17	0.19
<i>Eigenvalue</i>	3.6	1.5
<i>Per cent variance</i>	57	25
<i>Canonical correlation</i>	0.58	0.62

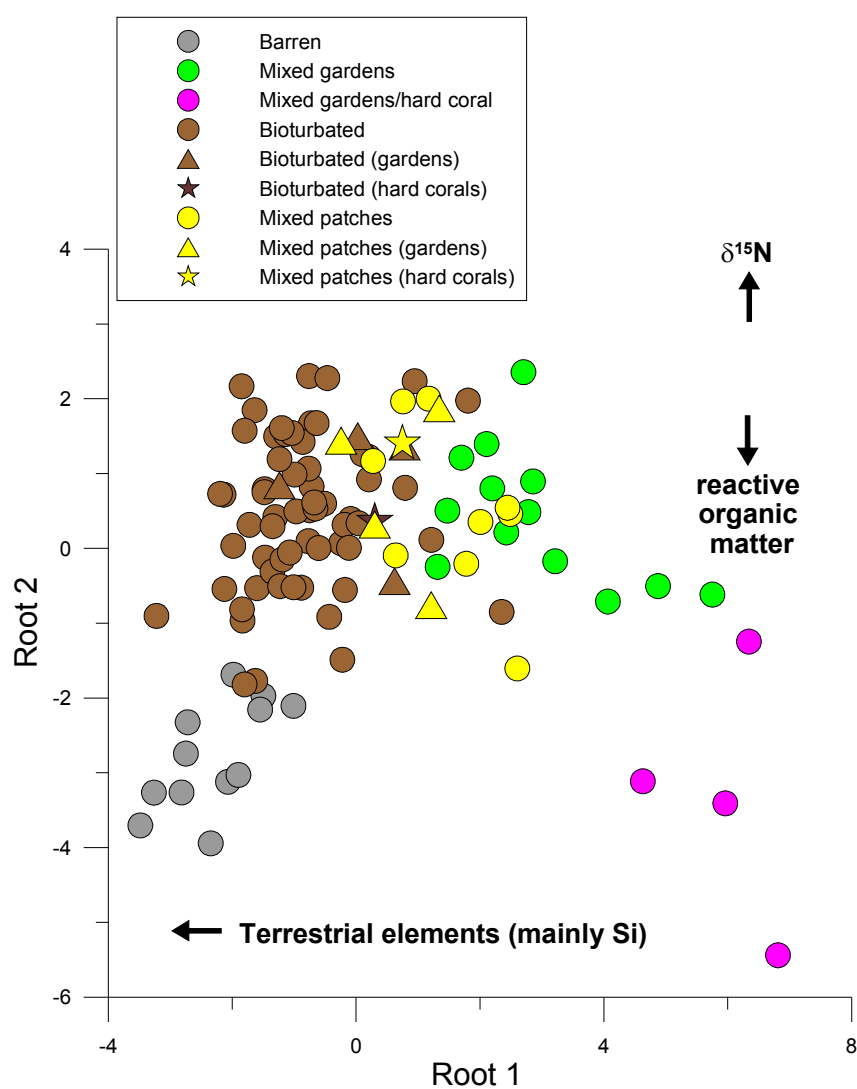


Figure E6: Scatter-plot of DFA canonical scores for the analysis on video-based habitat communities. Note that the occurrences of hard corals and gardens in benthic sleds are indicated for stations in which they were not observed in towed-video.

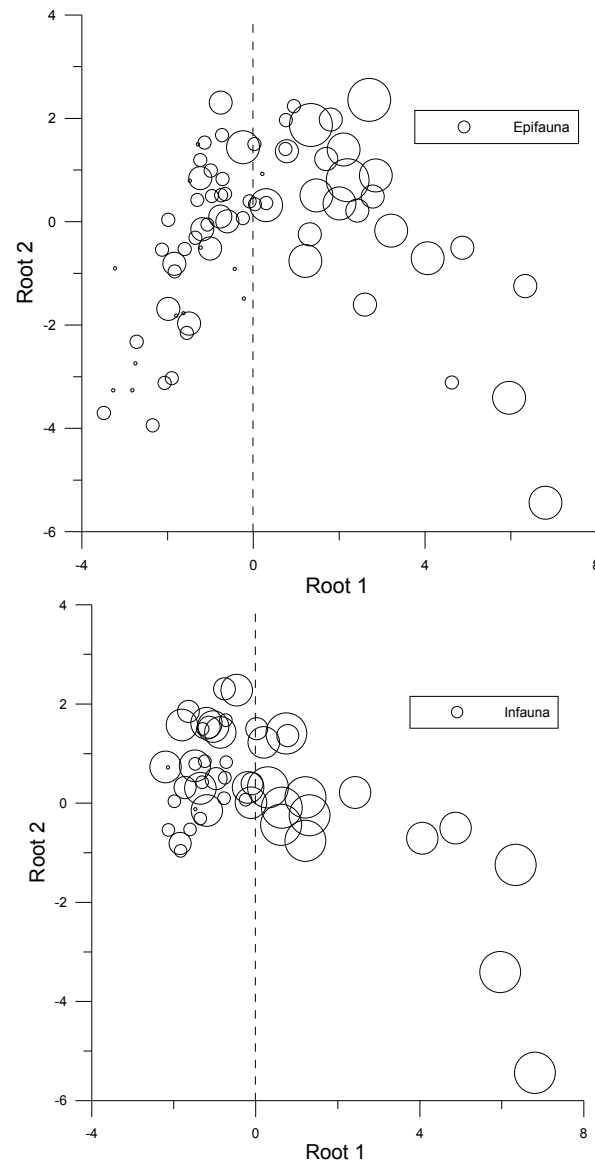


Figure E7: Scatter-plots of root 1 versus root 2 scores. Increasing bubble sizes reflect increases in species richness of (a) infauna and (b) and epifauna. Bubble sizes pertain to the species richness categories used in [Figure 2.20](#).

The changes in video-based communities from barren/bioturbated to mixed (patches, gardens, and gardens/corals) occurring after ~ 0.0 on root 1 of the DFA ([Figure E6](#)) is accompanied by general increases in both epifauna and infauna richness ([Figure E7](#)).

B2.4 Pockmark Analysis

Statistically-significant differences were found between pockmarked and non-pockmarked sediment for 18 parameters ([Table E5](#)). Pockmarked DHV sediments are distinguished sedimentologically in having lower gravel percentages, smaller mean grain-sizes, larger particle surface areas (PSA) and higher mud percentages than non-pockmarked sediments. The finer texture of the pockmarked sediments is reflected in the lower backscatter values of these sediments compared to non-pockmarked sediments. With the exception of $\delta^{15}\text{N}$, which was lower in pockmarks, the organic matter freshness indicators point to higher reactivity in the non-pockmarked sediments, *e.g.* lower C:N ratios, higher TCO_2 fluxes and higher values for the

reaction coefficient (k). The solid-phase of DHV pockmarked sediment also had statistically higher Ba concentrations than non-pockmarked sediments.

There were only four stations situated within pockmarks in Area D plains. These small sample sizes raise into question the validity of the statistical comparisons in Table E5. However, there were consistencies between DHVs and plains in the respect that both data-sets showed lower backscatter values in pockmarks and higher C:N ratios (potentially indicative of lower organic matter reactivity). Based on these albeit limited data, pockmarked plain sediments in Area D were also more Si-rich than surrounding sediments.

Table E5. Results of t-tests and Mann Whitney U tests comparing pockmarked and non-pockmarked DHV (Area A) and plain (Area D) sediments. Only parameters in which statistically significant differences were found are shown (N= 20 for pockmarked DHV sediment, 11 for non-pockmarked DHV sediment, 21 for non-pockmarked plain sediment and 4 for pockmarked plain sediment).

FEATURE	VARIABLE	TEST	MEAN VALUES (\pm 1SD) FOR POCKMARKED SEDIMENT	MEAN VALUES (\pm 1SD) FOR NON-POCKMARKED SEDIMENT	P-VALUE
DHV Area A	Mud (%)	t-test	27.8 \pm 9.5	17.2 \pm 7.4	0.002
	Mean grain size (μ m)	t-test	100.2 \pm 22.1	153.2 \pm 71.8	0.008
	Gravel (%)	t-test	1.2 \pm 1.3	5.9 \pm 9.3	0.009
	TCO ₂ flux (μ mol g ⁻¹ d ⁻¹)	t-test	0.09 \pm 0.08	0.17 \pm 0.08	0.009
	Backscatter (dB)	t-test	-31.7 \pm 2.7	-29.2 \pm 2.5	0.01
	C/N	MWU	8.1 \pm 0.2	8.0 \pm 0.5	0.03
	pH	t-test	7.75 \pm 0.12	7.65 \pm 0.11	0.03
	Zn (ppm)	MWU	15.7 \pm 2.7	16.0 \pm 5.1	0.03
	δ^{15} N	t-test	5.5 \pm 0.4	6.0 \pm 0.6	0.04
	Ba (ppm)	t-test	35.6 \pm 8.1	30.0 \pm 6.2	0.05
	PSA (m ² g ⁻¹)	t-test	5.4 \pm 1.3	3.0 \pm 2.1	0.05
	k (y ⁻¹)	t-test	0.07 \pm 0.08	0.17 \pm 0.15	0.05
Plains Area D	Si (mg kg ⁻¹)	t-test	163471 \pm 26341	111902 \pm 27330	0.002
	Si/Ca (mol)	t-test	1.2 \pm 0.3	0.69 \pm 0.25	0.002
	Al (CFB) (mg kg ⁻¹)	MWU	29337 \pm 3199	35672 \pm 11516	0.007
	Si (CFB) (mg kg ⁻¹)	t-test	380386 \pm 37698	315231 \pm 46742	0.02
	C:N (mol)	t-test	8.5 \pm 0.6	7.9 \pm 0.5	0.03
	F (mg kg ⁻¹)	t-test	344.8 \pm 57.2	266.9 \pm 63.6	0.03
	P (mg kg ⁻¹)	t-test	451.7 \pm 46.9	507.5 \pm 52.9	0.04
	Backscatter (dB)	t-test	-21.6 \pm 0.7	-20.5 \pm 1.0	0.05

* Calculated using the Kozeny-Carman equation (Bear, 1972) with mean grain-size and porosity as input variables.

B2.5 Background CO₂ concentrations, and evidence for sub-surface fluid migration

There were no statistical differences between pore-water TCO₂ concentrations in pockmarked and non-pockmarked sediments (Table E5). TCO₂ pools in the full suite of Bonaparte sediments (0-2 cm) had concentrations that ranged from 1.5 to 12.0 μ mol cm⁻³. These concentrations were tightly coupled with %porosity (Figure E8). TCO₂ pools in sediment reflect reactions that increase or decrease dissolved inorganic carbon (DIC) concentrations (e.g. organic matter degradation and CaCO₃ precipitation/dissolution), and processes that transport the DIC through sediment interstices and/or out of the sediment into the water column (e.g. diffusion, advection). The highest pore water TCO₂ concentrations were not found in the sediments with the highest reactive

phytopigment concentrations, e.g. terraces and banks, but rather in a sub-set of DHV sediments. This sub-set of DHV sediments is otherwise noted for having amongst the highest porosities and lowest intrinsic permeabilities in the data-set (Figure E8). The high TCO_2 concentrations in the DHV sediments is likely due to the effect of restricted pore water exchange on the residence time of pore waters. TCO_2 concentrations do not appear to build-up to the same extent in the more permeable sediments (e.g. terraces and banks) receiving higher reactive organic matter loads.

A pore water anomaly was observed at a bank site with particularly high backscatter values (e.g. -12.8 dB; Stn. 56B, SOL5117). The salinity of pore water at this station was 24 PSU compared to a background of concentrations averaging 34.1 ± 0.5 PSU (SOL5117 only). The TCO_2 concentration at this site was also amongst the lowest in the data-set, and the station deviated slightly from the main trend in the porosity- TCO_2 data (Figure E8). The low salinity at this station 56 (SOL5117) may be due to groundwater discharge, and raises the possibility that the banks, at least on the eastern side of the Bonaparte Gulf, are groundwater discharge features. However, pore water freshening is often found in association with cold seeps where it is attributed to the dehydration of clay minerals. This is another potential explanation for the anomalous pore-water salinity at station 56 (SOL5117).

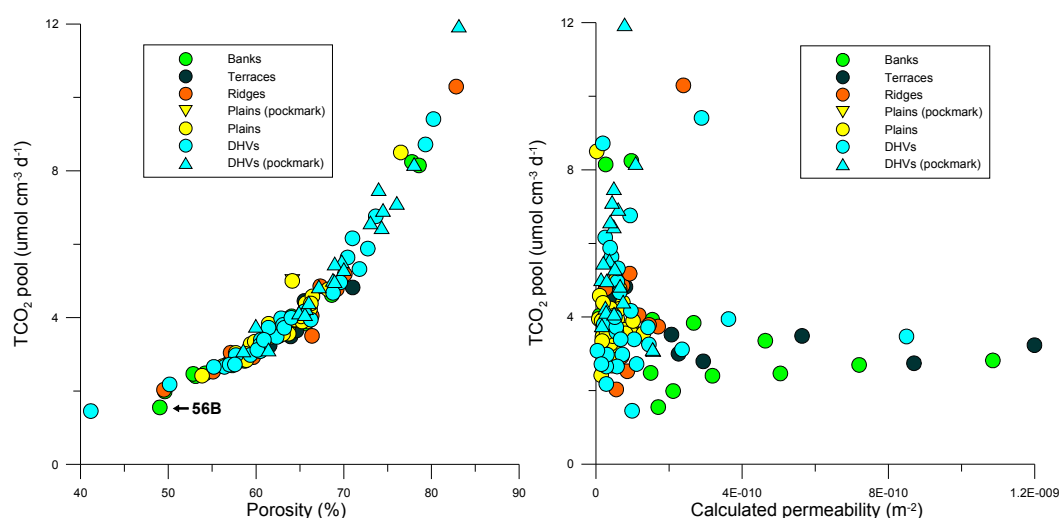


Figure E8: The TCO_2 concentrations of pore water in surface sediments in the Bonaparte Gulf, and (a) the variation of these concentrations with porosity; and (b) the variation of these concentrations with intrinsic(calculated) permeability calculated using the Kozeny-Carmen equation (Bear, 1972). Station 56 (SOL5117) in (a) is highlighted because a salinity anomaly was observed at this station.

Appendix F: Geophysics

F1. DATA PROCESSING AND ANALYSIS

F1.1 Multibeam bathymetry

The multibeam bathymetry data were processed using Caris HIPS/SIPS v6.1 software, and included: i) running algorithms that corrected for tide and vessel pitch, roll and heave, and ii) software filters and visual inspection of each swath line to remove any remaining artefacts and noisy data (e.g. nadir noise and data outliers). A bathymetry editing process was conducted during the survey, using IVS Fledermaus 3D visualisation software (v.7.2). The HDCS files from Caris were imported into IVS3D DMagic to produce a Combined Uncertainty Bathymetry Estimator (CUBE) surface. This surface was edited manually within the IVS 3D Editor tool. Final bathymetry surfaces were created within Caris using the edits from Fledermaus and then exported as a surface grid (bathymetric map) for display and analysis. Final processing to minimise tidal bursts was completed after the survey using a co-tidal solution in Caris.

F1.2 Multibeam backscatter

The Simrad EM3002 multibeam backscatter data were processed using the multibeam backscatter CMST-GA MB Process v10.10.17.0 toolbox software co-developed by the Centre for Marine Science and Technology (CMST) at Curtin University of Technology and GA (described in Gavrilov et al., 2005). The fully processed backscatter strengths were corrected for transmission loss and insonification area, and were normalised to the transmitted pulse length. The process also involved removal of the system transmission loss, removal of the system model, calculation of the incidence angle, correction of the beam pattern, calculation of the angular backscatter response within a sliding window of 100 pings with a 50% overlap in a 1° bin, removal of the angular dependence and restoration to the backscatter strength at an angle of 25° (Daniell et al., 2010).

Video-derived data on substratum were used to investigate the relationship between backscatter signal and associated hard/rock ground (see [Section 2.8](#) in main report). The angular backscatter response curves of a selected hard/rock ground were extracted. Of those selected response curves, the lowest angular backscatter response curve was associated with mixed epifaunal patches and sponge and octocoral gardens, and the highest one was associated with mixed gardens with hard corals. The lowest angular backscatter response curve was identified and extracted, one for each study area. For each study area, the probability (p-value) of the hard/rock ground was estimated by comparing the lowest angular backscatter response curve and all other angular backscatter response curves for incidence angles between 0° and 60° using the Kolmogorov-Smirnov goodness of fit. Finally, the inverse distance weight (IDW) interpolation technique was used to produce a continuous layer of the p-value of the hard/rock ground for each study area.

F1.3 Sub-Bottom Profiler

An Applied Acoustics CSP-1200 “Sparker” sub-bottom system was deployed to collect shallow (<70 metres below sea floor: mbsf) sub-surface data in study areas during multibeam swath operations. It was equipped with the Squid 500 sound source (300 – 800 J) and Mark 4 channel hydrophone array for data collection; both were towed at a speed of 4.5 to 5 knots (8 – 9 km hr⁻¹) in Beaufort Sea States of 0 to 2. The array was towed 40 m astern of the vessel and at a depth of 3.5 m. Data were processed using a C-View (Applied Acoustics Engineering) processing unit firing at a rate of 1 s⁻¹ with a record length of 500 ms. The process involved application of a band-pass filter (60-600 Hz), removal of false triggers and application of normal move-out corrections. Data from all four channels were stacked, the amplitudes scaled, and a correction applied. Finally, they were converted to a SEG Y format. Assuming a seawater sound speed of 1,500 m/s, depths were estimated from the two-way travel time.

F2. RESULTS

F2.1 Multibeam bathymetry

A total of 1938 km² was mapped (bathymetry and backscatter) within the four study areas (Areas A to D), mostly concentrated in the high priority areas of Area A and D ([Table D1](#)). Cumulative mapped areas were 426 km² (Area A), 133 km² (Area A-remapped), 472 km² (Area A1), 406 km² (Area B) 240 km² (Area C) and 261 km² (Area D). Area A1 was added in 2010 to the west of Area A. This western extension was found to have a wider range of depths (25-173 m) and a more complex morphology than the original Area A that was mapped in 2009. Area A-remapped was mapped in 2010 to determine if any detectable changes had occurred in seabed topography since the 2009 survey. It was found that seabed morphology was almost completely identical with a 98.86% measure of similarity. The differences (1.14%) were in the order of 10-20 cm that reflected the location of the north-to-south survey lines, and are interpreted as systematic errors in the tide models used to process these data. Improved sea-level data would be required to reduce these residuals, but are currently unavailable due to the remoteness of this location. This indicates that no measurable change in seabed morphology has occurred within this area during the 11 months between the consecutive surveys. Areas A and C exhibited relatively wider depth range than Areas B and D. Apart from the shallow water depths over Moss Shoal, Area B is relatively flat with few banks and valleys in the middle. Area D is simpler than other study areas. It mainly comprised relatively flat bottom indicated by the narrowest depth range.

Areas A and C comprised the more complex morphology than Areas B and D. Pockmarks were identified in Areas A and D. They are found on the floors of the valley (Areas A and D) and also within bedform fields (Area A). A comprehensive description of the geomorphology is contained in [Appendix D](#). The total data acquired for the two survey amounts to 165 Gigabytes of raw multibeam swath data.

F2.2 Multibeam backscatter

Backscatter values varied between the study areas and the geomorphic features ([Figures F1-4](#)). High backscatter is typically associated with shallow reef and bank features, while low backscatter is associated with soft sediments within valleys and channel features. Areas A and C have the greatest range in backscatter values whereas areas B and D have lower ranges of backscatter values, indicating a smaller variation in substratum types across these areas ([Figure F5](#)). Bank environments had the highest backscatter values (mean -14.38 dB; range -22.16 to -5.63 dB from sampling locations), which along with video observations indicated areas of hard substratum ([Figure F6](#)). In contrast, valleys had the widest range of backscatter values (mean -26.39 dB; range -46.79 to -16.76 dB from sampling locations) representing a mix of soft and hard substrata ([Figure F6](#)). Mixed gardens with hard corals represented the video-based habitat with the highest backscatter values, with a mean of -14.24 dB and a range from -21.97 to -5.63 dB from sampling locations. In contrast, bioturbated habitats had the lowest value and widest range of backscatter with a mean of -24.89 dB and a range from -46.79 to -12.03 dB from sampling locations ([Figure F7](#)).

The p-value of the hard/rock ground varied from 0 to 1 (see [Section 2.8](#) in main report). An obvious pattern between the presence of mixed gardens and reef-forming hard corals and the p-value of hard/rock ground was observed. High p-value is typically associated with the hard/rock ground on which mixed gardens and hard corals were found, and in contrast low p-value is associated with the soft ground. Setting the p-value ≥ 0.05 to class hard or else to class soft, the acoustic classes were compared to the video-derived classes and the overall classification accuracy was 74%. If however the threshold is increased to p-value ≥ 0.2 , the overall classification accuracy increases to 82%.

F2.3 Sub-Bottom Profiler

A total of 966 line-kms of sub-bottom profiler (SBP) data were collected from the four study areas over the two surveys. Cumulative survey distances for each survey were 340 km (GA-322) and 626 km (GA-325) (Figures 3.1, 3.5, 3.9, 3.13 in Heap et al 2010; 3.1, 3.3, 3.5 in Anderson et al 2011). The extent of sub-bottom penetration varied between areas, ranging up to ~140 m, with greatest penetration occurring in regions of relatively flat seabed, with less penetration over relatively rugged ground (e.g. Area C). Multiple sub-bottom reflections were recorded at each of the four study areas.

Detailed analysis of SBPs from GA-325 were undertaken for each study area in which SBPs were recorded. SBP was not recorded within Area C during survey GA-325.

Area A

A total of 18 lines of sub-bottom profile (SBP) data were collected in Area A from GA-325, primarily from the region where new multibeam data was collected. Two stratigraphic units were observed within the top 100 m of the sediment column. The lower unit is highly stratified and generally lying flat and conformable with the seabed surface. The upper unit conformably overlies the lower unit. This unit is less reflective but shows regular stratification, except where infilled channels occur. In many of the channels, the cut and fill deposition results in a complex stratigraphy, the result of channel development. The upper unit varies in thickness from less than 5 m to greater than 40 m. SBP data from the 2009 surveys indicates areas where the lower unit forms the seabed, particularly in the north. The base of the lower unit was not observed in the data collected. The lower unit is interpreted to be late Quaternary in age and the contact between units is the early Holocene sub-areal surface. Channel development occurred during sea level lowstand at the last glacial maximum.

Features present in the sub-bottom profiles include erosional terraces, cold seeps forming at the seafloor through gas chimneys, buried channels, and drowned reefs in the northwestern region (Section 3 in main report). The channel and bank morphology of Area A, as seen in cross section, suggests differences in tidal current strength and sediment texture. Almost all the terraces that form the boundaries of the channels display evidence of erosion and, in many areas, the development of a moat at the base of the terrace. In addition, the erosional terrace morphology suggests possible slope instability, though higher-resolution profiling is required to confirm this. Disturbed stratigraphy also occurs where gas chimneys are identified. In most cases these chimneys occur throughout the entire profile, cutting through both the upper and lower units. Gas chimneys are most common within the channels but also occur close to the terraces on the bank. Being that the gas is derived from depth, the possibility exists that the source is thermogenic.

The increase in terrace slopes due to erosion and the movement and release of gas through the sediment column constitute the primary geological hazards, as observed from the SBP data. This data suggests that both processes are ongoing and could be a more significant hazard in areas where these processes interact together.

Area B

A total of 9 lines of sub-bottom profile data were collected in Area B from GA-325. Two stratigraphic units were observed within the top 100 m of the sediment column. The lower unit is highly stratified and dips slightly to the West-Northwest based on the few SBP lines. The upper unit is less reflective but shows regular stratification, except where infilled channels occur, and lies unconformably over the lower unit. Biogenic gas masking obscures the stratigraphy in several areas, particularly in the southern portion of Unit B. The upper unit varies in thickness from less than 25 m to greater than 35 m and is absent in a few locations. The base of the lower unit was not observed in the data collected. The lower unit is interpreted to be late Quaternary in age and the contact between units is the early Holocene sub-areal surface. Channel development occurred during sea level lowstand at the last glacial maximum.

Features present in the sub-bottom profiles include, cold seeps forming at the seafloor through gas chimneys, erosional terraces, biogenic gas masking and buried channels ([Section 3](#) in main report). In addition, one surficial fault was observed in the northern part of Unit B. The gas chimneys occur primarily within the channels, often associated with disturbed stratigraphy. In most cases these chimneys occur throughout the entire profile cutting through both the upper and lower units. Again the migration of the gas through the stratigraphy suggests a possible thermogenic source, whereas the gas masking is biogenic.

Area D

A total of 17 lines of sub-bottom profile data were collected in Area D from GA-325, including the region of new multibeam data collection. As in Areas A and B, two stratigraphic units were observed within the top 100 m of the sediment column, separated by the sea level lowstand sub-aerial surface. The lower unit is highly stratified and generally flat lying, generally conformable with the seabed surface. The upper unit is less reflective and in areas transparent. The significant number of channels and extensive existence of gas results in more complex stratigraphy in the upper unit. The upper unit varies in thickness from absence to greater than 40 m and where it occurs, is conformable with the underlying unit. The base of the lower unit was not observed in the data collected. The lower unit is interpreted to be late Quaternary in age and the contact between units is the early Holocene sub-aerial surface. Channel development occurred during sea level lowstand at the last glacial maximum.

Features present in the sub-bottom profiles include, cold seeps forming at the seafloor through gas chimneys, biogenic gas masking, and buried channels ([Section 3](#) in main report). The gas chimneys occur primarily in the channels and often are surrounded by disturbed stratigraphy. In most cases these chimneys occur throughout the entire profile, cutting through both the upper and lower units, again making interpretation of the source of the gas problematic. Extensive areas of biogenic gas masking occur in the northwest quadrant of Area D.

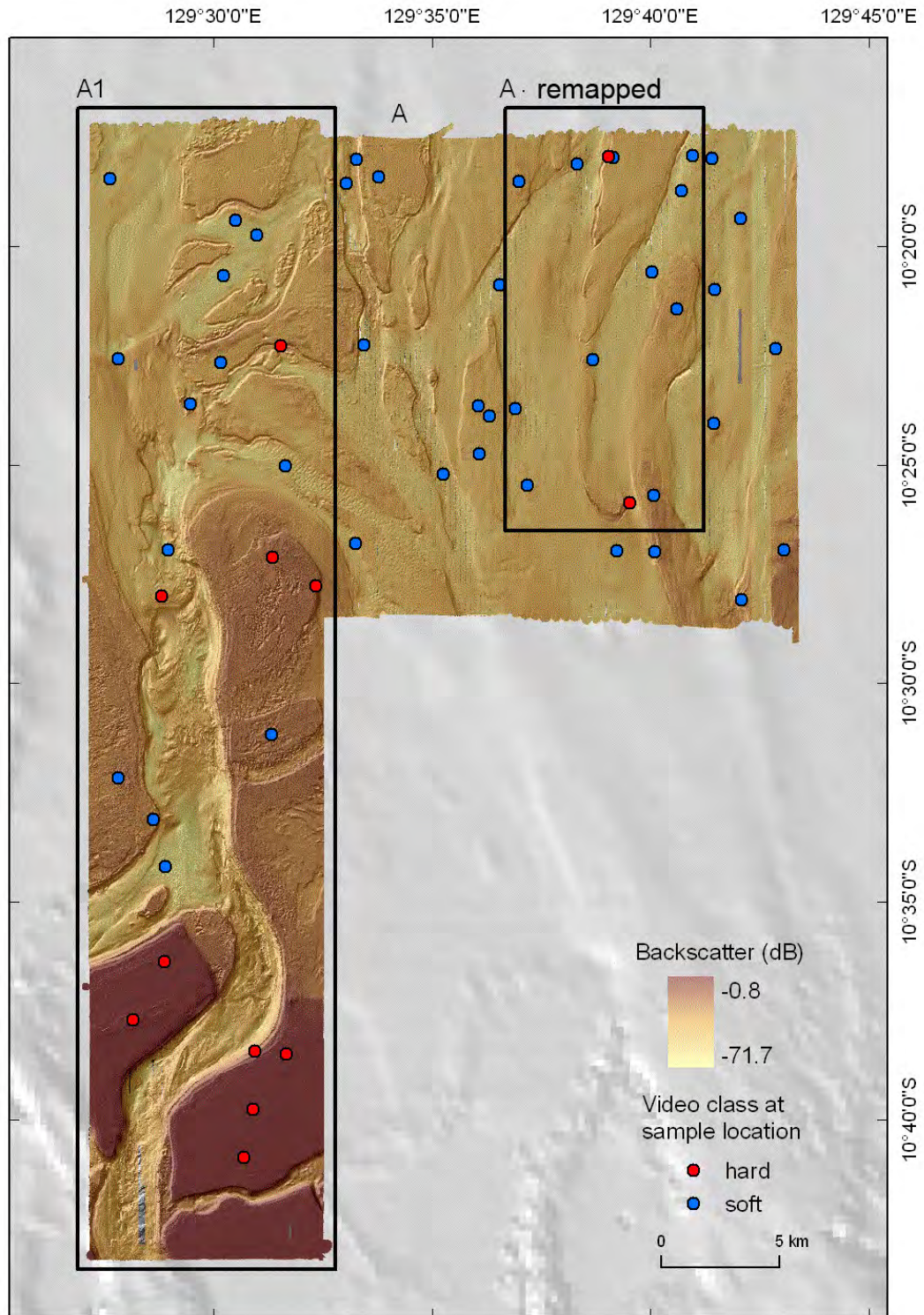


Figure F1: False colour backscatter image of Areas A, A1 and A-remapped, overlaid with video-derived classes at sample location. All areas inside the black boxes mapped during survey GA-325 and all others during survey GA-322.

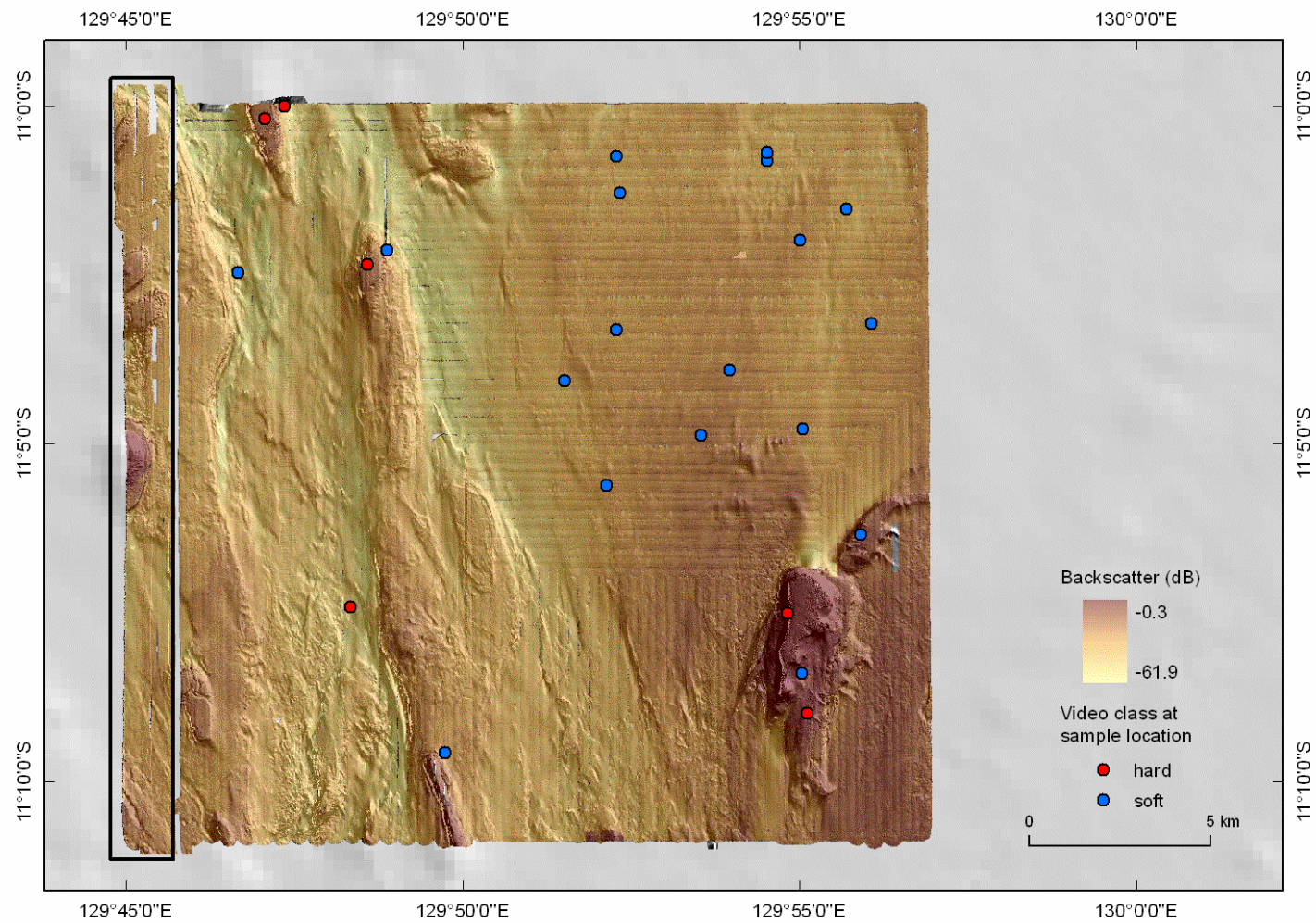


Figure F2: False colour backscatter image of Area B, overlaid with video-derived classes at sample location. All areas inside the black boxes mapped during survey GA-325 and all others during survey GA-322.

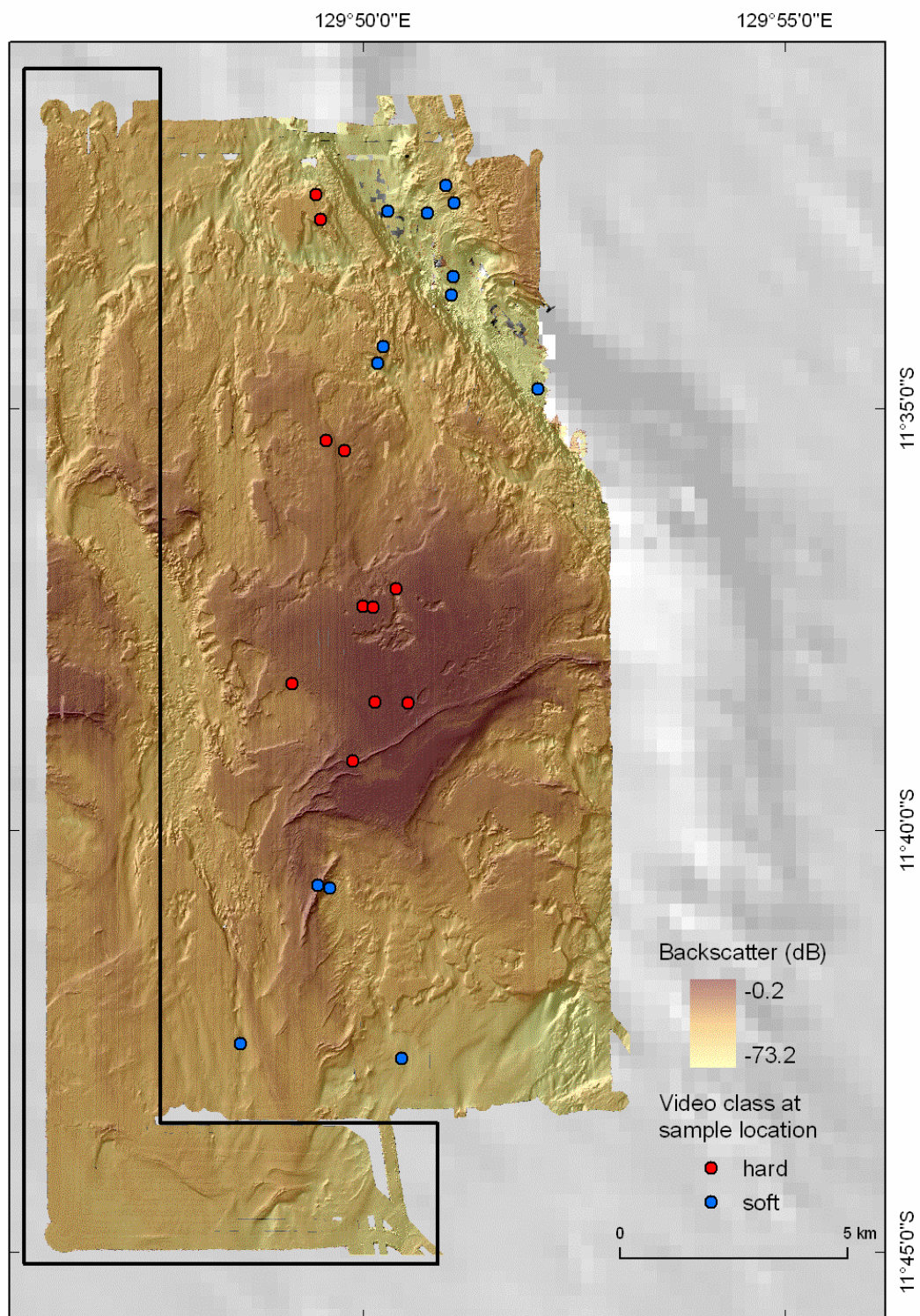


Figure F3: False colour backscatter image of Area C, overlaid with video-derived classes at sample location. All areas inside the black boxes mapped during survey GA-325 and all others during survey GA-322.

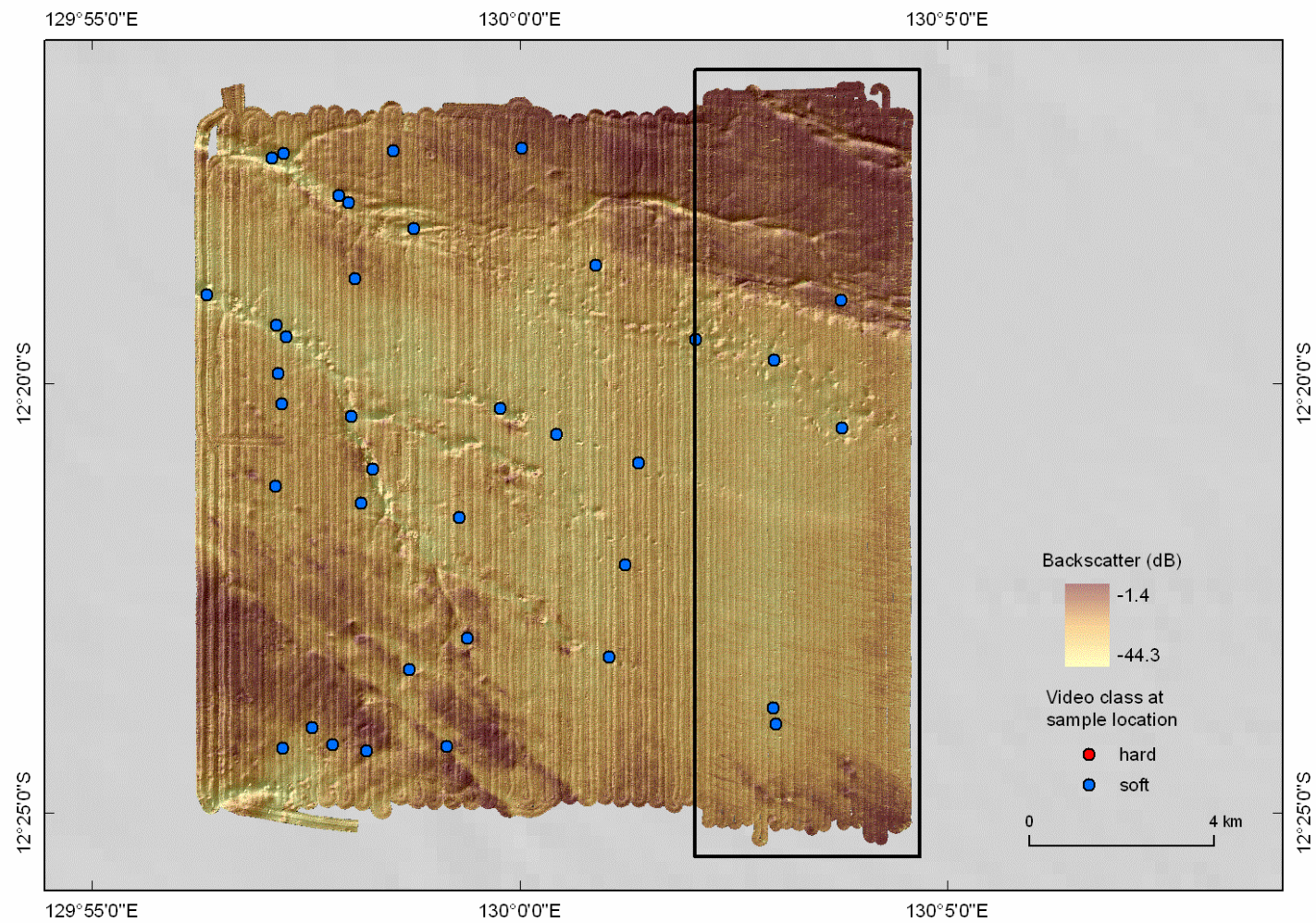


Figure F4: False colour backscatter image of Area D, overlaid with video-derived classes at sample location. All areas inside the black boxes mapped during survey GA-325 and all others during survey GA-322.

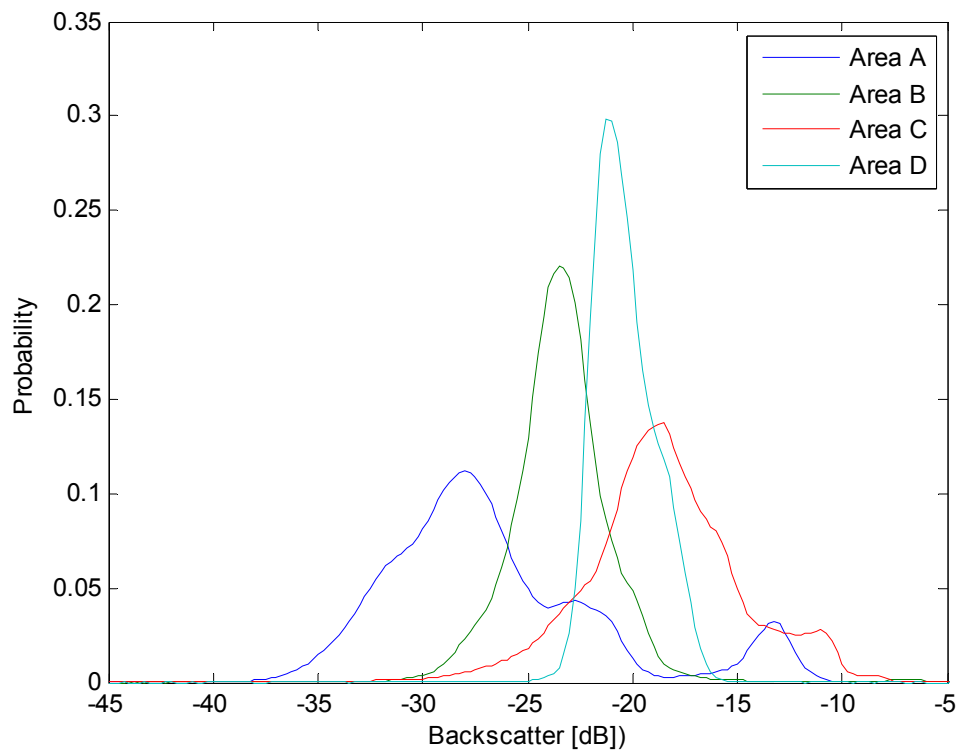


Figure F5: Histograms of backscatter values for four study areas.

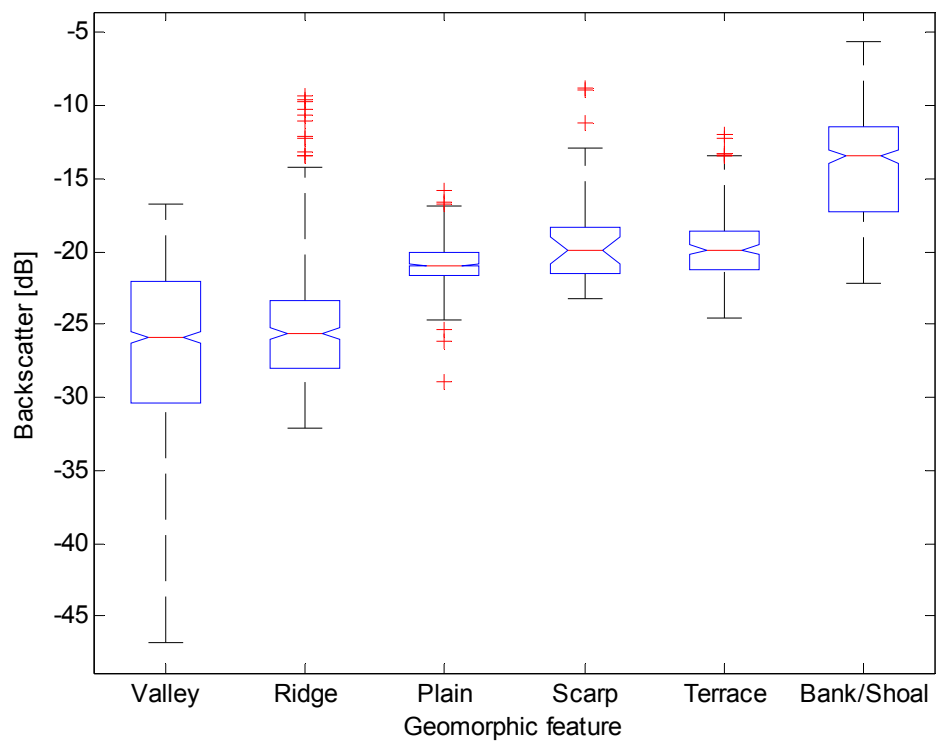


Figure F6: Boxplots of backscatter values grouped into geomorphic features.

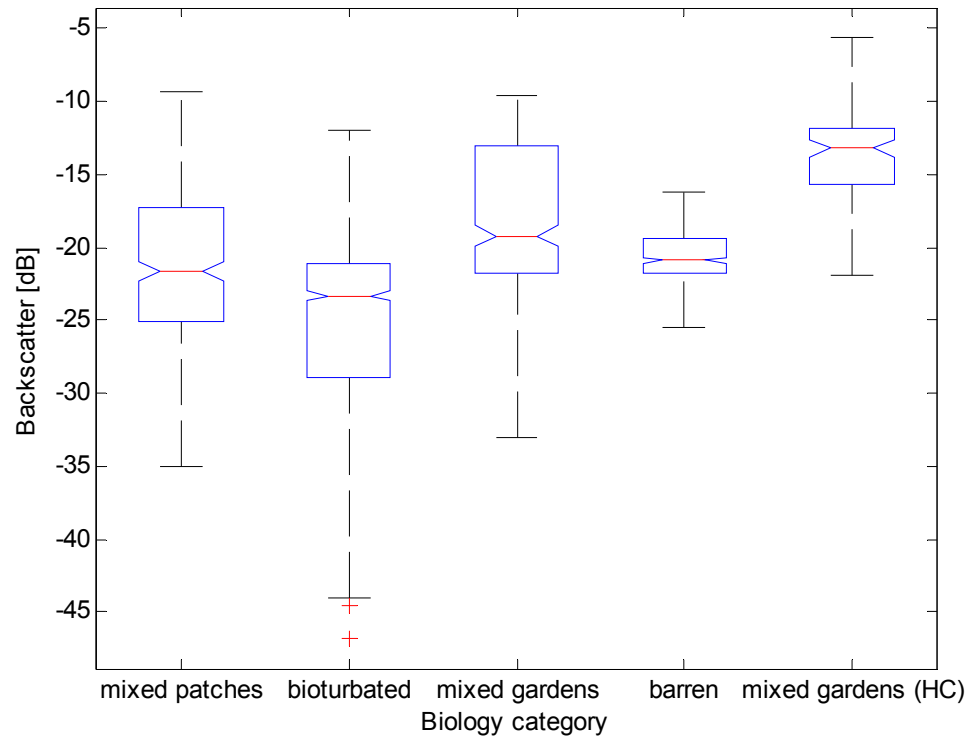


Figure F7: Boxplots of backscatter values grouped into video-derived biology category.

Appendix G: Physical Oceanography

G1. INTRODUCTION AND DATA SOURCES

The Joseph Bonaparte Gulf and Timor Sea region (JBG-TS) is influenced by a complex interplay of oceanographic processes. The region is dominated by strong tidal currents that are overprinted by weak wind-driven currents, and occasional tropical cyclones that make a short-lived, but energetic impact during the summer months. The gulf experiences an arid-tropical climate. Rainfall is highly seasonal, falling almost entirely in summer and autumn. Winds are generally weakest during summer from the northwest to southwest and strongest during winter from the southeast.

Information for the first part of this review, covering the regional oceanography of the JBG-TS, was drawn from key journal references, the CSIRO Atlas of Regional Seas (CARS), the National Marine Bioregionalisation of Australia GIS (Department of Environment and Heritage, 2005), and the Australian Bureau of Meteorology. The second part of the review, specifically targeted to the focus areas visited during marine surveys GA-322 and GA-325 onboard the *RV Solander*, presents oceanographic observations made from fixed moorings deployed during those surveys.

G2. REGIONAL OCEANOGRAPHY

The following sub-sections present both the annual mean and monthly means representative of seasonal values for sea surface temperature (SST) and seafloor temperature and sea surface salinity. Primary productivity (PP) in surface waters and the mixed layer depth (MLD) are also presented. The information is a subset of the National Marine Bioregionalisation GIS, which was drawn from the CARS data base.

G2.1 Temperature

On a global scale ocean temperature varies with latitude and largely reflects the intensity of solar radiation incident on the surface of the oceans. The ocean temperature influences the range of species present in a region. It also influences oceanic circulation through its effect on density and pressure gradients. Localised spatial and temporal variation in oceanic temperature often indicates the incursion of ocean currents from outside the region and the mixing of different water masses.

The sea surface temperature (SST) over the JBG-TS is characteristic of tropical ocean waters. Typical values for SST over the gulf in January and April are 28–31°C (Figure G1a, b) and in July and October are 24–26°C (Figure G1c,d). There is a diabathic thermal gradient in SST across the gulf that switches seasonally; decreasing SST with distance toward the shelf edge in January and April and increasing in July and October. This reflects the smaller thermal inertia of the very shallow waters in the southern gulf area.

The pattern of seafloor temperatures in the JBG-TS broadly mirrors the bathymetry (Figure G2). The coolest temperatures in the region of interest are on the outer shelf, particularly in the Malita Graben and the numerous channels dissecting the outer shelf edge, where they are typically 18–20°C and fall as low as 9–10°C in the deepest channel. On the inner shelf where the waters are very shallow and well-mixed, the seafloor temperature is much closer to the SST values just described.

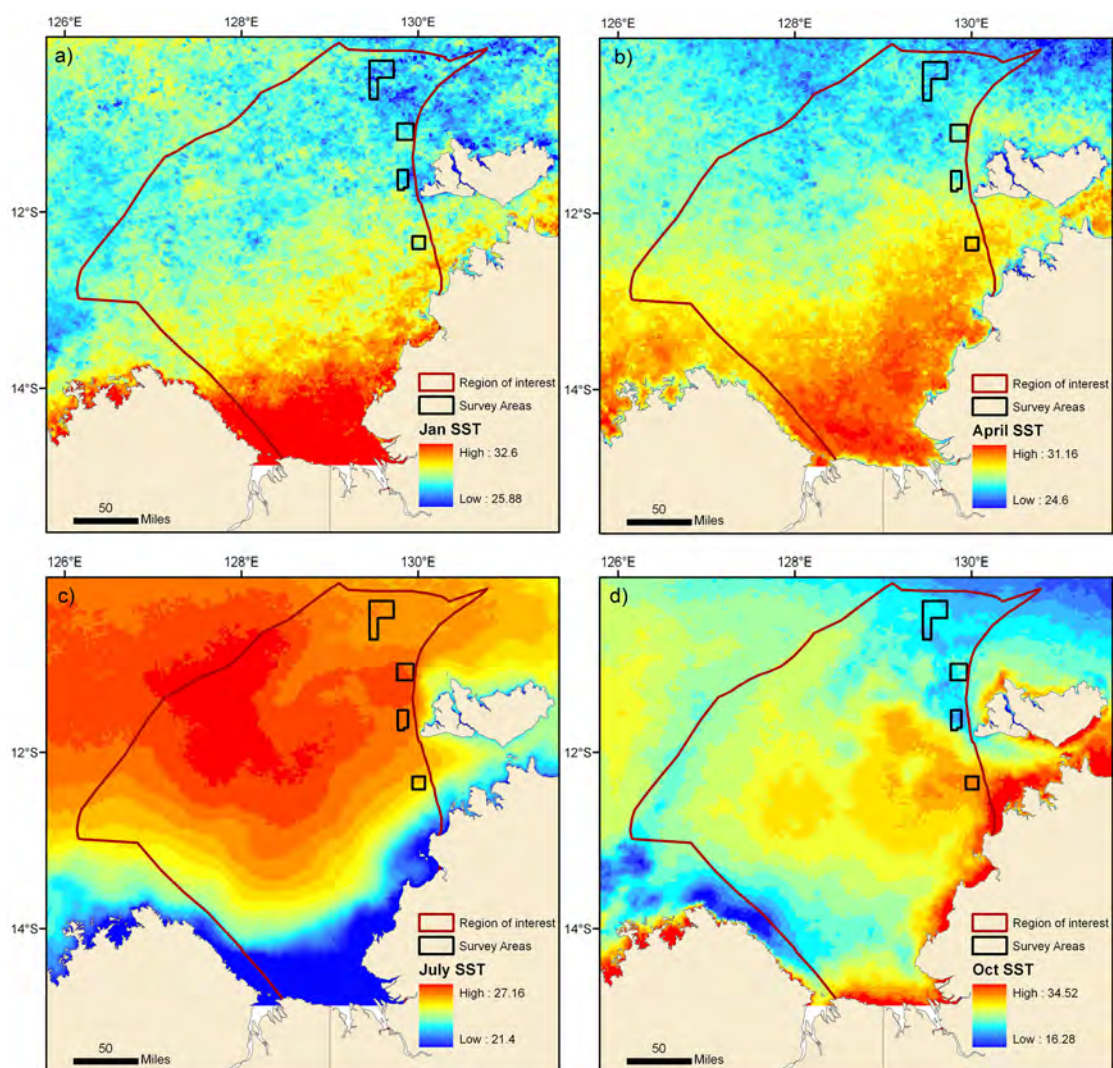


Figure G1: Mean sea surface temperature (SST) for a) January, b) April, c) July, and d) October over the JBG-TS obtained from the National Marine Bioregionalisation GIS (Department of Environment and Heritage, 2005).

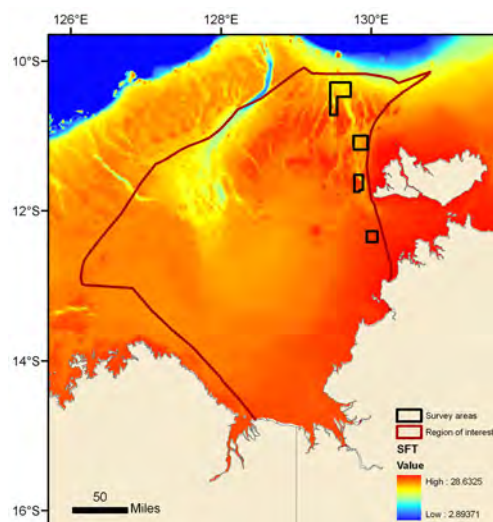


Figure G2: Annual mean seafloor temperature over the JBG-TS obtained from the National Marine Bioregionalisation GIS (Department of Environment and Heritage, 2005).

G2.2 Salinity

On a global scale ocean-surface salinity largely reflects the balance between evaporation and precipitation. The ocean salinity influences circulation through its effect on density and pressure gradients. Together salinity and temperature determine density and distinguish water masses. Localised spatial and temporal variation in salinity often indicates the incursion of ocean currents from outside the region and the mixing of different water masses.

The annual mean surface salinity across the gulf is mostly uniform at around 34–35, with marginally larger salinities in the southern gulf waters where warmer SST is likely to lead to greater evaporation (Figure G3).

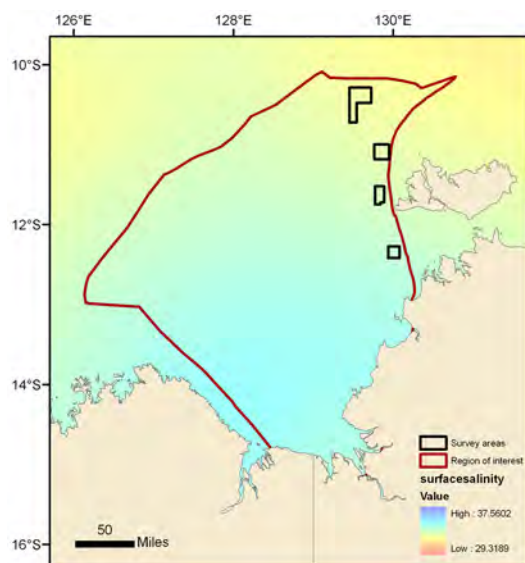


Figure G3: Annual mean surface salinity over the JBG-TS obtained from the National Marine Bioregionalisation GIS (Department of Environment and Heritage, 2005).

G2.3 Primary Productivity

Photosynthetic primary productivity is the amount of carbon fixed by organisms (marine plants and algae) through the synthesis of organic matter using energy derived from solar radiation. Put simply, it is a food source derived from carbon dioxide, water and sunlight that supports the rest of the marine ecosystem. The amount of photosynthetic primary production in a region reflects both the amount of solar radiation (light energy) and the supply of mineral nutrients (i.e. nitrate, phosphorus, iron and silica) (Thurman and Trujillo, 2004).

Primary productivity in the JBG-TS is consistently greatest in the coastal waters of the southern and eastern gulf, with values of the order $1400\text{--}1800\text{ mg m}^{-2}\text{ d}^{-1}$ persisting throughout the year (Figure G4). Across most of the remainder of the gulf, primary productivity is generally in the range of one hundred to a few hundred $\text{mg m}^{-2}\text{ d}^{-1}$ for most of the year. The peak season is winter when primary productivity levels across most of the gulf are of the order $1000\text{ mg m}^{-2}\text{ d}^{-1}$, and significantly greater in the coastal zone (Figure G4c).

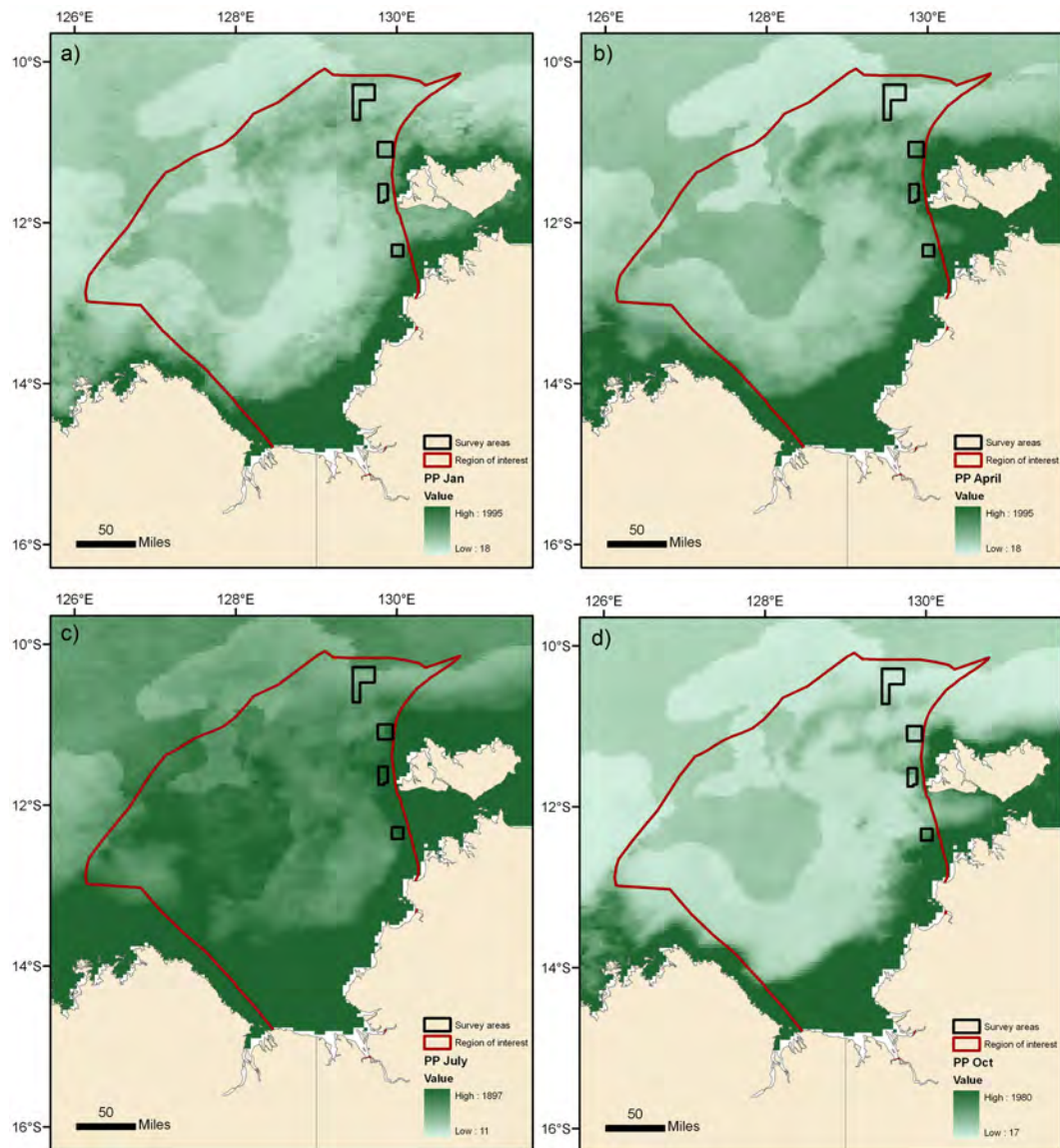


Figure G4: Mean primary productivity (PP) for a) January, b) April, c) July, and d) October over the JBG-TS obtained from the National Marine Bioregionalisation GIS (Department of Environment and Heritage, 2005).

G2.4 Mixed Layer Depth

The surface mixed layer of the ocean has a comparatively constant salinity, temperature and density. It represents the thickness of the water column that is regularly mixed and therefore exposed to the atmosphere. The mixed layer depth is determined by the turbulence in the upper water column and is therefore influenced by the strength of atmospheric winds, waves and tidal currents. The annual mean mixed layer depth over much of the JBG-TS is up to 40 m where water depth allows (Figure G5). Most of the gulf waters are therefore regularly mixed throughout the entire water column. On the outer shelf where water depths are greater, vertical mixing is less and the mixed layer depth is 25–30 m.

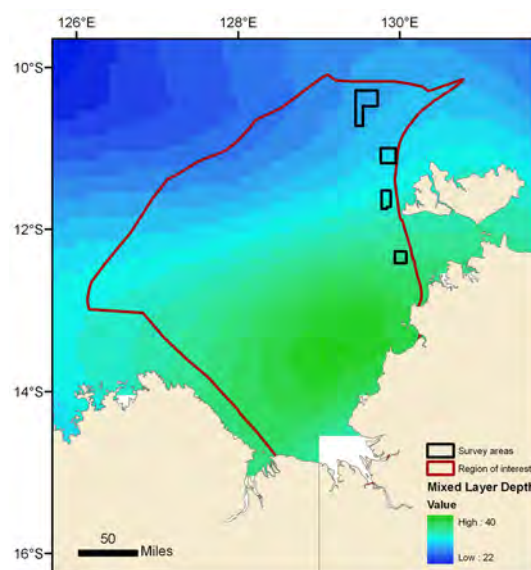


Figure G5: Annual mean mixed layer depth (MLD) over the JBG-TS obtained from the National Marine Bioregionalisation GIS (Department of Environment and Heritage, 2005).

G2.5 Ocean circulation

An idealised representation of the wind-driven circulation of the gulf, modelled by Condie (2011), is shown in [Figure 2.1](#) of the main report. Off the shelf edge there is a persistent westward current throughout the year. Within the gulf, during the monsoon season (January) the wind-driven currents are broadly-directed from west to east and during the trade wind season (July) from east to west.

Modelled wind-driven currents inside the Joseph Bonaparte Gulf are universally weak; achieving speeds of $<0.1 \text{ m s}^{-1}$ (Condie, 2011). The strongest modelled wind-driven currents in the study region occur on the outer shelf in the vicinity of Area D, where they reach of the order of 0.1 m s^{-1} (see Condie, 2011).

G2.6 Tides

The coastal bays and river entrances in the southern Joseph Bonaparte Gulf, e.g. Cambridge Gulf, have some of the largest tide ranges in Australia. The spring tide range at Wyndham, in Cambridge Gulf, is 7.9 m (Anon., 2009). The tides are classified as mixed semi-diurnal. The stronger semi-diurnal components of the tide rotate clockwise around the gulf and the weaker diurnal components rotate anti-clockwise (Louis and Radok, 1975).

The strongest tidal current measurements previously recorded in the Joseph Bonaparte Gulf are from the Victoria River entrance, reaching 3.5 m s^{-1} , and the Ord River entrance (Cambridge Gulf), reaching 3.0 m s^{-1} . Tidal current velocities on the inner shelf immediately seaward of these entrances reach 1.6 m s^{-1} (Coleman and Wright, 1978). Recent measurements of tidal currents in the eastern JBG-TS are presented in [Section G3](#).

G2.7 Waves

The wave climate was determined from wave conditions hindcast using the WAM model – a third generation ocean wave prediction model (Hasselmann et al., 1988). Implementation of the WAM model for the Australian region (AusWAM) was performed by the Australian Bureau of Meteorology using their high resolution atmospheric model on a 0.1° grid (e.g. Greenslade, 2001).

The hindcast wave conditions are significant wave height H_s , mean wave period T_m and wave direction D . The data set used here are 6-hourly time on the grid for the period 1 March 1997 to 29 February 2008 inclusive (11 years). The WAM model integrates the basic transport equation describing the evolution of a two-dimensional ocean wave spectrum without any assumptions concerning the evolving spectral shape. Energy dissipation due to whitecapping is included in the model, and energy dissipation due to bottom friction as well as refraction is included in the finite-depth version of the model (Hasselmann et al., 1988). Depth-induced wave breaking, however, is not included. For this reason and the limited grid resolution compared to the increased bathymetric complexity in shallow water, the AusWAM hindcasts may be of limited value for water depths <20-25 m (Hughes and Heap, 2010). For the short wave periods characteristic of the study region, however, this restriction might be reduced to depths of <10-15 m.

The pattern of wave heights across the area is broadly shore-parallel bands of increasing wave height in an offshore direction (Figure 3.9 in main report); this is true for all the percentiles shown and reflects the greater impact of wave diffraction and frictional dissipation in shallow water depths compared to offshore. It also reflects the greater fetch distances available offshore. The eastern gulf tends to be less energetic than the western gulf, because it is the lee shore for the wind regime primarily responsible for larger waves (i.e. SE Trades). Mean and 50th percentile values for H_s inside the gulf are typically <1 m. The 95th percentile values inside the gulf range up to 2 m, and up to 2.5 m further offshore (Figure 3.9 in main report).

The most energetic seasons with respect to significant wave height are centred on January and July (Figure 3.10 in main report). While July delivers the largest waves in the region they mostly occur outside of the gulf waters; significant wave heights inside gulf waters are restricted to <1 m, due to the short fetch distance associated with the southeasterly wind regime at this time of year. The northwesterly wind regime during January results in relatively smaller waves across the region overall, but waves up to 1.2 m penetrate into gulf waters, due to the favourable fetch (Figure 3.10 in main report). The small wave heights, <0.8 m, that persist across the entire region outside the monsoon and trade wind seasons demonstrates that the wave climate is dominated by locally-generated sea; very little swell penetrates the region.

The wave climate for the region is dominated by locally-generated sea conditions, as confirmed by Figure 3.11 in the main report. The time series of the mean wave period shows that a period of 5-6 s is typical and it reaches 10 s only during short-lived events. The raw time series and the box-and-whisker summary plots confirm previous comments that on average the largest wave heights occur during January and June. Figure 3.11c shows, however, that extreme wave heights of up to 8 m can occur between December and March. This is the cyclone season for this region. The four largest events occurred in December 1998, March 2004 and 2005, and January 2008. The cyclones responsible for these events are listed in Table 3.1 in the main report and their tracks are shown in Figure G6 below.

The largest significant wave height at the location presented in Figure G15, about 8 m, was associated with the second most intense cyclone, TC Ingrid. Category 2 and 3 cyclones TC Helen and TC Fay produced similar wave heights to those generated by the most intense cyclone, TC Thelma. The wave heights at a specific location depend not only on the wind speed, but the track of the cyclone, which affects the fetch distance. It appears that all cyclone categories are therefore capable of producing significant wave heights of over 5 m in outer gulf waters.

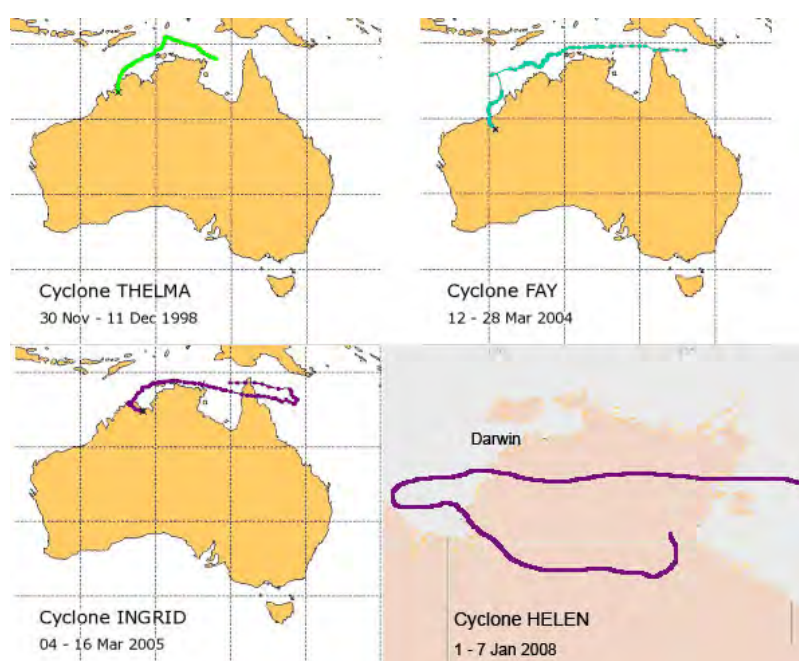


Figure G6: Map of cyclone tracks for: (a) TC Thelma; (b) TC Fay; (c) TC Ingrid; and (d) TC Helen. Information was compiled from the Australian Bureau of Meteorology and the Joint Typhoon warning Centre (see <http://australiasevereweather.com/cyclones/index.html>).

G3. OCEANOGRAPHIC OBSERVATIONS IN THE SURVEY AREAS

G3.1 Summary of oceanographic moorings

During marine surveys GA-322 and GA-325, four moorings were deployed, but during the 2010 survey only three were recovered. Details of the moorings including instrument type, location, survey area, depth and temporal coverage are listed in [Table G1](#).

Table G1. Summary of oceanographic moorings deployed in the eastern Joseph Bonaparte Gulf during Geoscience Australia Surveys GA-322 and GA-325. Times are in UTC.

INSTRUMENT	LATITUDE	LONGITUDE	AREA AND DEPTH (M)	DEPLOYMENT	RECOVERY
ADCP	-11°32.783	129°51.157	C, 100	28/08/09 04:10	22/09/09 09:22
Bruce (ADV)	-11°34.235	129°50.241	C, 50	28/08/09 01:50	22/09/09 06:47
Big Jim (PC-ADP)	-11°35.468	129°49.563	C, 33	28/08/09 00:35	22/09/09 05:57
Little Jim (Hydra)	-11°38.679	129°50.556	C, 22	27/08/09 23:20	21/09/09 12:40
ADCP	-10°23.754	129°36.775	A, 97	01/08/10 09:11	23/08/10 03:50
Bruce (ADV)					Not recovered
Big Jim (PC-ADP)	12°18.760	129°57.870	D, 44	31/07/10 11:47	25/08/10 20:00
Little Jim (Hydra)	11°38.355	129°50.143	C, 24	31/07/10 22:52	25/08/10 08:00

The ADCP moorings consisted of a RD Instruments Workhorse Sentinel 600 kHz acoustic Doppler current profiler (Serial No. 5581). The ADCP measures the 3-dimensional current vector in contiguous bins vertically through the water column. The instrument was programmed to obtain profiles of current velocity extending from 2–40 m above the seabed with measurements (sample bin elevations) spaced 1.00 m apart. In each bin a total of 60 pings were averaged over 600 s to provide current velocity time series with a sampling interval of 10 minutes for each bin elevation.

The Hydra moorings consisted of a Sontek Hydra 5 MHz ADV Ocean Probe (Serial No. A959H). The ADV provides a point measurement of the 3-dimensional current vector at 1 m above the bed. The instrument was programmed to record 3 nested burst sampling regimes: (1) sample rate of 0.2 Hz for 120 s every 30 minutes; (2) sample rate of 2 Hz for 1024 s every 60 minutes; and (3) 10 Hz for 10 minutes every 120 minutes. This provided data suitable for investigating tidal currents, waves and turbulence.

The PC-ADP moorings consisted of a Sontek PC-ADP acoustic Doppler current profiler (Serial No. H104). The PC-ADP measures the 3-dimensional current vector in contiguous bins vertically through the water column. The instrument was programmed to obtain profiles of current velocity extending from 0–1.2 m above the seabed with measurements (sample bin elevations) spaced 5 cm apart. The sample rate was 1 Hz for 1024 s bursts every 60 minutes. In addition to providing information on near-bed (boundary layer) tidal currents, the sampling regime also provided wave information through the PUV technique.

G3.2 Area A

Area A, located on the outer shelf, had one mooring placed in ca. 100 m water depth during the 2010 survey (Table G1). Time series of the tidal water level is shown in Figure G7 and the amplitudes and phases of the harmonic constituents are listed in Table G2. The form factor, based on the ratio of the amplitudes of the diurnal to semi-diurnal constituents, is 0.54. This classifies the tide as mixed, mainly semi-diurnal. Based on the 3 weeks of data available, the amplitudes of M2 and S2 (Table G2) indicate that the mean spring range is 1.93 m and the mean neap range is 0.72 m.

Table G2. Amplitude and G-Phase of the principal tidal constituents measured in Area A during 2010 (ADCP, see Table G.2).

CONSTITUENT	AMPLITUDE	PHASE	CONSTITUENT	AMPLITUDE	PHASE
O1	0.2008	176.81	S2	0.3014	218.36
K1	0.3171	199.30	M4	0.0033	245.80
M2	0.6638	150.91	S4	0.0018	153.87

The current magnitude between 2 and 40 m above the bed is shown in Figure G7, and reached of the order of 0.5 m s^{-1} . The lowest part of the water column, ca. <10 m above the seabed, was characterised by reduced current speeds suggesting the presence of significant bed shear. The phasing between the water level record and east and north components of the current indicate that the tide flooded to the south-southeast and ebbed to the north-northwest (Figure G8); and is consistent with the dominant semi-diurnal components of the tide wave rotating clockwise around the gulf (see Section G2.6). While the current vector close to the seabed was broadly symmetrical in distribution with a slight bias to the south-southeast, the current at mid water depth had a clear bias to the north-northwest (Figure G9). This is clearly evident in the progressive vector plot, which shows that the net-drift at the seabed and mid water depth were in opposite directions during the deployment period (Figure G10).

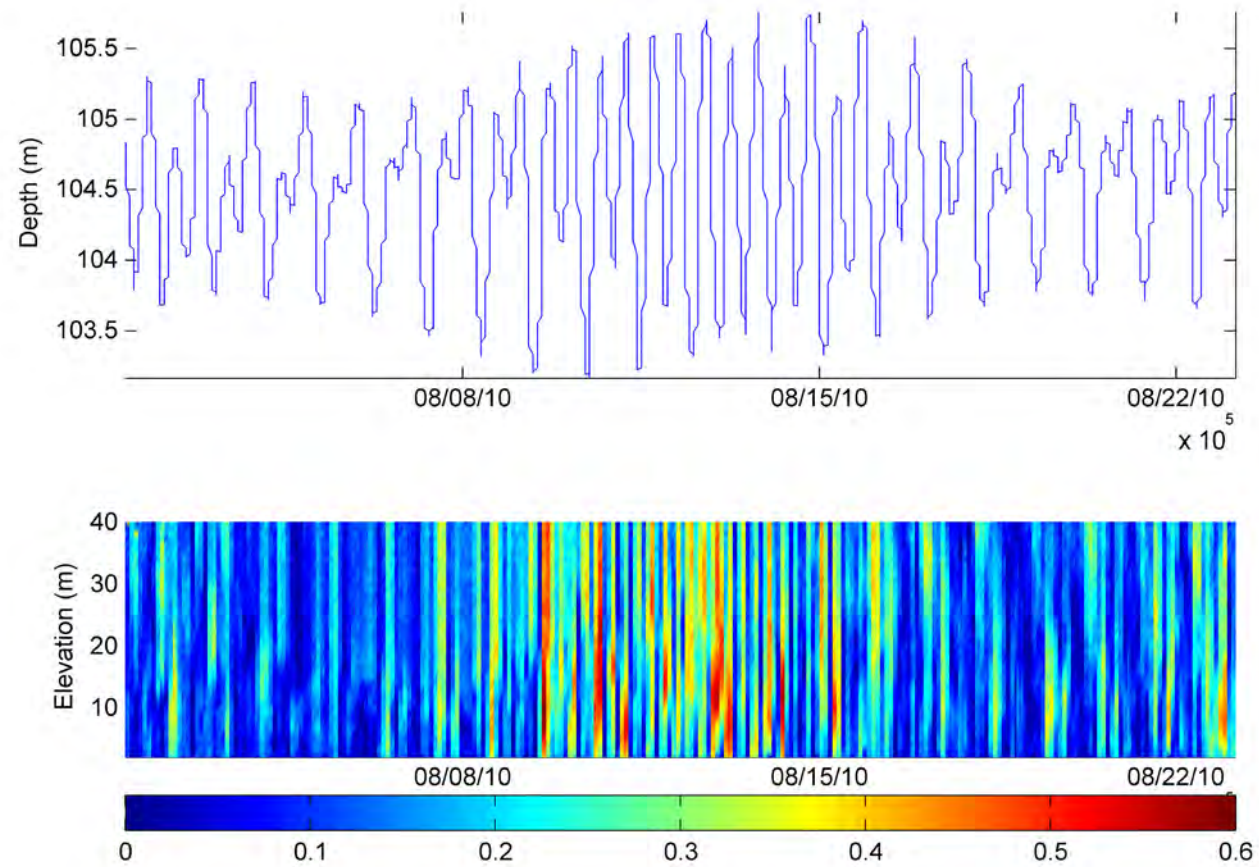


Figure G7: Time series data from the ADCP mooring deployed in Area A during 2010 (see [Table G1](#)); water depth (top panel) and current speed (m s^{-1}) between 2 and 40 m above the seabed (bottom panel).

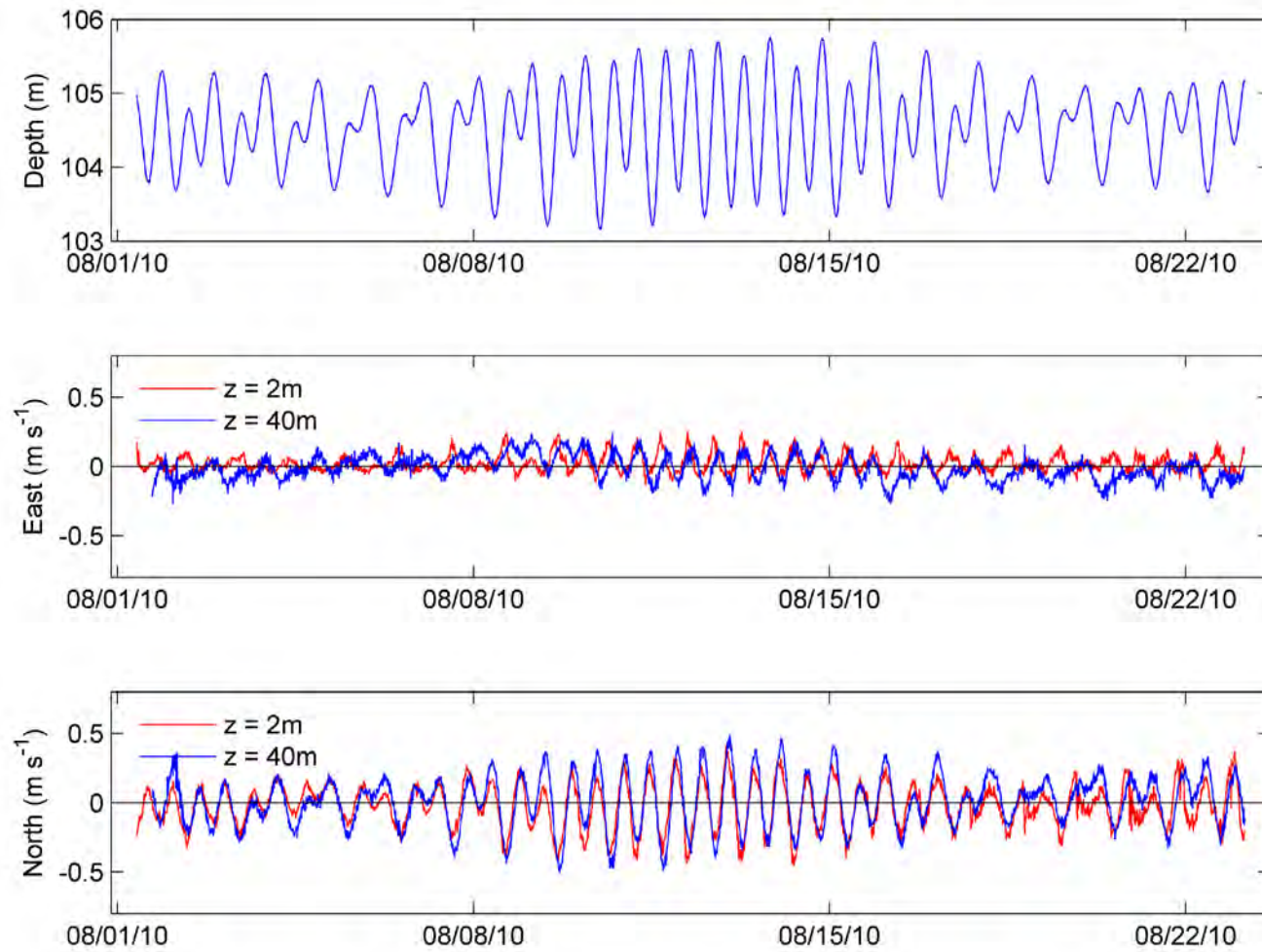


Figure G8: Time series data from the ADCP mooring deployed in Area A during 2010 (see [Table G1](#)); water depth (top panel), east vector component at 2 m and 40 m above the seabed (middle panel) and north vector component at 2 m and 40 m above the bed (bottom panel).

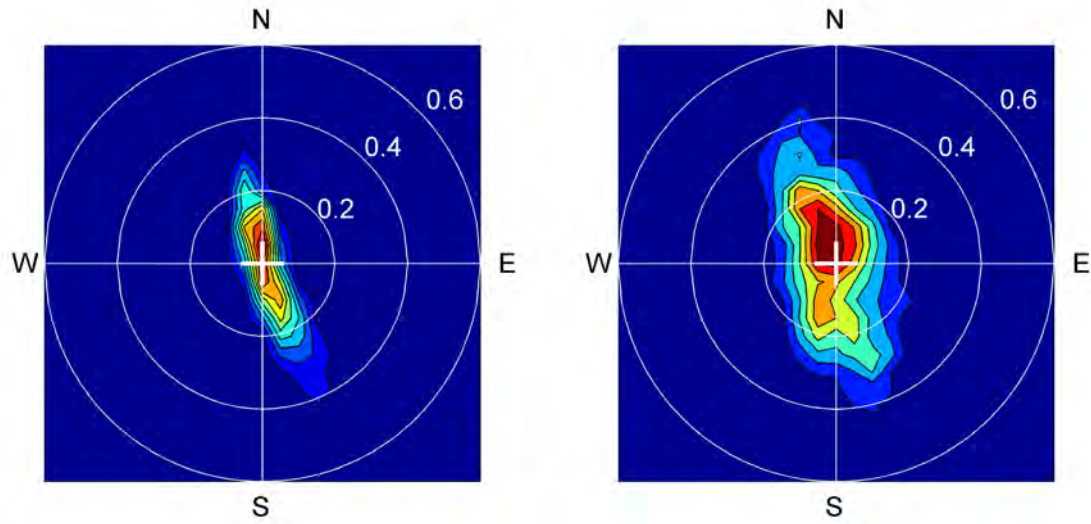


Figure G9: Data from the ADCP mooring deployed in Area A during 2010 (see [Table G1](#)); contoured histograms of the east and north components of the current vectors at 2 m (left panel) and 40 m (right panel) above the seabed.

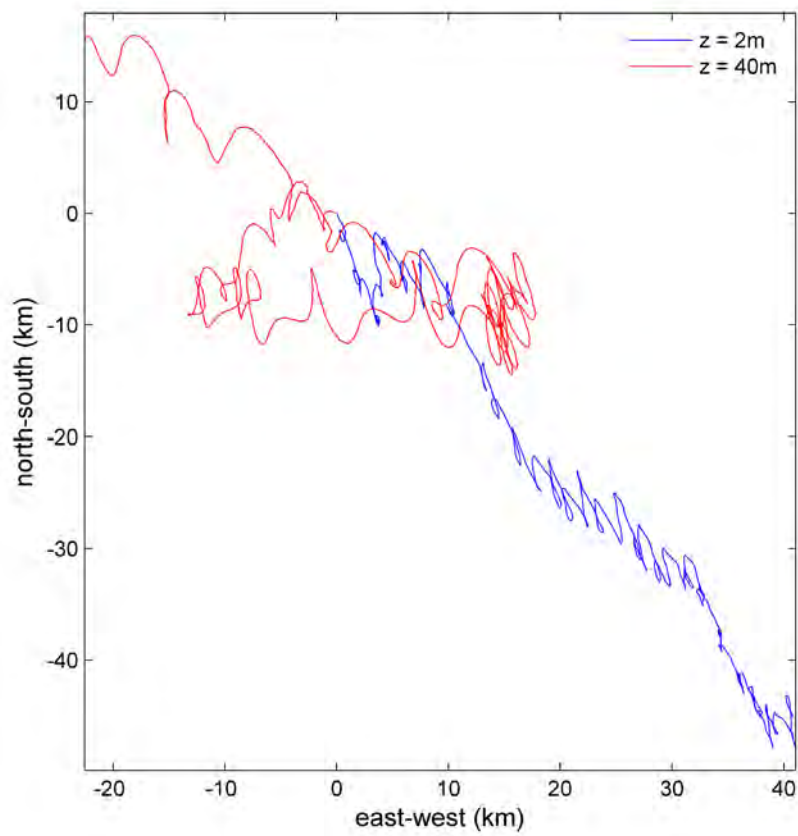


Figure G10: Data from the ADCP mooring deployed in Area A during 2010 (see [Table G1](#)); progressive vector plot for 2 m and 40 m above the seabed.

G3.3 Area C

In Area C, located on the mid shelf, moorings were placed in ca. 20, 30, 50 and 100 m water depth during the 2009 survey (Table G1). At the deepest site the current speed reached of the order of 1 m s^{-1} (Figure G11). The presence of strong bed shear is evident with current speeds at 41 m above the bed being about twice those at 2 m above the bed (Figure G11– G13). The current vector was broadly consistent over the 40 m of water column with peak ebb and flood magnitudes roughly equal, but a stronger persistence in the ebb currents directed to the north-northwest (Figure G13). This resulted in the net-drift, both near the seabed and mid water depth, toward the north-northwest (Figure G14).

At the shallowest site, also occupied in 2009, the current speed again reached of the order of 1 m s^{-1} , but at this site these magnitudes were observed at 1 m above the bed, suggestive of a much larger depth-averaged current speed (Figure G15). The current was aligned almost north-south at this site and the tidal current vector was evenly distributed (Figure G16), resulting in a net drift over the deployment period towards the west (Figure G17). A mooring was also placed close to this site during the 2010 survey. Interestingly, the observed current was quite different. The peak current speed was more modest, reaching of the order of 0.25 m s^{-1} at 1 m above the bed (Figure G18). The current was broadly aligned north-northwest to south-southeast, with peak velocities being greatest toward the north-northwest (Figure G19), resulting in a net-drift toward the north-northeast over the deployment period (Figure G20).

At the site located in 33 m water depth the peak current speed reached of the order 0.3 m s^{-1} at 1 m above the seabed (Figure G21). The current was aligned almost north-south at this site and the tidal current vector was evenly distributed (Figure G22), resulting in a net drift over the deployment period towards the west (Figure G23). Waves were also recorded at this site. During the deployment period significant wave height was typically ca. 0.20 m and peaked at 0.55 m, whereas peak period varied between 5 and 15 s (Figure G21).

Bonaparte Basin

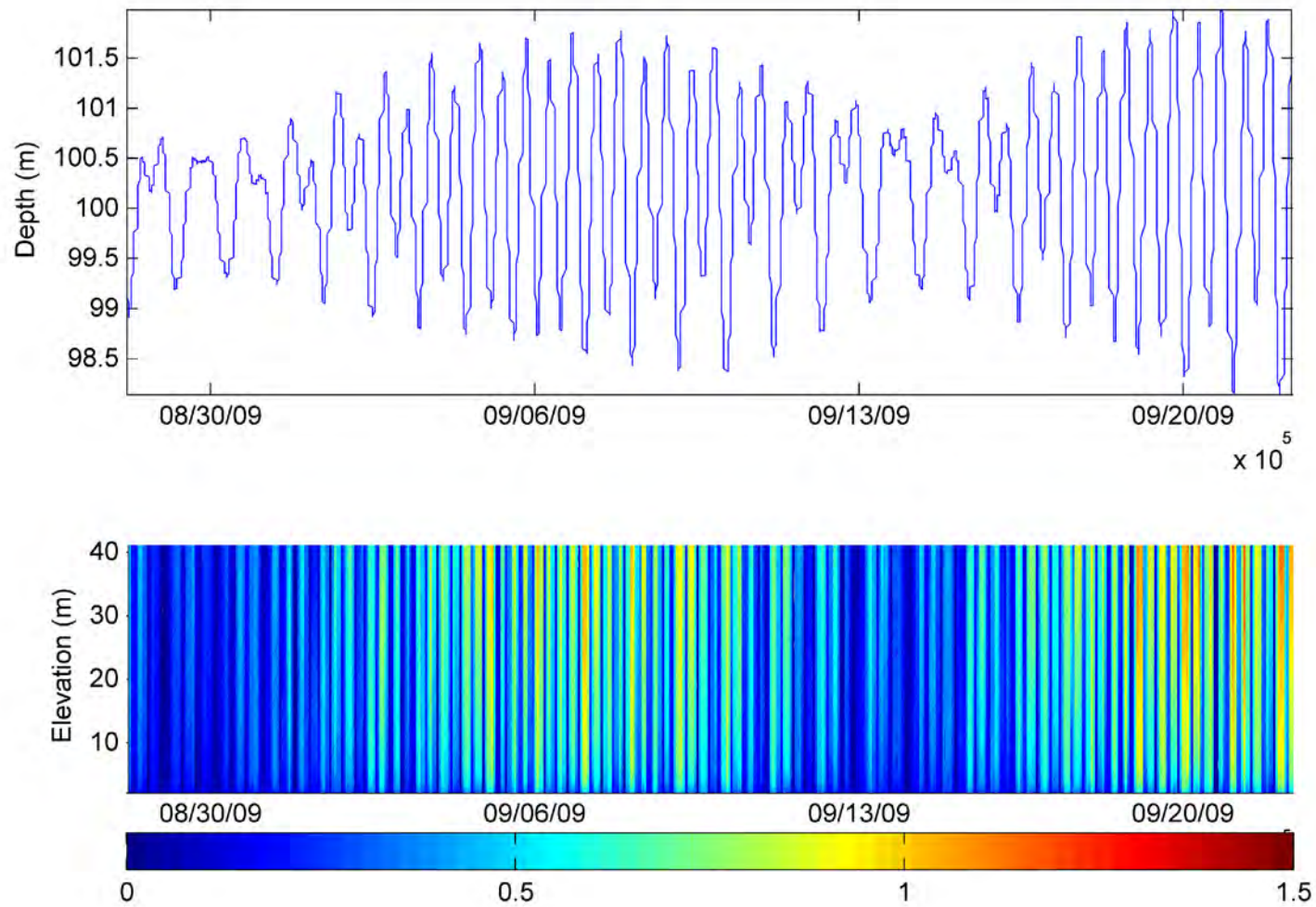


Figure G11: Time series data from the ADCP mooring deployed in Area C during 2009 (see [Table G1](#)); water depth (top panel) and current speed (m s^{-1}) between 2 and 40 m above the seabed (bottom panel).

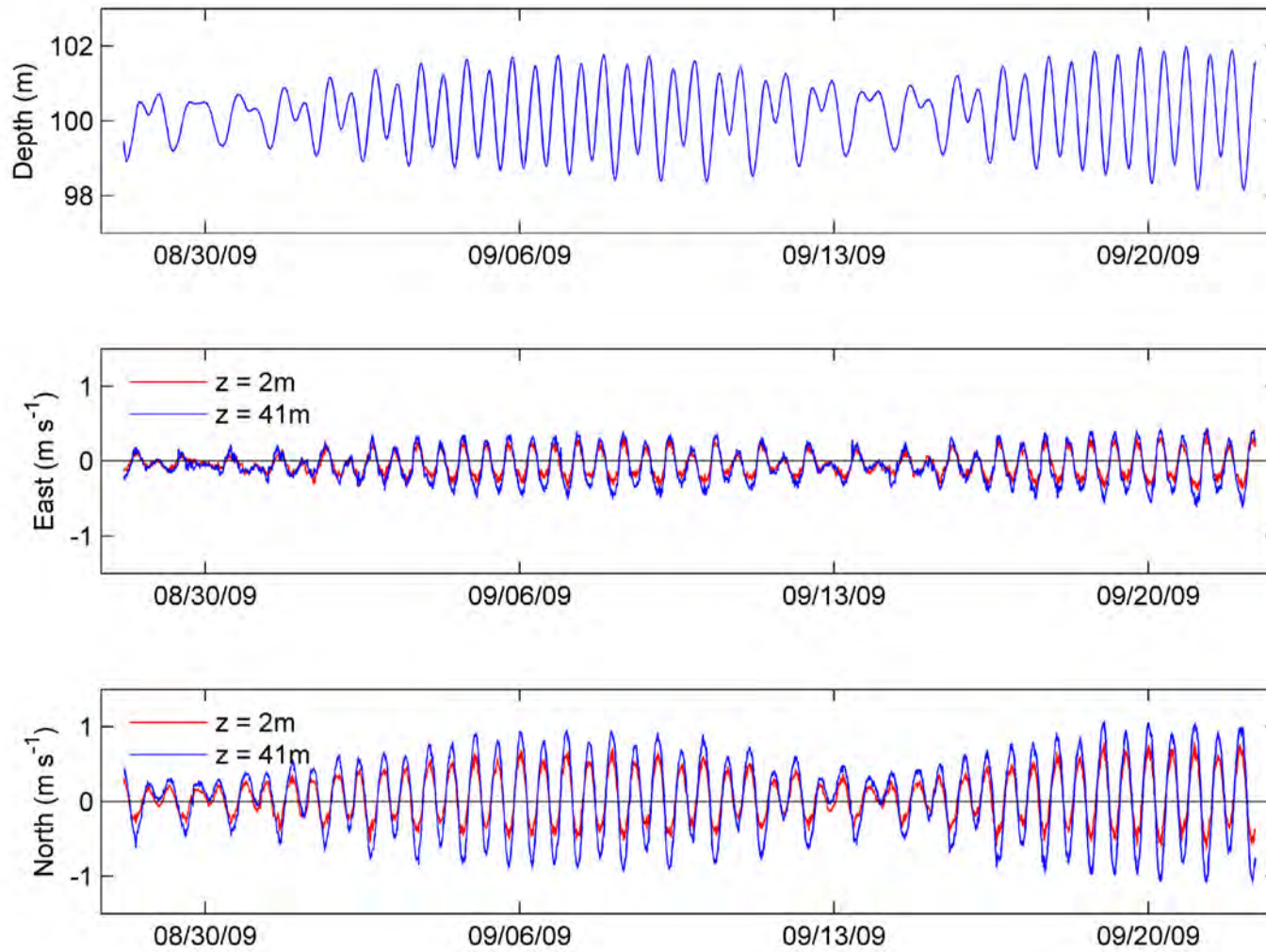


Figure G12: Time series data from the ADCP mooring deployed in Area C during 2009 (see [Table G1](#)); water depth (top panel), east vector component at 2 m and 41 m above the seabed (middle panel) and north vector component at 2 m and 41 m above the seabed (bottom panel).

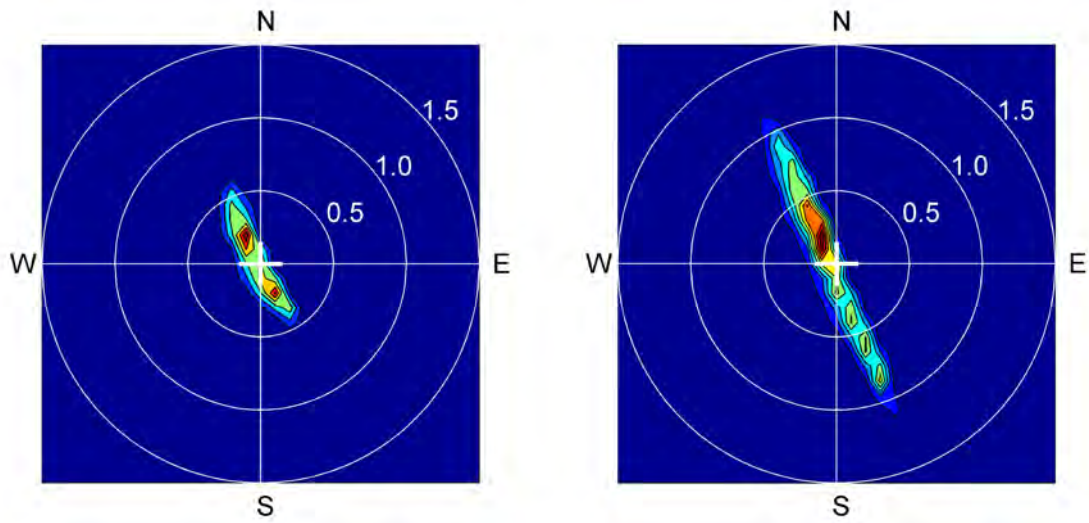


Figure G13: Data from the ADCP mooring deployed in Area C during 2009 (see [Table G1](#)); contoured histograms of the east and north components of the current vectors at 2 m (left panel) and 41 m (right panel) above the seabed.

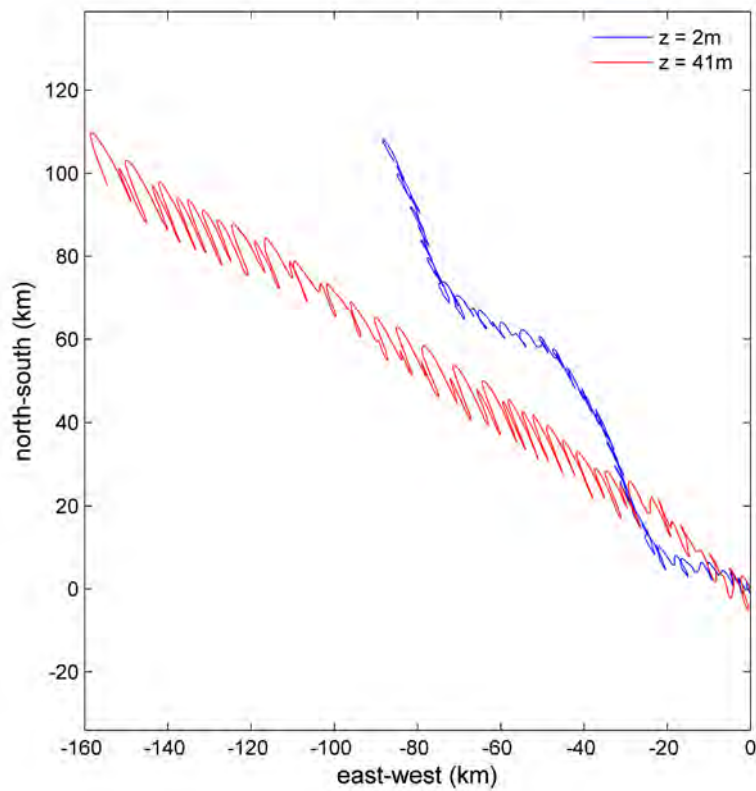


Figure G14: Data from the ADCP mooring deployed in Area C during 2009 (see [Table G1](#)); progressive vector plot for 2 m and 40 m above the seabed.

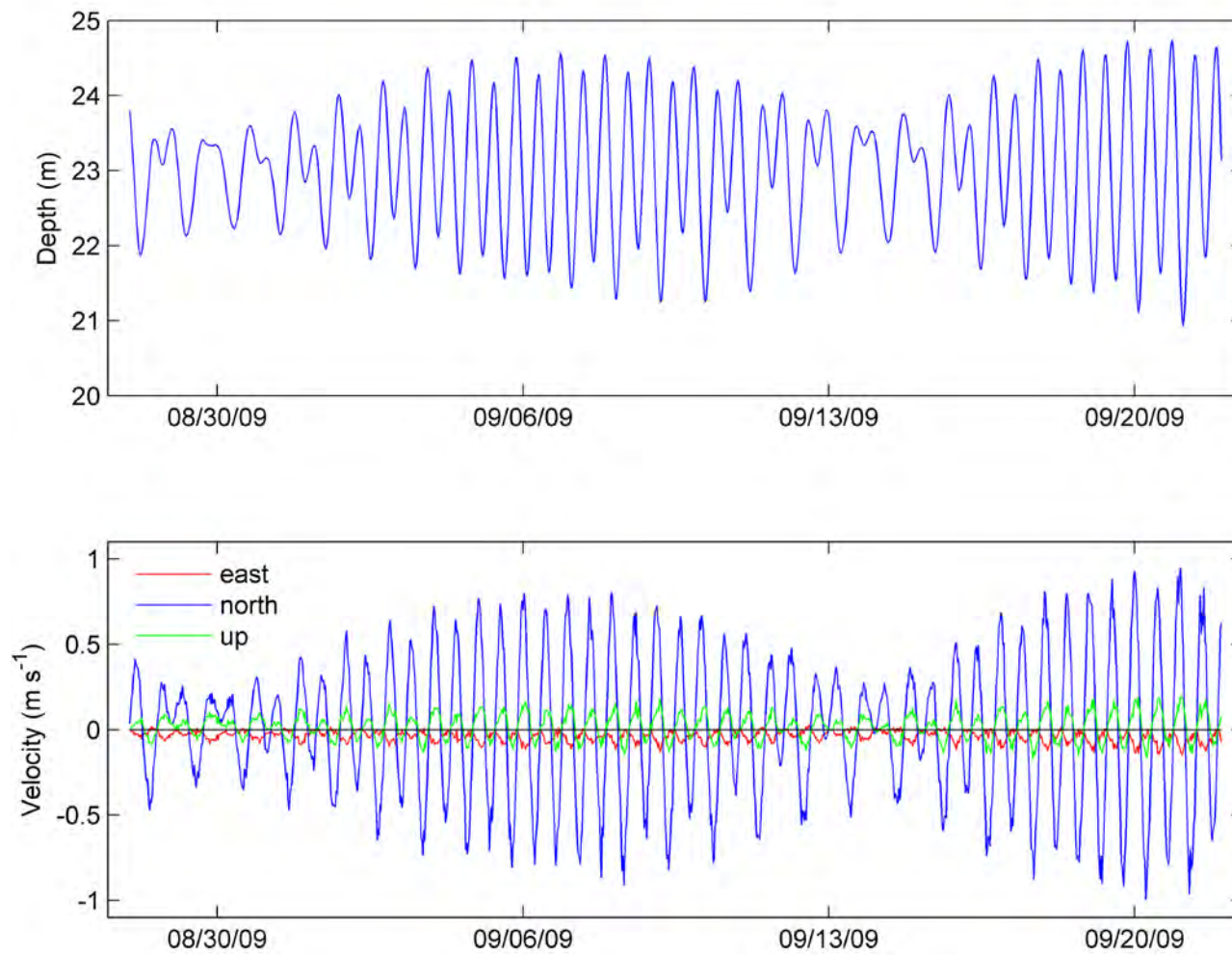


Figure G15: Time series data from the Hydra mooring deployed in Area C during 2009 (see [Table G1](#)); water depth (top panel), east, north and vertical vector components at 1 m above the seabed (bottom panel).

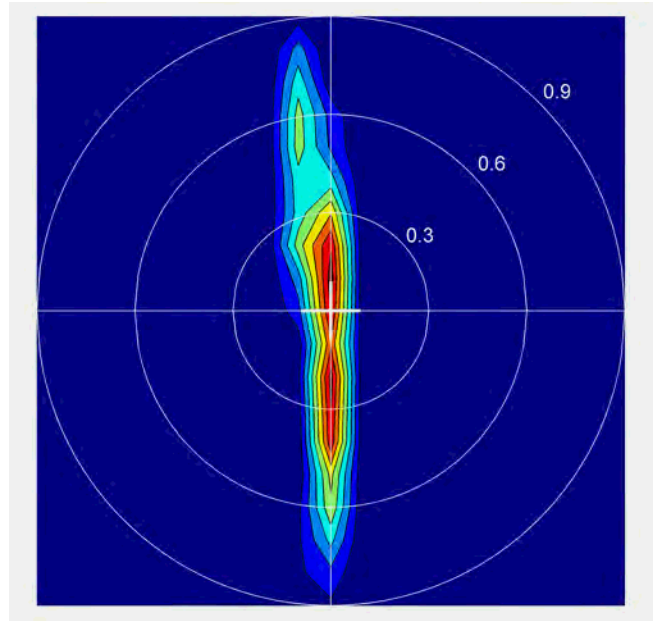


Figure G16: Time series data from the Hydra mooring deployed in Area C during 2009 (see [Table G1](#)); contoured histogram of the east and north components of the current vectors at 1 m above the seabed.

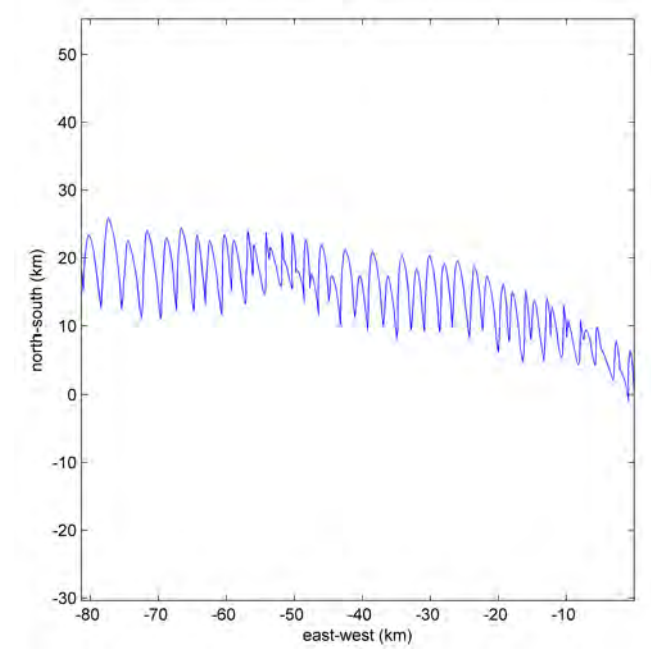


Figure G17: Data from the Hydra mooring deployed in Area C during 2009 (see [Table G1](#)); progressive vector plot for 1 m above the seabed.

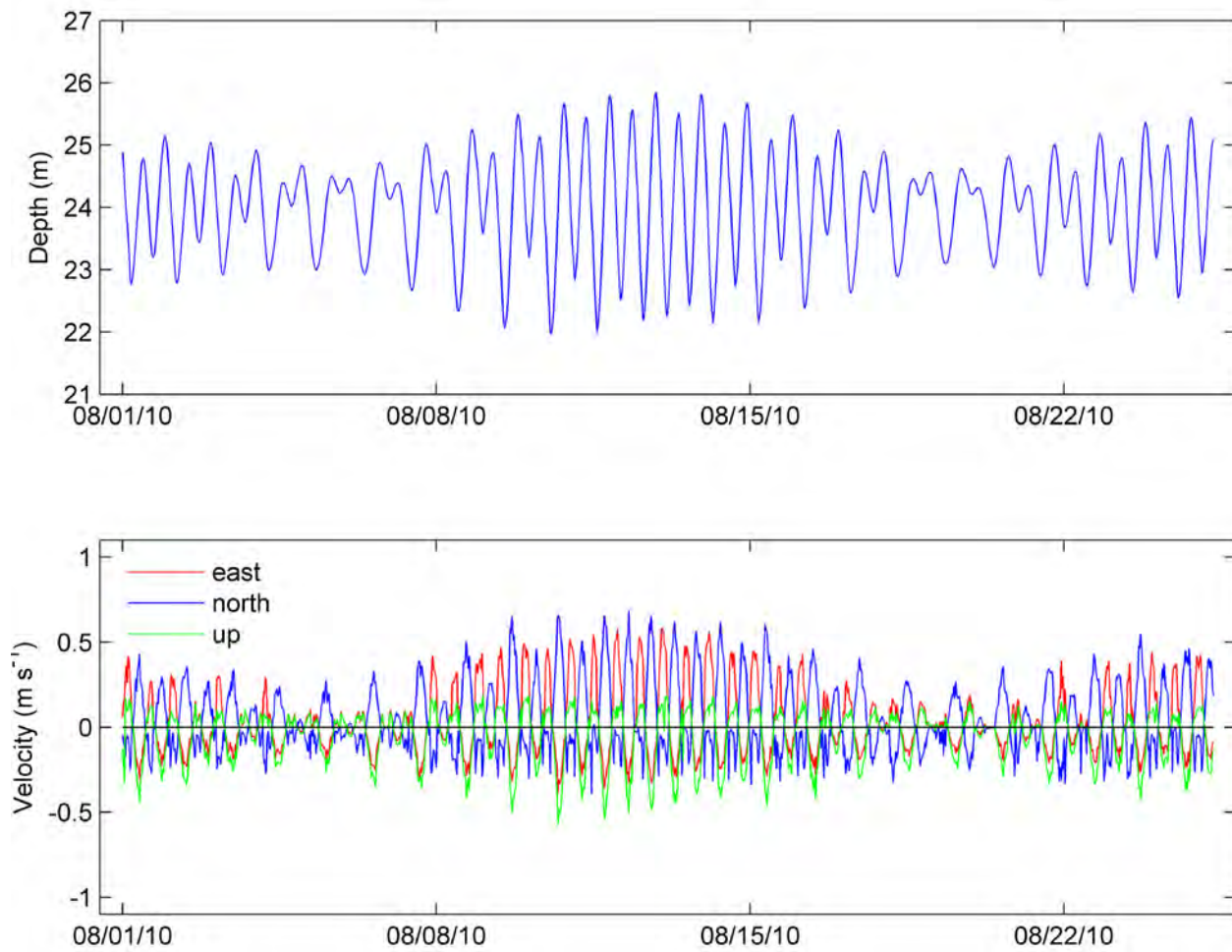


Figure G18: Time series data from the Hydra mooring deployed in Area C during 2010 (see [Table G1](#)); water depth (top panel), east, north and vertical vector components at 1 m above the seabed (bottom panel).

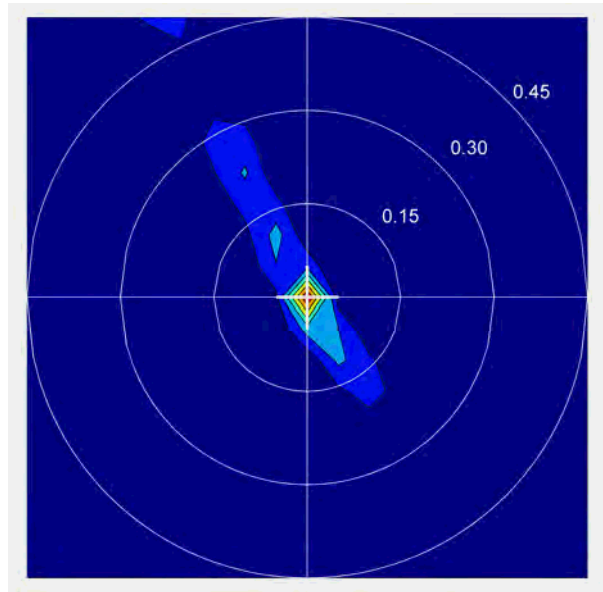


Figure G19: Time series data from the Hydra mooring deployed in Area C during 2010 (see [Table G1](#)); contoured histogram of the east and north components of the current vectors at 1 m above the seabed.

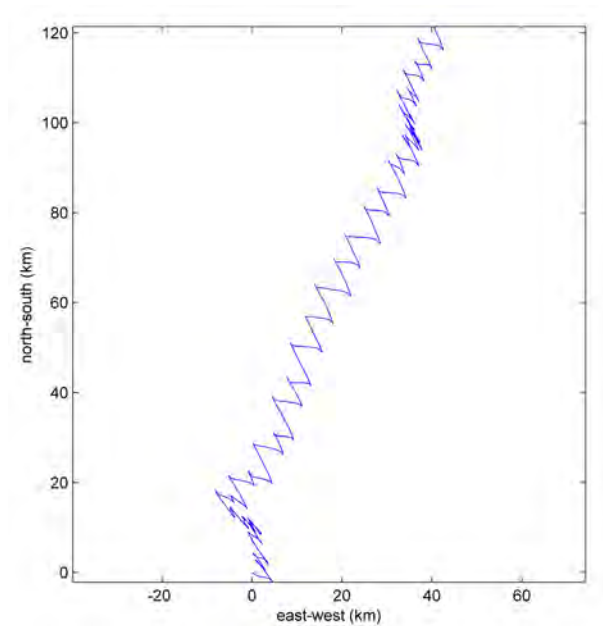


Figure G20: Data from the Hydra mooring deployed in Area C during 2010 (see [Table G1](#)); progressive vector plot for 1 m above the seabed.

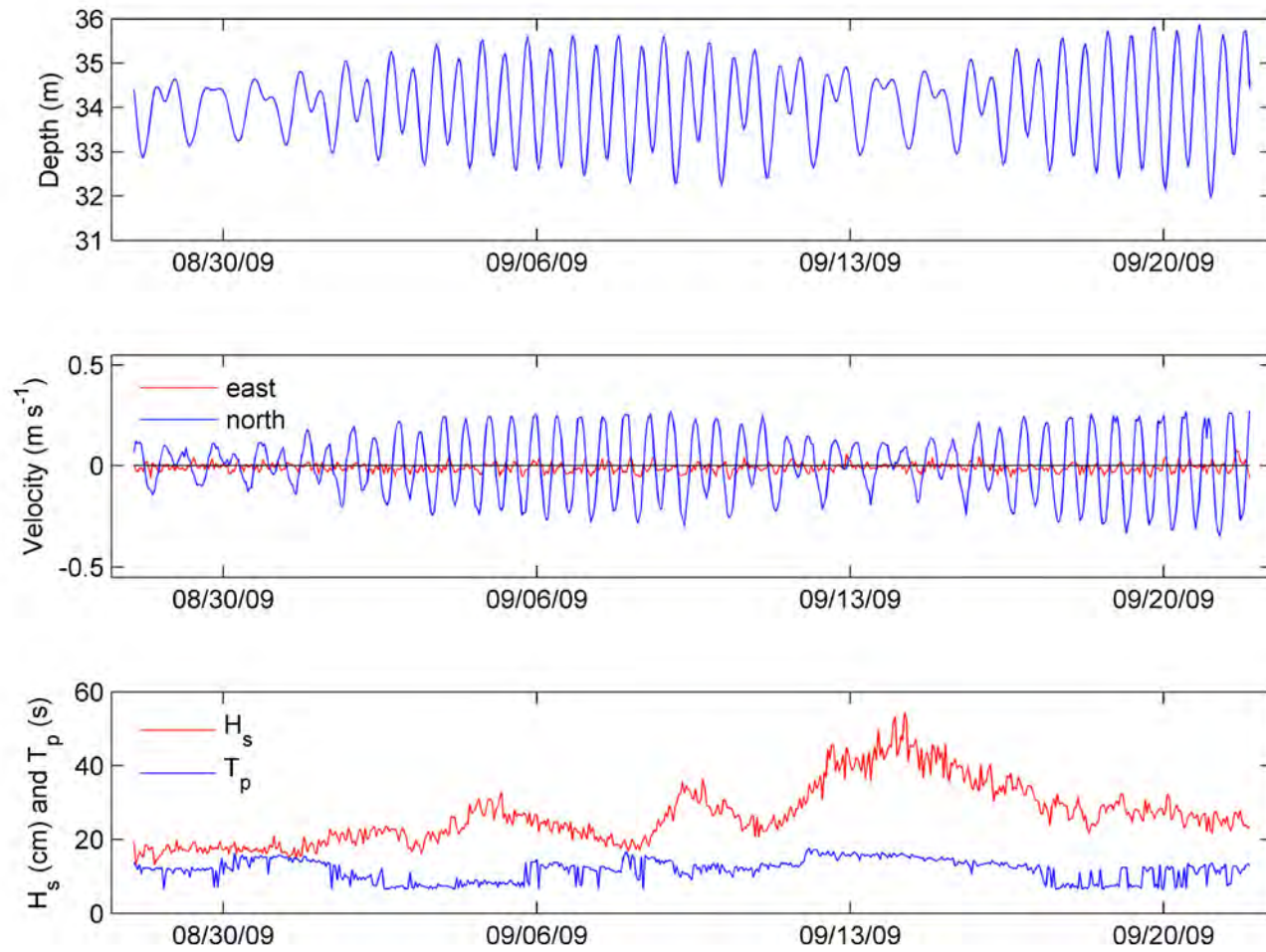


Figure G21: Time series data from the PC-ADP mooring deployed in Area C during 2009 (see [Table G1](#)); water depth (top panel), east and north vector components vertically-averaged over the first 1 m above the seabed (middle panel), and significant wave height and peak period (bottom panel).

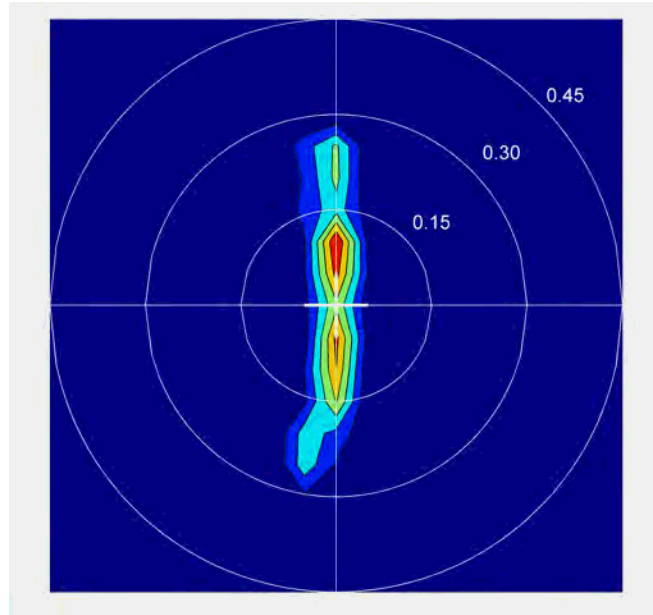


Figure G22: Time series data from the PC-ADP mooring deployed in Area C during 2009 (see [Table G1](#)); contoured histogram of the east and north components of the current vectors at 1 m above the seabed.

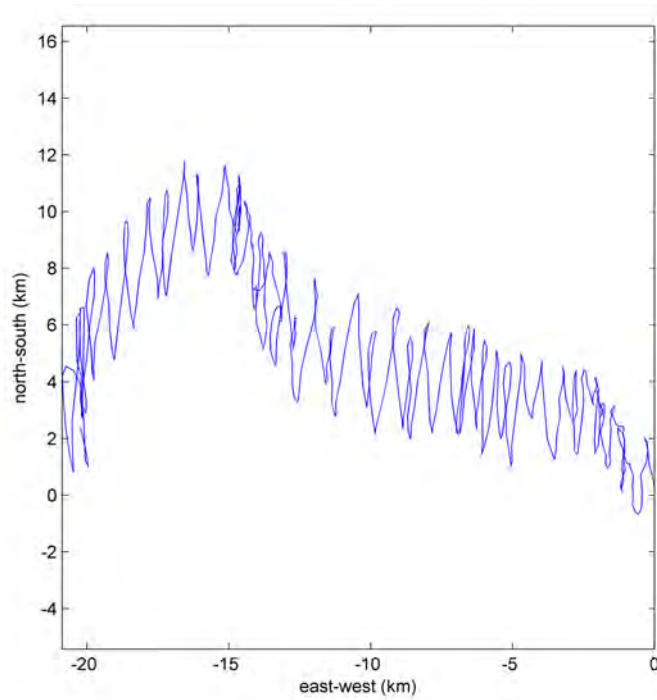


Figure G23: Data from the PC-ADP mooring deployed in Area C during 2009(see [Table G1](#)); progressive vector plot for 1 m above the seabed.

G3.4 Area D

Area D, located on the inner shelf, had one mooring placed in ca. 45 m water depth during the 2010 survey (Table G1). Time series of the tidal water level is shown in Figure G24 and the amplitudes and phases of the harmonic constituents are listed in Table G3. The form factor, based on the ratio of the amplitudes of the diurnal to semi-diurnal constituents, is 0.37. This classifies the tide as mixed, mainly semi-diurnal. Based on the nearly 4 weeks of data available, the amplitudes of M2 and S2 (Table G2) indicate the mean spring range is 4.23 m and the mean neap range is 1.06 m. The tide at this location on the inner shelf is larger in range than the tide measured on the outer shelf (cf. Table G2 and G3). The phase of the diurnal constituents is similar between the inner and outer shelf, however, the semi-diurnal constituents on the outer shelf lead those on the inner shelf, again supporting the notion that the semi-diurnal tide rotates around the gulf in a clockwise direction.

Table G3. Amplitude and G-Phase of the principal tidal constituents measured in Area D during 2010 (PC-ADP, see Table G2).

CONSTITUENT	AMPLITUDE	PHASE	CONSTITUENT	AMPLITUDE	PHASE
O1	0.3015	178.40	S2	0.7903	284.74
K1	0.4899	200.31	M4	0.0162	86.68
M2	1.3245	226.58	S4	0.0056	216.22

At this site on the inner shelf peak current speeds reached of the order 0.5 m s^{-1} at 1 m above the seabed (Figure G24). The current was aligned west-northwest to east-southeast at the site, broadly in alignment with the coastline, and the tidal current vector was roughly evenly distributed (Figure G25), resulting in a net drift over the deployment period towards the south (Figure G26). Waves were also recorded at this site. During the deployment period significant wave height was typically ca. 0.20 m and peaked at 0.40 m during two events, whereas peak period varied between 6 and 18 s (Figure G24).

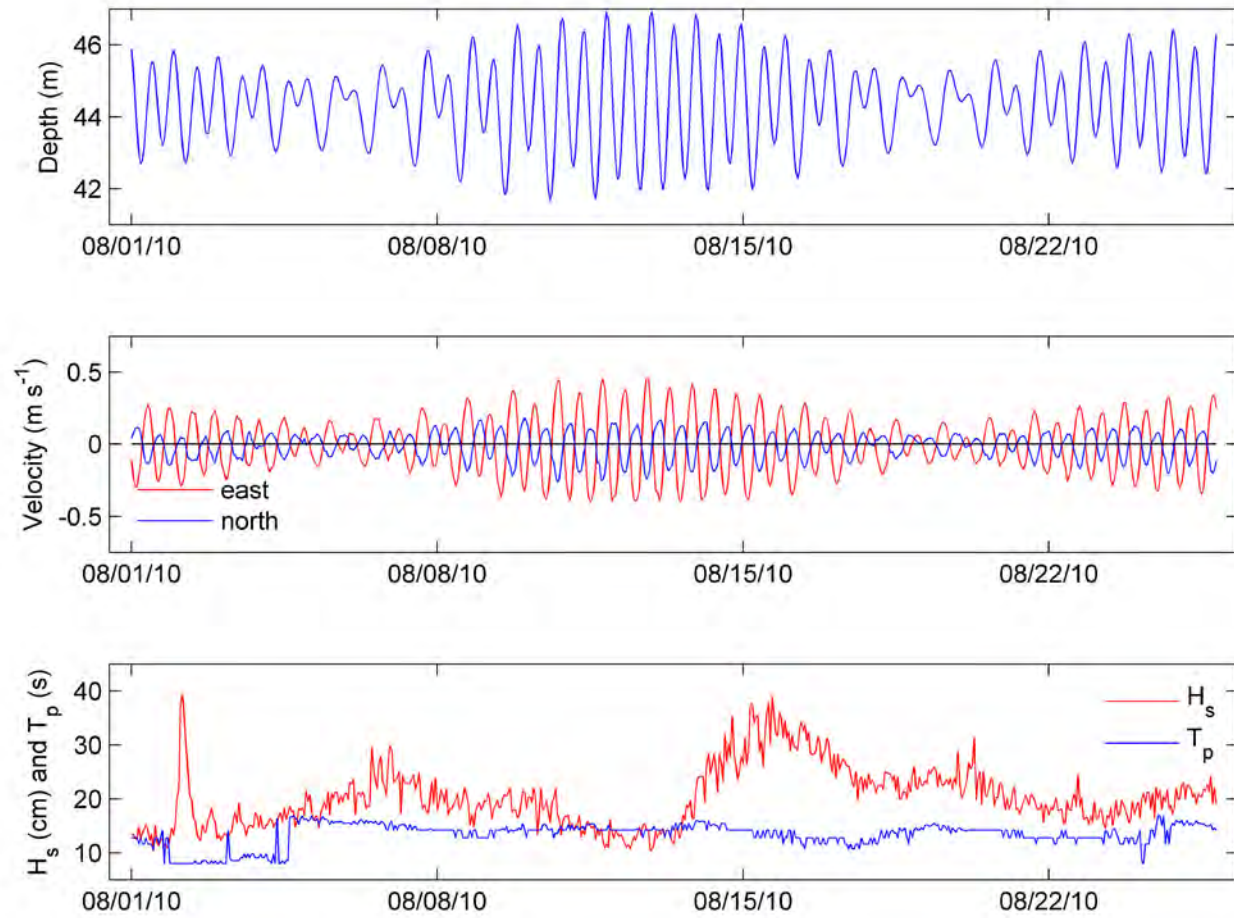


Figure G24: Time series data from the PC-ADP mooring deployed in Area D during 2010 (see [Table G1](#)); water depth (top panel), east and north vector components vertically-averaged over the first 1 m above the seabed (middle panel), and significant wave height and peak period (bottom panel).

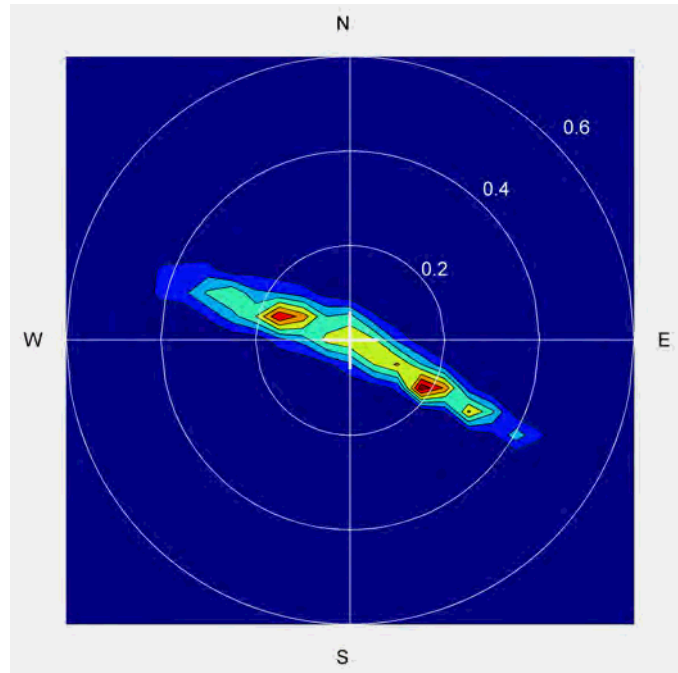


Figure G25: Time series data from the PC-ADP mooring deployed in Area D during 2010 (see [Table G1](#)); contoured histogram of the east and north components of the current vectors at 1 m above the seabed.

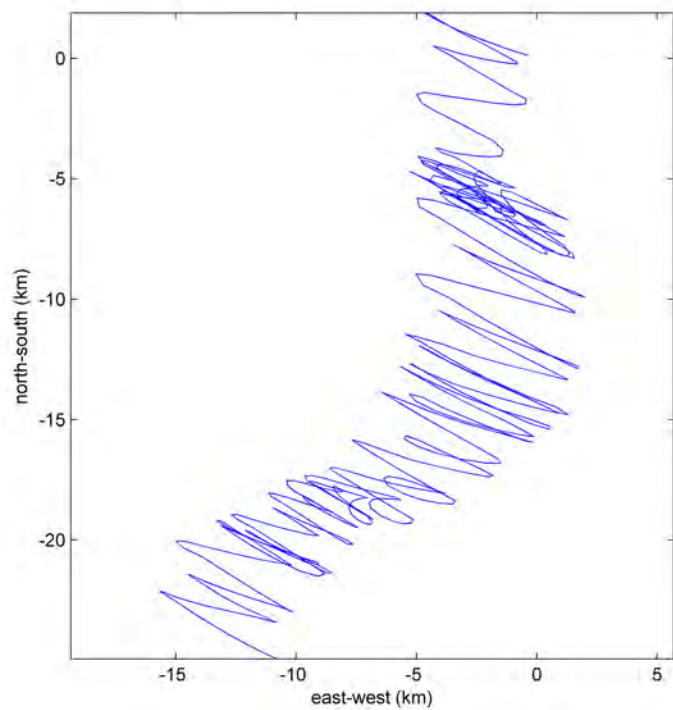


Figure G26: Data from the PC-ADP mooring deployed in Area D during 2010 (see [Table G1](#)); progressive vector plot for 1 m above the seabed.

Appendix H: GIS Data

H1. OVERVIEW

GIS files provided with this report include raw and processed data, and spatial interpretation of physical and ecological properties of the seabed. Data extent and scale varies: High-resolution local extent datasets were collected for four survey areas during 2009-11 as part of collaborative surveys by Geoscience Australia and the Australian Institute of Marine Science. Regional scale datasets covering the Joseph Bonaparte Gulf - Timor Sea region of interest have been extracted from Geoscience Australia's marine national scale datasets or databases. Complete national scale datasets and associated publications are available at www.ga.gov.au/marine.html

Datasets provided include those released as part of existing Geoscience Australia products. For access to other datasets used in creation of maps and spatial analysis, contact the data owner. Note that some datasets have been re-sampled from coarser resolutions. Regional datasets and local vector datasets are provided in Geographic WGS 84. Local geophysical grids are provided in WGS 84 UTM Zone 52S.

Details of data provided with this report are summarized in [Section H2](#). This data is intended for use in environmental interpretation as described in this report. Detailed metadata for all files is included and should be read before using datasets for other applications. Note that all data was current at the time of publication, and the confidence of interpreted products varies based on density and quality of the data that underpin them.



© Commonwealth of Australia (Geoscience Australia) 2011.

With the exception of the Commonwealth Coat of Arms and where otherwise noted, all material in this publication is provided under a Creative Commons Attribution 3.0 Australia Licence.

H2. SUMMARY OF SPATIAL DATASETS

H2.1 Administrative data

FILE NAME	FORMATS	EXTENT	GRID RESOLUTION/POSITIONAL ACCURACY
Region_of_interest	ESRI shapefile	Regional	-
Coast_250k	ESRI shapefile	Regional	250 m
AEEZ_limit	ESRI shapefile	Regional	250 m
Cities_towns	ESRI shapefile	Regional	-
SOL4934_SOL5117_surveyareas	ESRI shapefile	Regional	-

H2.2 Ecology

FILE NAME	DATA TYPE	FORMATS	EXTENT	GRID RESOLUTION/POSITIONAL ACCURACY
Video_habitats	Classification	ESRI	Local	10 m

Infaunal_richness	Classification	shapefile ESRI	Local	10m
Gardens_corals	Classification	shapefile ESRI	Local	10m
Epifaunal_richness	Classification	shapefile/ ESRI	Local	10m
Camera_4934_5117_transects	Video locations	shapefile ESRI	Local	10m
Sleds_4934_5117_transects	Benthic sled locations	shapefile ESRI	Local	10m

H2.3 Geophysics

FILE NAME	DATA DESCRIPTION	FORMATS	EXTENT	GRID RESOLUTION/POSITIONAL ACCURACY
Bathy_250m	Gridded bathymetry	ArcGRID	Regional	250 m
Pr_stb_newa	Probability of rock substrate	ArcGRID	Local	10 m
Pr_stb_newb	Probability of rock substrate	ArcGRID	Local	10 m
Pr_stb_newc	Probability of rock substrate	ArcGRID	Local	10 m
Pr_stb_newd	Probability of rock substrate	ArcGRID	Local	10 m
Bksct_a10m	Backscatter	ArcGRID	Local	10 m
Bksct_b2_10m	Backscatter	ArcGRID	Local	10 m
Bksct_b10m	Backscatter	ArcGRID	Local	10 m
Bksct_c10m	Backscatter	ArcGRID	Local	10 m
Bksct_d10m	Backscatter	ArcGRID	Local	10 m
Bathy_a10m	Bathymetry	ArcGRID	Local	10 m
Bathy_b2_10m	Bathymetry	ArcGRID	Local	10 m
Bathy_b10m	Bathymetry	ArcGRID	Local	10 m
Bathy_c10m	Bathymetry	ArcGRID	Local	10 m
Bathy_d10m	Bathymetry	ArcGRID	Local	10 m

H2.4 Physical seabed properties

FILE NAME	DATA DESCRIPTION	FORMATS	EXTENT	GRID RESOLUTION/POSITIONAL ACCURACY
Sediment_sample_locations	Locations and metadata	ESRI shapefile	Regional	0.1 decimal degrees
SOL5117_SOL4394_samples	Locations and assays	ESRI shapefile	Local	-
Gravel	Interpolated sediment properties	ArcGRID	Regional	0.01 decimal degrees
Sand	Interpolated sediment properties	ArcGRID	Regional	0.01 decimal degrees
Mud	Interpolated	ArcGRID	Regional	0.01 decimal degrees

Regional_geomorphic_features	sediment properties Clipped from the national scale geomorphology dataset	ESRI shapefile	Regional	250 m
JBG_geomorphology_all_areas	Detailed geomorphology for survey areas	ESRI shapefile	Local	0.01 decimal degrees
Jbg_5_class_Seascapes	Physical habitat classification	ESRI shapefile	Regional	0.01 decimal degrees
Fv_25cell_jbg	Physical habitat classification	ArcGRID	Regional	0.01 decimal degrees

H2.5 Oceanography

FILE NAME	DATA DESCRIPTION	FORMATS	EXTENT	GRID RESOLUTION/POSITIONAL ACCURACY
Prim_prod	Mean annual primary productivity	ArcGRID	Regional	Resampled to 0.01 decimal degrees
Seabed_exp	Output of GEOMACS model	ArcGRID	Regional	Resampled to 0.01 decimal degrees
Sf_temp		ArcGRID	Regional	Resampled to 0.01 decimal degrees

Instructions for the CD-ROM

Seabed Habitats and Hazards of Joseph Bonaparte Gulf and Timor Sea, Northern Australia by Przeslawski, R., Daniell, R., Anderson, T.J., Barrie, V., Heap, A., Hughes, M., Li, J., Potter, A., Radke, R., Siwabessy, J., Tran, M., Whiteway, T., Nichol, S. 2011. Geoscience Australia, Record 2011/40, 69 pp.

This CD-ROM contains the above-titled report as: Record 2011_40.pdf.

View this .pdf document using Adobe Acrobat Reader (click Adobe.txt for information on readers).

Double-click on **Record2011_40.pdf** to launch the document

Directories on data CD-ROM

Record2011_40_Appendix A
Record2011_40_Appendix B
Record2011_40_Appendix C
Record2011_40_Appendix D
Record2011_40_Appendix E
Record2011_40_Appendix F
Record2011_40_Appendix G
Record2011_40_Appendix H